Crosstalk of lysosomes, autophagy and apoptosis in dioxin-induced chloracne *in vitro*.

Emma Louise Woodward

Thesis submitted in fulfilment of the requirements of the regulations for the degree of Doctor of Philosophy

Institute of Cellular Medicine

Faculty of Medical Sciences

Newcastle University

September 2016

Abstract

Chloracne is a hyperkeratotic acneform skin disease caused by exposure to 2,3,7,8-tetrachlorodibenzo–p-dioxin (TCDD), a potent agonist of the aryl-hydrocarbon receptor (AhR). Despite the known role of TCDD exposure in the pathogenesis of chloracne, the molecular mechanisms mediating the disease remain poorly defined.

Using a previously optimised *in vitro* primary human keratinocyte epidermal equivalent model, we demonstrated the temporal regulation and development of a significantly reduced viable cell layer and compacted stratum corneum over 7 days with 10nM TCDD. These morphological changes were paralleled by cumulative AhR protein degradation and increased mRNA levels of CYP1A1. One of the key findings was a significant increase in the expression of the apoptotic marker, caspase-3 whilst there was no significant effect on Ki67 staining. Furthermore, TCDD treatment caused de-regulated epidermal differentiation as evidenced by increased mRNA expression but decreased protein expression of late differentiation markers. Treatment with TCDD also resulted in an induction of LC3 lipidation and endogenous LC3 protein expression as well as decreased P62 protein expression, well-established markers of autophagy induction. Interestingly, co-treatment of epidermal equivalents with TCDD and the lysosomal inhibitor, bafilomycin or cathepsin D inhibition (by pepstatin A or shRNA knockdown) resulted in restoration of the viable cell layer and reduction in TCDD-induced caspase-3 expression. Similar results were also seen after blockade of the autophagy pathway by ATG7 knockdown. Results also demonstrated lysosomal function and autophagy are required for TCDD-induced AhR degradation, indicating a potential role for chaperone-mediated autophagy. Collectively these data suggest exposure to TCDD results in deregulated epidermal differentiation, induction of autophagy, reduction of a viable cell layer and caspase-3 dependent cell death, likely mediated via lysosomal processing. Results provide an insight into the pathophysiology of chloracne, and demonstrate novel findings including TCDD-induced autophagy and potential role of lysosomal function in TCDD-induced death and AhR degradation.

Dedication

This work is dedicated to my grandpa, Brian Woodward, who would have loved to have seen my finished thesis.

Acknowledgements

This project was jointly funded by the Biotechnology and Biological Sciences Research Council (BBSRC) and AstraZeneca.

I would like to thank my supervisor Professor Nick Reynolds for your help throughout my PhD, particularly for all the meetings and discussions whilst writing up this thesis. I would also like to thank my supervisor Professor Penny Lovat, I couldn't have done this without your continued support, guidance and kindness throughout the project!

Thank you to my industrial supervisors Dr Mark Graham and Dr Lyn Rosenbrier Ribeiro at AstraZeneca for collaborating and the insightful discussions and knowledge. Thanks also to Dr Hilary Lewis and particularly Dr Rachel Rowlinson at AstraZeneca for your expertise and conducting the proteomics study.

I would also like to acknowledge Dr Ali Forrester who showed me the ropes at the beginning of this project and for answering my questions as the project progressed! Additional thanks also to Dr Alex Laude, Dr Trevor Booth and Dr Rolando Berlinguer Palmini for your help and guidance with imaging and inevitable troubleshooting!

Thanks to all the members of Dermatology I have had the privilege to work with, both past and present, for creating such a lovely working environment. I would particularly like to thank Martina, Laura and Keith for the second-to-none technical and statistical support but most importantly your incredible friendship both inside and outside of the lab (Wing Kee visits!). To Carole for all your advice and patience, Dhanisha for your positivity and Ashleigh…we made it!

A huge thank you to my family and friends, particularly my amazing parents for their endless love and support in everything I do, I'm so grateful. Finally, Adam, thank you for always believing in me, your patience and encouragement, especially over the last four years!

Declaration

This thesis is submitted for the degree of Doctor of Philosophy at Newcastle University. The research was performed in the Dermatological Sciences department in the Institute of Cellular Medicine under the supervision of Professor Nick J. Reynolds and Professor Penny E. Lovat. This thesis is my own work. I certify that none of the data offered in this thesis has previously been submitted by me for a degree or any other qualification at this, or any other university.

Table of Contents

List of Figures

List of Tables

Abbreviations

2D - Two dimensional

3D - Three dimensional

3-MA - 3-Methyladenine

AD - Atopic dermatitis

AhR - Aryl hydrocarbon receptor

AHRR - Aryl hydrocarbon receptor repressor

AIF - Apoptosis inducing factor

AIP - AhR interacting protein

ANOVA - Analysis of variance

Apaf-1 - Apoptosis protein-activating factor-1

ARNT - AhR nuclear translocator

ATG - Autophagy related gene

ATP - Adenosine triphosphate

BAD - Bcl-2-associated death promoter

Baf - Bafilomycin

BAK - Bcl-2 homologous antagonist/killer

BAX - Bcl-2-like protein 4

Bcl-2 - B cell lymphoma-2

BCL-W - Bcl-2-like protein 2

BEC-1 - BECLIN-1

bHLH-PAS - Basic Helix-Loop- Helix Per/ARNT/Sim

BIK - Bcl-2-interacting killer

Blimp1 - B lymphocyte-induced maturation protein 1

CAD - Caspase activated DNase

cDNA - Complementary DNA

CK10- Cytokeratin 10 (aka keratin 10)

CMA- Chaperone mediated autophagy

Ct - Cycle threshold

CTSD - Cathepsin D

CYP - Cytochrome P450

DISC - Death inducing signalling complex

DMSO - Dimethyl sulfoxide

DNA - Deoxyribonucleic acid

dNTPs - Deoxynucleotide

E.coli - Escherichia coli

EDC - Epidermal differentiation complex

EGF - Epidermal growth factor

EGFR - Epidermal growth factor receptor

ERK - Extracellular signal–regulated kinases

FADD - Fas-associated death domain protein

FBS - Fetal Bovine Serum

FFPE - Formalin fixed and paraffin embedded

FICZ - 6-formylindolo[3,2-b]carbazole

FLG - Filaggrin

GAPDH - Glyceraldehyde 3-phosphate dehydrogenase

GFP - Green fluorescent protein

H&E - Haemotoxilin and eoisin

HaCaT - Immortalised keratinocyte cell line

HAH - Halogenated aromatic hydrocarbons

HIV - Human immunodeficiency virus

HKGS - Human keratinocyte growth supplement

Hsp90 - Heat shock protein 90

IF - Immunofluorescence

INV - Involucrin

IPA - Ingenuity pathway analysis

K1 - Keratin 1

K14 - Keratin 14

K5 - Keratin 5

kDa - Kilodalton

Kg - Kilogram

LAMP - Lysosome associated membrane protein

LB - Lysogeny broth

LC3 - Microtubule associated protein light chain 3

LMP - Lysosomal membrane permeabilisation

LOR - Loricirn

mg - Milligram

ml - Millilitre

mM - Millimolar

MMLV - Moloney Murine Leukemia Virus

MMP - Mitochondrial membrane permeabilisation

MOMP - Mitochondrial outer membrane permeabilisation

MPT - Mitochondrial permeability transition pore

mRNA - Messenger ribonucleic acid

mTOR - Mammalian target of rapamycin

MTT - Thiazolyl blue tetrazolium bromide

NES - Nuclear export signal

NHEKs - Normal human epidermal keratinocytes

NHS - National Health Service

NIKS - Near diploid immortalised human keratinocytes

NLS - Nuclear localisation signal

nm - Nanometres

nM - Nanomolar

NT - Non target

p23 - Prostaglandin E synthase 3

P62 - Nucleoporin P62

PAH - Polycyclic aromatic hydrocarbons

PBS - Phosphate buffered saline

PCD - Programmed cell death

PCR - Polymerase chain reaction

PDT - Photo dynamic therapy

Pep A - Pepstatin A

pg - Picogram

PSA - Penicillin streptomycin amphotericin B

qPCR - Quantitative PCR

RIP1 - Receptor-interacting protein 1

ROS - Reactive oxygen species

SEM - Standard error of the mean

shBEC - Short hair pin ribonucleic acid BECLIN-1

shCTSD - Short hair pin ribonucleic acid cathepsin D

shNT - Short hair pin ribonucleic acid non target

shRNA - Short hair pin ribonucleic acid

siATG7 - Short interfering ribonucleic acid ATG7

siNT - Short interfering ribonucleic acid non target

siRNA - Short interfering ribonucleic acid

SNARES - Soluble N-ethylmaleimide-sensitive factor attachment protein

SRB - Sulphorhodamine B

TCDD - 2,3,7,8-Tetrachlorodibenzo-p-dioxin

TCDF - 2,3,7,8-Tetrachlorodibenzofuran

TE - Trypsin Ethyleneiamine tetraacetic acid

TGM - Transglutaminase

TNF - Tumour necrosis factor

TNFR - Tumour necrosis factor receptor

TRADD - TNF receptor-associated death domain

ULK - UNC51-like kinase

UV - Ultraviolet

V-ATPase - Vacuolar ATPase

VCL - Viable cell layer

VPS34 - Vacuolar protein sorting 34

XRE – Xenobiotic response element

µg - Microgram

µL - Microliter

µm - Micrometre

µM - Micromolar

Chapter 1 Introduction

1.1. Structure and function of skin

The skin consists of two layers, the epidermis and the dermis and provides protection against external agents such as chemical injury and physical stress. Made up of dermal fibroblasts and extracellular matrix proteins, the principal function of the dermis is to support the epidermis by providing both a blood supply and growth factor mediated regulatory signals (Loertscher *et al*., 2001a). Conversely, the upper layer or epidermis is a stratified squamous epithelium, mainly comprised of keratinocyte cells and organised into viable cell layers (VCL). These layers or strata are known as the basal, spinous and granular layer and at the top, a final cornified layer. Each layer has a distinct functional characteristic (Loertscher *et al*., 2001a). In addition to keratinocytes, melanocytes, Merkel cells and langerhan cells are also present in the epidermis. Briefly, melanocytes are involved in pigmentation of the skin and produce melanosomes which contain melanin (Wickett and Visscher, 2006). Langerhans cells are dendritic cells found in the basal and suprabasal layers within the epidermis and are involved in antigen presentation and adaptive immune system (Cumberbatch *et al*., 2003, Wickett and Visscher, 2006). Merkel cells serve as mechanoreceptors and as such are concentrated in areas which give the greatest tactile response e.g. the fingertips (Svensson, 2009). However, the work in this project focused on monolayer and epidermal skin equivalent models derived from primary human keratinocytes alone.

1.1.1. Epidermal differentiation

Keratinocytes undergo a continuous differentiation process to maintain epidermal structure (as shown in Fig 1.1) and regeneration of skin.

Undifferentiated stem cells, located in the **basal membrane**, have a distinct intracellular cytoskeleton composed of an extensive network of keratin 5 and keratin 14 filaments (Nelson and Sun, 1983, Fuchs, 1990). Proliferating keratinocytes in the basal layer are able to generate new cells that lose their proliferative ability and subsequently begin to differentiate (Eckert *et al*., 2005, Eckhart *et al*., 2013). These post-mitotic but metabolically active cells move up into the suprabasal layers of the

epidermis, firstly into the **spinous layer**. Within the basal and spinous layers are desmosomes, intercellular junctions required for hyper-adhesion between cells, forming a lattice shape and maintaining epidermal structure (Fuchs, 1990, Franke *et al*., 1987, Thomason *et al*., 2010). These differentiating keratinocytes then start to express keratin 1 and keratin 10, replacing keratin 5 and 14 and start to produce envelope proteins such as involucrin, deposited on the inner surface of the plasma membrane (Rice and Green, 1979, Fuchs, 1990).

Cells then move into the **granular layer**, characterised by keratohyalin granules which contain pro-filaggrin as well as lipid filled lamellar bodies (Sutter *et al*., 2011). Although at this stage pro-filaggrin is not able to bind to keratins, it is later de-phosphorylated and proteolysed to produce filaggrin monomers (Sandilands *et al*., 2009). It is in the granular layer cells are transformed into corneocytes. In this cornification process, organelles are destroyed, DNA is degraded and the plasma membrane is replaced with a cornified envelope, made of cross-linked proteins and lipids. Proteins expressed in the granular layer include transglutaminase 1 (TGM-1), TGM3 and TGM-5, involucrin as well as keratin 1 and keratin 10.

The **cornified layer** consists of dead flattened, enucleated cells and terminally differentiated corneocytes which are eventually sloughed from the surface and removed from the epidermis (Proksch *et al*., 2008). These corneocytes are held together by tight and adheran junctions, keratin filaments and cornified envelope proteins (Baroni *et al*., 2012).

Intracellular structural proteins are extremely important in the formation of the epidermal barrier and provide cellular strength (Sutter *et al*., 2011). Within the cornified layer, filaggrin aggregates to keratin filaments, helping to form flattened corneocytes and provides a uniform scaffold for cornified envelope assembly (Candi *et al*., 2005, Proksch *et al*., 2008). The cornified layer is also reinforced by other structural proteins, including loricrin, involucrin and trichohyalin crosslinked by transglutaminase enzymes (TGM1 and TGM3) to ceramides and small proline rich proteins (Furue *et al*., 2014).

Many structural proteins have been located on the epidermal differentiation complex (EDC) locus on the 1q21 human chromosome and loss of function mutations in these proteins can be the underlying cause of skin diseases (Sutter *et al*., 2011, Kypriotou *et al*., 2012).

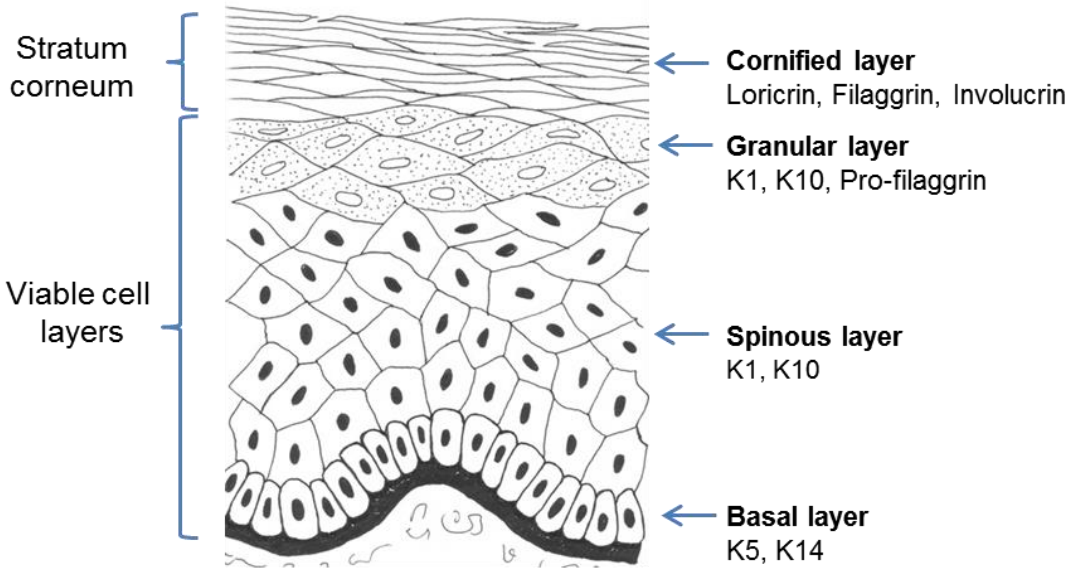

Figure 1.1 Schematic of the epidermis.

The epidermis consists of viable cell layers and stratum corneum, with each layer expressing distinct differentiation protein markers. Adapted from, Wickett and Visscher (2006)

1.1.2. Metabolism within the skin

As previously described (section 1.1) the skin is constantly exposed to the environment and provides protection from mechanical and chemical threats. Therefore, it is no surprise that drug metabolising activity has been found in the skin and it is capable of biotransformation of drugs or chemicals that penetrate through the stratum corneum (Svensson, 2009, Pannatier *et al*., 1978). The expression and localisation of xenobiotic metabolising enzymes within the skin has been extensively reviewed (Svensson, 2009, Oesch *et al*., 2007, Oesch *et al*., 2014).

One of the most important groups of Phase I metabolising enzymes are cytochrome P450 enzymes, heme-containing membrane proteins capable of xenobiotic metabolism via oxidation reactions. Substrates for CYP450 enzymes range from ingredients in cosmetics to allergens and carcinogens present in the atmosphere. Numerous CYP450 enzymes have been detected in the skin at both mRNA and protein level, including CYP1A1, CYP2B6, CYP2E1 and CYP3A5 (Baron *et al*., 2001,

Saeki *et al*., 2002, Vyas *et al*., 2006). Although activity in the skin may be less compared to the liver, other Phase I metabolising enzymes, have been detected in the skin. This includes flavin-dependent monooxygenases, alcohol dehydrogenases, and epoxide hydrolases.

After Phase I metabolism, in which the substrate is modified by introducing a reactive or polar group, Phase II metabolism begins. Phase II enzymes conjugate the active metabolite with a charged group such as glutathione to allow for easier transportation across membranes. Numerous Phase II enzymes have been identified in skin including glutathione-S-transferase, UDP-glucuronosyltransferase, sulfotransferase and N-acetyltransferase (Oesch *et al*., 2007).

1.2. Aryl hydrocarbon receptor

The aryl hydrocarbon receptor (AhR) is an intracellular mediator of the xenobiotic signalling pathway. It belongs to the bHLH–PAS (basic Helix-Loop-Helix-Per/ARNT/Sim) family of proteins and is a ligand activated transcription factor expressed in various mammalian tissues including the skin (Song *et al*., 2002, Abel and Haarmann-Stemmann, 2010). The AhR has a uniform molecular structure, comprised of three functional domains and unlike other members of the bHLH-PAS family, can bind to endogenous xenobiotics (Hao *et al*., 2013).

1.2.1 AhR pathway activation

In the absence of ligand binding the AhR resides in the cytoplasm in an inactive complex with the chaperone protein **p23** (prostaglandin E synthase 3) a dimer of **hsp90** (heat shock protein 90) and **AIP** (AhR interacting protein) also known as XAP-2 (HBV X-associated protein 2) (Sorg, 2014) (Fig 1.2).

AhR is activated by a variety of lipophilic compounds able to diffuse through the plasma membrane. Upon ligand binding AhR dissociates from its chaperone proteins and the AhR-ligand complex binds to **ARNT** (AhR nuclear translocator) (Sorg, 2014). The AhR-ligand-ARNT complex translocates into the nucleus and then binds to its

cognate DNA sequence (TNGCGTG) in the promoter regions of AhR target genes, known as xenobiotic response elements (**XRE**) (Hao *et al*., 2013, Denison *et al*., 1988, Ma, 2011). Binding to XRE causes altered transcription of target genes e.g. glutathione-s-transferase and UDP-glucoronosyltransferases as well as CYP genes, particularly CYP1A1 all of which are involved in xenobiotic metabolism.

The location of a transcription factor such as AhR, can affect gene regulation. Localisation of nuclear proteins is often determined by a nuclear localisation signal (NLS), which causes the protein to be transported into the nucleus, or alternatively a nuclear export signal (NES) (Ikuta *et al*., 2009). The AhR possesses both NLS and NES sequences and as such, is continuously shuttled between the cytoplasm and nucleus (Ikuta *et al*., 1998, Ikuta *et al*., 2009, Hao *et al*., 2013). It is thought that phosphorylation or de-phosphorylation of an amino acid near the NLS or NES can impact the balance between nuclear import or export and subsequent localisation of the protein in the cell (Zhang *et al*., 2001, Ikuta *et al*., 2009). As well as exposure to exogenous ligands, AhR localisation and activity can be affected by cellular confluency (Ikuta *et al*., 2009).

1.2.2. Degradation and regulation of AhR with the AhR substrate TCDD

AhR degradation is thought to occur within the cytoplasm of the cell after a nuclear export signal (NES) initiates nuclear translocation. Research suggests levels of AhR are tightly regulated and the ubiquitin-proteasome pathway is responsible for degradation. Initial studies demonstrated when cells were treated with TCDD in the presence of MG-132 a 26S proteasome inhibitor AhR degradation was blocked in a dose-dependent manner (Davarinos and Pollenz, 1999). MG-132 is thought to also have off-target effects and inhibit lysosomal proteases and calpains, however, when cells were treated with a more specific calpain inhibitor (ALLM) inhibition of AhR degradation did not occur (Davarinos and Pollenz., 1999). Later studies also revealed AhR is ubiquitylated and inhibition of the 26S proteasome caused TCDD-induced CYP1A1 expression to increase (Ma and Baldwin, 2000). Additionally, results showed ligand activated AhR had a reduced half-life (around 3 hours) compared to stable cytoplasmic AhR (around 28 hours) and this reduction in half-life was blocked by the 26S proteasome inhibitor (Ma and Baldwin, 2000).

As well as AhR targeting xenobiotic metabolism genes, the AhR/ARNT complex also targets the aryl hydrocarbon receptor repressor (AhRR) an integral part of AhR signalling (Mimura *et al*., 1999). The AhRR acts as a negative feedback loop, however, the mechanisms by which AhRR represses AhR signalling is not fully understood (Hao *et al*., 2013). It has been suggested AhRR is able to form heterodimers with ARNT, blocking AhR-ARNT binding to xenobiotic response elements (XREs) and subsequent upregulation of target genes (Mimura *et al*., 1999).

This ability to reduce the over-expression of enzymes such as CYP1A1 is particularly useful as such metabolic reactions can produce reactive oxygen species (ROS) which if accumulated can induce oxidative stress, leading to DNA damage amongst other consequences (Tigges *et al*., 2013).

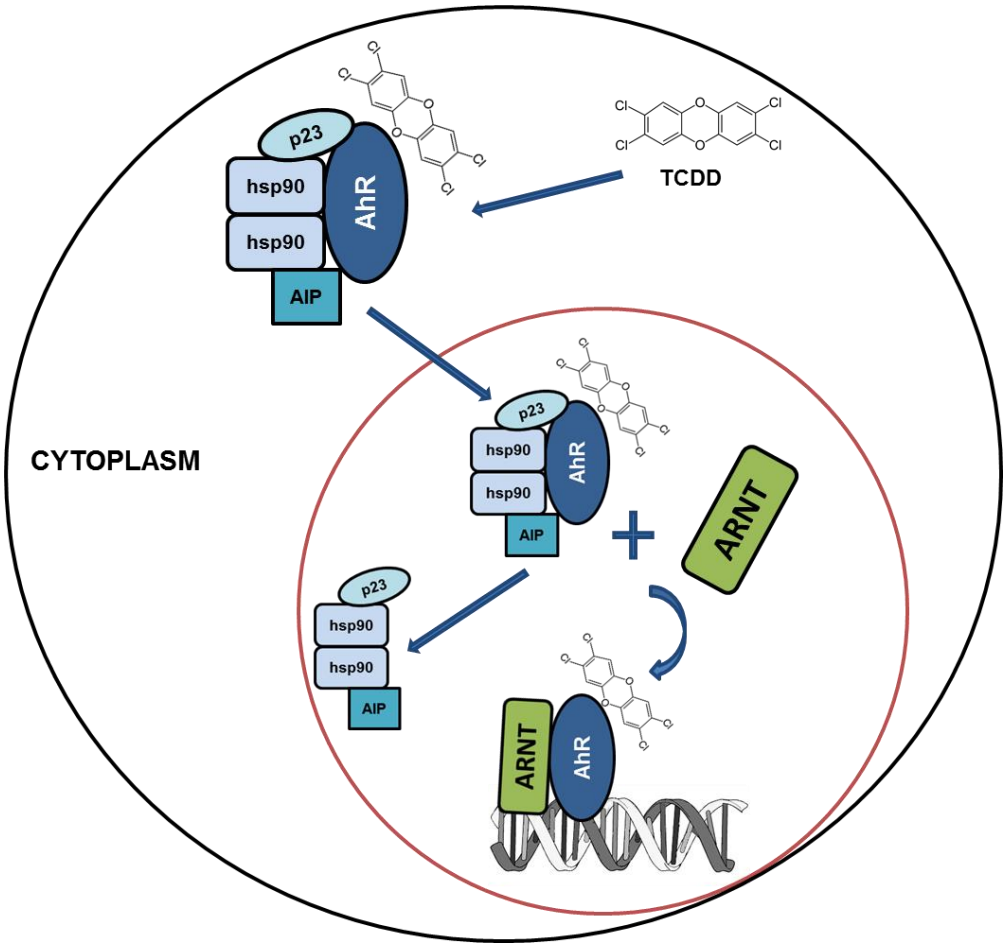

Figure 1.2 Schematic of AhR signalling within the cell.

Upon ligand binding, AhR is translocated into the nucleus of the cell, where it dissociates from chaperone proteins and forms a dimer with ARNT. AhR-ARNT then binds to XREs on target genes, causing up-regulation of transcription.

1.2.3. AhR ligands

The AhR is well known for its involvement in the toxic effects of dioxins and synthetic ligands such as poly-cyclic aromatic hydrocarbons (PAHs) (Tian *et al*., 2015). Indeed, the majority of high affinity AhR ligands identified are synthetic, with the more stable halogenated aromatic hydrocarbon (HAH) molecules (e.g. TCDD and TCDF) being most potent compared to PAH molecules (e.g. benzo(a)pyrene) which have a lower affinity (Denison and Nagy, 2003, Murray *et al*., 2014).

However, more recently, ligands with alternative non-halogenated structures have been identified including several drugs which have off-target effects such as omeprazole (a treatment gastroesophageal reflux disease) and tranilast (an anti-allergy drug) (Jin *et al*., 2014, Murray *et al*., 2014). Furthermore, endogenous and plant based ligands have also been identified and thought to play a role in the physiological function of AhR under normal or healthy conditions. In fact, it has been suggested that a variety of naturally occurring chemicals from the diet, can activate or inhibit the AhR pathway (Denison and Nagy, 2003). For example, phytochemicals such as flavonoids have been found exert both agonistic (e.g. galagin) and antagonistic (e.g. luteolin) effects when interacting with the AhR, although results have been cell line-dependent (Zhang *et al*., 2003, Murray *et al*., 2014). UV irradiation of tryptophan can also generate compounds with a high affinity for the AhR, the most active derivative being 6-formylindolo[3,2-b]carbazole (FICZ), thought to be a physiological AhR agonist (Nguyen and Bradfield, 2008). Indeed, FICZ (10nM) was found to rapidly induce CYP1A1 mRNA expression in HaCat cells, with maximal induction after just 3 hours (Wei *et al*., 1998).

1.2.4. TCDD

The AhR is known as an intracellular mediator for the xenobiotic signalling pathway and as such, it is responsible for the majority of all toxicological responses to the dioxin, 2,3,7,8-tetrachlorodibenzo-p-dioxin (TCDD) as shown in Fig 1.2.

TCDD is a halogenated hydrocarbon and a potent toxin which has a high affinity for the AhR. It is highly lipophilic with a long elimination half-life, staying in the body for

up to 11 years (Sorg *et al*., 2009). Indeed, dioxin-like compounds cause sustained induction of target enzymes such as CYP1A1, compared to the transient induction by other AhR agonists (Wincent *et al*., 2009). Very low levels of dioxin are present in the environment, often released as waste products from industrial processes such as herbicide and pesticide manufacturing. However, it can be released from natural phenomena such as volcanic eruptions or forest fires. Due to its long half-life, TCDD can accumulate in animal fat and plant tissue; as such human populations are primarily exposed through the food chain (Pelclova *et al*., 2006). The maximum accepted daily dose for humans is 4pg/kg (Saurat *et al*., 2012).

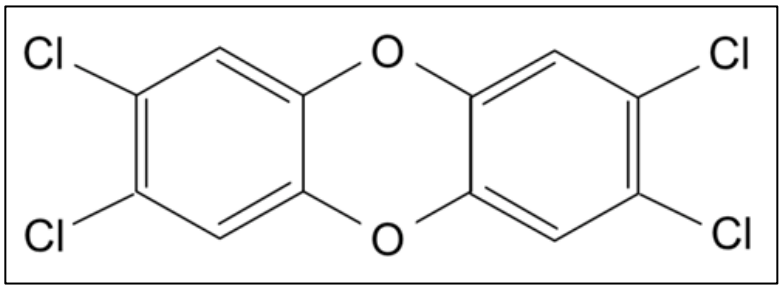

Figure 1.3 Molecular structure of 2,3,7,8-tetrachlorodibenzo-p-dioxin (TCDD).

TCDD has a planar structure with four chlorine atoms, hence the term “chloracne”.

1.3. Chloracne

TCDD is classified as a known human carcinogen, shown in laboratory animals to promote the formation of neoplastic lesions in areas such as the liver and skin (Knerr *et al*., 2006; Ray and Swanson, 2009). However, after abnormally high TCDD exposure, one of the most consistent outcomes of systemic poisoning is the development of a form of acne, “chloracne” and as such development of chloracne is used as a specific marker of dioxin toxicity (Saurat *et al*., 2012, Ju *et al*., 2012). First described in 1887, chloracne was originally thought to be the result of chlorine exposure, although now many chloracnegenic agents have been identified, with the most potent being dioxins (Ju *et al*., 2009). One of the most notable cases of TCDD poisoning was that of Viktor Yuschenko, a Ukrainian presidential candidate, who received a dose 50,000 fold greater than normal exposure in 2004 (Sorg *et al*., 2009). Another infamous case occurred in 1976, when exposure to more than 2kg of

TCDD released into the atmosphere, after an explosion at a chemical plant, resulted in 135 cases of chloracne developing in Seveso, Italy (Ju *et al*., 2009, Baccarelli *et al*., 2005).

After exposure through inhalation, ingestion or direct contact, *acne vulgaris* like lesions, primarily non-inflammatory comedones and cysts, develop often within a few weeks (Ju *et al*., 2012). Distribution is initially on the face and neck but can then extend to the trunk and other extremities (Ju *et al*., 2009) and in contrast to acne vulgaris, sebum excretion is generally reduced (Gawkrodger *et al*., 2009). Hyperkeratosis or abnormalities in keratinocyte differentiation within the follicle is also often detected, causing keratotic plugs to form (Pastor *et al*., 2002) as well as thinning of the follicular wall (Ju *et al*., 2012).

The cellular and molecular pathogenesis of chloracne remains incompletely understood, although most effects seem to be mediated via the AhR (Ju *et al*., 2012). As such, there is no known treatment or therapy for chloracne, other than avoiding further exposure to chloracnegens. Some patients have seen improvements after retinoid or corticosteroid treatment and dermabrasion, but in general chloracne is resistant to most tested treatments (Ju *et al*., 2009).

Figure 1.4 Viktor Yushenko pre and post poisoning with TCDD.

Images of Viktor Yushenko pre poisoning with TCDD (A) then 5 months (B) 3 years (C) and 11 years (D) post poisoning with TCDD. Image adapted from (Sorg *et al*., 2009).

1.3.1. Mice models of chloracne

The degree and range of TCDD-induced effects vary significantly between animal species and although AhR knockout animals have helped in understanding the endogenous role of AhR in other organs e.g. liver (Lahvis *et al*., 2000, Loertscher *et al*, 2002) chloracne affects both hair follicles and the interfollicular epidermis and as such suitable animal models are difficult to derive. Nevertheless, mouse models with differing AhR alleles are available which have provided some mechanistic insight. Mice with a responsive AhR allele (Ah^b) able to bind ligands with a high affinity and mice with an unresponsive allele (Ah^d) able to bind ligands with a low affinity, have been developed (Thomas *et al*., 1972, Loertscher *et al*., 2002). Mice with the Ah^b allele did develop an array of pathologies; however, as with most strains of mice, TCDD treatment failed to induce chloracne. Studies have also been carried out using mice with a hairless mutation (Knutson and Poland, 1982, Puhvel *et al*., 1982). Although TCDD induced a "chloracne-like" phenotype, including epidermal hyperkeratosis, hyperplasia and loss of sebaceous glands, results between strains of hairless mice varied. In addition, the mice are genetically sensitised and as such results should be viewed with caution. Due to the lack of data in both adult haired mice and developing mouse skin, Loertscher *et al* (2002) pursued an alternative method of *in utero* TCDD exposure. TCDD was delivered to the mother by oral gavage, and interestingly, results revealed alterations in terminal differentiation in foetal mouse skin, with TCDD inducing filaggrin protein expression (Loertscher *et al*., 2002).

However, as discussed by Murray *et al* (2014) there are several structural differences between mouse and human AhR which may affect function and explain the differences in TCDD toxicities. Firstly, the interaction with hsp90 is much more stable in mouse AhR than human. In addition, differences in binding affinity to ligands is evident, of importance, mouse AhR binds TCDD with tenfold higher affinity than human AhR (Ramadoss and Pardew, 2004, Murray *et al*., 2014). There is also low amino acid sequence homology between human and mouse AhR, particularly in the caboxy-terminal region of the protein which contains the transactivation domain (Murray *et al*., 2014).

1.3.2. Human models of chloracne

Due to the drawbacks of using animal models and differences in AhR activity between species, human keratinocyte cell lines such as the HaCaT cell line and primary cells obtained from human tissue biopsies are often used. Normal human epidermal keratinocytes (NHEKs) are particularly useful as they retain cellular structures and regulatory components involved in normal differentiation, even though they are a submerged culture (Sutter *et al*., 2011). Although monolayer cultures can be used to study biochemical and molecular mechanisms, organotypic models or epidermal equivalents more accurately reproduce the morphology and differentiation of human epidermal tissue (Loertscher *et al*., 2001a, b).

This project will incorporate both monolayer cultures and epidermal equivalents. The epidermal equivalent models were developed and used in previous research projects within the Reynolds lab (Forrester thesis). Briefly, primary human keratinocytes are seeded at high confluence onto a polycarbonate membrane and the following day raised to the air liquid interface. After culturing for 12 days a fully formed, fully stratified epidermis will develop and can be treated accordingly. Cultured 3D models like this have previously been found to accurately mimic native skin, including barrier protein expression (De Breij *et al*., 2012, El Ghalbzouri *et al*., 2008, Thakoersing *et al*., 2011)

Other forms of organotypic models are available and have been used by other groups to explore chloracne; for example, Loertscher *et al*. (2001b) used a full thickness system consisting of dermis and epidermis with primary human fibroblasts and near-diploid immortalised human keratinocytes (NIKs).

However, although skin equivalents, both epidermal and full thickness, represent useful models to investigate the effects of TCDD on human skin, these models lack appendages. Thus, tissues from chloracne lesions would obviously be gold standard when investigating the histopathology behind the phenotype (Saurat *et al*., 2012). However, cases of abnormally high TCDD exposure are rare and therefore studies on these lesions and biopsies are limited and few papers have been published.

1.4. AhR and role in the skin

Research over the years has revealed involvement of the AhR in numerous physiological processes and cross-talk between pathways, from the immune response (Quintana, 2013) to a role in cancer (Feng *et al*., 2013). However, recently the role of AhR in epidermal homeostasis and disease has become a popular area of research and revealed interesting findings as detailed below.

As previously described (section 1.1.3) skin is the first pass organ for dermal exposure and therefore as expected it is more than capable of metabolising xenobiotics (Tigges *et al*., 2013). One example of this is the presence of AhR which, when activated by ligands such as polycyclic aromatic hydrocarbons (PAHs), induces Phase I and Phase II enzymes capable of metabolising such ligands (Tigges *et al*., 2013).

Although the molecular mechanisms involved in the toxicity of TCDD and the chloracne phenotype are not fully understood, research has delineated the ability of TCDD to alter epithelial morphology and homeostasis (Loertscher *et al*., 2002). TCDD and the effect it has on keratinocyte differentiation has been well studied *in vitro*. In organotypic skin models dosed with TCDD, keratinocyte differentiation was altered, with a fully differentiated cornified layer developing quicker than in vehicle treated control models (Loertscher *et al*., 2001b). Interestingly, there was also no reported change in apoptosis induction or proliferation (Loertscher *et al*., 2001b). In monolayer, TCDD has been reported to increase protein expression of involucrin and filaggrin (Sutter *et al*., 2009). In addition, TCDD induces expression of genes in the human epidermal differentiation complex found on chromosome 1q21 (Kennedy *et al*., 2013).

However, the mechanism by which TCDD regulates these differentiation genes is not entirely known. Geng *et al*. (2006) found when ARNT null human keratinocytes were exposed to TCDD, filaggrin mRNA was not increased and therefore ARNT may be involved in this regulation. In contrast, Sutter *et al*. (2011) found using NHEKs that TCDD-activated AhR bound a small fragment of DNA upstream of the transcriptional start sites of the filaggrin gene. These start sites contained one of two candidate xenobiotic response elements and when the XRE sites were mutated the increased transcription of filaggrin disappeared (Sutter *et al*., 2011). Sutter *et al* (2009) also

suggest a role for epidermal growth factor receptor (EGFR) signalling, in dioxin induced keratinocyte differentiation and indeed, as a regulator or AhR. They reported dioxin induced filaggrin and CYP1A1 mRNA expression was repressed by epidermal growth factor (EGF) and propose EGF inhibits recruitment of the transcriptional co-activator protein p300 to the CYP1A1 gene (Sutter *et al*., 2009, Hankinson, 2009).

Research has also indicated that AhR may have a function in wound healing. Ikuta *et al*. (2009) carried out full thickness skin wounding on AhR -/-, AhR wildtype and AhR +/- mice and found that during the early phase of wound healing, AhR deficiency increased wound closure (Ikuta *et al*., 2009). In addition, Carvajal-Gonzalez *et al*. (2009) found in wild type and AhR knockout mice that loss of AhR expression increased migration of keratinocytes and increased skin re-epithelialisation whilst not effecting cell proliferation. Similarly, Moirangthem *et al*. (2013) found wound healing to be disrupted and poor when wild type mouse models of cutaneous wound healing were exposed to TCDD.

As discussed, it is well established that AhR activation by exogenous ligands such as TCDD induces terminal differentiation. However, Van den Bogaard *et al* (2015) recently explored the physiological role of AhR in keratinocyte differentiation, without exogenous ligand activation, using both murine and human models (Van den Bogaard *et al*., 2015). Results demonstrated AhR -/- primary keratinocytes had a significant reduction in differentiation gene and protein expression including involucrin and loricrin, which was in accordance with AhR +/+ primary keratinocytes treated with AhR antagonists (Van den Bogaard *et al*., 2015). Treatment of epidermal skin equivalent models with AhR antagonists also led to defects in stratification and reduced stratum corneum thickness. Finally, levels of nuclear AhR were also increased in differentiated primary mouse keratinocytes grown in monolayer.

Psoriasis is a chronic autoimmune skin disease which results in scaly, itchy and often painful patches of skin. In a study using both patient skin psoriasis biopsies and a psoriasis mouse model, Di Meglio *et al* (2014) suggests AhR signalling plays a role in preventing excessive skin inflammation. Interestingly, in the immiquimod-induced inflammatory mouse model, the endogenous AhR ligand FICZ was found to reduce inflammation and in AhR-deficient mice psoriasis was exacerbated compared to AhR control mice. In addition, the study found expression of a subset of psoriatic genes

decreased in the presence of the AhR agonist FICZ whilst the AhR antagonist CH223191 induced expression (Di Meglio *et al*., 2014, Colonna, 2014).

In corroboration with these findings, AhR was also recently suggested to have a role in coal tar treatment of atopic dermatitis (AD) (Van den Bogaard *et al*., 2013). AD is an inflammatory skin disease thought to be triggered by both environmental factors for instance allergens and genetic factors such as impaired skin barrier function. Mutations of the gene filaggrin are now known to represent an important cause of atopic eczema with ~50% of moderate to severe cases harbouring a mutated filaggrin allele. Within the European population, the 5 most commonly mutated alleles lead to severe truncation of filaggrin mRNA and reduced (hetereozygote) or absent (homozygote) filaggrin protein. Topical application of coal tar has been used to help treat AD for over 2000 years and is made up of over 10,000 organic compounds including many polycyclic aromatic hydrocarbons (Van den Bogaard *et al*., 2013). CYP450 enzymes help detoxify and metabolise such compounds and are found to be induced in coal tar treated patients. Using primary keratinocytes from both healthy patients and those with filaggrin-mutated AD, Van de Bogaard *et al*. (2013) used monolayer and organotypic models to investigate the effect of coal tar. The group observed that within 4 hours of coal tar treatment, AhR translocated from the cytoplasm into the nucleus, indicating coal tar was bound to AhR. Coal tar also induced levels of CYP1A1 and CYP1B1 and increased differentiation proteins such as filaggrin, loricrin and hornerin. In skin equivalents, terminal differentiation markers were also expressed earlier after coal tar treatment. In all, results indicate coal tar activates AhR and results in increased epidermal differentiation.

Together, these data underscore the physiological role of AhR in skin, its potential utility as a pharmacological target and the fact that CYP1A1 induction is not synonymous with toxicity and chloracne induction.

1.5. Autophagy

Autophagy is a catabolic lysosomal degradation pathway for cytoplasmic material. Unlike the ubiquitin proteasome system, autophagy is able to degrade long lived proteins and damaged organelles. There are three types of autophagy which only differ in the way material is delivered into the lysosome (Eskelinen, 2005). The term autophagy in general refers to macroautophagy, which describes the formation of a double membrane around a targeted region of the cell cytoplasm. The resultant vesicle then fuses with a lysosome for degradation. In microautophagy lysosomes engulf cytosolic components through direct invagination of the lysosomal membrane. In contrast, chaperone mediated autophagy (CMA) is characterised by its selectivity of substrates it degrades (Cuervo *et al*., 1996, Eskelinen, 2005). In this case, cytosolic proteins containing a KFERQ-like pentapeptide sequence are unfolded by chaperone proteins and translocated across the lysosomal membrane via a LAMP2A receptor (Kaur and Debnath, 2015). This is in contrast to macro or micro autophagy when substrates are engulfed or sequestered in bulk.

1.5.1. Process of autophagy

Autophagy is essential for normal cellular homeostasis and is generally a survival pathway activated in times of nutrient deprivation or stress to maintain cellular energy (Shpilka *et al*., 2012). It also has important roles in other processes such as cell development and defence mechanisms (Shpilka *et al*., 2012). Initially when autophagy is induced, a small isolation membrane or phagophore is formed and elongates to engulf part of the cytoplasm, as illustrated in Figure 1.5. This results in a double membrane autophagosome which then fuses with a lysosome, creating an autolysosome. The inner membrane of the autophagosome and the cytoplasmic material are then degraded and recycled (Shpilka *et al*., 2012). The proteases cathepsin D and B are translocated from the golgi body and are the main lysosomal proteases involved with the autophagy process (Aymard *et al*., 2011).

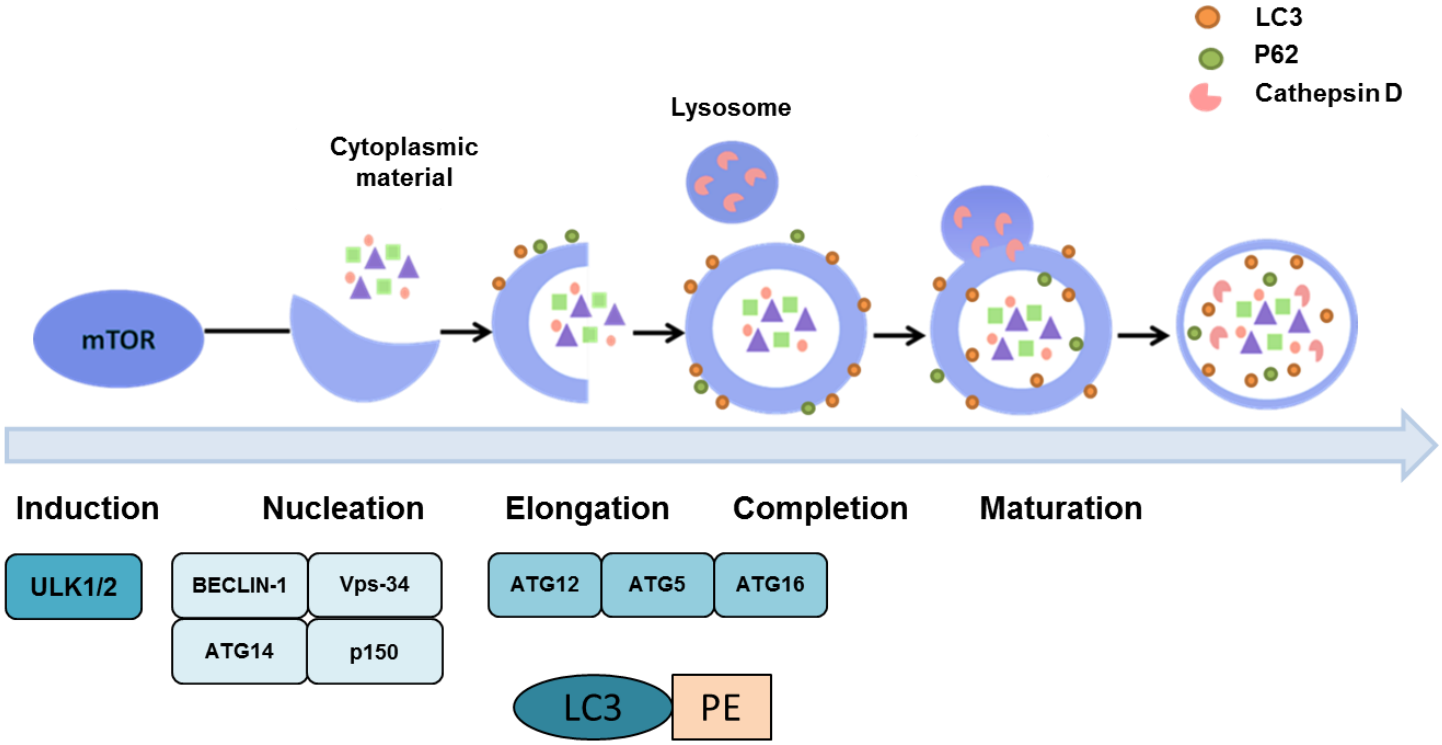

Figure 1.5 The autophagy pathway.

Schematic demonstrating the key stages of autophagy: induction, nucleation, elongation, completion and maturation including known regulatory genes at each stage. The schematic also illustrates recruitment and then degradation of LC3 and P62 by proteases such as cathepsin D

1.5.2. Autophagy genes and autophagy regulation

Research into genes associated with autophagy originally began in yeast mutants; however, homologs for many of these genes have been found in higher eukaryotes, suggesting the process of autophagy has been conserved from yeast to man (Eskelinen, 2005). Over 30 autophagy related genes (given the nomenclature ”ATG”) have been discovered and the process of autophagy is divided into distinct stages controlled by ATG related proteins.

Mammalian target of rapamycin (mTOR) is a member of the phosphatidylinositol 3-kinase-related kinase protein family and acts as a central regulator. In normal conditions, mTOR is activated causing inhibition of autophagy. However, when autophagy is induced in response to nutrient deprivation or stress, mTOR is phosphorylated and activates the ULK1/2 protein kinase complex (Mizushima *et al*., 2010). Members of the ULK (UNC51-like kinase) complex then assemble at the phagophore assembly site, or isolation membrane (Kaur and Debnath, 2015).

Of note, although nucleation is thought to occur from the endoplasmic reticulum, studies have recently suggested other sources of membrane may contribute to autophagosome formation, including mitochondria, plasma membrane and endosomes (Kaur and Debnath, 2015, Axe *et al*., 2008, Hailey *et al*., 2010, Ravikumar *et al*., 2010).

The activated ULK complex then targets a class III PI3 kinase complex, which mediates the nucleation phase and consists of BECLIN-1, VPS34 (vacuolar protein sorting 34), the serine/threonine kinase p150 and ATG14 (Mizushima *et al*., 2010, Kaur and Debnath, 2015, He and Klionsky, 2009). This subsequently leads to the development of a pre-autophagosomal structure from the membrane. Interestingly, binding of anti-apoptotic BCL-2 (discussed in section 1.6.1) to BECLIN-1 can block autophagy and dissociation of BECLIN-1 from BCL-2 is required for autophagy induction (He and Klionsky, 2009).

Elongation of this membrane around cytoplasmic material and completion of the double membraned autophagosome is mediated by recruitment of two conjugation systems. ATG12 is conjugated after activation by ATG7 (an E1 activating enzyme) this is then transferred to ATG10 (an E2 conjugating enzyme) and covalently

attached to ATG5 (He and Klionsky, 2009). The ATG12-ATG5 conjugate then interacts with ATG16 and attaches to the phagophore. The second conjugation system involves lipidation of protein 1 light chain 3 (LC3) to phosphatidylethanolamine (PE) resulting in the conformational change to LC3II, this LC3 I/II flux is often used as an autophagic marker for example through western blotting, immunofluorescence or dual tagged mCherry-GFP-LC3 live cell imaging (Mizushima *et al*., 2011, Eskelinen, 2005, Kaur and Debnath, 2015). The scaffold protein P62, which shuttles ubiquitylated proteins into the autophagosome, is also required. This is later broken down when the completed autophagosome fuses with a lysosome to form an autolysosome and again often used as an autophagic marker.

Although genes involved in formation of autophagosomes are well documented, the process of lysosome and autophagsosome fusion is still being delineated (Shen and Mizushima, 2014). However, studies have suggested a role for soluble N-ethylmaleimide sensitive factor attachment protein receptor (SNARES), a family of proteins involved in membrane mediated transport events (Jahn *et al*., 2006). Indeed it has been suggested that autophagosome lysosome fusion is mediated by SNARE proteins: syntaxin 17, SNAP-29 and VAMP8 or VAMP7 (Shen and Mizushima, 2014, Itakura and Mizushima, 2013, Mizushima, 2014).

1.5.3. Autophagy in the skin

Recent studies have suggested a role for autophagy in skin homeostasis. Results demonstrate autophagy is involved in keratinocyte differentiation and may be used as a signal initiating keratinocyte commitment to differentiation *in vitro* (Aymard *et al*., 2011). However, mice studies performed by Rossiter *et al* (2013) found autophagy was most likely to be involved in the later stages of differentiation and although autophagy was present in the epidermis and mutant mice had increased corneocytes, it was not essential for barrier function. Autophagy may also have a role in determining skin colour. Differences in skin colour are due to the presence of melanin in the epidermis and the amount of melanosomes produced in melanocytes, which are then transferred into keratinocytes (Murase *et al*., 2013). Using keratinocytes derived from both Caucasian and African American skin, Murase *et al* (2013) found autophagy to be responsible for the degradation and subsequent

reduction of melanosomes in different skin types. Therefore, the level autophagy and level of reduction determining the skin colour, for example in Caucasian skin autophagic activity was higher.

Interestingly, a recent study in monolayer primary human keratinocytes, explants and mouse tissue has explored autophagy marker expression in developing epidermis and again found autophagy plays an integral role in epidermal differentiation. Autophagy was found to be constitutively active in the granular layer and likely mediated by epidermal MTORC1 (Akinduro *et al*., 2016). Of note, in human psoriatic skin biopsies LC3 marker expression was found to be reduced, suggesting autophagy was impaired and could potentially be targeted therapeutically to restore epidermal barrier function (Akinduro *et al*., 2016).

1.5.4. Cell death and autophagy

Caspases are cysteine proteases and have long been associated with cell death, particularly apoptosis. There are 12-13 distinct caspases coded for in the human genome with at least seven contributing to cell death, and others being involved in processes such as inflammation (Kroemer and Martin, 2005). In terms of apoptosis, these seven caspases can be split into initiators or effectors, all of which begin as pro-enzymes and require activation (Kroemer and Martin, 2005).

In some cases, as hypothesised in the preceding PhD project, (Forrester thesis) caspase-independent cell death can occur. An example of this is autophagy, although primarily thought of as a cell survival mechanism; it can be associated with cell death. This was demonstrated in work on mouse embryonic fibroblasts, lacking pro-apoptotic BAX and BAK (Wei *et al*., 2001). Even though the cells were resistant to apoptosis, when dosed with apoptosis inducing agents cell death still occurred. The cells had increased autophagic vacuoles as well as increased levels of ATG proteins and therefore autophagic cell death was thought to be involved (Wei *et al*., 2001). Autophagic vacuoles are also linked with degenerating neurons in Alzheimer's and Parkinson's disease and it is hypothesised that autophagy is involved with cell death during neurodegeneration (Anglade *et al*., 1997).

Autophagic cell death still remains relatively controversial and indeed cells often display both apoptotic and autophagic markers. Many researchers believe that although large scale autophagy can occur, it is unlikely the cell dies through excessive autophagy alone and cross talk with apoptosis has been well documented (Kroemer and Levine, 2008). However, the Cell Death Committee defines autophagic cell death as death, which can be rescued by the inhibition of autophagy, by knockdown of two or more autophagy genes. Even if autophagy markers such as LC3 upregulation or P62 degradation are present, if the cell death is not blocked by autophagy inhibition, it is not autophagic cell death (Galluzzi *et al*., 2012).

1.6. Apoptosis

The term “apoptosis” was first used in 1972 by Kerr, Wyllie and Currie to describe a form of cell death with distinct morphological features (Elmore, 2007, Kerr, Wyllie and Currie, 1972). Since then, apoptosis has been recognised as a specific form of programmed cell death (PCD), resulting in the elimination of cells. Apoptosis is required for a variety of biological systems including homeostasis, particularly in developing tissues and organs in which the balance between cell division and PCD is crucial to maintain appropriate cell numbers and tissue turnover (Fuchs and Steller, 2015). However, apoptosis can also act as a protective mechanism or “quality control” in which infected or damaged cells are eliminated if they have irreparable DNA damage or disrupted cell cycle for example. Inappropriate apoptosis i.e. too little or too much has also been implicated in diseases such as Parkinsons disease (Venderova and Park, 2012) Alzheimers disease (Shimohama, 2000) as well as many cancers (Wong, 2011). Apoptosis is characterised by specific morphological changes to the cell, identified by light and electron microscopy, including cell shrinkage, nuclear condensation/fragmentation and membrane blebbing (Ouyang *et al*., 2012, Hacker, 2000). Pyknosis, or chromatin condensation is the most distinguishing feature of apoptosis (Elmore, 2007). Key biochemical changes also occur, namely degradation of DNA by endogenous DNases producing double-stranded DNA fragments but also protein cleavage and cross-linking (Saraste, 2000). Another key feature of apoptosis, distinguishing it from other forms of cell death such as necrosis, is that apoptotic cells are quickly phagocytosed and degraded within

phagolysosomes. Therefore, apoptotic cells do not release their cellular contents into the surrounding tissue and there is no inflammatory response (Savill and Fadok, 2000). Although sometimes difficult to distinguish between, unlike necrosis, apoptosis is a controlled form of PCD, is energy-dependent and does not affect large fields of cells (Elmore, 2007).

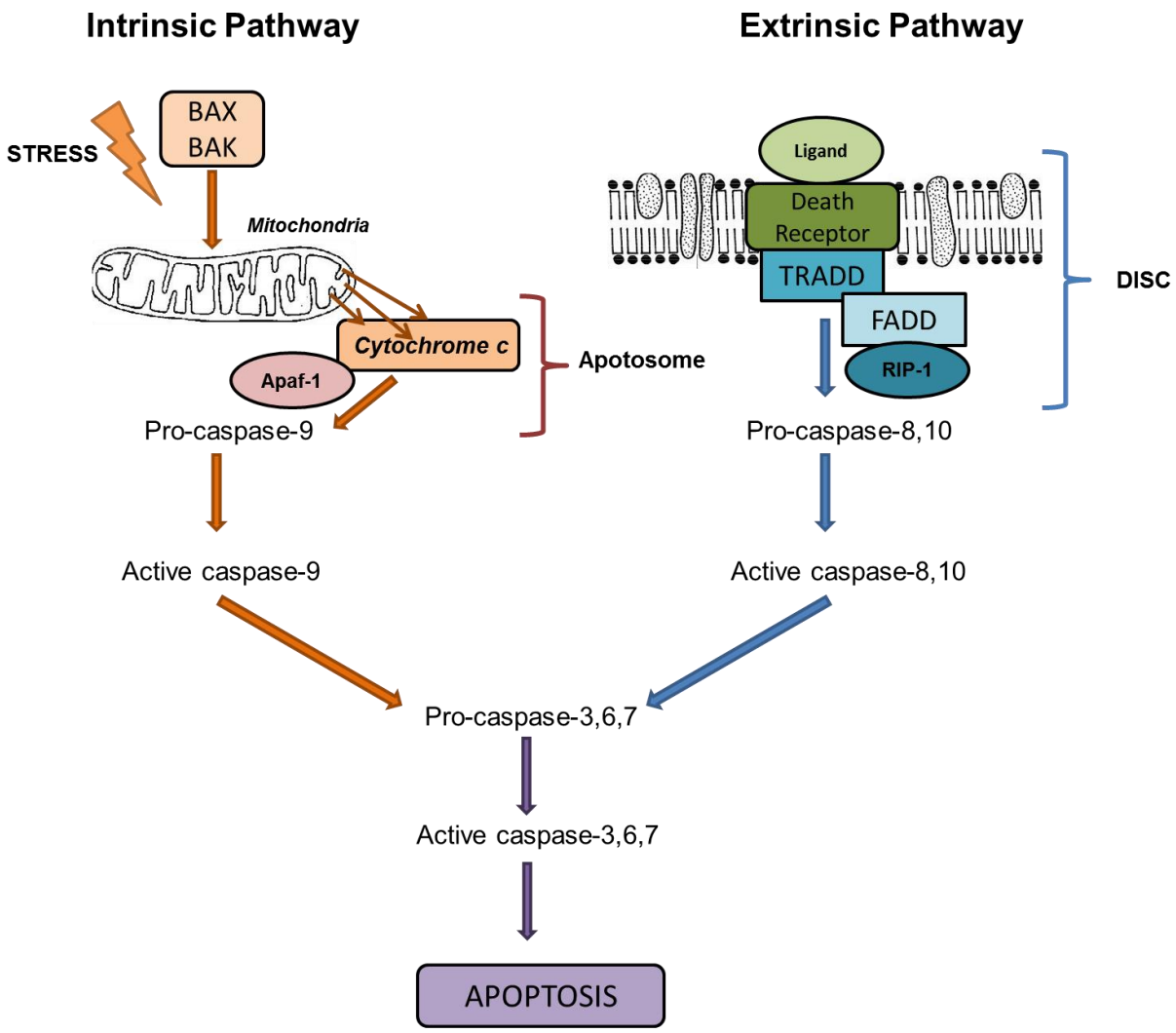

Figure 1.6 Regulation of apoptosis.

Schematic depicting the intrinsic (mitochondrial) pathway of apoptosis involving the formation of apotosomes and activation of pro-caspase 9. Schematic also depicts the extrinsic pathway of apoptosis, in this example involving TRADD (TNF receptor associated death domain) and activation of pro-caspase 8 or 10. Eventually both pathways converge and activate pro-caspase 3,6 or 7 which is then activated and induces apoptosis.

1.6.1. Regulation of apoptosis

Activation and completion of apoptotic cell death requires a complex cascade of molecular events involving a variety of cysteinyl aspartate proteases, or caspases. There are two main apoptotic pathways, the intrinsic (mitochondrial) pathway or extrinsic (death receptor) pathway, eventually however, both pathways result in the cleavage of caspase-3 and subsequent initiation of an execution pathway (Elmore, 2007) (Fig 1.6). This induces the previously defined morphological and biochemical changes to the target cell and subsequent phagocytosis.

The extrinsic pathway involves transmembrane receptor-mediated interactions, initiated when ligands bind to death receptors present on the cell surface. These death receptors are often members of the tumour necrosis factor (TNF) receptor gene superfamily (Elmore, 2007, Locksley *et al*., 2001) and have a cysteine rich extracellular domain and a cytoplasmic “death domain” allowing transmission of a death signal from the cell surface (Ashkenazi and Dixit, 1998). One of the more well-known death receptors is TNFR1 (TNF receptor 1) and corresponding ligand, TNF-α (Wong, 2011). Briefly, upon ligand binding, intracellular adaptor proteins are recruited for example, in the case of TNFR, the adaptor protein TRADD (TNF receptor-associated death domain) FADD (Fas-associated death domain protein) and RIP1 (receptor-interacting protein 1) are recruited. The ligand-receptor-adaptor protein complex is known as the death inducing signalling complex (DISC) which can then activate pro-caspase-8 (Wong, 2011, Kischkel *et al*., 1995). Activated caspase-8 then initiates the execution phase of apoptosis by cleaving other downstream caspases (Wong, 2011).

The intrinsic or mitochondrial pathway, involves a variety of non-receptor mediated stimuli, such as irreversible genetic damage, growth-factor deprivation or hypoxia, which produce intracellular signals that can act on targets within the cell (Elmore, 2007). This results in the opening of the mitochondrial permeability transition pore (MPT) as well as loss of mitochondrial potential. This increased permeability of mitochondria allows pro-apoptotic molecules to be released into the cytosol and subsequent activation of caspases (Saelens *et al*., 2004). Pro-apoptotic molecules are divided into two groups. The first group includes cytochrome *c* which activates the caspase-dependent mitochondrial pathway by binding and activating Apaf-1

(apoptosis protein-activating factor-1) and pro-caspase-9, which in turn activates caspase-9 in an ATP dependent manner (Chinnaiyan, 1999, Elmore, 2007). The second group contains pro-apoptotic markers which are released much later from the mitochondria, when the cell is already committed to die. This group includes AIF (apoptosis inducing factor) Endonuclease G and CAD (Caspase activated DNase) (Elmore, 2007).

Apoptotic mitochondrial events can also be controlled or regulated by members of the Bcl-2 (B cell lymphoma-2) family. These can be pro-apoptotic, e.g. BAX and BAK which induce permeabilisation of the mitochondria, allowing release of pro-apoptotic molecules such as cytochrome *c* (Youle and Strasser, 2008). This release of pro-apoptotic proteins sequestered between the outer and inner mitochondrial membranes is known as MOMP (mitochondrial outer membrane permeabilisation) (Chipuk and Green, 2008). Anti-apoptotic members e.g. BCL-W generally have four domains similar in sequence (BH1 to BH4) and are thought to inhibit BAX and BAK (Cory and Adams, 2002, Youle and Strasser, 2008). There is also a third class of BH3-only proteins e.g. BAD and BIK which have a conserved BH3 domain and are able to bind and regulate the anti-apoptotic Bcl-2 proteins to promote apoptosis (Youle and Strasser, 2008.)

However, regardless of which pathway is activated, both the extrinsic and intrinsic pathway activates the execution phase of apoptosis. In this phase, a series of effector caspases including caspase-3, caspase-6 and caspase-7 are activated and subsequently cause the morphological and biochemical changes described in section 1.6, by cleaving proteins involved in nuclear membrane and cytoskeletal structure, DNA repair, and replication systems (Slee *et al*., 2001, Elmore, 2007, Raj *et al*., 2006). Caspase-3 is considered to be the most important, as any initiator caspase can activate it including caspase-8 (extrinsic pathway) caspase-9 (intrinsic pathway) or caspase-10.

1.6.2. Apoptosis in skin

Apoptosis is essential for organ development and tissue turnover and as such, plays a role in skin, maintaining epidermal thickness and eliminating pre-malignant cells

(Raj *et al*., 2006). As described in section 1.1.2 epidermal keratinocytes undergo cornification, a unique form of terminal differentiation and programmed cell death, resulting in the formation of the outermost skin barrier (Eckhart *et al*., 2013). In contrast to normal homeostasis, in keratinocyte cornification, dead cells are not removed and instead play a vital role and function. There are similarities between apoptosis and cornification at both the molecular and cellular level such as loss of an intact nucleus, changes to the cytoskeleton and involvement of mitochondrial events (Lippens *et al*., 2005). In addition, proteins such as cathepsins are implicated in both apoptosis and epidermal differentiation. However, Lippens *et al* (2005) propose cornification does not involve apoptosis and although caspases are expressed in the epidermis, there is a lack of evidence to show pro-apoptotic caspases are required for normal skin formation (Lippens *et al*., 2000). In contrast, Allombert-Blaise *et al* (2003) suggest epidermal differentiation involves apoptotic cell death machinery. The study reported mitochondrial membrane potential decreased in calcium differentiated normal human keratinocytes and HaCaT cells, as seen in apoptosis. In addition, although it did not coincide with immediate apoptosis, cytochrome *c* was also released during epidermal maturation and interestingly; treatment with the general caspase inhibitor zVAD^{fmk} prevented the formation of a normal stratum corneum in an *in vivo* skin equivalent model (Allombert-Blaise *et al*., 2003).

A variety of agents have been shown to induce apoptosis in the skin, one of most well researched being UV irradiation. The most well studied is UVB (wavelength of 290-320nm) due to its physiological relevance and ability to induce DNA damage and mutations which could lead to malignancy (Ananthaswamy and Pierceall, 1990). Numerous studies have shown UVB irradiation induces release of cytochrome *c*, activation of caspases and mitochondrial depolarisation in keratinocytes, leading to the induction of apoptosis (Raj *et al*., 2006). Indeed, apoptosis induction by UV irradiation is thought to be a cellular repair mechanism to eliminate cells with irreparable DNA damage and as such research to gain further understanding is desirable (Takasawa *et al*., 2005). Interestingly, a study in HaCaT cells demonstrated the differences between apoptotic pathways induced by UVB and UVC irradiation. Whilst apoptotic cells appeared after only 8 hours after UVB irradiation, in UVC irradiated cells, apoptosis did not occur until much later. Furthermore, caspase-8 activation only occurred in UVB irradiated cells whilst UVC irradiated cells induced much greater release of pro-apoptotic markers cytochrome *c* and Smac/DIABLO as

well as activation of caspase-9 (Takasawa *et al*., 2005). Consequently, Takasawa *et al* (2005) suggests UVB irradiation induces both the intrinsic and extrinsic apoptotic pathways whilst UVC induced apoptosis only via the intrinsic pathway.

1.7. Cathepsins

Cathepsins can be divided into two categories: aspartic proteases such as cathepsin D and E and cysteine cathepsins of which there are 11 known in human. Of these, cathepsins B, C, H and L are ubiquitously expressed but others show more regulated expression (Repnik *et al*., 2012). Most cathepsins are endo-peptidases, initiating digestion at non-terminal peptide bonds, although cathepsins X and C are exo-peptidases, initiating digestion at terminal peptide bonds of the molecule, whilst cathepsin B and H use both actions (Repnik *et al*., 2012). Cathepsins have broad specificity, are generally stable and function well at acidic pH (Repnik *et al*., 2012). Although cathepsins have been implicated in a variety of pathologies and physiological functions, this project focuses primarily on their role in autophagy (section 1.5) skin homeostasis (sections 1.7.2) and apoptosis after lysosomal membrane permeabilisation (section 1.8).

1.7.1. Cathepsin D

Cathepsin D, a focus of this project, is normally found within lysosomes and synthesised as a pro-enzyme, pro-cathepsin D (52kDa) which matures after proteolytic cleavage into an intermediate active enzyme (48kDa). This then forms a mature active form, consisting of heavy (34kDa) and light (14kDa) chains linked by non-covalent bonds (Benes *et al*., 2008). Cathepsin D has a GC rich motif in the promoter region to which Sp1, a basal transcription factor, can bind (Wang *et al*., 1999). It also has a core sequence of a XRE to which the AhR/ARNT complex binds and both Sp1 and AhR are needed for maximal basal activity (Wang *et al*., 1999).

1.7.2. Cathepsins in skin

Cathepsins have also been implicated in epidermal differentiation and skin. For example, studies in rat keratinocytes, demonstrated expression of cathepsins B, H and L increased when keratinocytes were calcium differentiated (Tanabe *et al*., 1991). Similarly, cathepsin L activity has also been found to increase after 1-2 days then decrease again as differentiation progresses. Through studies with cathepsin L knockout mice, cathepsin L has also been implicated as an important regulator of keratinocyte and melanocyte differentiation during hair follicle morphogenesis (Tobin *et al*., 2002). Indeed, knockout mice had several abnormalities including, defective terminal differentiation of keratinocytes during the formation of the hair canal, abnormal hair cycling and disrupted exiting of hair shafts to the skin surface (Tobin *et al*., 2002). Furthermore, cathepsin K, known for its role in degrading collagen, is expressed in scarred skin and keloids, but not normal skin (Runger *et al.,* 2007). In contrast, work with cultured fibroblasts found cathepsin K to be highly expressed and co-localisation studies with LAMP1, found cathepsin K to be associated with lysosomes in which exogenous collagen I and collagen IV was internalised (Quintanillla-Dieck *et al*., 2009). Finally, in a clinical trial evaluating the efficacy and safety of the cathepsin K inhibitor balicatib for osteoporosis, one patient developed scleroderma with morphea lesions developing 9 months after beginning the trial (Peroni *et al*., 2008) again suggesting cathepsin activity can influence epidermal differentiation and regulation.

However, of interest to this project, cathepsin D has also been found to have a role in regulation and activation of transglutaminase 1 (TGM-1) (Egberts *et al*., 2004). Treatment with cathepsin D increased activity of TGM-1, an important cellular component involved in crosslinking of proteins in the cornified envelope. When pepstatin A was used to inhibit cathepsin D, TGM-1 activity decreased (Egberts *et al*., 2004). In addition, cathepsin D knockout mice have been found to have reduced TGM-1 and cornified envelope proteins such as filaggrin and involucrin as well as a skin phenotype similar to that of the disease lamellar ichthyosis (Egberts *et al*., 2004).

1.8. Lysosomes and LMP

Lysosomes are single membraned, digestive organelles present in the cytoplasm of almost all eukaryotic cells (Shen and Mizushima, 2014). Within the lysosome are more than 50 acid hydrolases, including lipases, nucleases and phosphotases specific for degradation of a range of macromolecule targets (Mindell, 2012, Eskelinen, 2006). These targets may be extracellular material captured by phagocytosis or endocytosis, or derived from the cell itself through autophagy (Gomez-Sintes *et al*., 2016). A key feature of a lysosome, therefore, is its acidic environment (pH 4.5-5.0) to maintain optimum enzymatic activity (Shen and Mizushima, 2014).

The lysosomal membrane, a single phospholipid bilayer, mediates a variety of functions including fusion with other organelles and controlling the passage of material into the lysosomal lumen (Saftig *et al*., 2010).

The membrane contains over 20 lysosomal membrane glycoproteins. One of the most important being the vacuolar type H(+)-ATPases (V-ATPases) which uses ATP to pump protons into the lumen of the lysosome and help create an acidic environment (Mindell, 2012). In addition, LAMP1 and LAMP2 (lysosome associated membrane protein 1 and 2) make up approximately 50% of all lysosomal membrane proteins (Saftig *et al*., 2010). *In vivo* studies suggest both proteins have a similar function as mice are viable after LAMP1 or LAMP2 knockout, but double knockout is embryonic lethal (Eskelinen, 2006). However, LAMP1 and LAMP2 only have 37% amino acid homology, and studies have found the phenotype in LAMP2 deficient mice is far more severe than LAMP1 knockout alone. LAMP2 also undergoes alternative splicing, forming LAMP2 A, B and C isoforms, which show specific tissue expression and function (Lichter-Konecki *et al*., 1999, Eskelinen, 2006).

Interestingly, lysosomes are now considered a significant component of cell death machinery. Lysosomal membrane permeabilisation (LMP) in which the contents of the lysosome, including cathepsins, are leaked into the cytosol initiating degradation of cellular components, can induce cell death. The extent of LMP determines the morphological features of cell death (Aits and Jaattela 2013). Complete disruption of

the lysosome provokes uncontrolled death by necrosis, which cannot be attenuated by treatment with inhibitors of lysosomal hydrolases.

In contrast, partial or selective LMP induces the intrinsic pathway of apoptosis (Boya and Kroemer, 2008, Kagedal *et al*., 2001). This apoptotic cell death is activated through MOMP (as described in section 1.6.1) and can be attenuated using cathepsin inhibitors, primarily against cathepsin B and D. Therefore, cathepsins are thought to be the main executors (Gomez-Sintes *et al*., 2016). Destabilisation of lysosomes and subsequent pore formation allowing for cathepsin release, can be induced by a range of stimuli including lysomotropic agents such as hydroxychloroquine and antibiotics (Boya *et al*., 2003) DNA damage (Emert-Sedlak *et al*., 2005) and reactive oxygen species (ROS) (Castino *et al*., 2007).

Interestingly, LMP has been shown to be regulated by proteins of the Bcl-2 family, also involved in apoptosis regulation. In particular, studies have demonstrated the pro-apoptotic BAX translocates to the lysosomal membrane after treatment rather than mitochondrial membrane, inducing LMP and cathepsin dependent cell death (Bove *et al*., 2014, Gomez-Sintes *et al*., 2016). Furthermore, cathepsins have been shown to induce cleavage of pro-apoptotic BID, which promotes translocation of Bax and Bak to the mitochondria inducing MMP and caspase-dependent cell death a (Droga-Mazovec *et al*., 2008, Gomez-Sintes *et al*., 2016). Together these demonstrate the complex crosstalk and overlap between cell deaths pathways.

1.9. Aims

The overall theme of this project was to increase understanding of the mechanism behind the TCDD-induced chloracne phenotype, whilst also further delineating the physiological role of AhR in the skin.

Preliminary work with the chloracne phenotype model (Forrester Thesis) revealed TCDD induced a significant reduction in viable cell layer thickness and compacted stratum corneum. Results also suggested TCDD treatment altered differentiation marker expression and induced autophagic activity. In addition, Ingenuity Pathway Analysis (IPA) revealed a link between cathepsin D and AhR (as described in section 1.7.1) and subsequent studies revealed cathepsin D expression was increased by AhR activity.

Therefore, the main focus of this research was to explore the mechanisms underlying TCDD induced morphological changes in an optimised epidermal equivalent model. Specific aims were to:

1. Reproduce a robust and reliable chloracne phenotype model using epidermal skin equivalents and consider the effect of TCDD treatment over time.
2. Explore the possible induction of apoptosis or caspase-dependent cell death after TCDD treatment
3. Investigate the hypothesis of TCDD-induced autophagy activity and autophagy regulated effects on epidermal differentiation, AhR expression and apoptosis.
4. Investigate the role of lysosomal function, specifically cathepsin D in epidermal differentiation, AhR expression and apoptosis.

Chapter 2 Materials and Methods

2.1. Laboratory work and reagents

All laboratory work was carried out in accordance with Newcastle University health and safety regulations and when necessary, in containment level two hoods under sterile conditions. Unless otherwise stated, reagents were purchased from Sigma Aldrich, UK and prepared according to manufacturer's instruction.

2.2. Tissue samples

Healthy adult foreskin tissue samples were obtained after informed consent from patients undergoing surgery and used to culture keratinocytes (Todd and Reynolds, 1998). Immediately after removal, skin samples were placed in keratinocyte growth media (MCDB 153) supplemented with 2% penicillin streptomycin amphotericin B (PSA) (Lonza biologics, UK) and stored at 4°C until collection. Ethical approval for this has been granted by Newcastle and North Tyneside research ethics committee (Ref 08/H0906/95+5_Lovat). This PhD project was funded by both BBSRC and AstraZeneca.

2.2.1. Primary cell culture

Upon arrival, foreskin samples were logged and washed in a Corning 10cm sterile petri dish (SLS, UK) with phosphate buffered saline (PBS) to remove any residual blood. Excess subcutaneous tissue, fat and blood vessels were then removed with sterile forceps and scissors. Using a scalpel, a grid pattern was cut into the epidermis to allow penetration of dispase II (Roche Diagnostics Ltd, UK) before the sample was placed in dispase II in PBS (0.2%) and 10% PSA solution and stored at 4°C overnight. The following day, the epidermis was removed from the dermis and placed into a universal tube containing 0.05% trypsin/EDTA (Lonza, UK) and incubated in the water bath at 37°C for 5 minutes. The trypsin was then neutralised with Dulbecco's Modified Eagle's Medium (DMEM) (Lonza, UK) media supplemented with 10% Fetal Bovine Serum (FBS) (DMEM/FBS) and centrifuged at 3000G for 5 minutes. The supernatant was removed, and the pellet re-suspended in 18-20ml of

MCDB 153 medium or Epilife (Life Technologies, UK) both of which were supplemented with 1% PSA and 1% human keratinocyte growth supplements (HKGS) (Life Technologies, UK) and placed into a T175 tissue culture flask. After 24 hours, any excess epidermis was removed and the media replaced with fresh. Cells were incubated at 37°C in a humidified atmosphere of 5% carbon dioxide in air and the media replaced with fresh media every 2-3 days.

Whilst the majority of experiments were carried out in MCDB 153 media, epidermal equivalents were cultured in Epilife, however, both mediums provided a complete culture environment for primary keratinocytes and equally as effective.

2.2.2. Cell passaging of primary keratinocytes

At 70% confluence primary keratinocytes were passaged, to prevent epidermal differentiation. Old media was removed and the cells washed with PBS before adding 5ml trypsin/EDTA (Lonza, UK) and incubation at 37°C for 5 minutes to allow the cells to detach and neutralisation of the trypsin/EDTA by addition of 10mls of DMEM/FBS. Cells were then pelleted by centrifugation for 5 minutes 3000g, the supernatant removed and the cell pellet re-suspended in complete Epilife or MCDB 153. Primary keratinocytes were then subsequently reseeded at a 1/3 of the original cell number, approximately 1 million cells per T175 in 20mls of media and cultured up to a maximum of 4 passages. Alternatively, cells were counted using a haemocytometer and seeded for monolayer experiments. Monolayer experiments were generally either conducted in 6 well plates in which 100,000 cells/well were seeded in 2ml of media, or 48 well plates in which 10,000 cells/well were seeded in 500µl of media, and treated for 5 days unless otherwise stated. Primary human keratinocytes were also seeded in to epidermal skin equivalent models (see section 2.4)

2.2.3. Cell passaging of HEK293T cells

The transformed human embryonic kidney (HEK) 293 cell line originates from 1973 (Graham *et al*., 1977) and is widely used in cell biology. The HEK293T cell line is a derivative of the HEK293 cell line and often used for viral packaging due the addition

of a temperature sensitive allele of SV40 T antigen. This allows amplification of vectors carrying the SV40 region of replication and subsequently increases expression when transiently transfected (Lin *et al*., 2014). Cells were cultured in DMEM media supplemented with 10% FBS (DMEM/FBS) and 1% PSA and incubated at 37°C in a humidified atmosphere of 5% carbon dioxide in air. Media was replaced with fresh every 2-3 days and at 80% confluence cells were passaged as described above (section 2.2.2). Cells were subsequently re-seeded into T175 flasks at 1/3 of the original density in 20ml of media. Alternatively, cells were seeded into sterile 10cm petri dishes in which 250,000 cells were seeded into 10ml of media. HEK293T cells were cultured up to 20 passages and frozen stocks were stored in liquid nitrogen in 10% DMSO (Fisher Scientific, UK) and 90% FBS.

2.3. Treatments with chemical agents

In experiments with monolayer primary keratinocytes, cells were seeded appropriately (see section 2.2.2) into 6 well plates or 48 well plates and allowed to attach overnight prior to treatment. Epidermal skin equivalents were seeded and cultured for a minimum of 12 days before treatment (see section 2.4). In all experiments, treatment was every 48 hours for up to 7 days in either complete MCDB 153 or Epilife media.

The dioxin 2,3,7,8-Tetrachlorodibanzo-*p*-dioxin (TCDD) (Supelco, Sigma Aldrich, UK) was diluted in dimethylsulfoxide (DMSO) to a concentration of 10µM in the fume hood and kept at room temperature in the poisons cupboard. The final concentration in all experiments was 10nM TCDD unless otherwise stated. Control monolayer cells or epidermal skin equivalents were all treated with the same dilution of DMSO, 1:1000.

The autophagy and lysosomal inhibitor bafilomycin A1 was dissolved in DMSO to a stock solution of 10µM and stored at -20°C in aliquots. The final concentration in all experiments was 5nM and treatment was throughout the time course.

Cathepsin D inhibitor pepstatin A was dissolved in DMSO to a stock solution of 10mg/ml and stored at -20°C in aliquots. The final concentration used in all experiments was 10µg/ml and treatment was throughout the time course.

In differentiated monolayer primary keratinocyte experiments, cells were seeded into 6 well plates (100,000cells/well) in complete MCDB 153 and allowed to attach overnight. The following day, media was replaced with high calcium MCDB 153 to induce differentiation. For this, complete MDCB 153 media was supplemented with 1mol/L calcium chloride ($CaCl_2$) (BDH laboratory supplies, UK), 70µl of $CaCl_2$ was added to 50ml of complete MCDB 153 media to give a final concentration of 1.3mM calcium. Cells were differentiated for 5 days whilst being treated appropriately.

2.4. Epidermal Equivalents

To produce epidermal equivalents, primary keratinocytes were initially seeded (0.5-1 $x10^6$ cells/insert) onto 12mm diameter; 0.4uM Millicell inserts (Millipore, Ireland) in a 6 well plate and cultured overnight in 2ml Epilife containing 1.5mM $CaCl_2$ (high calcium Epilife). Subsequently, epidermal equivalents were raised to the air/liquid interface by removing media from inside the insert and replacing the media on the outside with high calcium Epilife supplemented with vitamin C (5µg/ml). Epidermal equivalents were then incubated at 37°C for 12 days and media outside the insert replaced every other day with fresh high calcium Epilife supplemented with vitamin C. At day 12 post seeding, the epidermal equivalents, then completely differentiated, were subjected to treatment with chemical agents as described within each experiment every 48 hours for up to 7 days, with control epidermal equivalents treated with vehicle (DMSO) at a concentration of 1:1000.

At the end of each treatment period, epidermal equivalents were harvested by removal of the media in each supporting well, washing twice with PBS and cutting around the insert using a sterile scalpel before washing the epidermal equivalent again in PBS. Each epidermal equivalent was then cut into 4 sections.

For immunohistology and haemotoxylin and eosin (H&E) staining, sections were placed into 4% paraformaldehyde (100µl of 37-40% paraformaldehyde in 900µl PBS) and left overnight at 4°C to become formalin fixed. The following day, samples were washed in PBS and placed into histology cassettes then processed and embedded in paraffin by Cellular Pathology, Royal Victoria Infirmary, Newcastle upon Tyne. H&E was then performed (as described in section 2.4.2).

For immunofluorescent staining (as described in section 2.6) sections were mounted in OCT (Thermo Scientific) over liquid nitrogen onto cork discs (VWR, UK) and stored at -80°C until required.

Epidermal equivalents sections were also snap frozen in Eppendorf tubes in liquid nitrogen and used for RNA extraction for subsequent qPCR experiments (as described in section 2.8) or protein extraction for subsequent immunoblotting (as described in section 2.5)

2.4.1. H&E staining of Epidermal Skin Equivalents

After fixation (as described in section 2.4) the formalin fixed paraffin embedded (FFPE) samples were sectioned (4µm) using a microtome and baked onto SuperFrost Plus slides (VWR, UK) overnight at 60°C. Sections were then stained with H&E (both stains purchased from Pioneer Research Chemicals Limited, UK). Briefly, excess paraffin was removed by immersion of sections in histoclear (AGTC Bioproducts, UK) for 20 minutes at room temperature. Sections were then dehydrated in ethanol and submerged in haemotoxylin (5 seconds), and rinsed well in tap water (10 minutes) then submerged into eosin for 5 seconds and rinsed in tap water. Sections were then de-hydrated in ethanol and cleaned in histoclear before being mounted with a glass coverslip using DPX hard mount (Thermo Scientific, UK). Images of the sections were captured at 20x magnification using a Zeiss Axioimager microscope (Carl Zeiss Ltd, UK) and with measurements of the viable cell layer obtained using Image J Software (National Institutes of Health, USA). For each experiment 6 measurements were taken, spread evenly throughout each 20x H&E image of an epidermal equivalent, and data expressed as the mean viable cell layer thickness, relative to vehicle (DMSO) control ±SEM.

2.5. Immunoblotting

Following 48 hours after the final treatment of monolayer primary keratinocytes seeded in 6 well plates, cells were lysed for protein. Whilst on ice, media was removed; each well washed with 2ml ice-cold PBS and then 120µl/well of RIPA lysis

buffer was added. RIPA lysis buffer was supplemented with 10µl of 100x phosphatase inhibitor cocktail, 10µl 100xprotease inhibitor cocktail, and 10µl of EDTA was added per ml. Using a cell scraper cells were collected into Eppendorf tubes and vortexed for 5 seconds then sonicated using a probe sonnicator (Soniprep 150, MSE) for 3 x 5 seconds. Samples were then centrifuged at 4°C at 16000g for 5 minutes.

Conversely, epidermal equivalents were lysed in urea lysis buffer to solubilise the cytoskeleton. Per epidermal skin equivalent section, 120µl of urea lysis buffer was added (8M urea, 50mM Tris-HCL pH 8.0, 1mM NaF, 1mM Na_3VO_4, 1mM PMSF, 0.25% SDS and 1x complete EDTA containing protease inhibitor cocktail) prior to vortexing to remove the polycarbonate membrane and sonication for 3x5 seconds (as described above) then centrifugation for 5 minutes at 4°C at 16000g.

Both monolayer and epidermal equivalent protein concentrations were determined using a BCA protein assay kit (Pierce, UK) according to manufacturer's instructions before proteins were separated through a NuPage gel electrophoresis system (Life Technologies, UK). Protein samples (60µg where possible) were combined with LDS sample buffer (4X) containing lithium dodecyl sulfate at a pH of 8.4 to help denature the protein, as well as reducing agent (10X) containing 500 mM dithiothreitol (DTT) to reduce the protein. The ratio of 6.5:2.5:1, protein: LDS: reducing agent was maintained for all experiments. Samples were then incubated at 70°C in a heat block for 10 minutes and stored in -20°C freezer until required.

Samples were then defrosted at room temperature, incubated at 70°C for 10 minutes and briefly centrifuged in a microfuge, before proteins were separated through 4-12% NOVEX Bis-Tris pre-cast gels (Life technologies, UK). In all experiments, 10-20µg protein was loaded and samples run in NuPAGE MES/SDS running buffer with 500µl/L of NuPAGE antioxidant added. Proteins were then transferred onto nitrocellulose membrane (GE Healthcare Lifesciences) using a BioRad mini-Trans Blot system with NuPAGE transfer buffer (cat number NP0006-1).

Membranes were then blocked in TBS-T (Tris-Base, NaCl, pH 7.6 and Tween-20 (Fisher Scientific, UK) 1ml/L) containing 5% skimmed milk for 1 hour at room temperature. Following 3 X 5 minute washes in TBS-T, membranes were incubated with primary antibodies overnight at 4°C, diluted as detailed in Table 1. Following 3 X 5 minute washes in TBS-T membranes were then incubated with appropriate hydrogen-peroxidase secondary antibody (Vectorlabs, UK), again as described in

Table 1 prior to 3 X 5 minute washes and detection of primary antibody expression using an ECL plus kit (Amersham GE healthcare) according to manufacturer's instructions. Imaging was carried out using a phosphoimager (Fujifilm FLA-3000) or Licor Odyssey FC system and with densitometry carried out using ImageJ software or Image Studio software (version 5.0) to quantify protein expression relative to GAPDH loading control.

Table 1 Summary of antibodies and respective incubation conditions used for immunoblotting

Protein	Manufacturer and item number	Primary conditions in TBS-T	Secondary conditions in TBS-T	Weight (kDa)
AhR Rabbit polyclonal	SantaCruz #sc-5579	1:1000 in 5% milk O/N 4°C	1:2000 in 5% milk 1 hour at RT	95
LC3 Rabbit polyclonal	Cell signalling #2775	1:2000 in 5% BSA O/N 4°C	1:2000 in 5% milk 1 hour at RT	LC3I = 18 LC3II = 16
CTSD Rabbit polyclonal	Calbiochem #219361	1:4000 in 5% milk O/N 4°C	1:2000 in 5% milk 1 hour at RT	Pre/pro = 54 Pro = 48 Active = 34
Loricrin Rabbit Polyclonal	Biolegend #905101	1:10000 in 5% BSA O/N at 4°C	1:5000 in 5% milk 1 hour at RT	38
ATG7 (APG7) Goat polyclonal	SantaCruz #sc-8668	1:2000 in 5% milk O/N at 4°C	1:2000 in 5% milk 1 hour at RT	71
Beclin-1 Mouse monoclonal	BD Bioscience #612112	1:1000 in 5% milk O/N at 4°C	1:4000 in 5% milk 1 hour at RT	60
GAPDH Mouse polyclonal	Chemicon international #MAB374	1:10000 in 5% BSA 1 hour at RT	1:5000 in 5% milk 30 minutes at RT	37

2.6. Immunofluorescence staining

Sections of OCT processed epidermal equivalents (4µm) were cut using a cryostat onto SuperFrost Ultra Plus slides (VWR, UK) and stored at -20°C until required. Upon staining, slides were defrosted at room temperature and washed with PBS for 1 minute to wash off excess OCT. A hydrophobic pen was used to mark the tissue area prior to fixation for 10 minutes in ice cold acetone, methanol, acetone/methanol or 4% paraformaldehyde at room temperature, depending on the optimised fixative method for each specific antibody. Sections were washed again with PBS and permiablised with 0.2% Triton-X-100 (Fisher Scientific, UK) for 10 minutes at room temperature. After washing 3 times with PBS containing 0.05% Tween 20 (Fisher Scientific, UK) (PBS-T) sections were then blocked in goat serum for 30 minutes (1:60) in PBS containing 2% BSA (PBS/BSA) before further washing in PBS-T and incubation with primary antibody or isotype control (dilution antibody dependent, as described in Table 2) for 1 hour at room temperature. Sections were subsequently washed again 3 times in PBS-T, blotted and then incubated with specific AlexaFluor® 568 secondary antibody (ThermoFisher Scientific, UK) (1:300 in PBS-BSA) with Hoechst nuclear stain (1:3000) (Life Technologies, UK) for 1 hour at room temperature in the dark. After 3 final washes with PBS-T, sections were then mounted with a glass cover slip using Mowiol mounting medium (consisting of glycerol, Mowiol 4-88, distilled water and 0.2M Tris buffer pH 8.5) and stored at 4°C in the dark. Image analysis was conducted by confocal microscopy using a Nikon A1 Upright microscope and with all images captured with a 20x objective and with 1.54 magnification and processed using Nikon Elements software. Tiled images of epidermal equivalents stained for caspase-3 or Ki67 were captured using a Zeiss Axioimager and images acquired at 10x magnification using Zen 2 Pro software (Zeiss, Germany). For quantification of immunofluorescent staining, image J was used to measure intensity of differentiation marker expression. One representative image per epidermal equivalent was used and data expressed relative to vehicle control, or siNT/shNT vehicle control in knockdown studies.

Table 2 Summary of antibodies used for immunofluorescence staining

Protein	Manufacturer and item number	Primary conditions in PBS-BSA
Filaggrin Mouse monoclonal	Novocastra #NCL-Filaggrin	1:50
Loricrin Rabbit Polyclonal	Biolegend #905101	1:200
CK10 Mouse monoclonal	Novocastra #NCL-CK10	1:200
P62 (SQSTM1) Mouse monoclonal	Santa Cruz #sc-28359	1:50
LC3 Rabbit polyclonal	Cell signalling #2775	1:100
Active Caspase-3 Mouse monoclonal	R&D Systems #MAB835	1:500
LAMP2 Mouse monoclonal	BD Biosciences #555803	1:200
Cathepsin D Mouse monoclonal	Abcam #ab6313	1:200
Ki67 (MIB-1) Mouse monoclonal	Dako #M724001-2	1:100

2.7. Cell viability assays

Both MTT (3-(4,5-dimethylthiazol-2-yl)-2,5-diphenyltetrazolium bromide) and SRB (sulfohodamine B) colorimetric assays were used as a measure of cell viability. Specifically, the SRB assay measures total cellular protein content based on the ability of SRB to bind to basic amino acid residues (Voigt *et al*., 2005). In contrast, the MTT assay, requires the reduction of yellow MTT to a purple formazan product by metabolically active and therefore, viable cells (Stockert *et al.,* 2012).

For both assays, primary human keratinocytes were seeded at a density of 10,000 cells per well into 48 well tissue culture plates (Corning, SLS, UK) in a volume of 500µl of complete MCDB 153 media before being left to attach over night at 37°C. Cells were then treated accordingly.

For commercial MTT assays, cell viability was assessed by the addition of 40µl of MTT in PBS (5mg/ml) to each well with continued incubation for 3.5 hours at 37°C prior to the removal of the MTT solution and the direct addition of 300µl/well of MTT solvent (4mM HCL and 0.1% Nondent P-40 in isopropanol). Following agitation, 150µl from each well, was placed into a 96 well plate and absorbance measured at 590nM using a SpectraMax 250 plate reader (Molecular Devices, UK).

For SRB assays, cell viability was assessed by removing media from each well and replacing with 200µl/well of freshly made 10% trichloracetic acid and incubating for 1 hour at 4°C. Plates were then washed 5 times by immersion in distilled water and allowed to air dry. Once dry, 200µl of 0.4% (W/V) SRB dissolved in 1% (V/V) glacial acetic acid was added to each well for 30 minutes at room temperature. Plates were then washed with 1% glacial acetic acid 5-10 times until all residual dye was removed and then dried at 60°C for 1 hour or at room temperature overnight. The protein bound SRB was then solubilised in 400µl of 10mM unbuffered Tris base (pH 10) and the plate agitated on an orbital shaker for 10 minutes before, as for MTT cell viability assays, 150µl of the solution was taken from each well into a 96 well plate and absorbance measured at 530nm using a SpectraMax 250 plate reader.

2.8. qPCR

2.8.1. RNA Extraction

Before any RNA work was carried out, the lab area was thoroughly cleaned and decontaminated with RNase ZAP (Thermo Fisher Scientific, UK). Additionally, all water used was nuclease-free.

RNA was extracted from epidermal equivalent samples using a ReliaPrep tissue kit (Promega, UK) following manufacturer's instructions with certain modifications. Epidermal equivalents were initially disrupted on ice using a pellet pestle in BL lysis buffer supplemented with 1% 1-Thioglycerol and all polycarbonate membranes removed. Samples were then centrifuged for 5 minutes at 14,000g to remove excess debris prior to RNA precipitation and purification according to the manufacturer's protocol. After an on-column DNase digestion (Promega, UK) step, RNA was initially eluted with 15µl of nuclease free water into PCR tubes with a second identical elution step to ensure collection of RNA. RNA concentration was then determined using a NanoDrop (NanoDrop 2000 Thermo Scientific, UK) and samples stored at -80°C prior to use.

2.8.2. Reverse Transcription

Preparation of cDNA from epidermal equivalents was carried out using a standardised amount of RNA in each reaction, random hexamers and dNTPs. Moloney murine leukaemia virus enzyme (MMLV), DTT (DL-Dithiothreitol) and buffers were then used in a 20µl reaction with the recombinant ribonuclease inhibitor, RNase OUT, according to manufacturer's instruction (all from Life Technologies, UK). Reverse transcription was carried out using standard PCR cycle conditions in an Applied Biosystems GeneAmp PCR system 9700 machine (Invitrogen, UK). cDNA was then diluted appropriately for gene expression qPCR assays.

2.8.3. Real time qPCR

Exon-spanning probe based assays were purchased from a variety of suppliers (Table 3) and consisted of two primers (forward and reverse) and a hydrolysis probe. Primers were used at 400nM and probes at 100nM. These were used in combination with GoTaq probe master mix according to manufacturer's instructions (Promega, UK). Total volume per reaction was reduced to 10µl and reaction mixes were sealed before being briefly centrifuged on a plate spinner. Subsequent PCR was performed using a StepOne plus qPCR machine (Life Technologies, UK) and standard PCR cycle conditions were used:

1. 50°C for 2 minutes
2. 95°C for 10 minutes
3. 95°C for 15 seconds
4. 60°C for 60 seconds
5. Plate read
6. Steps 3-5 were repeated 40 times

mRNA expression was determined through C_t (cycle threshold) value. C_t values are the relative measure of target per reaction, and defined as the number of PCR cycles needed to exceed background levels of the target, also known as the threshold. C_t values are inversely proportional to the amount of target nucleic acid in the sample; therefore, a lower C_t value means a greater amount of target nucleic acid is present.

Histone H4 expression was used as a validated housekeeping gene and the Delta-Delta C_t method was used for analysis (Livak and Schmittgen. 2001) without PCR efficiency correction. The difference between the two C_t values was expressed as fold change.

Table 3 qPCR targets and assay ID

Target	Assay ID
AhR	Hs.PT.56a.38998805 FAM/TAMRA (IDT, UK)
Cyp1a1	Hs.00153120_m1 FAM/NFQ (ThermoFisher Scientific, UK)
Loricrin	Hs.PT.58.27761511 FAM/TAMRA (IDT,UK)
CK10	Hs.PT.58.38635764 FAM/TAMRA (IDT, UK)
Filaggrin	Hs.PT.58.24292320 FAM/TAMRA (IDT, UK)
Involucrin	Universal Prove Library (UPL) Probe number 16 Cat number 04686896001 Roche Design Centre, UK
Histone H4	Forward: 5'- CAC CAC GCT TGG TCT TGC TC -3' Reverse: 5'- GCC AGC TGG GTT CCA ATC TT -3' Probe: CTC TAA GGG AGT TTC CCA CCC CCA GGG FAM/TAMRA (IDT, UK)

2.9. ShRNA Lentiviral knockdown in primary keratinocytes

For long term knock down, primary keratinocytes were transduced with short hair-pin (sh)RNA.

Glycerol stocks of competent *E.Coli* with lentiviral shRNA pGIPZ vectors for cathepsin D (CTSD) and BECLIN-1 (Open Biosystems) (Table 4) were purchased. Glycerol stocks of *E.Coli* previously transformed with shRNA packaging plasmid (*pCMVdeltaR*8.91) and envelope plasmid (*pMD*2.G) were already available in the lab. Each shRNA vector contained target shRNA, GFP and puromycin resistance genes under the control of a constitutive CMV promoter. As such, transduced keratinocytes could be identified using puromycin selection and green fluorescence in image analysis.

Initially, bacterial colonies were spread and grown on lysogeny broth (LB) agar plates with 50µg/ml ampicillin under standard sterile conditions. Single colonies were selected and expanded in LB broth at 37°C. Plasmid DNA was then purified using a hi-speed Maxi-Prep kit (Qiagen, UK) according to manufacturer's instructions.

Table 4 Lentiviral constructs purchased

Target	Construct known as	Catalogue Number/Sequence
Cathepsin D	CTSD (708)	V3LHS_382708 Mature Antisense AGTTCTTGAGCACCTCGGG
BECLIN-1	BEC-1 (3409)	V3LHS_349509 Mature Antisense TTTCTGCCACTATCTTGCG
	BEC-1 (3412)	V3LHS_349512 Mature Antisense AAAATTGTGAGGACACCCA
	BEC-1 (3414)	V3LHS_349514 Mature Antisense TCACTGTCATCCTCATTCA
	BEC-1 (3413)	V3LHS_349513 Mature Antisense TCCGTAAGGAACAAGTCGG
Non silencing	NT	RHS4346

The following sections outline the procedures including transfection into HEK293T cells and transduction of primary keratinocytes, all of which were adapted from the Trono laboratory, Switzerland (Klages *et al.,* 2000 and Naldini *et al.,* 1996).

2.9.1. Production of virus in HEK293T cells

HEK293T cells were cultured as described in section 2.2.3 and seeded at 250,000 cells per 10cm culture petri dishes in 10ml of complete DMEM/FBS and left to attach overnight at 37°C. Medium was then removed carefully and replaced with 10ml transfection media (DMEM/FBS no PSA). The HEK293T cells were then transfected using standardised calcium precipitation.

Briefly, a mixture containing 5µg of envelope plasmid, 15µg of packaging plasmid and 20µg of target shRNA plasmid, was mixed in a sterile Eppendorf tube and the volume adjusted to 250µl with special water (0.63mM hepes buffered water, pH 7.3) and 250µl of 0.5M $CaCl_2$ solution was then added. This was mixed with 500µl of 2X HeBS (HEPES-buffered saline solution) whilst air bubbling and left to stand for no longer than 40 minutes to avoid formation of too large a precipitate. The precipitate was then added slowly; dropwise onto the HEK293T cells and dishes gently rocked for 10 seconds to ensure the media and precipitate were well mixed. Cells were then incubated overnight at 37°C.

The following day, medium was removed; the cells washed with warm PBS and the media replaced with 10ml viral production media (DMEM with 20% FCS and PSA) before continued incubation for 3 days at 37°C at 5% CO_2 in air as normal. After this time, the viral supernatant was collected into a 50ml falcon tube and centrifuged at 1900g for 5 minutes. The virus was then sterilised through 0.45µm filters (Millipore, UK) aliquoted and stored at -80°C for up to 6 months.

2.9.2. Transduction of primary keratinocytes

Primary keratinocytes were seeded in complete Epilife medium into 6 well tissue culture plates at a density of 100,000cells/well in 2ml media per well and left to attach overnight. The following day, media was removed, the cells washed in PBS, and the medium replaced with 2ml of a viral supernatant mix. This contained 3ml of appropriate virus, 9ml of DMEM/FBS with no PSA and 4ug/ml hexadimethrine bromide. Following centrifugation of plates at 310g for 90 minutes at room temp, the viral supernatant was removed, cells washed with PBS and the medium replaced

with 2ml of fresh complete Epilife. After 48 hours further incubation at 37°C to allow transgene expression, cells were detached with trypsin/EDTA as described in section 2.2.2 and placed into T175 flasks in a volume of 20ml complete Epilife containing 1µg/ml puromycin to select successfully transduced keratinocytes. Images were taken after a further 48 hours with the fluorescent microscope (DMRIB Leica) to check for GFP and transduction efficiency. Cells were then allowed to expand prior to inclusion in epidermal skin equivalents with high calcium Epilife as described in section 2.4.

2.10. Transient siRNA knockdown of ATG7 in primary keratinocytes

The siRNA for ATG7 was purchased from life Technologies, UK and already available in the lab (Lovat group). A Stealth RNAi negative control medium GC content siRNA was purchased from Thermo Fisher Scientific (Table 5).

siRNA constructs were transfected into primary keratinocytes using lipofectamine LTX plus (ThermoFisher Scientific, UK) according to manufacturer's recommendations. Keratinocytes were seeded into 6 well plates (100,000/well) in 2ml complete MCDB 153/well and allowed to culture to approximately 70% confluency (usually requiring at least overnight incubation at 37°C). Media was then removed from keratinocytes and cells washed with PBS prior to replacement with 1ml/well of Opti-MEM (Life Technologies, UK) and the dropwise addition of 250µl of combined transfection siRNA containing mix, ensuring the final concentration of siRNA was 40nM. Incubation was then continued for 6 hours at 37°C before removing the siRNA media mix, a brief wash with PBS and replacement of the media with 2ml of complete MCDB 153. The following day, cells were treated appropriately every 48 hours.

For experiments in which keratinocytes were cultured in monolayer and differentiated, the media was changed 24 hours after transfection to high calcium complete MCDB153 medium, replacing the medium every 48 hours for 5 days to induce differentiation whilst cells were treated appropriately,

For siRNA mediated knockdown of ATG7 in epidermal equivalents, primary keratinocytes were first seeded into T75 flasks in 12ml complete MCDB 153 media and allowed to culture to approximately 70% confluency at 37°C. The same

transfection protocol was used, but volumes were scaled up appropriately by adding 2ml of the combined transfection siRNA mix into 7ml Opti-MEM. The cells were then allowed to become confluent before trypsinising, counting and seeding as normal into epidermal equivalent models as described in section 2.4.

Table 5 siRNA constructs purchased

Target	Construct known as	Catalogue Number/Sequence
ATG7	ATG7	Catalogue No:1299001 siRNA ID: HSS116182 (Made to order)
Non silencing	NT	Catalogue No:12935300

2.11. Fractionation of epidermal skin equivalents for proteomic analysis

Optimisation of epidermal equivalent fractionation was carried out prior to preliminary proteomic analysis performed in collaboration with AstraZeneca. Initially, whole cell lysates of epidermal equivalents lysed in urea buffer (as described in section 2.5) were analysed however, results revealed proteins of interest were masked by cytoskeletal proteins present.

Consequently, the use of two different fractionation kits was tested. For this, larger samples of epidermal equivalents were lysed (1/2 compared to 1/4 of an epidermal equivalent usually lysed) to ensure protein concentrations in all fractions were high enough. Firstly, a NE-PER Nuclear Protein Extraction kit (Life technologies, UK) was used for cell lysis and stepwise extraction of cytoplasmic and nuclear protein fractions. Secondly, a Subcellular Protein Fractionation Kit (Life Technologies, UK) was employed to isolate cytoplasmic, soluble nuclear, chromatin-bound, membrane and cytoskeletal fractions from epidermal equivalents.

In both kits, fractions were separated using a reagent-based protocol following manufacturer's instructions. This involved initially lysing the sample with a pellet pestle, then the addition and incubation with a series of lysis buffers specific to each fraction followed by centrifugation steps. After each centrifugation step, the

supernatant (fraction of interest) was removed. Protein concentration of each fraction was then determined (as described in section 2.5) and samples stored at -80°C until shipment.

Although fractionation of samples was performed at Newcastle University, proteomics analysis was carried out by collaborator Dr Rachel Rowlinson at AstraZeneca, Macclesfield using a standardised protocol. Briefly, this involved preparation of samples and 50µg of sample was loaded onto a Synapt G2-si high definition mass spectrometer (Waters, UK) via a Nano Acquity LC using the 110min MS^E ion mobility method for data collection. Samples were processed using the Waters Progenesis Software. Results were then sent for analysis by Dr Simon Cockell (Bioinformatics Unit, Newcastle University).

2.12. Statistical analysis

All statistical analyses were performed using GraphPad Prism 6 (SanDiego, CA). Data unless stated otherwise were represented as the mean value of at least 3 replicates +/- the standard error of the mean (SEM). Individual figure legends describe the precise statistical analyses performed in a given experiment where “n” denotes the number of biological repeats, i.e. independent donors whilst “N” represents the number of technical repeats, i.e. number of wells analysed.

All protein expression data were quantified by densitometry from at least three different donors. Protein levels were normalised to GAPDH loading control values of the respective sample and expressed relative to vehicle control of an individual donor (to account for varied expression between varied skin donors). One-way ANOVA analysis was used to compare effects of experimental treatments, with Dunnett’s or Tukey’s multiple comparison tests. In experiments with more than two variables, for example in RNA interference studies, two-way ANOVA analysis was carried out with either Tukey’s or Bonferroni’s multiple comparison tests. Protein was normalised to GAPDH loading control of a given sample and expressed relative to protein expression following transfection with non-targeting siRNA or ShRNA (siNT or shNT) vehicle treated control.

In time and dose range experiments, a post-test for linear trend was also performed, giving a R^2 value and p value to determine whether there was a significant linear increase or decrease in samples.

mRNA expression data derived from delta C_t values, were from at least three individual donors all normalised to levels of histone H4 housekeeping gene within a given sample and expressed relative to vehicle control from the same original donor sample.

For MTT and SRB assays data were collected from kertainocytes derived from three different donors, all in triplicate, i.e. for each treatment three technical repeats were performed for each donor. For each donor, treated wells were expressed relative to to the mean absolute absorbance data derived from from the three vehicle treated control wells. Data was presented according to calcium conditions or treatment length and as such statistical analysis was performed using a simple one-way ANOVA with Dunnett's multiple comparison test.

Measurements of viable cell layer thickness with epidermal skin equivalents were derived using Image J software with 6 measurements taken along the length of each skin equivalent image and expressed relative to the mean thickness of vehicle control treated epidermal equivalents and represented as the mean relative viable thickness. Differing statistical analysis were applied depending on the number of variables and experiment. For analysis of epidermal equivalents treated over 3, 5 and 7 days, a two-way ANOVA with Bonferroni's multiple comparison test was performed. For simply comparing effects of treatments e.g. vehicle vs. TCDD treated epidermal equivalents, an unpaired t-test was used in order to compare differences between independent random measurements.

Finally, for analysis of the effect of chemical inhibitors or knockdown on TCDD induced apoptosis or proliferation in epidermal equivalents, tiled images of caspase-3 and Ki67 stained epidermal equivalents were acquired. Hoechst positive nuclei and caspase-3/Ki67 positive cells were counted manually. The mean percentage of caspase-3/Ki67 expressing cells compared to total Hoechst positive nuclei was then determined and data expressed as fold change relative to vehicle control, or vehicle treated siNT/shNT controls.

Statistical analysis was subsequently performed using two-way ANOVA with Tukey's multiple comparison post hoc correction test for all ATG7 or cathepsin D knockdown experiments or by one-way ANOVA with Tukey's multiple comparison test for analysis in treated (pepstatin A or bafilomycin) epidermal equivalents without knockdown.

For all experiments statistical significance was reported ****p<0.0001, ***p<0.001, **p=<0.01 and *p<0.05, where a value of <p= 0.05 was considered significant.

Chapter 3 Exposure to TCDD results in a chloracne phenotype associated with AhR degradation, autophagy induction and deregulated differentiation in a 3D epidermal equivalent model

3.1. Introduction

The most severe and typical form of TCDD cutaneous toxicity is chloracne, a chronic hyperkeratoic skin disorder with comedones and cysts, resulting in scarring and disfigurement (Ray and Swanson, 2009). However, the pathogenesis underlying chloracne is still incompletely understood and it seems resistant to most treatments (Ju *et al*., 2009). Since chloracne affects both hair follicles and the interfollicular epidermis, suitable animal models have proved difficult to derive. Not only this, there are significant differences between mouse and human AhR, with mouse AhR having increased affinity for ligands such as TCDD (Hao *et al*., 2013, Ema *et al*., 1994). Therefore, due to the drawbacks of using animal models, human keratinocyte cell lines such as the HaCaT cell line and normal human epidermal keratinocytes (NHEKs) are often used. Although monolayer cultures can be used to study biochemical and molecular mechanisms, organotypic models or epidermal equivalents more accurately reproduce the morphology and differentiation of human epidermal tissue (Loertscher *et al*., 2001a).

Although AhR activation by TCDD is thought to alter epidermal differentiation (Van den Bogaard *et al*., 2015, Forrester *et al*., 2014), the role of endogenous AhR signalling and direct impact on keratinocyte signalling still requires further research. Recent studies showing increased expression of AhR-related mRNA in skin biopsies derived from patients with atopic dermatitis and psoriasis has increased interest in this area (Kim *et al*., 2014). In addition, observations demonstrating coal tar, used in the treatment of atopic dermatitis, induces AhR pathway activation and the restoration of normal epidermal differentiation (Van den Bogaard *et al*., 2013) has further highlighted the role of AhR in regulating epidermal homeostasis. Further research reported the ability of AhR activating ligands to reduce inflammation associated with psoriasis, whilst AhR antagonists induced inflammation (Di Meglio *et al*., 2014). Collectively, this data suggests AhR regulates key homeostatic mechanisms in cutaneous biology and AhR may provide a valuable therapeutic target for cutaneous diseases such as atopic dermatitis.

Similarly, the molecular mechanisms mediating TCDD-induced toxicity and the resultant chloracne phenotype are not fully understood (Loertscher *et al*., 2002). *In vitro*, in both organotypic skin models and keratinocyte monolayer cultures, TCDD treatment results in the altered expression of epidermal differentiation markers

(Loertscher *et al*., 2001a, Sutter *et al*., 2009). In a previous study in the lab, TCDD treatment was also found to induce dysregulated differentiation in epidermal equivalents. However, in contrast to the literature TCDD treatment reduced filaggrin protein expression whilst TGM-1 expression was increased (Forrester *et al*., 2014).

Previous studies from the Reynolds lab (Forrester thesis) also reported that the induction of a TCDD chloracne phenotype was associated with increased autophagic activity. Electron microscopy of epidermal equivalents treated with TCDD found evidence of double membrane autophagosomes, as well as vacuolisation indicative of autophagy. Since autophagy also plays an integral role in normal skin homeostasis and epidermal differentiation (Yoshihara *et al*., 2015) these studies provide further support for the likely impact of TCDD on altered epidermal differentiation.

Building upon earlier preliminary studies, (Forrester *et al*., 2014), the principle aim of the present chapter was to further develop, refine and characterise a physiologically relevant and robust epidermal skin equivalent model of a TCDD-induced chloracne phenotype. Our focus was to characterise the mechanisms mediating TCDD-induced chloracne and the specific effects of TCDD on keratinocyte/epidermal differentiation, autophagy, apoptosis and the physiological role of AhR pathway activation in the skin.

3.2. Results

3.2.1. TCDD induces a chloracne phenotype in human 3D epidermal skin equivalents.

TCDD has previously been reported to induce a chloracne phenotype in epidermal skin equivalents *in vitro* (Forrester *et al*., 2014); however, the mechanisms mediating this effect remain incompletely understood. To further characterise mechanisms associated with TCDD-induced chloracne, human epidermal skin equivalents were generated and initially treated with 10nM TCDD or vehicle (DMSO) control systematically every 48 hours for a period of 3, 5 or 7 days. Histological staining of formalin fixed and paraffin embedded (FFPE) sections with haemotoxilin and eoisin (H&E), revealed as expected a reduction in the viable cell layer (Fig. 3.1), with apparent maximal effect after 7 days. This was in addition to a more compacted stratum corneum, again with maximal effect after 7 days treatment with TCDD (Fig. 3.1).

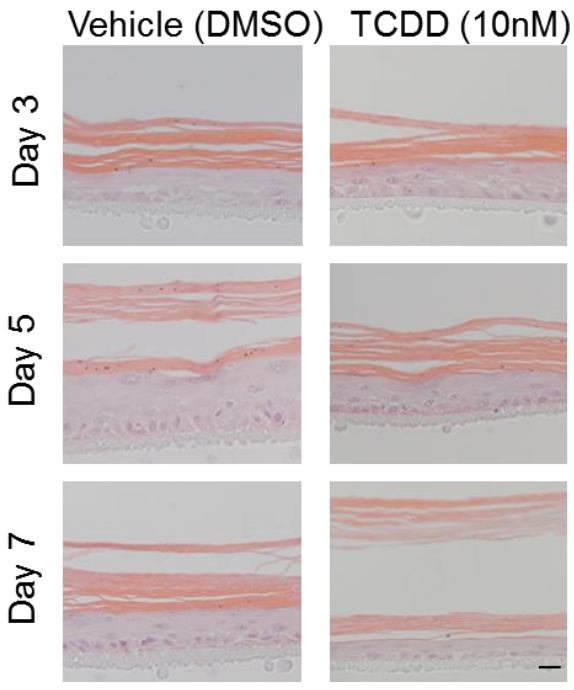

Figure 3.1 TCDD–induced chloracne in epidermal skin equivalents.

Representative immunohistochemical images of epidermal skin equivalents (n=3 independent donors) stained with H&E following treatment every 48 hours for 3, 5 or 7 days with vehicle (DMSO) or TCDD (10nM), scale bar=20µm.

Quantitative analysis of the viable cell layer demonstrated a significant decrease in the thickness of the viable cell layer in all epidermal skin equivalents treated for 3, 5 or 7 days with TCDD compared to those treated for identical time points with vehicle (DMSO) control (Two-way ANOVA with Bonferroni's multiple comparison test, $p<0.01$, $p<0.05$, $p<0.001$ Fig. 3.2A). This was more significant and notably greater in epidermal skin equivalents treated with TCDD for 7 days ($p<0.001$). Additional quantitative analysis also revealed a slight reduction in the viable cell layer thickness of epidermal skin equivalents treated with vehicle (DMSO) control after 7 days (Fig. 3.2B), although treatment with TCDD for 7 days still revealed a significant affect (Two-way ANOVA Bonferroni's multiple comparison test $p<0.0001$, Fig. 3.2B).

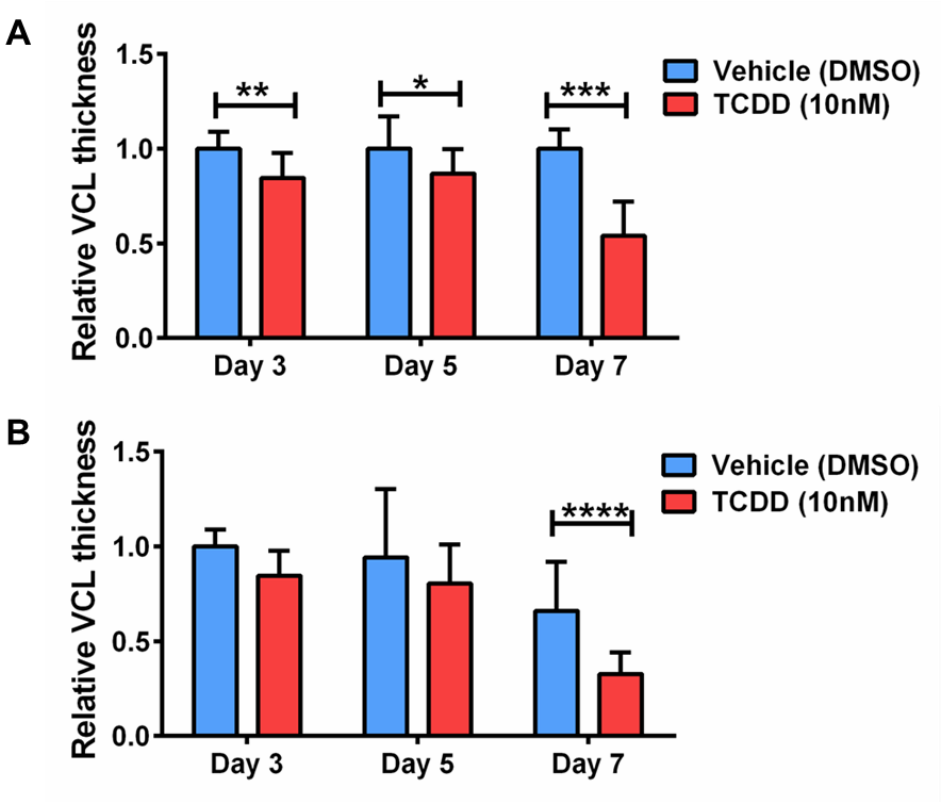

Figure 3.2 TCDD treatment induced a significant reduction in viable cell layer thickness in epidermal skin equivalents.

A) Mean viable cell layer thickness (VCL) of epidermal skin equivalents treated with vehicle (DMSO) control (blue bars) or TCDD (10nM) (red bars) every 48 hours for 3, 5 or 7 days 6 measurements were taken per treatment, per donor. Data is expressed relative the average VCL thickness taken from 6 images of vehicle (DMSO) control at day 3, 5 or 7 respectively (n=3 independent donors) ±SEM. B) Mean VCL thickness of epidermal skin equivalents treated every 48 hours for 3, 5 or 7 days with vehicle (DMSO) control (blue bars) or TCDD (10nM) (red bars). Date is expressed relative to the average VCL thickness taken from 6 images of vehicle (DMSO) control at day 3(n=3 independent donors). Statistics were acquired using two-way ANOVA Bonferroni's multiple comparison test, *** P< 0.0001.

These experiments were repeated on several occasions and collectively demonstrated the consistent induction of a TCDD-induced chloracne phenotype at 7 days, with a consistent and significant reduction in the viable cell layer (Un-paired t-test, p<0.0001, Fig. 3.3).

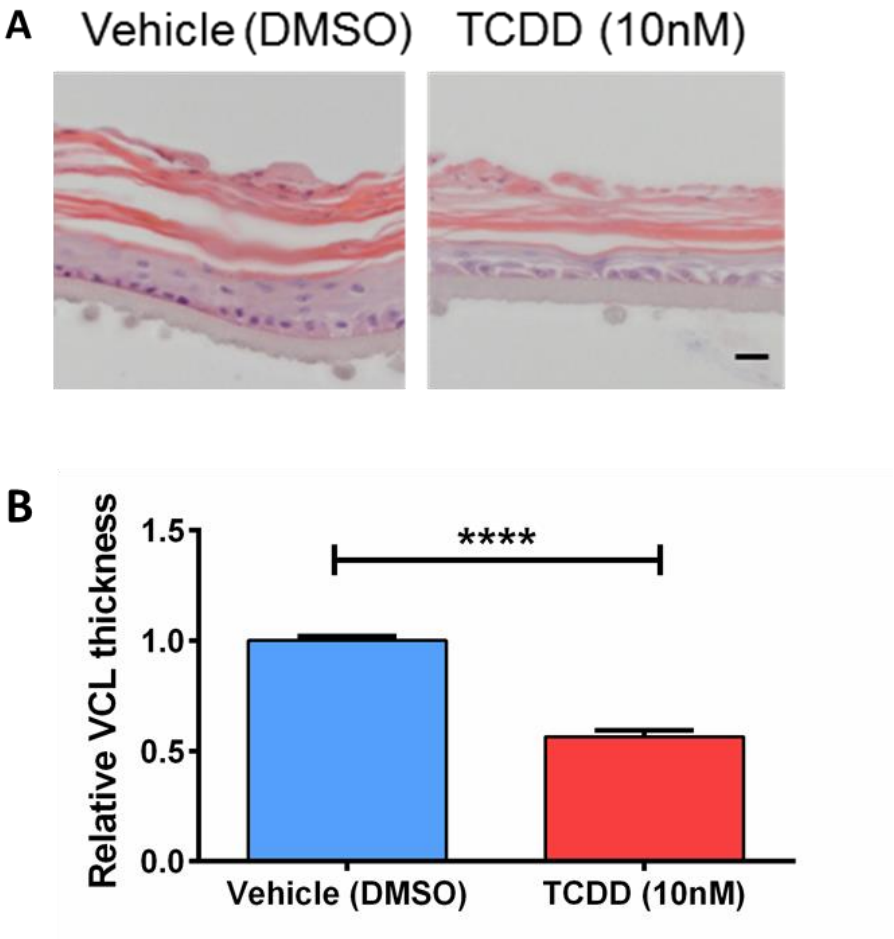

Figure 3.3 TCDD-induced reduced viable cell layer of the chloracne phenotype model is reproducible at 7 days.

A) Representative immunohistochemical images of epidermal skin equivalents (n=8 independent donors) stained with H&E following treatment with vehicle (DMSO) control or TCDD (10nM) every 48 hours for 7 days. Scale bar = 20µm B) Mean viable cell layer (VCL) thickness of epidermal skin equivalents treated with vehicle (DMSO) or TCDD (10nM) every 48 hours for 7 days. Each bar is expressed relative to vehicle (DMSO) control (n= 8 independent donors) ±SEM. Statistics were acquired by un paired t test ****p=<0.0001.

3.2.2. TCDD induces AhR degradation and CYP1A1 mRNA expression

As AhR activation leads to AhR protein degradation (Forrester *et al*., 2014, Ma and Baldwin, 2000), AhR protein expression in TCDD treated epidermal skin equivalents was determined by western blotting as a read out of AhR pathway activation in this model. Epidermal skin equivalents were treated with vehicle (DMSO) or TCDD (10nM) every 48 hours for 3, 5 or 7 days (Fig. 3.4).

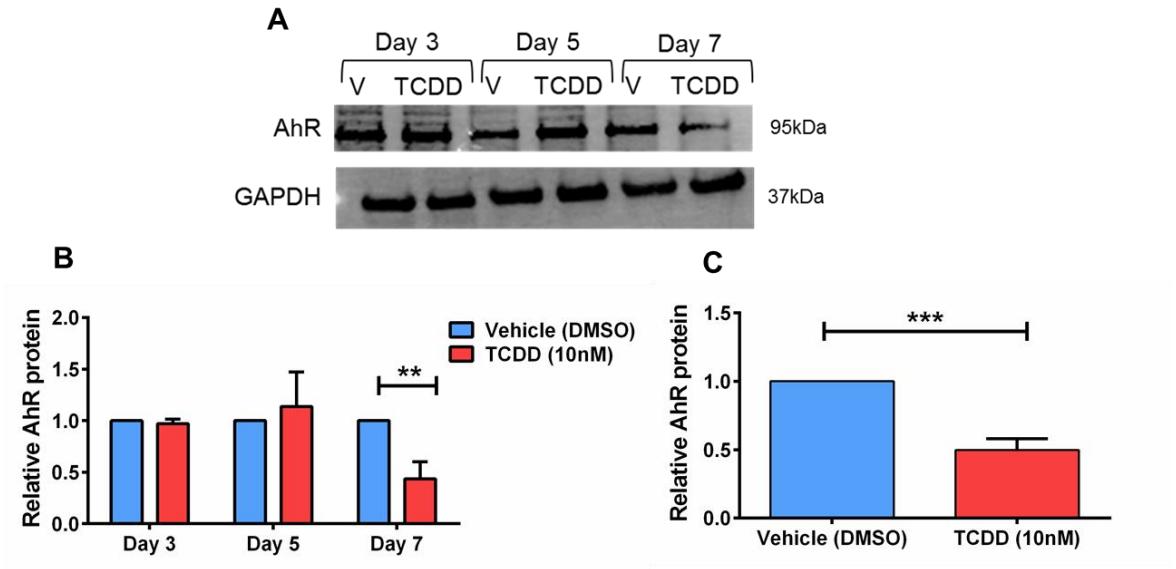

Figure 3.4 TCDD induces AhR protein degradation in epidermal skin equivalents.

A) Representative western blot of AhR protein expression in epidermal skin equivalents (n=3 independent donors) following treatment with vehicle (DMSO) control or TCDD (10nM) every 48 hours for 3, 5 or 7 days. B) Densitometric analysis of AhR protein expression after vehicle (DMSO) (blue bar) or TCDD (10nM) treatment (red bar) each bar is normalised to GAPDH loading control and relative to vehicle (DMSO) control at day 3, 5 or 7 (n=3 independent donors) ± SEM. Statistics were acquired by two-way ANOVA with Bonferroni's multiple comparison test **p= <0.01 C) Densitometric analysis of AhR protein expression after vehicle (DMSO) (blue bar) or TCDD (10nM) treatment (red bar) every 48 hours for 7 days each bar is normalised to GAPDH loading control and relative to vehicle (DMSO) control (n=7 independent donors) ±SEM. Statistics were acquired by paired t test ****p=<0.001.

Results showed relative to GAPDH loading control, AhR protein expression significantly decreased after 7 days treatment with TCDD compared to vehicle (DMSO) control (two-way ANOVA with Bonferroni's multiple comparison test, $p<0.01$, Fig. 3.4 A, B). Furthermore, repeated experiments of TCDD treatment in epidermal skin equivalents, derived from 7 independent donors, for 7 days confirmed the consistent and significant degradation of AhR protein expression (paired t-test,

p<0.001, Fig. 3.4 C). To gain further evidence of TCDD-induced activation of AhR, mRNA levels of AhR as well as CYP1A1 (as a downstream target of AhR activation) (Ma, 2001, Veldhoen *et al*., 2009) were quantified by qPCR of lysates prepared from epidermal skin equivalents treated for 7 days with either vehicle (DMSO) control or TCDD (10nM) (Fig. 3.5).

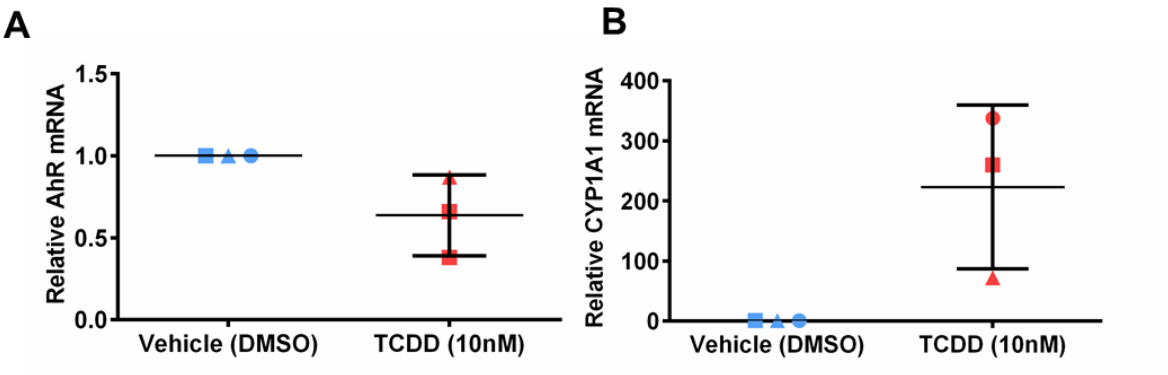

Figure 3.5 TCDD-induced AhR mRNA degradation and CYP1A1 mRNA induction.

A) AhR mRNA expression in epidermal skin equivalents (n=3 independent donors) following treatment with vehicle (DMSO) (blue symbols) or TCDD (10nM) (red symbols) every 48 hours for 7 days, each symbol is normalised to housekeeper gene H4 and relative to vehicle (DMSO) control , line represents mean value. Statistics were acquired by paired t-test (NS) B) CYP1A1 mRNA expression in epidermal skin equivalents (n=3 independent donors) following treatment with vehicle (DMSO) (blue symbols) or TCDD (10nM) (red symbols) every 48 hours for 7 days each symbol is normalised housekeeper gene H4 and relative to vehicle (DMSO) control, line represents mean value. Statistics were acquired by paired t-test (NS).

Results revealed a trend for decreased AhR mRNA expression and increased CYP1A1 mRNA in epidermal skin equivalents following 7 days treatment with TCDD further supporting the evidence for TCDD-induced AhR activation in a chloracne phenotype.

3.2.3. TCDD induces de-regulated epidermal differentiation in epidermal skin equivalents

Previous reports have shown that TCDD causes de-regulated differentiation, inducing a switch from proliferation to differentiation of keratinocytes (Berkers *et al*., 1995). In order to further delineate the impact of TCDD treatment on epidermal differentiation in the context of chloracne, the immunofluorescent expression of epidermal differentiation markers filaggrin, loricrin and cytokeratin 10 (CK10 or K10) was determined in epidermal skin equivalents treated with vehicle (DMSO) or TCDD (10nM) every 48 hours for 7 days (Fig. 3.6).

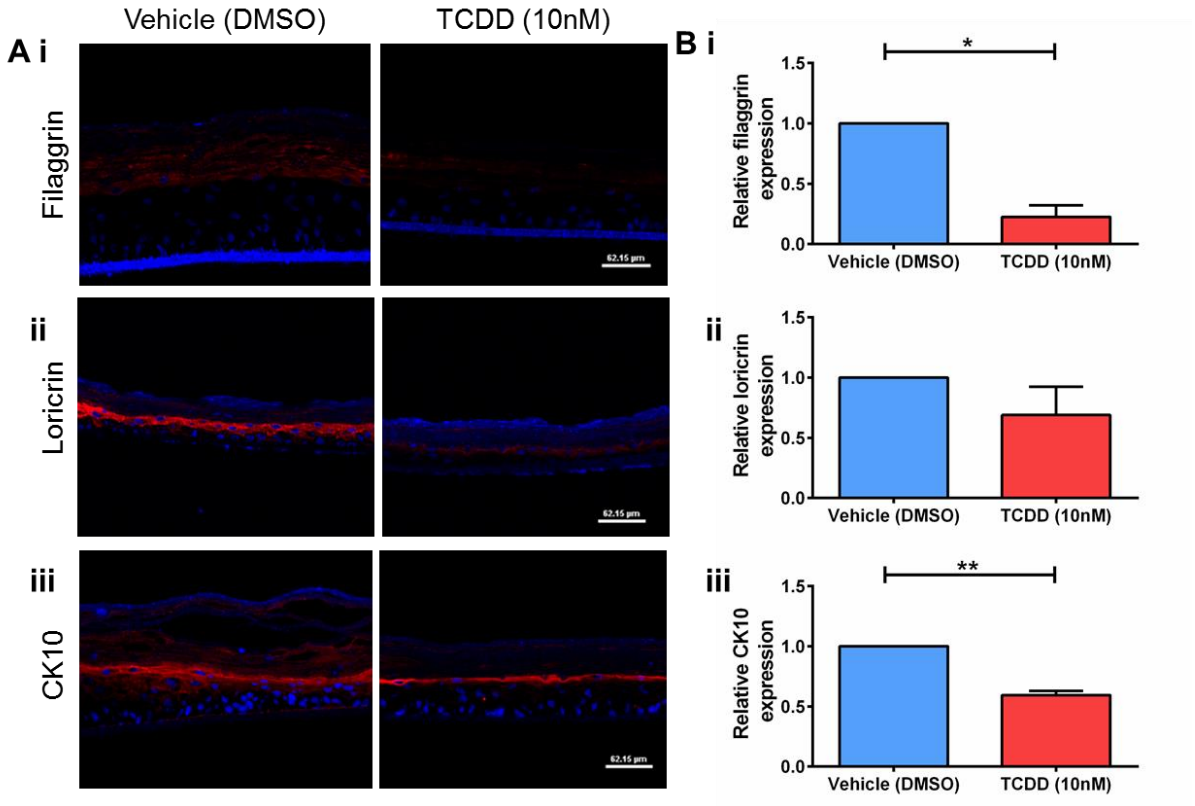

Figure 3.6 TCDD induces de-regulated expression of late epidermal differentiation markers.

A) Representative photomicrographs of epidermal equivalents treated with vehicle (DMSO) or TCDD (10nM) every 48 hours for 7 days depicting Hoechst nuclear staining (blue fluorescence) and filaggrin (i), CK10 (ii) or loricrin (iii) staining (red fluorescence). n=3 independent donors, scale bar 62.15µm. B) Mean relative filaggrin (Bi) loricrin (Bii) or CK10 (Biii) expression in epidermal equivalents treated for 7 days with vehicle (DMSO) (blue bars) or TCDD (10nM) (red bars). Each bar is expressed relative to vehicle (DMSO) control filaggrin (i) CK10 (ii) or loricrin (iii) expression, n= 3 independent donors, ± SEM. Statistics were acquired by paired t-test *p=<0.05, **p=<0.01

Results demonstrated a significant reduction in filaggrin expression (paired t-test $p<0.05$, Fig. 3.6 A, B i) and CK10 ($p<0.01$, Fig. 3.6 A, B iii) in response to treatment with TCDD (10nM) treatment for 7 days. Loricrin expression was also reduced, although this was not significant (Fig. 3.6 A, B ii). Conversely, analysis of mRNA expression of loricrin, filaggrin, CK10 and involucrin revealed opposing results (Fig. 3.7), in which TCDD induced an apparent increase in the mRNA expression levels of each marker (Fig. 3.7). Collectively, these data thereby suggest that a TCDD-induced chloracne phenotype is associated with deregulated epidermal differentiation.

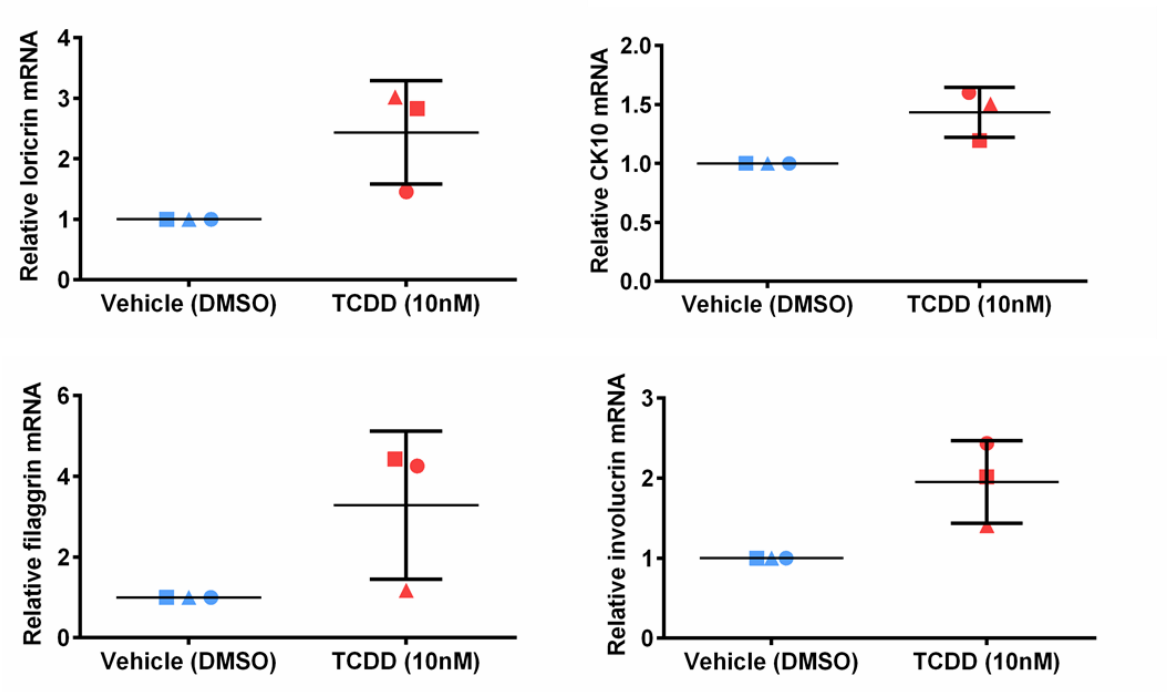

Figure 3.7 TCDD-induced mRNA expression of epidermal differentiation markers.

Loricrin, CK10, filaggrin or involucrin mRNA expression in epidermal skin equivalents (n=3 independent donors) following treatment with vehicle (DMSO) (blue symbols) or TCDD (10nM) (red symbols) every 48 hours for 7 days each symbol is normalised to housekeeper gene H4, relative to vehicle (DMSO) control, line represents mean value. Statistics were acquired by paired t-test (NS)

3.2.4. TCDD treatment causes no significant change in cell proliferation but does induce active caspase-3 staining in epidermal skin equivalents

To further delineate the TCDD-induced chloracne phenotype and specifically the mechanisms involved in the TCDD-induced reduction in viable cell layer, caspase-3 dependent cell death and cellular proliferation were explored. Human epidermal skin equivalents were generated and then treated with vehicle (DMSO) or TCDD (10nM) every 48 hours for 7 days. After harvesting, immunofluorescence staining on OCT frozen sections for caspase-3 or Ki67 was carried out. Images were taken along the entire length of the epidermal skin equivalents and Hoechst positive cells and caspase-3 or Ki67 positive cells were counted (Fig 3.8 A-D). Further representative tiled images of capsase-3 staining are also displayed in Appendix G.

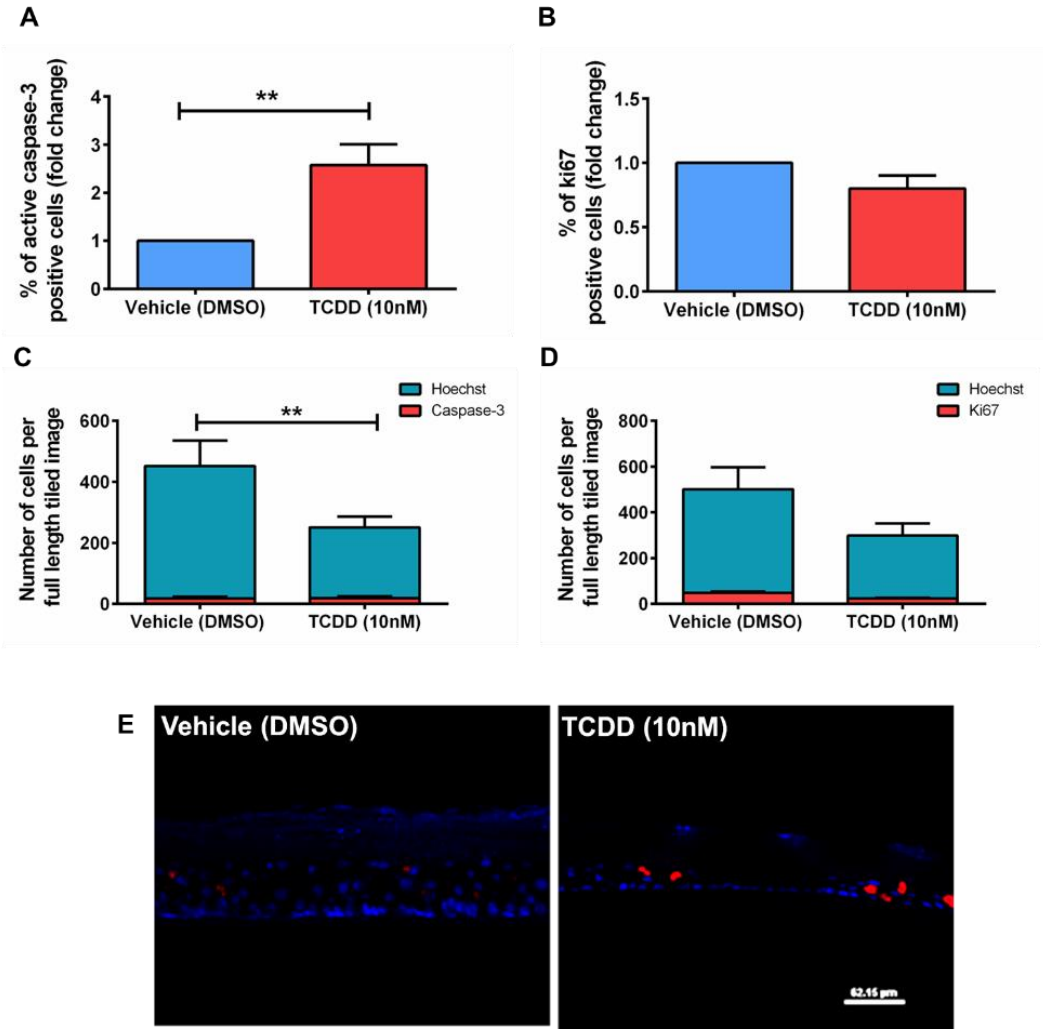

Figure 3.8 TCDD significantly induced caspase-3 positive cells but caused no change to proliferation.

Mean percentage of caspase-3 positive cells (A) or Ki67 positive cells (B) to Hoechst positive cells presented as fold change in epidermal equivalents treated with vehicle (DMSO) (blue bar) or TCDD (10nM) (red bar) every 48 hours for 7 days relative to vehicle (DMSO) control. n=7 (A) or n=3 (B) independent donors, ± SEM. Statistics were acquired by paired t-test **p=<0.01 (A) NS (B). Mean number of caspase-3 positive cells (C) or Ki67 positive cells (D) to Hoechst positive cells presented as raw number in epidermal equivalents treated with vehicle (DMSO) or TCDD (10nM) every 48 hours for 7 days relative to vehicle (DMSO) control. n=7 (C) or n=3 (D) independent donors, ± SEM. Statistics were acquired by two-way ANOVA with Bonferroni's multiple comparison test **p=<0.01 (C) NS (D). Representative photomicrographs (E) taken at 20x magnification of epidermal skin equivalents treated with vehicle (DMSO) or TCDD (10nM) every 48 hours for 7 days depicting Hoechst nuclear staining (blue fluorescence) or caspase-3 expression (red fluorescence). Scale bar=62.15µm

Statistical analysis revealed TCDD treated epidermal skin equivalents had significantly increased caspase-3 positive cells compared to vehicle (DMSO) alone (Paired t-test $p<0.01$ Fig. 3.8 A). This data suggests the reduced viable cell layer may be due to TCDD inducing a form of apoptotic cell death. In contrast, TCDD did not cause a significant change in proliferation, although staining for Ki67 was reduced slightly in TCDD treated epidermal skin equivalents (Fig. 3.8 B). Statistical analysis of the raw number of Hoechst positive cells and caspase-3 positive cells along the entire tiled image revealed a significant reduction in Hoechst positive cells (two-way ANOVA $p<0.01$) in TCDD treated epidermal equivalents compared to vehicle (DMSO) treated (Fig 3.8 C). Data also suggested the number of Ki67 positive cells decreased proportionally compared to number of Hoechst positive cells in TCDD treated epidermal equivalents compared to control (Fig 3.8 D). However, the number of caspase-3 positive cells remained similar to vehicle treated epidermal equivalents, despite the reduced number of cells in total after TCDD treatment (Fig 3.8 C).

3.2.5. TCDD induces autophagy in epidermal skin equivalents

Preliminary data leading to the present study suggested a TCDD-induced chloracne phenotype is associated with autophagy activation (Forester thesis). To provide further evidence for TCDD-induced autophagy activation, LC3 lipidation was also determined by western blotting in the same epidermal skin equivalents from sections 3.1.1 and 3.1.2, treated with vehicle (DMSO) or TCDD (10nM) every 48 hours for 3, 5 and 7 days (Fig 3.9) and probed for LC3II.

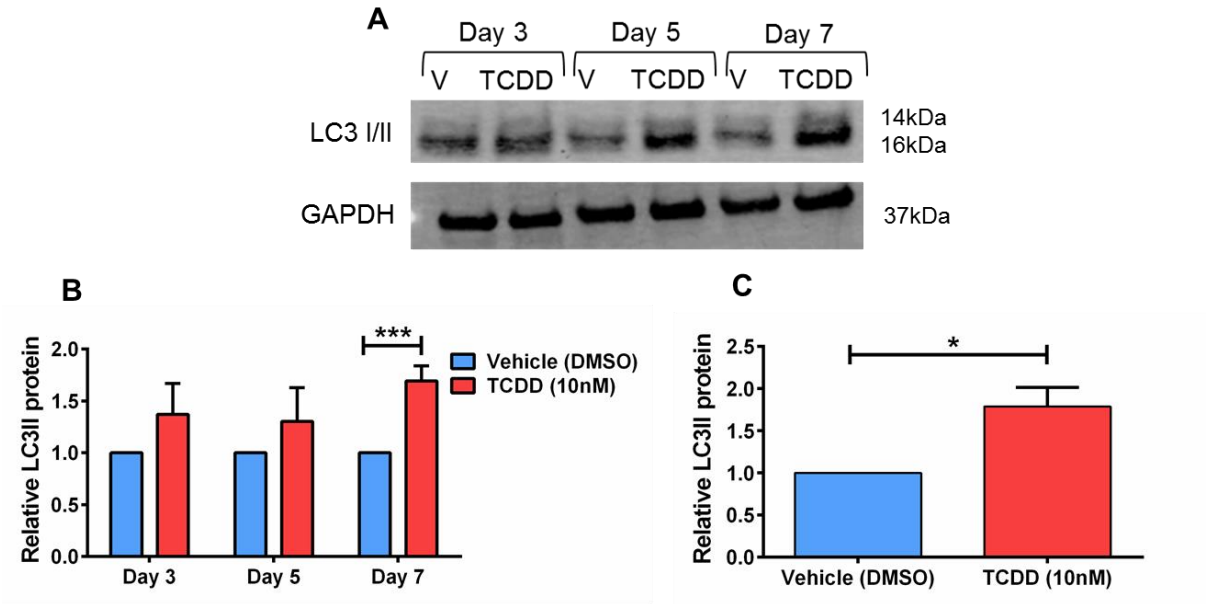

Figure 3.9 TCDD induces LC3II accumulation in epidermal skin equivalents.

A) Representative western blot of LC3 I/II protein expression in epidermal skin equivalents (n=3 independent donors) following treatment with vehicle (DMSO) control or TCDD (10nM) every 48 hours for 3, 5 or 7 days. B) Densitometric analysis of LC3II expression after vehicle (DMSO) (blue bar) or TCDD (10nM) treatment (red bar) every 48 hours for 3, 5 or 7 days. Each bar is normalised to GAPDH loading control relative to vehicle (DMSO) control at day 3, 5 or 7 (n=3 independent donors) ±SEM. Statistics were acquired by two way ANOVA with Bonferroni's multiple comparison test *p= <0.05) Densitometric analysis of LC3II protein expression after vehicle (DMSO) (blue bar) or TCDD (10nM) treatment (red bar) every 48 hours for 7 days each bar is normalised to GAPDH loading control relative to vehicle (DMSO) control (n=7 independent donors) ±SEM. Statistics were acquired by paired t test *p=<0.05.

Results demonstrated TCDD treatment gradually increased LC3II expression, compared to vehicle (DMSO) control over 7 days, supportive of autophagy induction (Fig. 3.9 A). Densitometric analysis further revealed significant induction of LC3II after treatment with TCDD for 7 days (two-way ANOVA with Bonferroni's multiple comparison test, $p<0.001$, Fig. 3.9 B). This effect was significantly reproducible following analysis in epidermal skin equivalents derived from 7 independent donors (Paired t-test, $p<0.05$, Fig. 3.9. C). Additional Immunofluorescence analysis of TCDD treated epidermal skin equivalents showed significant increased endogenous LC3 expression (Fig. 3.10 A i and ii) as well as significantly decreased expression of P62 (Fig. 3.10 Bi and ii) throughout the epidermis, following 7 days treatment with 10nM TCDD (paired t-test, $p<0.05$). Collectively these data strongly support that a TCDD-induced chloracne phenotype is associated with the activation of autophagy in the epidermis.

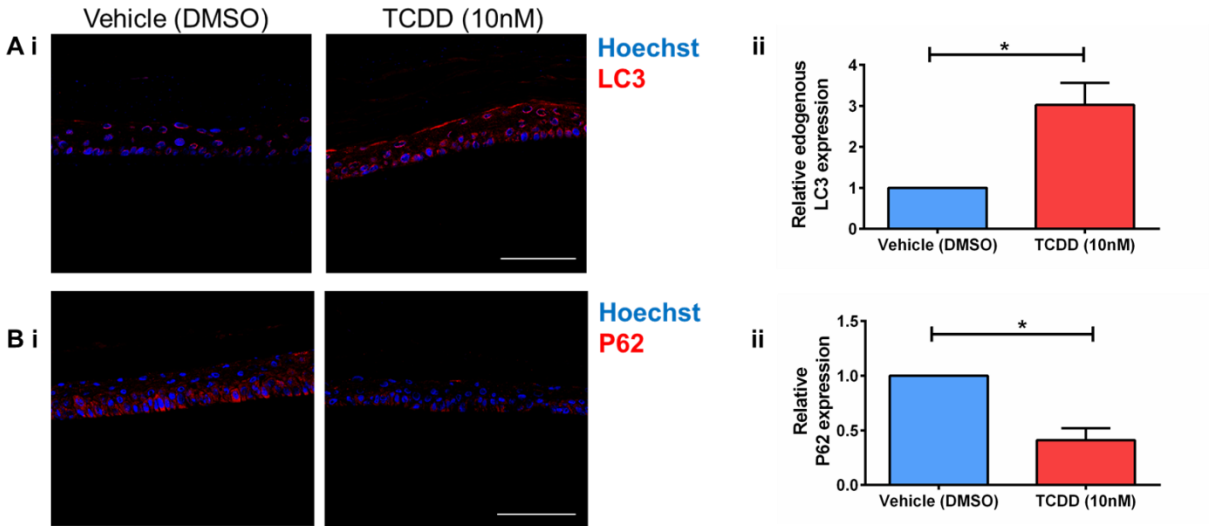

Figure 3.10 TCDD induced a significant increase in endogenous LC3 and P62 degradation in epidermal skin equivalents.

Representative photomicrographs of epidermal skin equivalents treated with vehicle (DMSO) or TCDD (10nM) every 48 hours for 7 days depicting Hoechst nuclear staining (blue fluorescence) or endogenous LC3 (Ai) or P62 expression (Bi) (red fluorescence). n=3 independent donors, scale bar=100µm. Mean LC3 (Aii) or P62 (Bii) expression of epidermal skin equivalents treated with vehicle (DMSO) or TCDD (10nM) every 48 hours for 7 days. Each bar is relative to vehicle (DMSO) control, n=3 independent donors, ± SEM. Statistics were acquired paired t-test ($p<0.05$).

3.3. Discussion

Using an optimised and robust *in vitro* human epidermal skin equivalent model, data from the present chapter characterises the time course and inter-relationship between histological changes, AhR activation, induction of autophagy and apoptosis and altered keratinocyte differentiation. Together this demonstrates TCDD treatment leads to a significantly reduced viable cell layer and more compact stratum corneum, typical of a chloracne phenotype observed *in vivo* (Forrester *et al*., 2014 and Ju *et al*., 2009). Whilst TCDD has previously been shown to induce a chloracne phenotype model within the lab, data demonstrating the temporal regulation and detailed time course of development over 7 days is novel.

In humans, chloracne is the most consistently observed pathology after TCDD exposure and therefore, dermato-pathology is the most widely accepted and reliable means of identifying associated toxicity (Neuberger *et al*., 1991, Loertscher *et al*., 2001b). To date, suitable animal models have been difficult to derive and as such, recent research has focussed on the use of organotypic skin equivalent models. Previous studies have described the development of a full thickness organotypic model, by co-culturing near immortalised diploid human keratinocytes (NIKS) and dermal fibroblasts (Loertscher *et al*., 2001b and De Abrew *et al*., 2014), which, although contain a dermal compartment still lacks appendages such as hair follicles. Although the application of TCDD to these models resulted in altered/de-regulated epidermal differentiation, there was no obvious reduction in viable cell layer thickness or the induction of a chloracne-like phenotype, reflective of an *in vivo* setting (Loertscher *et al*., 2001b and De Abrew *et al*., 2014). Nevertheless, studies by De Abrew *et al* noted the increase in intracellular spaces, between keratinocytes of the basal and suprabasal layers following treatment with TCDD (De Abrew *et al*., 2014). Interestingly, additional studies of primary human keratinocytes cultured in monolayer and subjected to treatment with TCDD demonstrated a reduction in cell number (Loertscher *et al*., 2001a). *In vivo*, observations of a TCDD mediated reduction in viable cell layer and compacted stratum corneum are evident within the follicle wall resulting in a follicular plug or comedone, both characteristic features of chloracne (Forrester *et al*., 2014 and Ju *et al*., 2009). In the present study, a consistent and distinct chloracne-like phenotype was evident after treatment with TCDD for 7 days.

This therefore, highlights the suitability of the model to elucidate the mechanisms behind the pathology of chloracne.

3.3.1. TCDD treatment activates the AhR pathway in epidermal skin equivalents

Results from the present study further confirmed the ability of TCDD to activate AhR signalling, specifically causing a reduction of AhR expression, both at the protein and mRNA level, as expected (Hao *et al*., 2013) in epidermal equivalents. Furthermore, consistent with previous studies, including studies on skin lesions from dioxin-exposed humans with chloracne (Tang *et al*., 2008, Sutter *et al*., 2011), TCDD treatment of epidermal skin equivalents also resulted in the induction of CYP1A1 mRNA induction after 7 days.

After exposure to exogenous ligands, AhR is thought to be degraded by the 26S proteasome ubiquitination pathway (Ma and Baldwin, 2000, Ma, 2011). Interestingly, previous reports noted TCDD-induced AhR degradation occurred quickly, but differed between cell types. In the normal lung cell line Hs 115. LU, for example, AhR degradation occurred after 2 hours, whilst maximal degradation in the colorectal adenocarcinoma cell line LS 180 only occurred after 16 hours of TCDD treatment (Pollenz *et al*., 2006). In contrast, TCDD induced AhR degradation in the present study was only significant at 7 days, and this coincided with CYP1A1 mRNA induction. Such variable time and magnitude of AhR degradation may be reflected by the use of differing *in vitro* models and as such in the present model this process may take longer. It would be interesting to explore the temporal changes in CYP1A1 induction after TCDD treatment and determine if the induction of CYP1A1 is also delayed in addition to AhR degradation. However, this late induction of CYP1A1 is indicative of the long half-life of TCDD and sustained induction of the AhR pathway is also seen *in vivo*. Saurat et al (2009) found CYP1A1 mRNA expression to be increased 170.1 fold above control in chloracne skin lesions, 5 months after TCDD poisoning.

As well as exposure to exogenous ligands, AhR localisation and activity can be affected by other factors. A study using the HaCaT cell line found at low confluency AhR was mainly localised in the nucleus, but at sub-confluent levels was localised

both in the nucleus and cytoplasm. In contrast, at 100% confluency AhR expression was predominantly in the cytoplasm, collectively suggesting confluency of keratinocytes may impact on cellular localisation. In addition to its effect of sub cellular localisation, the confluency of keratinocytes in monolayer also impacts on AhR activity: AhR activity apparently falls to basal levels in confluent cells (Ikuta *et al*., 2009, Ikuta *et al*., 2004). Of note, in murine keratinocytes differentiation status was also found to effect induction of genes in response to TCDD (Jones *et al*., 1997). Both proliferating and differentiating keratinocytes expressed AhR and ARNT proteins, but there was a higher induction of CYP1A1 and other target genes including CYP1B1 in the differentiating population. In the present epidermal equivalent model, primary human keratinocytes were seeded at high density and fully differentiated. Therefore, according to the literature, this may result in altered AhR activity and delayed AhR degradation following treatment with TCDD. It would be beneficial, therefore, to carry out immunofluorescence staining to establish localisation of AhR and explore any differential cellular distribution.

3.3.2. TCDD treatment de-regulates epidermal differentiation in epidermal skin equivalents

Results from the present study showed TCDD clearly de-regulates epidermal differentiation *in vitro*, with observed decreased protein, but increased mRNA expression of the differentiation-associated proteins loricrin, filaggrin and CK10. The induction of mRNA expression of late differentiation markers by TCDD is in keeping with published literature. For example, Sutter *et al* reported TCDD treatment of primary human keratinocytes cultured in monolayer resulted in increased filaggrin mRNA expression (Sutter *et al*., 2011). Additionally, TCDD treatment of NHEKs has been found to increase involucrin expression at both RNA and protein level (Gaido and Maness, 1994). In fact, TCDD has been found to increase the expression of 40% of genes of the epidermal differentiation complex (EDC) located on chromosome 1q21 in humans, which encodes for proteins involved in cornified envelope formation (Kennedy *et al*., 2013). This included increased expression of filaggrin and hornerin.

The observed reduction in filaggrin, loricrin and CK10 protein levels has also been previously reported. Proteomic analysis of primary monolayer keratinocytes, exposed

to TCDD reported significant suppression of filaggrin, keratin 1 and keratin 10 proteins (Hu *et al*., 2013). Furthermore, using the present epidermal equivalent model, Forrester *et al* (2014) found TCDD treatment caused aberrant changes in expression of filaggrin, involucrin and TGM-1. Protein expression of filaggrin and involucrin was downregulated by TCDD treatment, however, TGM-1 expression increased (Forrester *et al*., 2014). TGM-1 was not examined in the studies reported here.

In contrast, TCDD treatment of an organotypic skin model previously described, found a fully differentiated cornified layer developing quicker than in vehicle treated control (Loertscher *et al*., 2001a). TCDD treated cultures were found to have a more extensive layer of keratinised tissue compared to vehicle control and measurements taken from electron micrographs confirmed this, with the ratio of keratinised to monokeratinised layers being far greater in TCDD treated samples (Loertscher *et al*., 2001b). Of note, staining for differentiation markers revealed all markers were present in vehicle and TCDD treated equivalents, but the pattern of expression was altered by TCDD treatment. This was particularly notable in filaggrin, with expression reported as patchy in the granular layers and evident in cellular layers more proximal to the basal layer compared to control samples (Loertscher *et al*., 2001b), consistent with the findings reported here. Together this data suggested TCDD treatment alters both temporal and spatial expression of filaggrin. Similarly, altered expression of involucrin was also detected with evidence of expression in basal keratinocytes after TCDD treatment rather than supra-basal cells (Loertscher *et al*., 2001b). TGM-1 was found to also be irregular and disrupted after TCDD treatment. However, it should be noted that, in contrast to the present model, Loertscher *et al* (2001b) used a full thickness model with a dermis consisting of neonatal fibroblasts mixed with collagen. Additionally, near immortalised keratinocytes were seeded on top of the dermis, rather than primary keratinocytes. Models were also treated 2 hours post plating and cultured for only 8 days.

Results from the present study indicate TCDD treatment induces de-regulated differentiation, which is in keeping with the literature. However, in the present model keratinocytes are in culture, able to differentiate and the epidermis to stratify for 12 days before beginning treatment for a further 7 days with TCDD. As such, this treatment regime may alter the effect of TCDD treatment on differentiation, as the cells are mostly differentiated before treatment begins. The effect of adding

treatments at different time points during the generation of the human skin equivalents has been explored previously by Van den Bogaard *et al* (2015). In this study, AhR antagonists were added when keratinocytes were submerged (proliferation/attachment phase), after the culture had been brought to air/liquid interface or much later during the last phase of air/liquid culture. Interestingly, results demonstrated addition on antagonists in the last phase did not affect involucrin of filaggrin expression, whereas when added in the submerged or early air/liquid interface phase addition of AhR antagonists caused late differentiation marker expression to reduce and the stratification process was suppressed. Van den Bogaard also found differences between cultures on inert filters, as used in the present model, and skin equivalents using de-epidermised dermis. It would therefore, be interesting to explore this further in the present model, by treating with TCDD at different time points and then investigating full differentiation marker expression.

Adding to the complexity of autophagy, this process also plays an integral role in cellular differentiation and more over in epidermal differentiation (Aymard *et al*., 2011, Yoshihara *et al*., 2015). Interestingly, a recent study in monolayer primary human keratinocytes, explants and mouse tissue has explored autophagy marker expression in developing epidermis and again found autophagy plays an integral role in epidermal differentiation. Autophagy was found to be constitutively active in the granular layer and likely mediated by epidermal MTORC1 (Akinduro *et al*., 2016). Of note, in human psoriatic skin biopsies LC3 marker expression was found to be reduced, suggesting autophagy is impaired and could potentially be targeted therapeutically to restore epidermal barrier function (Akinduro *et al*., 2016).

As to whether TCDD-induced autophagy in the current model directly or indirectly impacts on the deregulation of epidermal differentiation is unclear and investigating the link between autophagy and loss of a viable cell layer following TCDD treatment of epidermal equivalents, is addressed in the following chapter.

3.3.3. TCDD treatment causes no significant change in cell proliferation but does induce caspase-3 staining in epidermal skin equivalents

Data in the present chapter also demonstrated TCDD treatment caused an increase in active caspase-3 staining. Caspase-3 is an executioner caspase, activated by either caspase-9 (intrinsic apoptosis) or caspase-8 (extrinsic apoptosis) and results in the induction of apoptosis (McIlwain *et al*., 2015). Therefore, it is frequently used as a marker for both apoptosis pathways and increased expression is associated with the initiation of cell death or apoptosis. The induction of apoptosis by TCDD treatment has been reported in a variety of models including human breast carcinoma cells (Lin *et al*., 2007), choriocarcinoma cells (Chen *et al*., 2010) and human neuronal cell lines (Morales-Hernandez *et al*., 2012). In contrast, work in primary human keratinocytes in monolayer found TCDD treatment caused a reduction in cell number, but apoptosis was not induced (Loertecher et al., 2001a). Nucleosomal fragmentation, morphological changes, and caspase-3 activity were all measured and there was no significant difference between TCDD treated or vehicle (DMSO) treated cells (Loertscher *et al*., 2001a). However, Loertcher *et al*. (2001a) conducted studies in monolayer as opposed to the more physiologically relevant epidermal skin equivalent model used in the present study. As such, the unique microenvironment of the epidermal skin equivalent model may account for differences in results. Regardless, data suggests TCDD-induced apoptosis may to some extent be responsible for the significant reduction in viable cell layer. In addition, the number of Hoechst positive cells was significantly reduced after TCDD treatment compared to vehicle (DMSO) control (Appendix G), further confirming the reduction in the number of viable cells after TCDD treatment.

To establish whether the TCDD-induced reduction in viable cell layer thickness was a consequence of decreased proliferation, Ki67 staining was also performed. However, TCDD treatment did not cause a significant change in Ki67 positive staining, although expression was reduced slightly. TCDD has previously been found to reduce proliferation in the ovarian cancer cell line OVCAR-3 and this was blocked by AhR siRNA knockdown (Li *et al*., 2014). In contrast, results in monolayer human keratinocyte cultures, after treatment for 48 hours with AhR antagonists, showed the percentage of Ki67 positive cells had reduced (Van den Bogaard *et al*., 2015). In the same study, however, Ki67 positive basal cells were increased in skin equivalent

models compared to untreated, again demonstrating the differences between monolayer and 3D cultures. Importantly in neither the Van den Bogaard study or the results reported here was a reduction in Ki67 staining observed following treatment of skin equivalents with TCDD. These data suggest that reduction in proliferation by TCDD does not account for the phenotype observed (reduced viable cell layer).

3.3.4. TCDD treatment induces autophagy in epidermal skin equivalents

As discussed, preliminary data (Forrester thesis) suggested TCDD treatment induced autophagy. Although not significant, in monolayer primary keratinocytes TCDD treatment increased LC3II protein expression with maximal effect at day 8 and a dose dependent downregulation of P62, detected through western blotting. Electron microscopy of epidermal equivalents also suggested autophagic induction. In TCDD treated epidermal equivalents, increased vacuolisation was noted as well as identification of both early and late autophagosomes, however, this was only performed in one donor (Forrester Thesis). In the present study, confirmation of autophagic activity in epidermal skin equivalents and potential role in the chloracne phenotype model was therefore pursued.

Interestingly, TCDD treatment of epidermal skin equivalents in the present study also resulted in a significant increase in protein expression of the autophagic marker LC3II (by western blotting) and endogenous LC3 (by immunofluorescence) with concurrent downregulation of P62. Although endogenous LC3 is ubiquitously expressed, immunofluorescent staining can accurately measure autophagosome number and increased puncta suggests increased autophagic activity (Mizushima *et al*., 2010, Klionsky et al., 2016). Indeed, in the present study, a variety of techniques to detect autophagic activity were harnessed and therefore results can be interpreted with confidence that TCDD induces an increase in autophagic activity or flux (Mizushima *et al*., 2010, Menzies *et al*., 2012). Autophagy, the principle catabolic process for the lysosomal mediated degradation and recycling of damaged/excess proteins and organelles, is a well-recognised mechanism of cell survival for which the induction of LC3II and decreased expression of P62 are accepted markers of the induction of this process (Mizushima *et al*., 2010, Klionsky *et al*., 2016). However, autophagy induction can also result in cell death (Tsujimoto and Shimizu, 2005), suggesting the

hypothesis that the observed TCDD mediated reduction in viable cell layer and likely cell death, observed in epidermal skin equivalents, may be mediated by autophagy. There is known cross talk between autophagy and apoptosis (Maiuri *et al*., 2007, Gozuacik and Kimchi, 2007) and this concept is supported by TCDD induced caspase-3 staining in the current study as well as previous observations of TCDD-induced cell death of primary human keratinocytes cultured in monolayer (Loertscher *et al*., 2001a). Nevertheless, the extent of TCDD-induced apoptosis appears to be model and cell type dependent.

In the context of skin, a link between autophagy and apoptosis has already been established; eravirenz, a retroviral therapy given to patients with HIV, causes phenotypic alterations in normal human keratinocytes (NHKs) (Dong *et al*., 2013) resulting in autophagy dependent cytotoxic effects. Senescent NHEKs also display excessive autophagic activity, resulting in their subsequent death (Gosselin *et al*., 2009), an effect again dependent on the level (i.e. excessive) of autophagy induction (Deruy *et al*., 2014).

In contrast, autophagy is also known to be involved in skin homeostasis (Yoshihara *et al*., 2015) and act as a cytoprotective mechanism after UV exposure (Misovic *et al*., 2013, Vitale *et al*., 2013). In addition, remifentanil an opioid analgesic was recently found to exert a protective mechanism in human keratinocytes subject to hypoxia-reoxygenation injury, again through activation of signalling pathways associated with autophagy (Kwon *et al*., 2015).

Whether the TCDD-induced loss of viable cell layer observed in the present study is mediated by the induction of cytotoxic autophagy and/or subsequent apoptosis or if autophagy is induced as a stress response to survive TCDD toxicity remains unclear, and is the subject of the subsequent chapter to this thesis.

In summary, data in the present chapter demonstrate TCDD induces a chloracne phenotype in a robust reproducible *in vitro* skin equivalent model, associated with the reduction of a viable cell layer, AhR degradation, and an increase in CYP1A1. TCDD also causes significant induction of autophagy, apoptotic cell death and the deregulation of epidermal differentiation. The intimate relationship between autophagy, cell death and deregulated differentiation in TCDD-induced cytotoxicity is addressed in the following chapter.

3.4. Summary

- TCDD treatment of epidermal equivalents induces a chloracne-like phenotype with a significantly reduced viable cell layer and compacted stratum corneum, after 7 days

- TCDD treatment activates AhR, causing AhR degradation and CYP1A1 induction

- TCDD causes de-regulated differentiation at protein and mRNA level

- TCDD induces caspase-3 cell death but causes no significant change to proliferation

- TCDD induces LC3II accumulation and P62 reduction, indicative of autophagy

Chapter 4 Exploring the interplay between de-regulated epidermal differentiation and autophagy in TCDD-induced chloracne 2D and 3D models

4.1. Introduction

The epidermal skin equivalent model optimised in the previous chapter is both reproducible and physiologically relevant. However, generation of such models is time consuming and relatively low throughput. Therefore, a monolayer primary human keratinocyte model of chloracne, particularly if differentiated, would be beneficial. Although not as physiologically relevant, it would provide a quicker and easier method to determine specific pathways of interest induced by TCDD treatment, without the complexity of the epidermal skin equivalent model. Such a model may be adapted for high-through put screening assays applicable for drug development (to minimise the risk of chloracne for example). Further relevant mechanisms or pathways of interest could then be verified and investigated in the TCDD-induced chloracne phenotype epidermal skin equivalent model.

Results from the previous chapter revealed 10nM TCDD treatment induced de-regulated differentiation. Epidermal skin equivalents are a well-established model to investigate differentiation, with keratinocytes migrating from the basal layers to stratum corneum and forming a fully stratified epidermis. However, it is also possible to differentiate monolayer primary keratinocytes by increasing extracellular calcium concentration. Although the precise mechanism is not fully understood, it is well known that calcium plays an integral part of keratinocyte differentiation (Shrestha *et al*., 2016). Under low or normal calcium conditions (0.05-0.1mM Ca^{2+}) keratinocytes proliferate and can grow rapidly. When extracellular calcium concentration is increased (1.2-1.3mM Ca^{2+}) cells start to differentiate, cell-cell contact increases and after 5 days a state of terminal differentiation is reached (Hennings *et al*., 1980, Pillai *et al*., 1990, Yuspa *et al*., 1989). This induction of differentiation by calcium has been well researched and involves many signalling pathways which help maintain cell-cell adhesion and increase intracellular calcium concentration, as reviewed by Bikle *et al* (2012).

This method of differentiating monolayer keratinocytes is frequently used in research, particularly when exploring the role or effect of differentiation in comparison to proliferating cells (Karlsson *et al*., 2010, Lanzafame *et al*., 2015). Of note, this method was used when exploring the physiological role of AhR of endogenous signalling in keratinocyte differentiation, by van den Bogaard *et al* (2015). Initially

monolayer primary keratinocytes were cultured in both growth media (0.05mM) and high calcium (0.12mM) differentiation-inducing media to investigate AhR dependent genes and the effect of AhR antagonists on differentiation. They then explored this further in epidermal equivalents models. Interestingly, monolayer human keratinocytes treated with AhR antagonists GNF351 and CH223191 showed impaired terminal differentiation with reduced expression of loricrin, filaggrin and hornerin, whilst similar results were seen in human skin equivalents. Results demonstrated impaired epidermal stratification and altered stratum corneum formation in the 3D model, although the timing of AhR antagonist treatment did alter the effect on differentiation marker expression, as discussed in Chapter 3, section 3.3.2 (Van den Bogaard *et al*., 2015).

Results from the previous chapter also revealed significant autophagy induction by TCDD treatment. As discussed, autophagy induction in keratinocytes has been well researched and is involved in many processes, from expression of early differentiation markers (Aymard *et al*., 2011) to acting as a cytoprotective mechanism after UV exposure (Misovic *et al*., 2013, Vitale *et al*., 2013). The role of autophagy in this chloracne phenotype model is yet to be determined and is therefore a key focus of this current chapter. To explore this, modulation of autophagy is essential and there are a variety of chemical inhibitors available to target specific points of the pathway. Autophagosome formation can be blocked using PI3-kinase inhibitors such as 3-MA or wortmannin, (Wu *et al*., 2010). Later stages in the pathway can also be targeted, using microtubule disrupting agents such as vinblastine which blocks autophagosome-lysosome fusion or bafilomycin A1, a V-ATPase inhibitor which also prevents autolysosome degradation (Mizushima *et al*., 2010, Yamamato *et al*., 1998). However, as expected, chemical inhibitors can have off-target effects. Therefore, it is useful to also pursue genetic modulation of the pathway to confirm data obtained with chemical inhibitors. Key autophagy genes can be knocked down, such as ATG7 (Aymard *et al*., 2011) or BECLIN-1 (Zhang *et al*., 2015) through stable (shRNA) or transient (siRNA) transfection.

Finally, TCDD treatment of epidermal skin equivalents caused significant reduction in viable cell layer thickness. TCDD could be inducing a variety of pathways or processes responsible for this reduction of viability. For example, TCDD has previously been found to simply reduce proliferation in ovarian cancer cells (Li *et al*., 2014) and a pre-osteoblast cell line (Yu *et al*., 2014). However, Ki67 staining in

epidermal skin equivalents in the previous chapter revealed TCDD caused no significant reduction in proliferation. Alternatively, reduced viable cell layer thickness may be due to the well documented induction of terminal differentiation by TCDD as shown in monolayer normal human keratinocytes (Sutter *et al*., 2011, Sutter *et al*., 2009). In the previous chapter TCDD was found to de-regulate differentiation causing increased mRNA expression of differentiation markers, whilst protein expression decreased. Although TCDD did not induce terminal differentiation fully, this de-regulation of differentiation could also affect viable cell layer thickness.

As discussed in Chapter 3, TCDD has also previously been reported to reduce cell number in NHEKs; although Loertecher *et al*. (2001a) found no evidence for apoptosis induction. Similarly, in previous studies (Forrester Thesis) data suggested TCDD induced a caspase-independent form of cell death. In contrast, there have been reports of increased caspase-3 staining after TCDD treatment in other non-keratinocyte cell models (Morales-Hernández *et al*., 2012, Huang *et al*., 2005). Interestingly, TCDD treatment was found to also induce increased caspase-3 positive staining in the present epidermal skin equivalent model. There is known cross talk between autophagy and apoptosis (Maiuri *et al*., 2007, Gozuacik and Kimchi, 2007) and whether in this model TCDD is inducing death through apoptosis or autophagy remains unclear.

The aims of this chapter therefore, were to develop a differentiated and un-differentiated monolayer primary human keratinocyte model in which TCDD caused AhR degradation, LC3II induction and reduced cell viability. Using this model as well as epidermal skin equivalents, the role of autophagy in TCDD induced de-regulated differentiation, AhR degradation and induction of cell death, was explored with both chemical inhibition and genetic modulation of the autophagy pathway.

4.2. Results

4.2.1. Effect of a TCDD dose response in monolayer primary human keratinocytes on AhR degradation and LC3II accumulation

The principle aim of this project was to investigate the mechanisms behind the TCDD-induced chloracne phenotype. After initial work with epidermal equivalents (Chapter 3) a more high-throughput model was pursued in order to determine pathways of interest. These individual pathways would then be investigated further in the more physiological relevant epidermal equivalent model.

Firstly, to establish an optimum treatment regime, monolayer keratinocytes cultured in 0.06mM calcium medium were seeded and treated the following day with vehicle (DMSO) and a range of TCDD concentrations (0.1nM, 1nM, 10nM or 20nM). The keratinocytes were then treated every 48 hours for a total of 7 days, and harvested every 24 hours. To confirm TCDD induced AhR degradation and LC3II induction, as seen in the epidermal equivalent model, expression was determined by western blotting (Fig. 4.1, Fig. 4.2, Fig. 4.3).

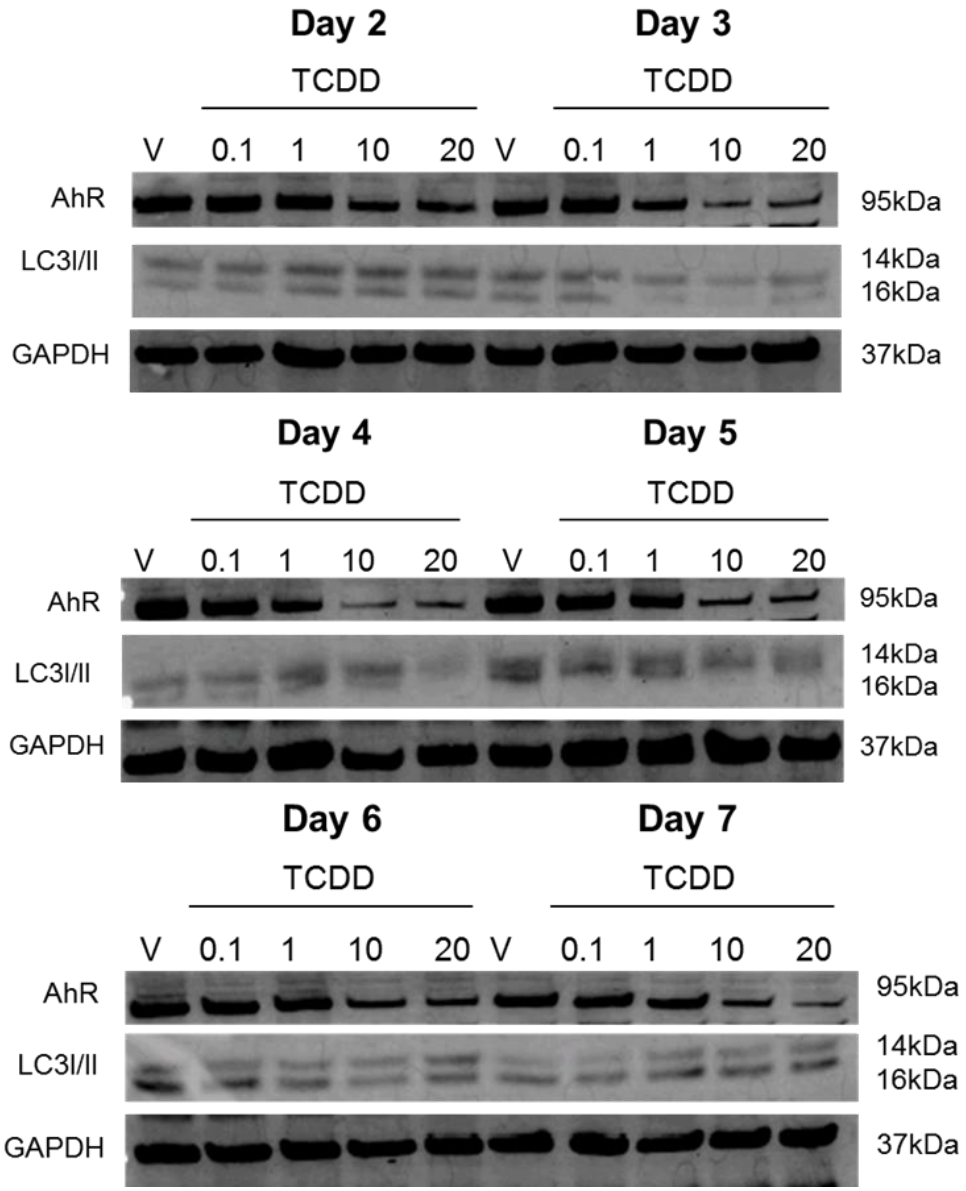

Figure 4.1 TCDD treatment alters AhR protein expression but not LC3II protein expression in monolayer primary keratinocyte cultures.

Representative western blots of AhR protein expression and LC3I/II expression in monolayer primary human keratinocytes (n=3 independent donors) following treatment with vehicle (DMSO) control, or TCDD (0.1nM, 1nM, 10nM or 20nM) every 48 hours for 7 days.

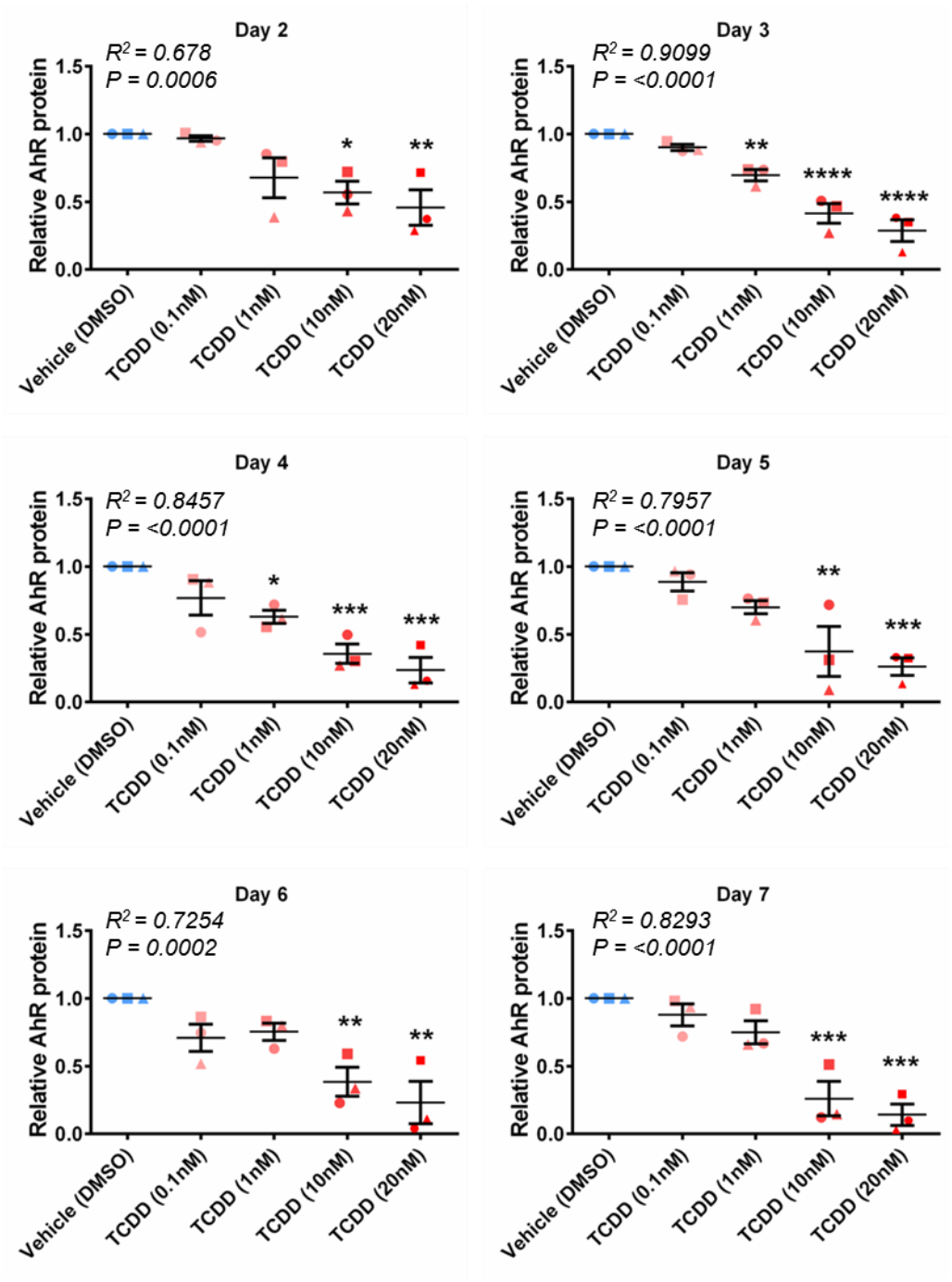

Figure 4.2 TCDD treatment induces dose dependent AhR protein degradation in monolayer primary keratinocyte cultures.

Densitometric analysis of AhR protein expression in monolayer primary human keratinocytes after treatment with vehicle (blue symbols) or TCDD (0.1nM, 1nM, 10nM or 20nM) (pink and red symbols) every 48 hours for 7 days. Each point is normalised to GAPDH loading control and expressed relative to vehicle (DMSO) control at each day. n=3 independent donors, ± SEM. Statistics were acquired by one-way ANOVA with Dunnett's multiple comparison test *p= <0.05, **p=<0.01, ***p= <0.001, ****p= <0.0001. A post-test for linear trend was also carried out (Individual R2 and P values displayed on graph)

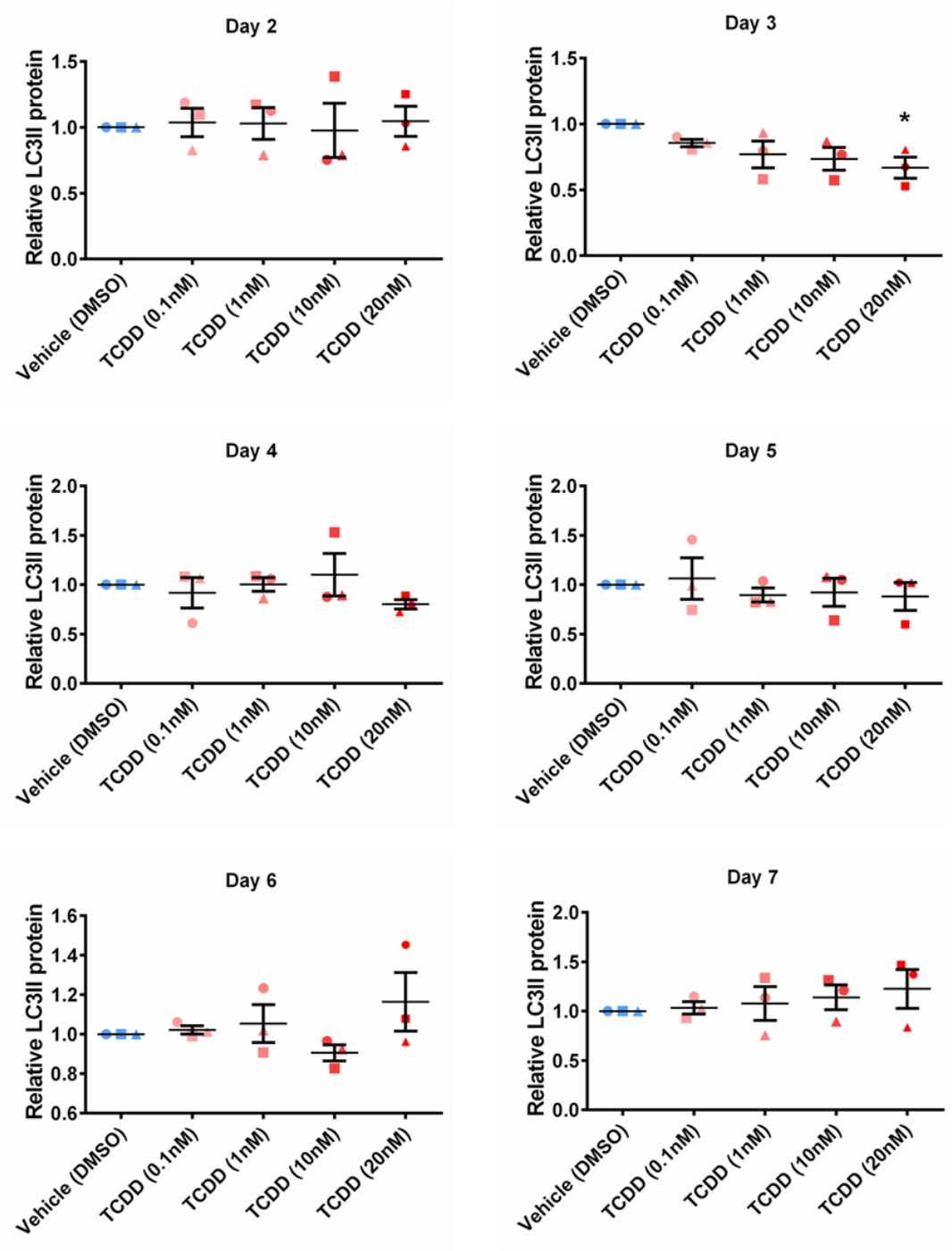

Figure 4.3 TCDD treatment does not induce a significant dose dependent increase in LC3II protein accumulation.

Densitometric analysis of LC3II protein expression in monolayer primary human keratinocytes after treatment with vehicle (blue symbols) or TCDD (0.1nM, 1nM, 10nM or 20nM) (pink and red symbols) every 48 hours for 7 days. Each symbol is normalised to GAPDH loading control and expressed relative to vehicle (DMSO) control at each day. n=3 independent donors, ± SEM. Statistics were acquired by one-way ANOVA with Dunnett's multiple comparison test *p= <0.05. A post-test for linear trend was also carried out (NS).

Densitometric analysis of AhR and LC3II protein expression on western blots were adjusted relative to GAPDH loading control and normalised to the vehicle controls at each respective time point. AhR protein expression decreased in a time and concentration dependent manner following treatment with TCDD and a dose/response curve was evident across most time points. Levels of expression were similar after treatment with both 10nM and 20nM concentrations, and seemed to flatten out, suggesting this was close to the top of a dose/response curve. Therefore, data clearly demonstrated functional interaction of TCDD with its cognate AhR receptor (Fig. 4.2). This was further verified by performing a post-test for linear trend which found this trend to be significant across all time points. Interestingly, 10nM and 20nM TCDD treatments caused significant reduction in AhR protein degradation across all time points (one-way ANOVA with Dunnett's multiple comparison test $p<0.05$, $p<0.01$, $p<0.001$) compared to vehicle (DMSO) control.

In contrast, TCDD treatment of monolayer primary keratinocytes cultures did not induce any significant increase in LC3II expression (Fig. 4.3) (one-way ANOVA with Dunnett's multiple comparison test). At day 7 there does appear to be a trend of increased LC3II expression as TCDD concentration is increased, however, this was not significant (one-way ANOVA with post-test for linear trend $p=0.2136$, $R^2=0.1492$). In general, unlike in TCDD treated epidermal equivalents, LC3II expression was very variable and overall did not seem to be significantly induced. This was also supported by the R^2 values which were all below 0.5, much lower than R^2 values for trend in AhR expression.

Of note, there was no significant change in LC3II or AhR protein expression in vehicle DMSO (1:1000) treated monolayer primary keratinocytes, over time (Appendix Fig D, [A and B]).

The concentration of TCDD used to produce the chloracne phenotype in epidermal equivalents is 10nM (Chapter 3). Therefore, statistical analysis was carried out to look into this concentration in monolayer in more detail (Fig. 4.4). Specifically, a two-way ANOVA was used to look at the difference between vehicle (DMSO) and TCDD treatment over time.

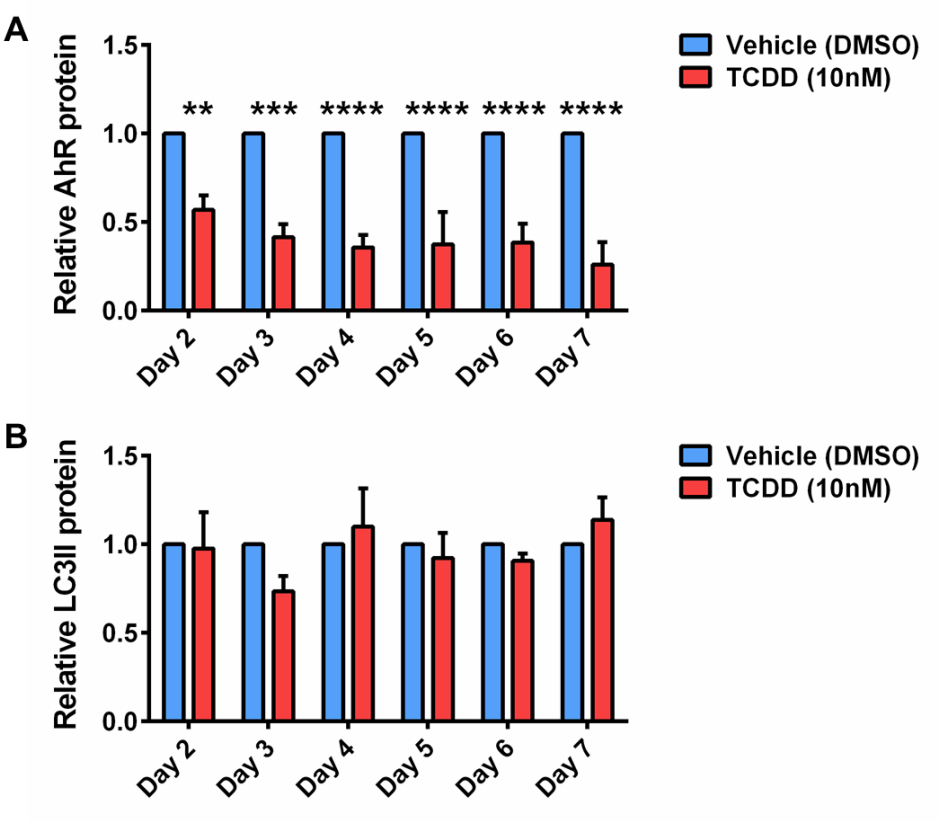

Figure 4.4 TCDD (10nM) treatment induces AhR protein degradation in monolayer primary keratinocyte cultures over time, but does not cause significant LC3II accumulation.

Densitometric analysis of A) AhR or B) LC3II protein expression in monolayer primary human keratinocytes after vehicle (blue bars) or TCDD (10nM) treatment (red bars) every 48 hours for 7 days. Each bar is normalised to GAPDH loading control and expressed relative to vehicle (DMSO) control at each day. n=3 independent donors, ± SEM. Statistics were acquired by two-way ANOVA with Bonferroni's multiple comparison test. A) **p=<0.01, ***p= <0.001, ****p= <0.0001 B) (NS)

Analysis revealed that relative to GAPDH loading control, AhR protein expression was significantly reduced after 10nM TCDD treatment of monolayer primary keratinocytes, at every time point. Although AhR degradation was significant at day 2 and 3 (two-way ANOVA with Bonferroni's multiple comparison test $p<0.01$ and $p<0.001$ respectively) degradation from day 4 onwards was more significant ($p<0.0001$). These data reinforce that TCDD was activating AhR from day 2.

In contrast there was no significant increase in LC3II expression with 10nM TCDD treatment across any time point (two-way ANOVA with Bonferroni's multiple comparison test). However, at day 4 and day 7 expression of LC3II was slightly increased.

4.2.2. High calcium conditions cause monolayer primary keratinocytes to differentiate after 5 days

After analysing the results of the time–dose response experiment (in which cells were treated every 48 hours for 7 days), the treatment regimen was modified. At 5 days 10nM TCDD treatment caused significant and reproducible AhR degradation and treating the cells for any longer may have caused cells to become over-confluent which may have caused increased variation in results. Therefore, in subsequent experiments monolayer primary keratinocytes were seeded, treated the following day and again 48 hours later then harvested at 5 days.

To further develop the high throughput monolayer model of chloracne, differentiation of keratinocytes was explored. As autophagy has been implicated in regulating keratinocyte differentiation (Akinduro *et al.,* 2016), we hypothesised that high calcium differentiation-promoting media might modulate induction of autophagy by TCDD. Calcium induced differentiation has been previously studied in many labs (Shrestha *et al*., 2016) and culture conditions used in the present study had been previously optimised in parallel studies within the lab (Martina Elias, unpublished observations). Data showed increasing extracellular calcium concentration to 1.3mM for 5 days caused a phenotypic loricrin expression to significantly increase. Filaggrin expression was technically difficult to detect and consequently expression was variable, therefore in present monolayer experiments loricrin alone was used as a terminal differentiation marker.

For the current study, primary keratinocytes were seeded and treated with vehicle (DMSO) or TCDD (10nM) in high (1.3mM calcium) and normal calcium conditions for 5 days. Loricrin expression was determined by western blotting to confirm calcium-induced differentiation was achievable (Fig. 4.5)

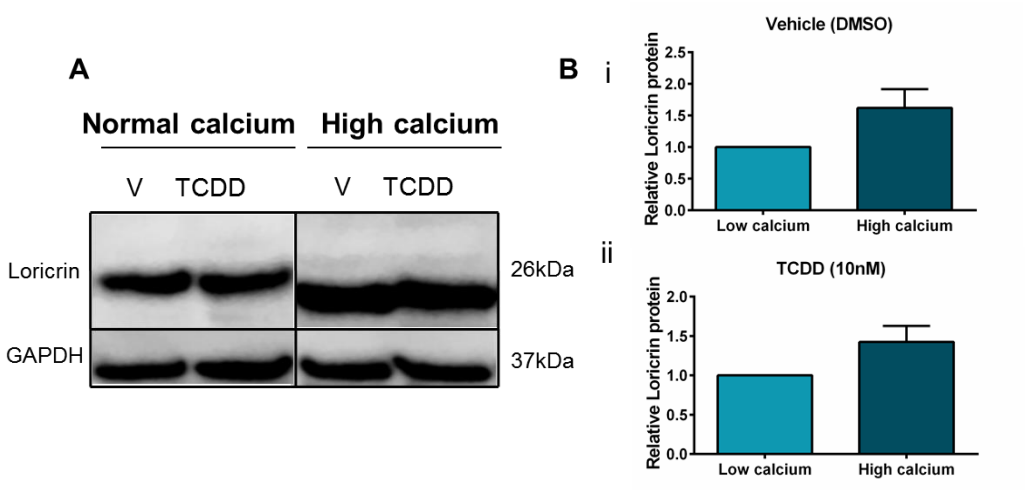

Figure 4.5 High calcium conditions induced differentiation with increased loricrin expression in monolayer primary human keratinocytes independent of treatment.

A) Representative western blot of loricrin protein expression in monolayer primary human keratinocytes following treatment with vehicle (DMSO) control or TCDD (10nM) every 48 hours for 5 days in normal and high calcium conditions. B) Densitometric analysis of loricrin expression after vehicle (DMSO) (i) or TCDD (10nM) (ii) treatment in normal calcium media (light blue bars) or high calcium media (dark blue bars) normalised to GAPDH loading control expressed relative to the respective treatments in normal calcium conditions, n=3 independent donors, ± SEM. Statistics were acquired by paired t-test (NS)

Results demonstrated, treatment of monolayer keratinocytes in high calcium media for 5 days did induce increased loricrin expression, relative to GAPDH loading control regardless of whether co-treated with TCDD or vehicle (Fig. 4.5 B) although not significant (paired t-test).

4.2.3. TCDD induces AhR degradation in differentiated and un-differentiated monolayer primary keratinocytes but does not cause a significant induction of LC3II

After confirming calcium induced differentiation in monolayer primary keratinocytes (Fig. 4.5) development of the monolayer model continued. Although earlier results (Fig. 4.4 B) suggested TCDD treatment did not induce LC3II expression in undifferentiated monolayer keratinocytes, in the fully differentiated epidermal equivalent model (which is grown under high calcium conditions) autophagy was clearly significantly induced by TCDD (Chapter 3 Fig. 3.9, Fig. 3.10). Therefore, to explore the role of differentiation further, monolayer primary keratinocytes were seeded and treated with vehicle (DMSO) or TCDD (10nM) every 48 hours for 5 days in both normal media and high calcium media. TCDD-induced AhR degradation and potential LC3II accumulation was explored by western blotting (Fig. 4.6).

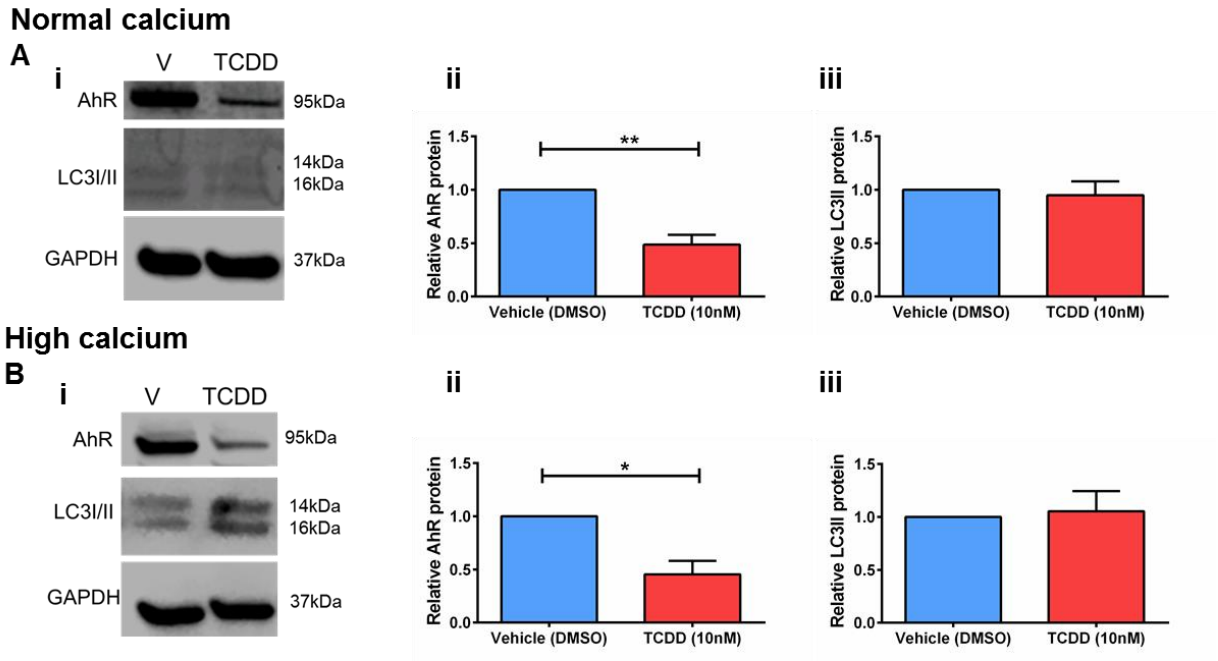

Figure 4.6 TCDD induces AhR degradation in differentiated and un-differentiated monolayer primary keratinocytes but does not cause a significant induction of LC3II.

Representative western blot of AhR protein expression and LC3II protein expression following treatment of monolayer primary human keratinocytes with vehicle (DMSO) control or TCDD (10nM) every 48 hours for 5 days in normal calcium (Ai) or high calcium (Bi). Densitometric analysis of AhR protein expression (A and B ii) or LC3II protein expression (A and B iii) after vehicle (blue bars) or TCDD (10nM) (red bars) treatment, normalised to GAPDH loading control expressed relative to vehicle (DMSO) n=4 (B) or n=7 (A) independent donors, ± SEM. Statistics were acquired by paired t-test

Results demonstrated TCDD treatment caused significant AhR degradation in primary keratinocytes treated in both normal (paired t-test $p<0.001$) and high calcium (paired t-test $p<0.05$) conditions (Fig. 4.6 A and B ii). In contrast, LC3II accumulation was not significantly induced after TCDD treatment, in either low or high calcium conditions (Fig. 4.6 A and B iii). However, there was a very slight increase in expression under high calcium conditions compared to normal calcium conditions as evident in Fig 4.6Bi although results were variable and more donors would be needed to confirm significance.

Overall data from monolayer experiments, using LC3II as a readout for autophagy induction, suggested TCDD did not significantly induce autophagy in either differentiated and un-differentiated cultures. However, results from both LC3II and P62 expression studies in epidermal skin equivalents (Chapter 3) did demonstrate TCDD caused significant autophagy induction. As such, the next phase of experiments continued to explore autophagy in monolayer but was approached from a different perspective, by manipulating autophagy flux.

4.2.4. Chemical inhibition of autophagy alters LC3II accumulation but has little effect on TCDD-induced AhR degradation in differentiated and un-differentiated monolayer primary keratinocyte cultures

To explore the role of autophagy further, the autophagy inhibitor bafilomycin A1 (bafilomycin) was initially used. Bafilomycin (as described in section 4.1) blocks autophagic flux by preventing fusion of lysosomes and autophagosomes. Monolayer primary keratinocytes were seeded and treated with vehicle (DMSO), TCDD (10nM), bafilomycin (5nM) or TCDD with bafilomycin co-treatment every 48 hours for 5 days in both normal media and high calcium media. Initially, the influence of blocking autophagy on TCDD-induced AhR degradation and potential LC3II accumulation was explored by western blotting.

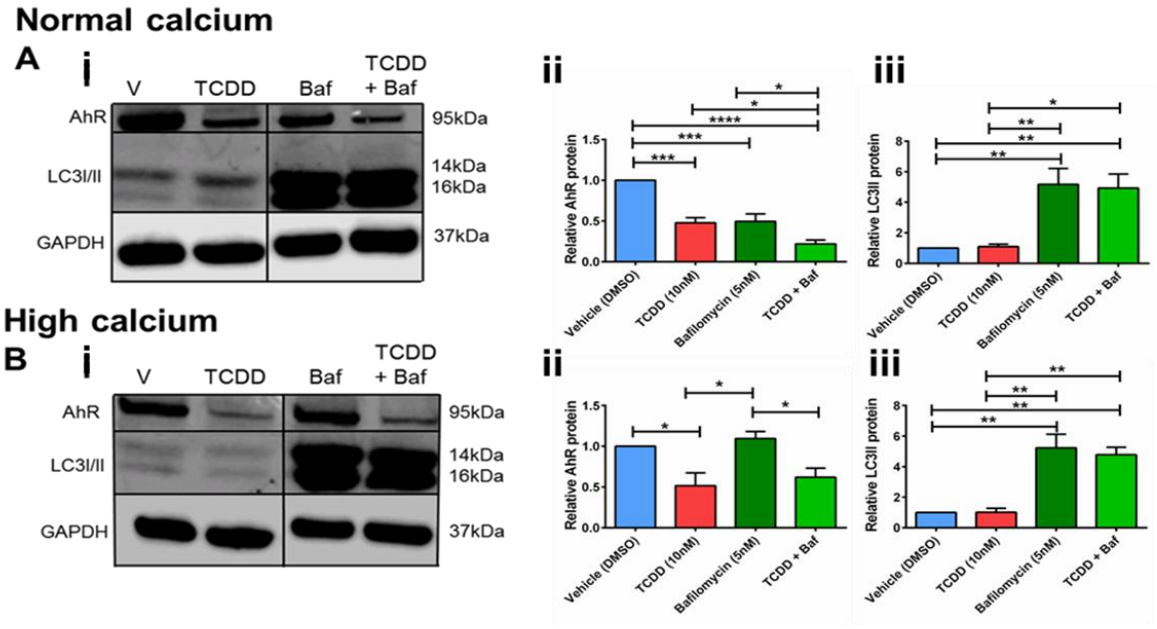

Figure 4.7 Bafilomycin co-treatment caused TCDD induced AhR degradation to be somewhat accentuated in normal calcium conditions, but had no effect in in high calcium conditions, whilst bafilomycin treatment in both conditions causes LC3II accumulation.

Representative western blot of AhR protein expression and LC3II protein expression following treatment of monolayer primary human keratinocytes with vehicle (DMSO) control, TCDD (10nM), bafilomycin (5nM) or TCDD with bafilomycin co-treatment every 48 hours for 5 days in normal calcium (Ai) or high calcium (Bi). Densitometric analysis of AhR protein expression (A and B ii) or LC3II protein expression (A and B iii) after vehicle (blue bars), TCDD (10nM) (red bars), bafilomycin (5nM) (dark green bars) or TCDD with bafilomycin co-treatment (light green bars). Each bar is normalised to GAPDH loading control expressed relative to vehicle (DMSO). n=4 (A) or n=3 (B) independent donors, ± SEM. Statistics were acquired by one-way ANOVA with Tukey's multiple comparison test *p= <0.05, **p=<0.01, ***p= <0.001, ****p=<0.0001.

Densitometric analysis revealed in normal (low) calcium conditions, TCDD (10nM) treatment caused significant AhR protein degradation (Fig. 4.7 A ii) (one-way ANOVA with Tukey's multiple comparison test, $p<0.001$). Bafilomycin treatment alone also caused a significant reduction in AhR protein expression ($p<0.001$), whilst bafilomycin co-treatment accentuated TCDD-induced AhR protein degradation, compared to TCDD treatment alone ($p<0.05$).

TCDD (10nM) treatment did not cause a significant increase in LC3II expression (Fig. 4.7 A iii), in contrast to results in epidermal equivalents. However, both bafilomycin treatment alone and co-treatment with bafilomycin caused a significant increase in LC3II accumulation compared to vehicle (DMSO) control ($p<0.01$), indicating bafilomycin did block or attenuate flux of basal autophagy.

In high calcium, TCDD (10nM) treatment caused significant AhR protein degradation compared to vehicle (DMSO) control (Fig. 4.7 B ii) (one-way ANOVA with Tukey's multiple comparison test, $p<0.05$). Interestingly, in contrast to results in normal calcium conditions, bafilomycin treatment alone caused slightly increased AhR protein expression above that of vehicle (DMSO) control, although not significant. In addition, bafilomycin co-treatment had no effect on TCDD-induced AhR protein degradation.

However, TCDD (10nM) treatment of monolayer primary keratinocytes again did not cause LC3II accumulation (Fig. 4.7 B iii) but bafilomycin treatment alone and co-treatment did induce LC3II expression significantly above vehicle (DMSO) control levels (one-way ANOVA with Tukey's multiple comparison test $p<0.01$) indicating bafilomycin blocked or attenuated flux of basal autophagy.

4.2.5. Chemical inhibition of autophagy alters loricrin expression in differentiated monolayer primary keratinocyte cultures

To investigate the potential role of autophagy in TCDD-induced de-regulated differentiation, monolayer primary keratinocytes were treated with vehicle (DMSO), TCDD (10nM), bafilomycin (5nM) or TCDD with bafilomycin co-treatment in high calcium conditions every 48 hours for 5 days. Expression of the differentiation marker loricrin was then determined by western blotting (Fig. 4.8).

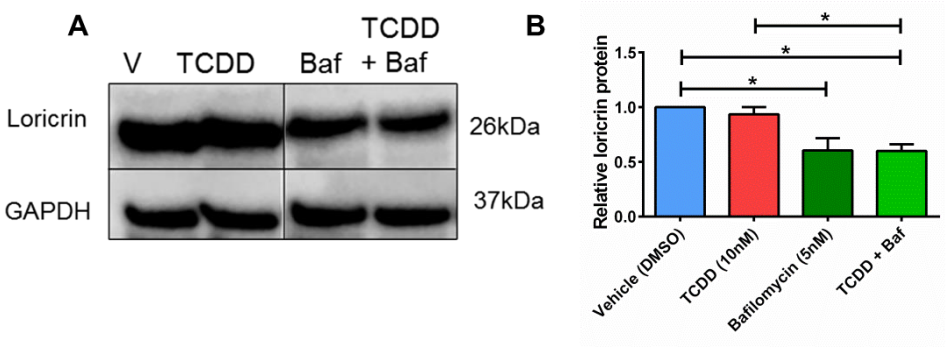

Figure 4.8 TCDD does not significantly alter loricrin protein expression in monolayer primary keratinocytes cultured in high calcium medium but bafilomycin treatment causes reduced expression.

A) Representative western blot of loricrin protein expression following treatment of monolayer primary human keratinocytes with vehicle (DMSO) control, TCDD (10nM), bafilomycin (5nM) or TCDD with bafilomycin co-treatment every 48 hours for 5 days in high calcium media. B) Densitometric analysis of loricrin expression after vehicle (blue bar), TCDD (10nM) (red bar), bafilomycin (5nM) (dark green bar) or TCDD with bafilomycin co-treatment (light green bar). Each bar is normalised to GAPDH loading control and expressed relative to vehicle (DMSO) n=3 independent donors, ± SEM. Statistics were acquired by one-way ANOVA with Tukey's multiple comparison test *p= <0.05

Densitometric analysis revealed TCDD (10nM) treatment of monolayer primary keratinocytes induced no significant change in loricrin protein expression compared to vehicle (DMSO) control (one-way ANOVA with Tukey's multiple comparison test). However, bafilomycin treatment alone caused loricrin expression to decrease significantly compared to vehicle (DMSO) control levels ($p<0.05$). Interestingly, bafilomycin co-treatment with TCDD also induced a decrease in loricrin expression, with significantly lower expression compared to both vehicle and TCDD (10nM) treated cells ($p<0.05$). However, levels were similar to that of epidermal equivalents

treated with bafilomycin alone and as such further investigation would be required to confirm if bafilomycin reduced loricrin expression in general, or if co-treatment blocked the TCDD induced effect. 4.2.6. TCDD treatment causes no significant reduction in cell viability in differentiated and un-differentiated monolayer primary keratinocytes

In the TCDD-induced chloracne phenotype, viable cell layer thickness is significantly reduced after TCDD treatment and TCDD induces caspase-3 positive staining (Fig. 3.3 and Fig. 3.8A). Therefore, to validate the high throughput monolayer primary keratinocyte model further, basic colorimetric cell viability/proliferation assays were performed. Assays included 3-(4,5-dimethylthiazol-2-yl)-2,5-diphenyltetrazolium bromide (MTT) assays (Fig 5.9) and Sulforhodamine B (SRB) assays (Fig. 4.10). Cells were seeded and treated with vehicle (DMSO), TCDD (10nM) bafilomycin alone (1.25nM, 2.5nM or 5nM) or TCDD with bafilomycin co-treatment, in both high and normal calcium conditions, every 48 hours for 3 or 5 days.

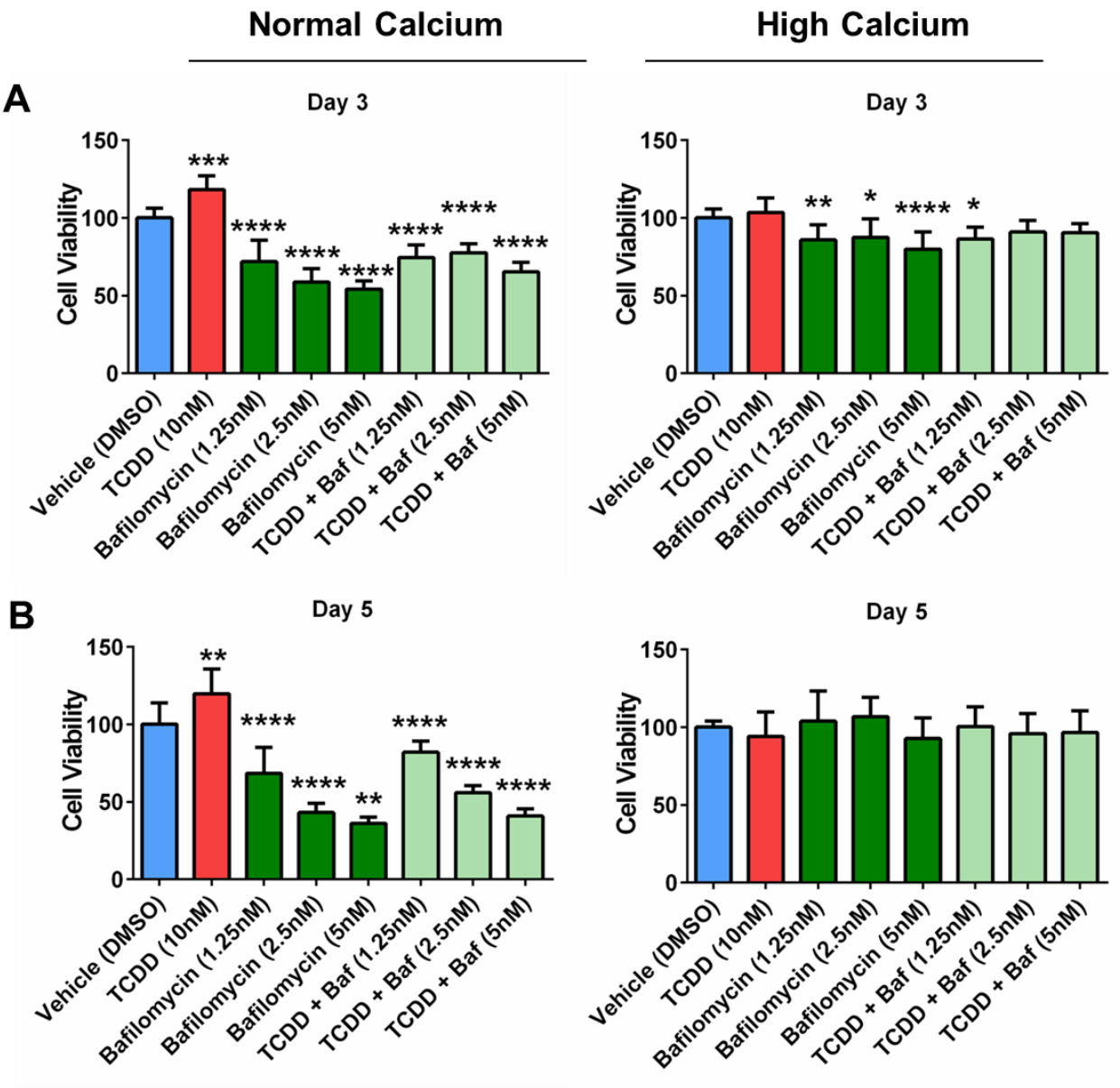

Figure 4.9 TCDD causes no significant induction of reduced cell viability at day 3 (A) or day 5 (B) in high or normal calcium conditions.

Analysis of cell viability (MTT assay) in monolayer primary human keratinocytes, in high and normal calcium following treatment with vehicle (DMSO) control (blue bars), TCDD (10nM) (red bars), bafilomycin (1.25nM, 2.5nM or 5nM) (dark green bars) or TCDD with bafilomycin co-treatment (light green bars), every 48 hours for 3 or 5 days. Each bar is normalised to GAPDH loading control expressed relative to vehicle (DMSO). n=3 independent donors, in triplicate (N=9) ± SEM. Statistics were acquired by one-way ANOVA with Dunnett's multiple comparison test *p=<0.05, **p=<0.01, ***p=<0.001, ****p=<0.0001.

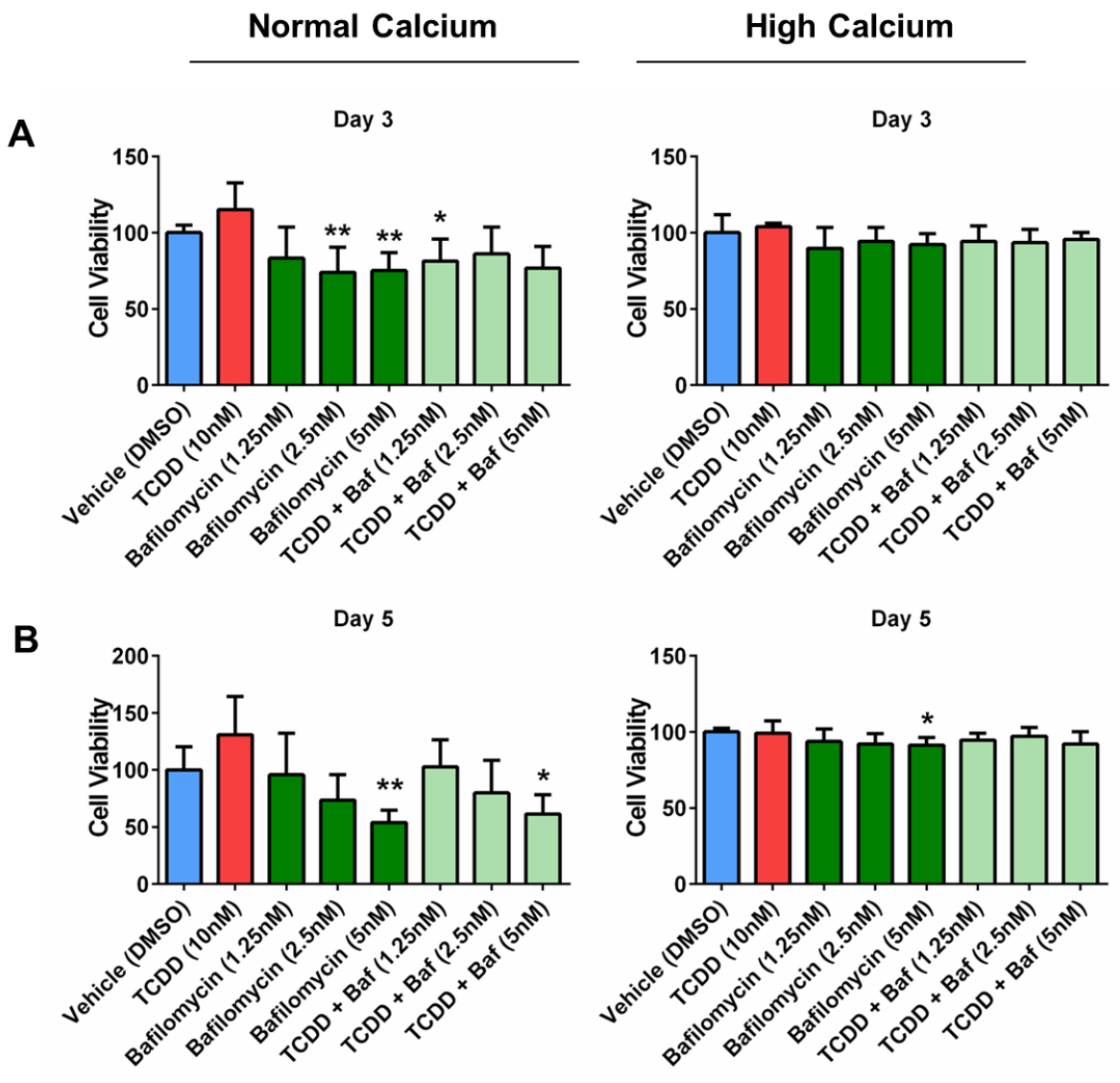

Figure 4.10 TCDD causes no significant induction of reduced cell viability at day 3 (A) or day 5 (B) in high or normal calcium conditions.

Analysis of cell viability (SRB assay) in monolayer primary human keratinocytes following treatment in normal and low calcium with vehicle (DMSO) control (blue bars), TCDD (10nM) (red bars), bafilomycin (1.25nM, 2.5nM or 5nM) (dark green bars) or TCDD with bafilomycin co-treatment (light green bar), every 48 hours 3 and 5 days. Each bar is normalised to GAPDH loading control expressed relative to vehicle (DMSO) control. n=3 independent donors, in triplicate (N=9) ± SEM. Statistics were acquired by one-way ANOVA with Dunnett's multiple comparison test *p=<0.05, **p=<0.01, ***p=<0.001, ****p=<0.0001.

In cells treated in normal calcium conditions, MTT assays (Fig. 4.9) revealed a significant increase with TCDD treatment at day 3 and day 5 compared to vehicle (DMSO) control (one-way ANOVCA with Dunnett's multiple comparison test, $p<0.001$ and $p<0.01$ respectively). Surprisingly, bafilomycin treatment alone caused a significant dose dependent decrease in cell viability at both day 3 and day 5 ($p<0.0001$, $p<0.01$). In cells treated with TCDD (10nM) with bafilomycin co-treatment (1.25nM, 2.5nM or 5nM) cell viability was also significantly reduced compared to vehicle (DMSO) control ($p<0.0001$). At day 5, this decrease in cell viability with bafilomycin co-treatment was also dose dependent, as concentration of bafilomycin increased, cell viability decreased ($p<0.0001$). However, at day 3 cell viability was slightly more variable. In general, cell viability was higher after treatment with TCDD and bafilomycin-co-treatment compared to cells treated with bafilomycin alone.

In cells treated in high calcium conditions, MTT assays revealed no significant change in cell viability at day 3 or day 5 with TCDD (10nM). At day 3, bafilomycin treatment (1.25nM, 2.5nM and 5nM) all caused a significant decrease in cell viability compared to vehicle (DMSO) control ($p<0.01$, $p<0.05$, $p<0.0001$ respectively). However, this decrease in cell viability was not as high as cells treated in normal calcium conditions. Interestingly, at day 5, bafilomycin treatment had no significant effect on cell viability. In addition, TCDD with bafilomycin co-treatment caused no significant change in cell viability, apart from a slight decrease in viability in cells treated for 3 days with TCDD and 1.25nM bafilomycin ($p<0.05$).

In cells treated in normal calcium conditions, SRB assays (Fig. 4.10) revealed a similar increase in cell number after treatment with TCDD (10nM) at day 3 and day 5 compared to vehicle (DMSO) control, but this was not significant (one-way ANOVA with Dunnett's multiple comparison test). At day 3, bafilomycin treatment alone caused significant reduction in viability at 2.5nM and 5nM ($p<0.01$). This was similar to results at day 5 where bafilomycin treatment caused a dose dependent decrease in cell viability, although only 5nM bafilomycin caused significant reduction ($p<0.01$). Co-treatment with TCDD and bafilomycin did decrease cell viability at day 3, but only TCDD with 1.25nM bafilomycin caused a significant change ($p<0.05$). In contrast, at day 5, co-treatment caused a dose dependent decrease in cell viability, with TCDD and 5nM bafilomycin causing a significant reduction in viability ($p<0.05$).

In cells treated in high calcium conditions, SRB assays revealed no significant change in cell viability at day 3 or day 5 in cells treated with TCDD (10nM). Additionally, the only significant change in cell viability was in cells treated with 5nM bafilomycin at day 5 ($p<0.05$). Bafilomycin treatment alone or co-treatment with TCDD caused no other significant change in cell viability at either day 3 or day 5 in high calcium conditions.

Bafilomycin treatment clearly attenuated basal flux of autophagy as evidenced by LC3II accumulation (Fig. 4.3, Fig. 4.4). However, bafilomycin acts primarily as a V-ATPase inhibitor, targeting lysosomal function and consequently blocking autophagy (as described in section 5.1). Therefore, although a useful tool when investigating autophagic flux, bafilomycin should really be used in the context of lysosomal activity. In the following chapter work with bafilomycin continues in epidermal skin equivalent models, investigating the role of the lysosome in the chloracne phenotype.

Therefore, to continue work exploring the role of autophagy in the present chapter, manipulation of specific autophagy genes was explored. Initially, knockdown of ATG7, required for autophagosome biogenesis (Komatsu et al., 2007) was established in monolayer (both un-differentiated and differentiated models). Once optimised, this was then taken into epidermal skin equivalents. Knockdown of BECLIN-1, involved in the beginning of the autophagy pathway, was also pursued and provided interesting results.

4.2.6. Successful siRNA knockdown of ATG7 in un-differentiated monolayer primary keratinocytes causes increased AhR and LC3II protein expression

Firstly, knockdown was established in un-differentiated monolayer primary keratinocytes. Cells were transfected with siRNA non-target (siNT) or siRNA ATG7 (siATG7). Cells were treated with either vehicle (DMSO) or TCDD (10nM) every 48 hours for 5 days. Initially, ATG7 protein expression was determined by western blotting, to verify knockdown. Protein expression of AhR and LC3II expression was then measured to investigate any effect of knockdown (Fig. 4.11).

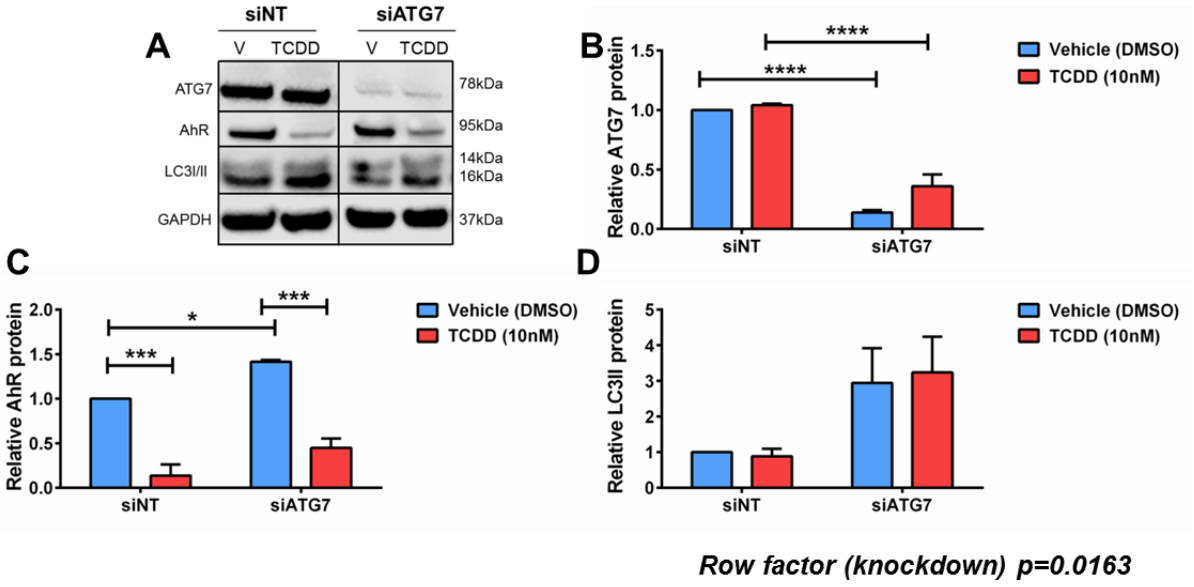

Figure 4.11 Successful siRNA knockdown of ATG7 in monolayer primary human keratinocytes causes increased AhR expression and LC3II accumulation.

A) Representative western blot of ATG7, AhR and LC3I/II protein expression following treatment of siNT or siATG7 transduced monolayer primary human keratinocytes with vehicle (DMSO) control or TCDD (10nM), every 48 hours for 5 days. Densitometric analysis of ATG7 (B) AhR (C) or LC3II (D) protein expression after vehicle (DMSO) (blue bar) or TCDD (10nM) (red bar) treatment. Each bar is normalised to GAPDH loading control relative to siNT vehicle (DMSO) control. n=3 independent donors, ± SEM. Statistics were acquired by two-way ANOVA with Tukey's multiple comparison test *p=<0.05, ***p=<0.001, ****p=<0.0001. Row factor (knockdown) is significant p=0.0163 (D).

Densitometric analysis revealed successful knockdown of ATG7 in siATG7 cells compared to siNT cells, regardless of treatment (two-way ANOVA with Tukey's multiple comparison test $p<0.0001$). AhR protein expression was significantly higher in vehicle treated siATG7 cells compared to vehicle treated siNT cells ($p<0.05$).

TCDD treatment in siNT cells induced significant AhR degradation (two-way ANOVA with Tukey's multiple comparison test $p<0.01$) compared to vehicle (DMSO) treatment, as expected. TCDD also induced significant AhR degradation in siATG7 cells ($p<0.001$). Interestingly, AhR expression was higher in TCDD treated siATG7 cells than in TCDD treated siNT cells. However, there was no significant change in LC3II expression in TCDD treated siNT cells, or TCDD treated siATG7 cells compared to vehicle controls, although in siATG7 cells, TCDD treatment did cause a slight increase in LC3II.

However, siATG7 knockdown in general caused an increase in LC3II expression. ATG7 is the conjugating enzyme for LC3, as such, by knocking down ATG7 it would be expected that LC3I expression would increase whilst LC3II expression would decrease due to lack of conjugation of LC3I to PE. Therefore, this data suggests functional ATG7 knockdown was not entirely successful and the autophagy pathway may not be fully attenuated.

4.2.7. Successful siRNA knockdown of ATG7 in differentiated monolayer primary keratinocytes does not cause significant increased AhR protein expression

Knockdown of ATG7 was also carried out in differentiated monolayer cells. Cells were transduced with siRNA non-target (siNT) or siRNA ATG7 (siATG7) and treated with either vehicle (DMSO) or TCDD (10nM) in high calcium (1.3mM) media every 48 hours for 5 days. Initially, ATG7 protein expression was determined by western blotting, to verify knockdown. Protein expression of AhR and LC3II expression was then measured to investigate any effect of knockdown (Fig. 4.12).

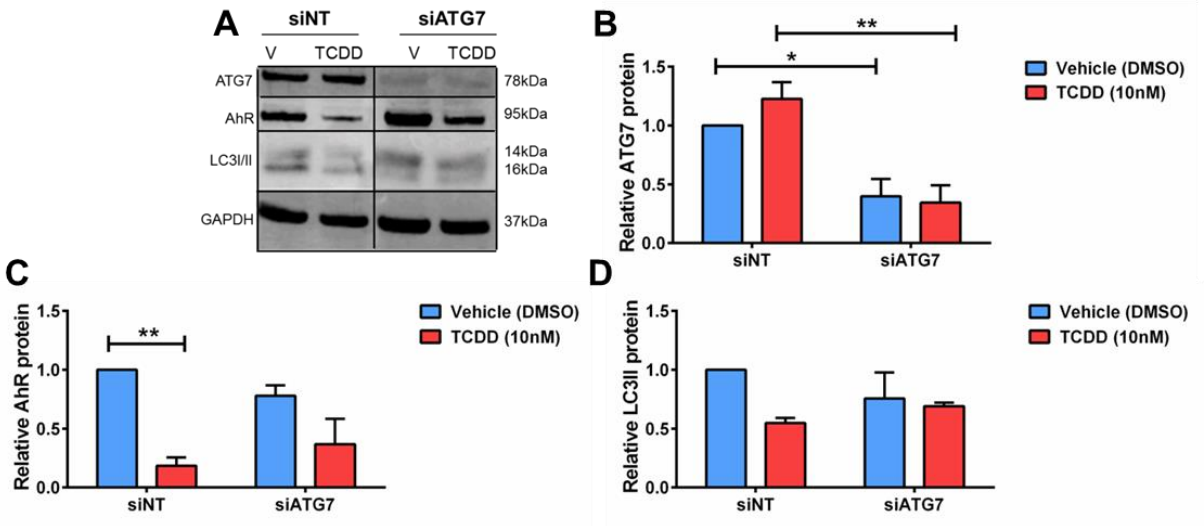

Figure 4.12 Successful siRNA knockdown of ATG7 in differentiated monolayer primary human keratinocytes causes no increase in AhR expression or LC3II accumulation.

A) Representative western blot of ATG7, AhR and LC3I/II protein expression following treatment of siNT or siATG7 transduced monolayer primary human keratinocytes in high calcium media with vehicle (DMSO) control or TCDD (10nM), every 48 hours for 5 days. Densitometric analysis of ATG7 (B) AhR (C) or LC3II (D) protein expression after vehicle (DMSO) (blue bar) or TCDD (10nM) (red bar) treatment. Each bar is normalised to GAPDH loading control expressed relative to siNT vehicle (DMSO) control. n=3 independent donors, ± SEM. Statistics were acquired by two-way ANOVA with Tukey's multiple comparison test *p=<0.05, ***p=<0.001, ****p=<0.0001

Densitometric analysis revealed successful knockdown of ATG7 in siATG7 cells compared to siNT cells after treatment with vehicle (DMSO) (two-way ANOVA with Tukey's multiple comparison test $p<0.05$) or TCDD (10nM) ($p<0.01$). In contrast to results in un-differentiated cells (Fig 4.11) siATG7 knockdown did not increase AhR

expression in vehicle treated cells and there was no significant change in LC3II accumulation after either vehicle (DMSO) or TCDD treatment.

TCDD treatment in siNT cells did induce significant AhR degradation (two-way ANOVA with Tukey's multiple comparison test $p<0.01$) compared to vehicle (DMSO) treatment, as expected. TCDD also induced AhR degradation in siATG7 cells, although not significant. However, there was no increase in LC3II expression in TCDD treated siNT or siATG7 cells compared to vehicle control cells.

4.2.8. siRNA knockdown of ATG7 in differentiated monolayer primary keratinocytes reduces loricrin protein expression

To investigate the impact of autophagy on TCDD induced de-regulated differentiation, the effect of ATG7 knockdown on loricrin expression was explored. Cells transduced with siNT and siATG7 were treated with vehicle (DMSO) or TCDD (10nM) every 48 hours for 5 days in high calcium (1.3mM) media. Loricrin expression was then determined by western blotting (Fig. 4.13).

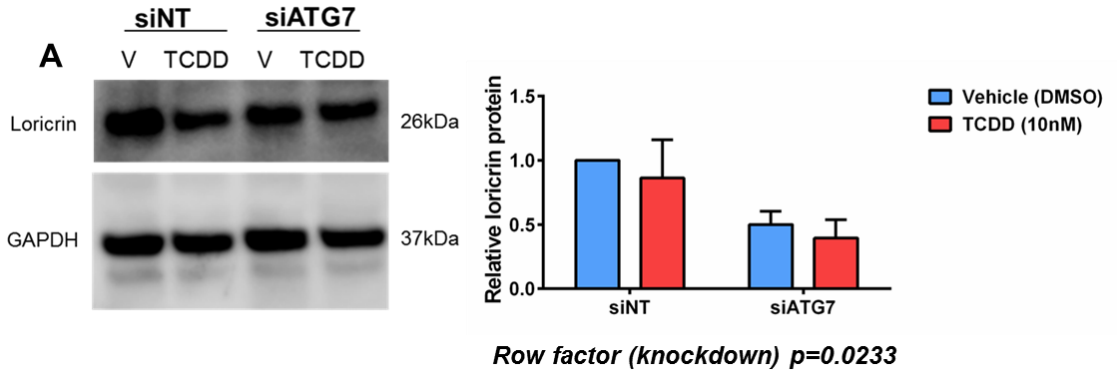

Figure 4.13 siATG7 knockdown reduces expression of loricrin in differentiated monolayer primary human keratinocytes.

A) Representative western blot of loricrin protein expression following treatment of siNT or siATG7 transduced monolayer primary human keratinocytes with vehicle (DMSO) control or TCDD (10nM), every 48 hours for 5 days in high calcium media. B) Densitometric analysis of loricrin expression after vehicle (DMSO) (blue bar) or TCDD (10nM) (red bar). Each bar is normalised to GAPDH loading control expressed relative to siNT vehicle (DMSO) control. n=3 independent donors, ± SEM. Statistics were acquired by two-way ANOVA with Tukey's multiple comparison test (NS). Row factor (knockdown) is significant p=0.0233

Densitometric analysis revealed a slight decrease in loricrin expression in TCDD treated siNT cells compared to vehicle treated. Interestingly, however, loricrin expression was lower in both vehicle (DMSO) treated and TCDD (10nM) treated siATG7 cells, compared to siNT (two-way ANOVA with Tukey's multiple comparison test, row factor p=0.0233).

4.2.9. Successful siRNA knockdown of ATG7 in epidermal skin equivalents causes increased AhR and LC3II protein expression

After successful knockdown in monolayer, siATG7 and siNT primary human keratinocytes were then seeded into epidermal equivalents, to establish a more physiologically relevant model. To understand the impact of knocking down ATG7 on AhR protein expression and LC3II accumulation, epidermal skin equivalents with siNT and siATG7 were generated and treated every 48 hours for 7 days with vehicle (DMSO) or TCDD (10nM). Western blotting was then used to determine ATG7, AhR and LC3II protein expression (Fig. 4.14).

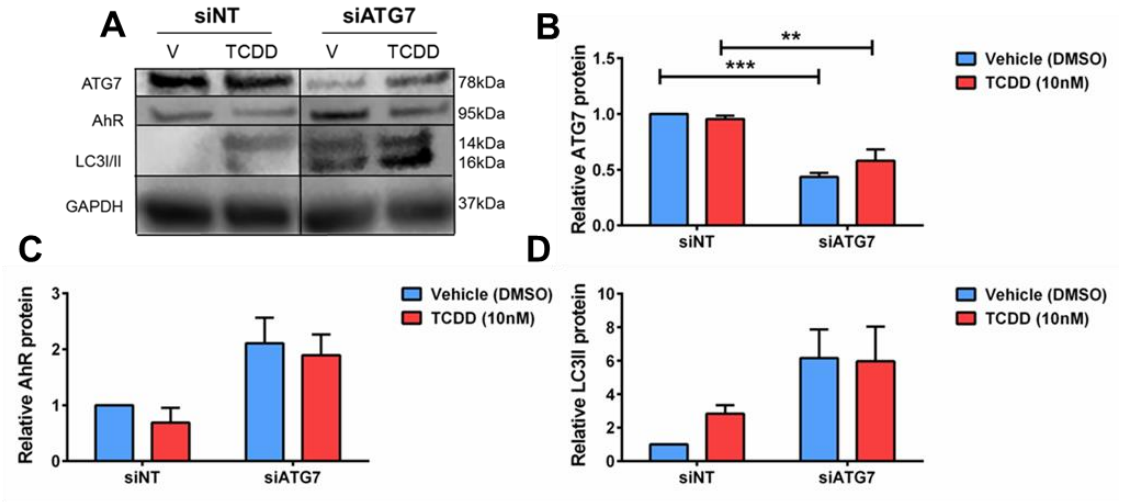

Row factor (knockdown) p=0.0074 ***Row factor (knockdown) p=0.0164***

Figure 4.14 Successful siRNA knockdown of ATG7 in epidermal equivalents causes an increase in AhR expression and LC3II accumulation.

A) Representative western blot of ATG7, AhR and LC3I/II protein expression following treatment of siNT or siATG7 transduced monolayer primary human keratinocytes in high calcium media with vehicle (DMSO) control or TCDD (10nM) treatment, every 48 hours for 5 days. Densitometric analysis of ATG7 (B) AhR (C) or LC3II (D) expression after vehicle (DMSO) (blue bar) or TCDD (10nM0 (red bar) treatment. Each bar is normalised to GAPDH loading control expressed relative to siNT vehicle (DMSO) control. n=3 independent donors, ± SEM. Statistics were acquired by two-way ANOVA with Tukey's multiple comparison test *p=<0.05, ***p=<0.001, ****p=<0.0001. Row factor (knockdown) is significant (C) p=0.0074, (D) p=0.0164.

Results revealed significant knockdown of ATG7 in siATG7 epidermal skin equivalents compared to siNT control, after both vehicle (DMSO) and TCDD (10nM) treatment (two-way ANOVA with Tukey's multiple comparison test, $p<0.001$ and $p<0.01$ respectively). AhR protein expression was also higher in siATG7 cells compared to siNT cells, regardless of treatment. In addition, siATG7 knockdown in general caused an increase in LC3II expression, suggesting the autophagy pathway had not been fully attenuated as shown previously (Fig. 4.11)

TCDD treatment in siNT and siATG7 cells causes little change to AhR protein expression and there was no significant AhR degradation compared to vehicle (DMSO) treatment. Although there was no significant change in LC3II expression in TCDD treated siNT cells, expression did increase, but there was no change in siATG7 cells compared to vehicle.

4.2.10. siRNA knockdown of ATG7 in epidermal skin equivalents prevents TCDD-induced reduced viable cell layer thickness

To further explore the role of autophagy in the TCDD-induced chloracne phenotype, particularly the reduction in viable cell layer thickness, siNT and siATG7 epidermal equivalents were generated and treated with vehicle (DMSO) or TCDD (10nM) every 48 hours for 7 days. Histological staining of formalin fixed and paraffin embedded (FFPE) sections with haemotoxilin and eoisin (H&E) was then carried out (Fig. 4.15).

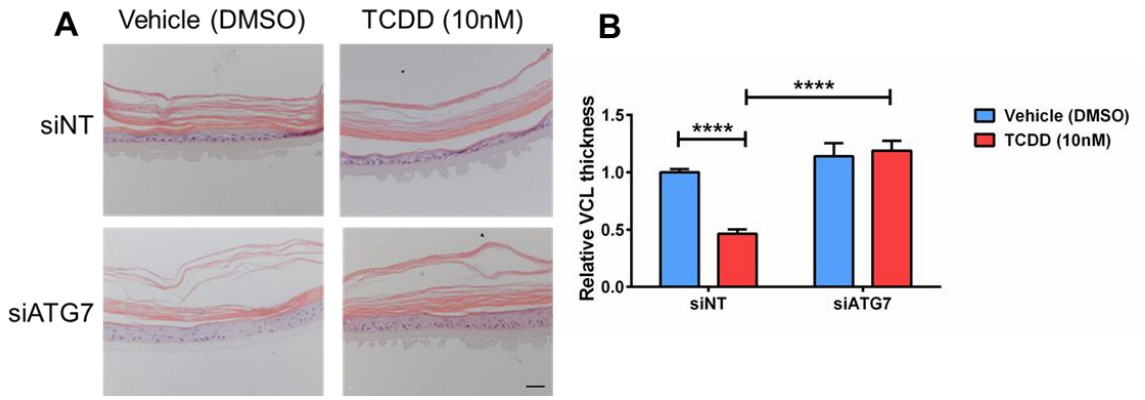

Figure 4.15 TCDD-induced reduced viable cell layer of the chloracne phenotype model is abrogated by siATG7 knockdown.

A) Representative immunohistochemical images of siNT and siATG7 transduced epidermal skin equivalents (n=3 independent donors) stained with H&E following treatment with vehicle (DMSO) control or TCDD (10nM) every 48 hours for 7 days. Scale bar = 20µm B) Relative mean viable cell layer (VCL) thickness of epidermal skin equivalents treated for 7 days with vehicle (DMSO) or TCDD (10nM) for 7 days. Each bar is expressed relative to vehicle (DMSO) control, n=3 independent donors, ± SEM. Statistics were acquired by two-way ANOVA. ****p=<0.001.

Quantitative analysis of viable cell layer thickness was performed and revealed as expected, TCDD treatment of siNT epidermal skin equivalents caused a significant reduction in viable cell layer thickness (two-way ANOVA with Tukey's multiple comparison test $p<0.0001$). Interestingly, siATG7 knockdown of epidermal skin equivalents treated with vehicle (DMSO) control caused no significant change in viable cell layer thickness. Notably, siATG7 knockdown significantly blocked TCDD-induced reduction in viable cell layer thickness ($p<0.0001$).

4.2.11. Effect of siRNA knockdown of ATG7 on filaggrin protein expression in epidermal skin equivalents

To explore the role of autophagy in the chloracne phenotype model, particularly the influence on TCDD-induced de-regulated differentiation, siNT and siATG7 knockdown epidermal skin equivalents were treated with vehicle (DMSO) or TCDD (10nM) every 48 hours for 7 days. After harvesting, immunofluorescence staining on OCT frozen sections for filaggrin was performed (Fig. 4.16).

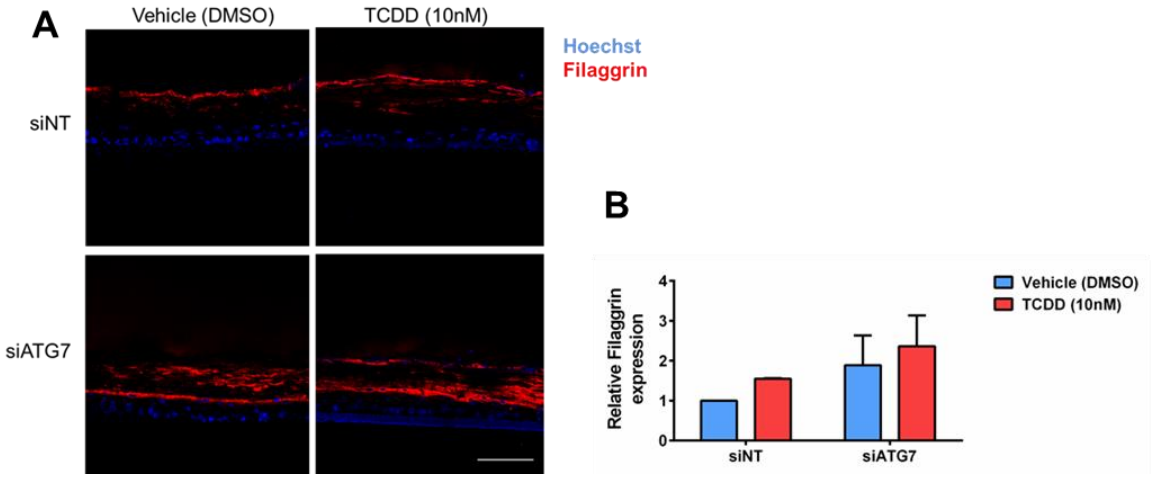

Figure 4.16 TCDD treatment induces filaggrin protein expression in siNT epidermal equivalents but not in siATG7 knockdown epidermal equivalents.

A) Representative photomicrograph of siNT and siATG7 epidermal skin equivalents treated with vehicle (DMSO) control or TCDD (10nM) every 48 hours for 7 days depicting blue Hoechst nuclear staining and Filaggrin expression (red staining). Scale bar = 100µm B) Mean filaggrin expression of siNT and siATG7 epidermal skin equivalents treated with vehicle (DMSO) or TCDD (10nM) every 48 hours for 7 days. Each bar is expressed relative to to siNT vehicle (DMSO) control, n=3 independent donors, ± SEM. Statistics were acquired by two-way ANOVA with Tukey's multiple comparison test (NS).

After quantification and statistical analysis (two-way ANOVA with Tukey's multiple comparison test) results suggested an increase in filaggrin expression after TCDD treatment in siNT and siATG7 epidermal skin equivalents compared to those treated with vehicle (DMSO) control however this was not significant. Filaggrin expression overall was higher in siATG7 knockdown epidermal skin equivalents compared to siNT regardless of treatment although again not significant and results were variable.

4.2.12. siRNA knockdown of ATG7 in epidermal skin equivalents abrogates TCDD-induced caspase-3 positive staining

To explore TCDD-induced cell death and the potential influence of autophagy, caspase-3 immunofluorescence was performed on frozen OCT sections of siNT and siATG7 epidermal skin equivalents treated with vehicle (DMSO) or TCDD (10nM) every 48 hours for 7 days (Fig. 4.17) raw values are presented in Appendix K.

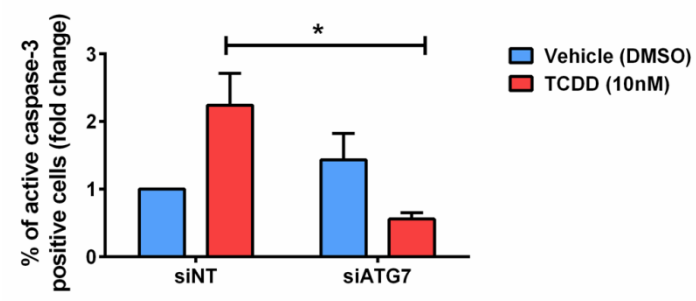

Figure 4.17 TCDD-induced increase of caspase-3 positive cells is prevented by siATG7

Mean percentage of caspase-3 positive cells presented as fold change in siNT and siATG7 transduced epidermal skin equivalents treated with vehicle (DMSO) or TCDD (10nM) every 48 hours for 7 days. Each bar is normalised relative to GAPDH loading control and expressed relative to siNT vehicle (DMSO) control n= 3 independent donors, ± SEM. Statistics were acquired by two-way ANOVA with Tukey's multiple comparison test *p=<0.05.

Images were taken along the entire length of each epidermal skin equivalent model and caspase-3 positive cells and Hoechst positive cells were counted. After quantification and statistical analysis (two-way ANOVA with Tukey's multiple comparison test) a clear trend was apparent. TCDD treatment of siNT epidermal skin equivalents caused increased caspase-3 positive staining relative to siNT vehicle treated. In general, siATG7 epidermal skin equivalents had less capase-3 positive staining compared to siNT epidermal skin equivalents. Of particular interest, TCDD treated siATG7 epidermal skin equivalents had significantly less caspase-3 positive cell staining compared to siNT TCDD treated epidermal skin equivalents ($p<0.05$).

4.2.13. Successful shRNA knockdown of BECLIN-1 alters morphology of epidermal skin equivalents

After successful siRNA knockdown of ATG7 in epidermal skin equivalents, a longer term lentiviral shRNA knockdown of another autophagy gene, BECLIN-1, was pursued. Initially, optimisation of the most effective BECLIN-1 shRNA construct to use was carried out in monolayer primary human keratinocytes (Appendix C). After this, keratinocytes were transduced with non-target control (shNT) or the selected BECLIN-1 (shBEC-1) shRNA lentivirus construct, then puromycin treated. Successful transfection efficiency was verified by imaging for GFP expression (Appendix F) and the cells were then expanded. Cells were seeded into epidermal equivalents and grown for 12 days then treated appropriately every 48 hours for a further 7 days. To establish whether successful knockdown of BECLIN-1 had occurred, epidermal equivalents were harvested and protein expression was established by western blotting (Fig. 4.18 A, B).

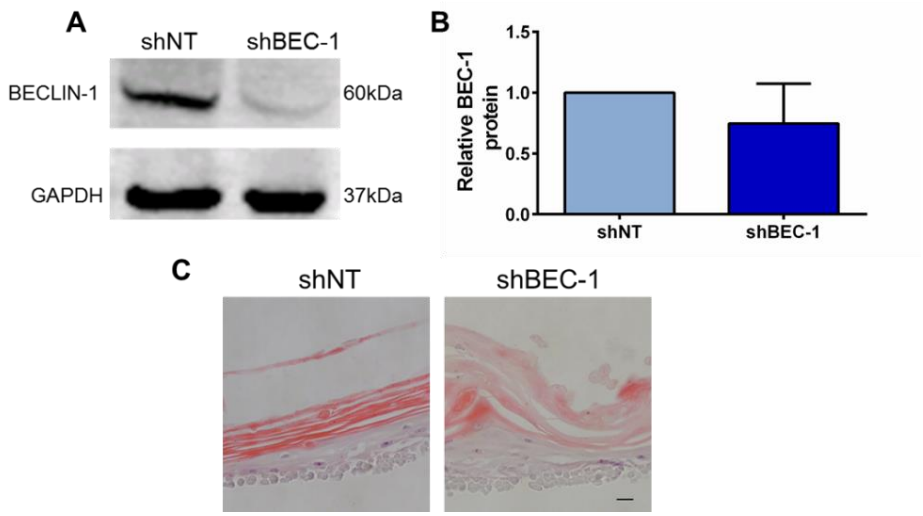

Figure 4.18 Successful BECLIN-1 shRNA knockdown causes altered morphology in epidermal skin equivalents.

A) Representative western blot of BECLIN-1 protein expression in epidermal skin equivalents. B) Densitometric analysis of BECLIN-1 expression in shNT and shBEC-1 epidermal skin equivalents. Expression is normalised to GAPDH loading control relative to shNT control. n=3 independent donors, ± SEM. Statistics were acquired by paired t-test (NS). C) Representative immunohistochemical images of shNT and shBEC-1 epidermal skin equivalents stained with H&E Scale bar = 20µm

Densitometric analysis showed successful knockdown, with decreased expression of BECLIN-1 in shBEC-1 epidermal skin equivalents compared to shNT control. However, unlike siATG7 knockdown epidermal equivalents, histological staining with haemotoxilin and eosin (H&E), revealed shBEC-1 epidermal skin equivalents to have repeatedly disrupted morphology compare to shNT (Fig. 4.18 C). Although time constraints precluded pursuit of further studies, these data suggest that BECLIN-1 might play a critical role in epidermal homeostasis and formation of an intact epidermal barrier.

4.3. Discussion

Despite optimisation of a high-throughput, monolayer chloracne model, including the use of high calcium differentiation promoting conditions, results from this chapter revealed differential effects of TCDD treatment in monolayer cultures and epidermal equivalents. Although earlier results provided clear evidence that TCDD significantly induced autophagy activation in epidermal skin equivalents (Chapter 3, Fig 3.9, Fig 3.10) there was no significant induction of LC3II in monolayer, in either normal or high calcium conditions. Furthermore, in contrast to results in epidermal skin equivalents, TCDD treatment in monolayer did not significantly reduce the number of viable cells. However, TCDD did cause significant AhR degradation in monolayer and as such these differential results are likely not due to differential activation of AhR. Rather, these data suggest that whether AhR activation activates autophagy is dependent on the specific environment and state of keratinocyte differentiation. Another key finding of this chapter was thorugh work in epidermal equivalents which indicated ATG7 knockdown blocked TCDD-induced caspase-3 expression above that of non-target control suggesting autophagy likely plays a role in TCDD-induced apoptosis.

4.3.1 Differences in response after TCDD treatment between monolayer and epidermal equivalent models of chloracne

Epidermal skin equivalents can be treated or genetically manipulated to provide a physiologically relevant model in which disease states can be researched. Nevertheless, parallel monolayer cultures can also be valuable particularly to develop more high-throughput systems when exploring biochemical and molecular pathways of interest. However, results in this chapter revealed key differences between epidermal skin equivalents and monolayer cultures.

AhR degradation is a hallmark for ligand binding and subsequent AhR activity (Ma and Baldwin, 2000) and as such AhR degradation can be used as a read out when comparing the effects of TCDD treatment in monolayer cultures and in epidermal equivalents. Results initially revealed TCDD treatment caused a dose-dependent

decrease in AhR protein expression in monolayer. Importantly, this decrease in expression, or increase in degradation continued throughout the time course suggesting TCDD was stable and not metabolically cleared by the cell, as seen in previous studies (Swanson and Bradfield, 1993, Pollenz *et al*., 2006).

However, after treatment with 10nM TCDD, results demonstrated that significant AhR degradation in monolayer occurred after only 24 hours. In contrast, AhR degradation did not occur until day 7 in epidermal skin equivalents (Chapter 3). Interestingly, similar differences in time taken for AhR degradation were seen between monolayer and epidermal equivalents (Forrester thesis). Thus, Forrester reported that in monolayer, AhR degradation occurred after only 2 days compared to 7 days in epidermal skin equivalents, although full time course experiments were not carried out (Forrester thesis). Studies in a variety of cell types have also previously shown differences in TCDD-induced AhR degradation, with degradation occurring as quickly as 3 hours post treatment in the breast tumour cell line T47D (Wormke *et al*., 2000) or 16 hours post treatment in HepG2 cells (Davarinos *et al*.,1999). Furthermore, other factors can affect AhR expression as discussed in Chapter 3, section 3.3.1, such as confluency which can alter AhR localisation and activity (Ikuta *et al*., 2009, Ikuta *et al*., 2004). Previous studies (Ikuta et al., 2009, Ikuta et al., 2006) demonstrated AhR localises to the cytoplasm when cells reach 100% confluency. Therefore, this may affect AhR degradation, as AhR is degraded in the cytoplasm. Perhaps this would explain why levels of AhR degradation increased over time in the monolayer study as cells became more confluent (reaching 100% confluency around day 5) and AhR localised to the cytoplasm. However, this hypothesis was not tested in the present study and results in high confluency epidermal equivalents do not support the idea, as one would expect AhR degradation to be quicker given the high number of cells seeded per insert. It should be noted, however, a 3D epidermal equivalent model in which cells are in contact and able to interact with other cells in all directions is very different to a simple monolayer. Therefore, to explore the effect of confluency further, it would be interesting to compare localisation of AhR in these two models and explore differences in transcriptional activity in monolayer, by measuring CYP1A1 expression.

In contrast to the significant and reproducible increase in LC3II expression after TCDD treatment seen in epidermal skin equivalents, LC3II expression did not significantly increase even at higher concentrations of TCDD in monolayer, at any

time point. There was a slight increase at day 4 after 10nM TCDD treatment and at day 7 after 10nM and 20nM TCDD treatment, but individual donors varied greatly. Consistent with these results, previous published studies have also found differences in autophagic flux between cells in monolayer (2D) and 3D cultures (Follo *et al*., 2016). For example, in malignant cancer cell lines grown in both 2D cultures and 3D multicellular spheroids, LC3II immunoblotting varied greatly. Autophagic flux was found to be higher in 2D in three cell lines and lower in 2D in the other three cell lines, compared to 3D cultures. These differences in 2D and 3D were also verified by LC3 immunofluorescence (Follo *et al*., 2016). However, bafilomycin treatment did successfully block LC3 flux in monolayer and caused accumulation of LC3II, suggesting basal autophagy was attenuated.

Although not the same treatment length as in epidermal skin equivalents, cells for monolayer experiments were still treated every 48 hours and harvested 48 hours post final treatment, as in epidermal equivalents. In addition, 7 days in monolayer culture may have affected the responsiveness of the cells, for example if they became over confluent. Furthermore, TCDD-induced AhR activity was significantly induced in both models and as such results were still comparable.

As well as un-differentiated monolayer cultures, in some experiments cultures were differentiated under high calcium conditions (1.3nM Ca^{2+}) throughout the treatment period. As epidermal equivalents are fully stratified and cells differentiated, it was important to investigate whether differentiation status altered the effect of TCDD treatment. As expected, data confirmed monolayer primary human keratinocytes did undergo differentiation when exposed to increased extracellular calcium concentration (1.3mM) for 5 days. Loricrin expression was increased regardless of treatment, in cells cultured in high calcium conditions compared to those in normal growth media (0.5mM Ca^{2+}). This confirmed the calcium differentiation technique previously optimised (Reynolds lab) was reproducible and effective.

However, one of the major issues with the monolayer chloracne model was in both high and low calcium conditions TCDD treatment did not cause any reduction in cell viability at 3 or 5 days, as assessed by SRB and MTT assays. In contrast, TCDD treatment in epidermal skin equivalents caused a dramatic and significant reduction in viable cell layer thickness and significantly induced active caspase-3 staining, indicative of apoptotic cell death (Chapter 3). In addition, bafilomycin treatment alone

in normal calcium conditions caused a significant decrease in cell viability in monolayer. Although initially an unexpected result, autophagy is a well-known cell survival mechanism, and can protect cells from apoptotic cell death (Thorburn, 2008). Therefore, if autophagy is blocked by bafilomycin, this protective homeostatic mechanism may be reduced, potentially accounting for loss of cell viability following treatment with bafilomycin. However, in contrast reduced cell viability after bafilomycin treatment was not seen in high calcium conditions, in differentiated cells. Interestingly, these results are in corroboration with siATG7 knockdown data in epidermal skin equivalents where ATG7 knockdown prevented TCDD-induced caspase-3 expression (Fig 4.17). These results suggest blocking autophagy, by bafilomycin treatment or ATG7 knockdown in differentiated models prevents cell death through apoptosis. Together these data highlight differential effects of autophagy in differentiated and undifferentiated models, whilst autophagy may be a cell survival mechanism in undifferentiated cells; it may have a cytotoxic effect in differentiated cells. Data also highlights the potential cross talk between autophagy and apoptosis in this system. However, further experiments would be required to confirm the specific role of autophagy in differentiated and undifferentiated cells and the effect on cytotoxicity. The effect of bafilomycin treatment on caspase-3 expression and the TCDD-reduced viable cell layer is explored further in Chapter 5 using the epidermal skin equivalent model.

To investigate the effect of TCDD on cell viability further, experiments were also carried out at different seeding densities to determine the effect of confluency on TCDD-induced reduced viability as studies have shown confluency can affect AhR activity (as discussed in Chapter 3 section 3.3). In addition, monolayer cultures were treated with TCDD for a longer period, up to 7 days but there was still no significant loss in cell viability in either experiment (see Appendix A and B). This result could be due to the lack of autophagy induction by TCDD in monolayer, compared to epidermal equivalents. However, this would need to be explored further as results in undifferentiated keratinocytes also suggested bafilomycin reduced cell viability.

Both SRB and MTT assays are high throughput assays frequently used to indicate reductions in cell number. However, these assays do not provide mechanistic insights into underlying mechanisms of cell death/loss of viability and results with colorimetric assays have previously been found to be variable under certain conditions (Van Tonder *et al*., 2015). Issues with the MTT assay include sensitivity to

compounds and environmental factors (Marqués-Gallego *et al*., 2010) which can lead to altered metabolism of MTT to formazan (Pagliacci *et al*., 1993) as well as underestimating cell number in a well (Haselsberger *et al*., 1996). SRB assays do have advantages over MTT assays and seem generally preferred; however, perhaps a more sensitive method providing mechanistic insight would be useful. To look into this further, and for completeness, immunofluorescence for caspase-3 could be pursued, in keeping with the staining carried out in epidermal skin equivalents (Chapter 3 Fig. 3.8 and Fig. 3.17). Cleaved caspase-3 in monolayer cultures was probed for by western blotting although the antibody used needs further optimisation as detection was not successful.

4.3.2. Effect of autophagy modulation on AhR expression and potential role of chaperone mediated autophagy in AhR degradation

As discussed in Chapter 1, section 1.2.2, AhR degradation is thought to be performed by the 26S proteasome system (Ma and Baldwin, 2000). Interestingly, however, research suggests cross-talk between autophagy and the ubiquitin-proteasome system, both of which are major protein degradation pathways (as reviewed by Lilienbaum, 2013).

Unlike autophagy, proteasome mediated degradation only occurs within the cytosol, rather than in lysosomes and it does not degrade as wide a spectrum of substrates. Proteasome mediated degradation also involves ubiquitination of target material, this ubiquitin “tagging” is used as a recognition motif (Kraft *et al*., 2010). Similarly, in a specific form of autophagy, chaperone mediated autophagy; substrates are also specifically targeted by ubiquitination but then delivered to the lysosome for degradation (Korolchuk *et al*., 2009).

This cross talk is evidenced by studies showing proteasome inhibition inducing autophagy (Ding *et al*., 2007) whilst genetic studies in mice revealed knockout of autophagy genes ATG5 or ATG7 caused accumulation of ubiquitinated proteins (Korolchuk *et al*., 2009, Hara *et al*., 2006, Komatsu *et al*., 2006).

Ma and Baldwin (2000) also discovered ubiquitination of AhR for degradation requires the ubiquitin activating enzyme E1. Interestingly, ATG7 is known to act as

an E1-like enzyme involved in two ubiquitin like reactions, ATG12 ubiquitination and LC3 lipidation which are required for the initiation of autophagy and formation of autophagosomes (Tanida *et al*., 2012). In addition, the autophagy marker protein P62, shown to be degraded in Chapter 3 after TCDD treatment, is a known ubiquitin-binding scaffold protein involved in chaperone-mediated autophagy. However, it has also been implicated in targeting material for proteasome degradation (Pankiv *et al*., 2009). Pankiv *et al* (2009) demonstrated P62 to be involved in the fast shuttling of material between nuclear and cytoplasmic compartments. As such they suggest P62 could be involved in the redistribution of proteins such as AhR which are degraded in the cytoplasm, if for example the nuclear export signal (NES) was inhibited.

Results from the present study support these findings and suggested autophagy modulation altered TCDD induced AhR degradation and AhR expression to some extent. Results were variable in monolayer studies and between calcium conditions, but transient knockdown of ATG7 in epidermal equivalents did reveal AhR expression to be increased after knockdown. However, as discussed previously, although ATG7 protein expression was reduced after knockdown, whether ATG7 function was fully attenuated remains unclear, as LC3II protein levels were unusually high (Fig 4.14). Experiments confirming successful autophagy inhibition after treatment with bafilomycin or ATG7 knockdown would need to be carried out to validate these results. In addition, measurement of other autophagy markers such as expression of P62 protein levels would be beneficial. Although the siRNA construct used for these experiments was previously optimised within the lab, it would also be useful to use additional siRNA constructs in order to confirm results and to assess which construct is most efficient within the present system. As such, whether ATG7 is specifically required for ubiquitination of AhR, or ATG7 knockdown prevents degradation by blocking chaperone mediated autophagy would need to be explored.

The present data supports the notion of crosstalk between autophagy and the ubiquitin protease pathway and suggests chaperone mediated autophagy may play a role in AhR degradation. To explore this hypothesis further, it would be interesting to measure AhR degradation after treatment with autophagy inducer rapamycin, and establish if AhR degradation was induced further. However, preliminary results (data not shown) with rapamycin treatment in monolayer keratinocytes did not show a significant change in AhR expression. However, given the issues with autophagy

induction in monolayer primary human keratinocytes, it would be preferential to treat epidermal equivalents with rapamycin.

The role of chaperone mediated autophagy in AhR protein degradation, specifically from the perspective of lysosomal function, is explored further in the following chapter.

4.3.3 TCDD-induced caspase-3 expression and reduction in viable cell layer thickness may involve autophagic activity

There are two principal forms of programmed cell death (PCD) which includes apoptosis (type 1) and autophagic cell death (type II). Autophagic cell death is a caspase-independent mechanism described as the large scale sequestration of cytoplasmic material by double-membraned autophagosomes (Kroemer and Levine, 2008). Cells undergoing autophagic cell death can appear vacuolated and have distinct non-apoptotic morphology. However, whether this increased vacuolization is actually indicative of defects in autophagosome maturation remains unclear (Kroemer and Levine, 2008). Autophagic cell death still remains relatively controversial and indeed cells often display both apoptotic and autophagic markers.

Many researchers believe that although large scale autophagy can occur, it is unlikely the cell dies through excessive autophagy alone (Kroemer and Levine, 2008). Instead, research suggests there is crosstalk between autophagy and apoptosis with interactions between autophagy and apoptotic machinery (Maiuri *et al*., 2007, Gonzalez-polo *et al*., 2005). Studies have shown autophagy preceding apoptosis and induction of apoptosis has been found to depend on autophagy activation. For example, work by Xue *et al* (1999) showed the autophagy inhibitor 3-MA was found to delay caspase-activation. Previous studies have also found BECLIN-1 knockdown to prevent feroniellin A (a novel organic furanocoumarin) induced-apoptosis and rapamycin increased feroniellin-induced apoptosis in lung cancer cells (Kaewpiboon *et al*., 2014). Interestingly, as found in the present study, inhibition of the autophagy pathway by chemical inhibitors (bafilomycin or 3-MA) or genetic inhibition by knockout of ATG7 or BECLIN-1 prevented cleaved caspase-3 activity and prevented apoptosis in CD4+ T cells (Espert *et al*., 2006).

Results from the current chapter indicate cross-talk between apoptosis and autophagy is occurring. Knockdown of siATG7 significantly blocked the TCDD-induced reduced viable cell layer in epidermal equivalents. Furthermore, TCDD-induced caspase-3 staining, indicative of apoptotic cell death, was also blocked by siATG7 knockdown. It is unlikely TCDD-induced autophagy in epidermal skin equivalents is solely a stress induced protective response, as blocking autophagy would exacerbate caspase-3 staining. Instead, caspase-3 staining is prevented with siATG7 knockdown. Therefore, it is hypothesised that TCDD induces autophagy and this induces death through apoptosis.

To further confirm TCDD-induced apoptosis, knockout of key apoptosis genes e.g. from the bcl-2 family (as discussed in section 1.6.1) or chemical inhibition of caspases through Z-VAD^{FMK} would be useful to confirm TCDD-induced apoptosis.

4.3.4. The role of autophagy in TCDD-induced de-regulated differentiation

Data in Chapter 3 revealed TCDD treatment of epidermal equivalents induced a reduction in differentiation protein expression. In addition, as discussed in Chapter 1, section 1.5.3, studies have shown autophagy plays a role in skin homeostasis and keratinocyte differentiation.

Specifically, studies in ATG7 knockout mice reveal autophagy to somewhat be required for and play a significant role in, differentiation (Yoshihara *et al*., 2015). Skin from ATG7 knockout mice was found to not only have impaired hair growth, but hyperkeratosis and reduced immunostaining of differentiation proteins including filaggrin, loricrin and involucrin. In addition, studies carried out on the HaCat cell line have suggested autophagy may be used as a signal to initiate keratinocyte commitment to differentiation *in vitro* (Aymard *et al*., 2011). In accordance with this, results in the present study demonstrated inhibition of autophagy by bafilomycin treatment or siATG7 knockdown, also altered differentiation patterns and caused loricrin expression to decrease in the differentiated monolayer model.

In addition, data from preliminary BECLIN-1 knockdown epidermal skin equivalent models found morphology of the skin equivalents to be disrupted to the extent that they were not useable. Although interesting, the role of BECLIN-1 in epidermal

homeostasis was not able to be explored further in this thesis. However, unpublished data (Lovat group, Newcastle University) has found a significant correlation between AMBRA-1 and epidermal differentiation. With AMBRA-1 found to promote differentiation. AMBRA-1 is an activating molecule in BECLIN-1 mediated autophagy and promotes the binding between BECLIN-1 and target kinase VPS34 (Yazdankhah *et al*., 2014). Together these data suggest both BECLIN-1 and AMBRA-1 may de-regulate differentiation. As morphology was disrupted, work with BCELIN-1 knockdown was not continued to explore the role of autophagy in the TCDD induced chloracne phenotype.

In contrast to monolayer studies and previous studies in epidermal equivalents (Chapter 3 Fig. 3.6), TCDD treatment appeared to increase filaggrin expression in siNT epidermal equivalents although this was not significant. Knockdown of ATG7 also caused increased filaggrin in vehicle treated epidermal skin equivalents, and expression was higher again in TCDD treated, although again this was not significant and individual donors varied greatly. This potential increase in filaggrin expression may be due to donor variability, but it is possible that the siRNA transfection process de-regulated the morphology of the epidermal equivalents somewhat and may have induced a compensatory acceleration of differentiation. However, regardless of the precise role of autophagy, as the literature suggests, autophagy can influence differentiation status and as such the study should be repeated to rule out donor variability.

Data in this chapter presents novel findings that autophagy is indeed involved in the chloracne phenotype model and is likely involved in TCDD-induced apoptotic cell death. Due to the issues discussed with monolayer keratinocytes, including variable results and lack of TCDD-induced autophagy, subsequent experiments were carried out in the more physiologically relevant epidermal skin equivalent models. Studies in the next chapter continue to explore mechanisms involved in the chloracne phenotype model. Focus is particularly on the potential role of the lysosome in TCDD-induced autophagy and apoptosis. In addition, the role of the lysosomal protease cathepsin D is explored, following on from preliminary data (Forrester thesis) which found TCDD induced cathepsin D expression

4.4. Summary

- TCDD treatment in monolayer cultures induced AhR degradation, but did not cause LC3II accumulation indicative of autophagy induction

- TCDD treatment in monolayer cultures did not cause a reduction in cell viability

- siATG7 knockdown in epidermal skin equivalents blocked the TCDD-induced reduction in viable cell layer

- TCDD induced increased caspase-3 staining in siNT epidermal skin equivalent models, indicative of apoptosis

- siATG7 knockdown in epidermal skin equivalent models prevented TCDD-induced caspase-3 positivity, suggesting autophagy causes apoptotic cell death

Chapter 5 Crosstalk of lysosomal processing in the TCDD-induced chloracne phenotype

5.1. Introduction

Degradation of cytoplasmic material via autophagy is dependent on lysosomal function and the two pathways are very much inter-related. As discussed in previous chapters, autophagy induction contributes to the TCDD induced chloracne phenotype model. The present chapter explores the potential role of lysosomal function, with a focus on the lysosomal protease cathepsin D, as outlined below.

Lysosomes are single membraned, digestive organelles present in almost all eukaryotic cells (Shen and Mizushima, 2014). Within the lysosome are more than 50 acid hydrolases, specific for degradation of a range of macromolecule targets (Mindell, 2012). Therefore, a key feature of a lysosome is its acidic environment (pH 4.5-5.0) to maintain optimum enzymatic activity (Shen and Mizushima, 2014). This acidic environment is maintained by the lysosomal membrane which contains over 20 lysosomal membrane proteins, one of the most important membrane proteins is the vacuolar type H(+)-ATPases (V-ATPases) which uses ATP to pump protons into the lumen of the lysosome and create an acidic environment (Mindell. 2012). Of note, bafilomycin used throughout this study targets lysosomal V-ATPases and alters acidification of the lysosome which has been found to prevent autophagosome and lysosome fusion (Yamamoto *et al*., 1998, Klionsky *et al*., 2008). Indeed, increasing the pH of acidic compartments independent of V-ATPases also effects fusion of autophagosomes and lysosomes (Kawai *et al*., 2007). Kawai *et al* (2007) hypothesise that autophagosome and lysosome fusion is regulated by pH to prevent inefficient fusion, as material would not be successfully degraded if the pH in the lysosome (and autolysosomes) is incorrect. In contrast, Mauvezin *et al* suggest lysosomal acidification is not a prerequisite for fusion, and that bafilomycin inhibits fusion independent of its effect on lysosomal pH (Mauvezin *et al*., 2015)

Although LC3II protein expression data suggested that bafilomycin caused basal autophagy blockade, it would perhaps be more appropriate to consider bafilomycin in the context of lysosomal activity. Indeed, literature published from early studies using bafilomycin and its subsequent binding to the lysosomal V-ATPase, found treatment reduced lysosomal degradation of target material, such as ^{125}I-labeled epidermal growth factor (EGF) in A431 cells (Yoshimori *et al*., 1991). Consequently, although

treatment with bafilomycin continued in this chapter in epidermal skin equivalents, results are considered from the perspective of its effects on lysosomal function.

As described in Chapter 1 (section 1.8) lysosomal membrane permeabilisation (LMP) in which the contents of the lysosome are leaked into the cytosol initiating degradation of cellular components, can induce cell death. The extent of LMP determines the morphological features of cell death (Aits and Jatattela, 2013). Complete disruption of the lysosome provokes uncontrolled death by necrosis, whilst, of importance to the present study, partial or selective LMP induces apoptosis (Boya and Kroemer, 2008). The release of cathepsins into the cytosol is now widely accepted to be associated with both intrinsic (Johansson *et al*., 2003) and extrinsic apoptosis (Guicciardi *et al*., 2000). Specifically, cathepsin D, B and L are all recognised as having a role in apoptosis signalling (Johansson *et al*., 2010, Repnik *et al*., 2010, Chwieralski *et al*., 2006). For example, inhibition of cathepsin D by treatment with pepstatin A in human foreskin fibroblasts prevented staurosporine-induced cytochrome *c* release, caspase activation and consequently delay cell death (Johansson *et al*., 2003). Similarly, in mouse models of acute kidney injury, inhibition of cathepsin D with pepstatin A improved kidney function, reduced apoptosis and improved cell viability even in hypoxic conditions (Cocchiaro *et al*., 2016)

Interestingly, studies have also already revealed AhR expression can influence lysosomal mediated apoptosis. In a study using the lysosomal sensitiser NPe6 and photo dynamic therapy (PDT) to induce lysosomal disruption and apoptosis, the development of apoptosis was delayed and expression of lysosomal contents was reduced in AhR deficient cells compared to the parental line (Caruso *et al*., 2004). Later studies also supported these findings, with AhR content effecting susceptibility to TNF-α induced apoptosis (Caruso *et al*., 2006).

The lysosomal aspartic protease cathepsin D is of particular interest in this project. Previous studies (Forrester thesis) found TCDD treatment of epidermal skin equivalents to de-regulate cathepsin D expression. Ingenuity Pathway Analysis (IPA) conducted by Astra Zeneca (Forrester thesis) also revealed interactions between cathepsin D and AhR as described in Chapter 1 sections 1.7.1). Data suggests a role for AhR in cathepsin D transcription, even in the absence of an AhR agonist (Wang *et al*., 1999). Cathepsin D has also been found to have a role epidermal

differentiation, particularly in regulation and activation of TGM-1 (as described in Chapter 1 section 1.7.2) a key transglutaminase enzyme required for cornification.

The aims of this chapter were therefore, to explore the role of lysosomal processing in a TCDD-induced chloracne phenotype model. Results have already demonstrated that TCDD significantly induces autophagy as well as caspase-3 positive staining, indicative of apoptotic cell death. In addition, data suggested autophagy, possibly chaperone-mediated autophagy, influenced levels of AhR degradation. Given the involvement of lysosomes in (macro) autophagy, chaperone mediated autophagy and apoptosis, it was important to also explore the role of lysosomal function. Cathepsin D was also of particular interest after previous preliminary data (Forrester Thesis) as well as the documented relationship with AhR and the role of cathepsin D in epidermal differentiation. Both chemical and genetic inhibition of lysosomal function and cathepsin D were performed in epidermal skin equivalents and the effect on AhR degradation, LC3II accumulation, differentiation and cell viability were explored.

5.2. Results

5.2.1. TCDD treatment induces LAMP2 expression in primary human epidermal skin equivalents.

The transmembrane glycoprotein LAMP2 (lysosomal associated membrane protein 2) is found in the lysosomal membrane and is ubiquitously expressed (Eskelinen, 2006). It plays a key role in lysosome biogenesis and is important in trafficking and fusion with autophagosomes (Saftig *et al*., 2010). Previous studies have suggested LAMP2 expression may be related to an increase in phagocytic or immunological responses as well as accumulation of lysosomes (Hua *et al* 1998, Wu *et al*., 2011). Therefore, immunofluorescence staining for LAMP2 was carried out to explore the effect TCDD treatment has on lysosome expression. Human epidermal skin equivalents were generated and then treated with vehicle (DMSO) or TCDD (10nM) every 48 hours for 7 days. After harvesting, immunofluorescence staining on OCT frozen sections revealed an increase in LAMP2 expression after TCDD treatment relative to vehicle control (Fig. 5.1). LAMP2 was detected in both the high suprabasal layer and basal layer, although only in the basal layer did expression appear to be induced after TCDD treatment. Quantification and statistical analysis (paired t-test) found this increased expression to be not significant, however, there was a clear trend.

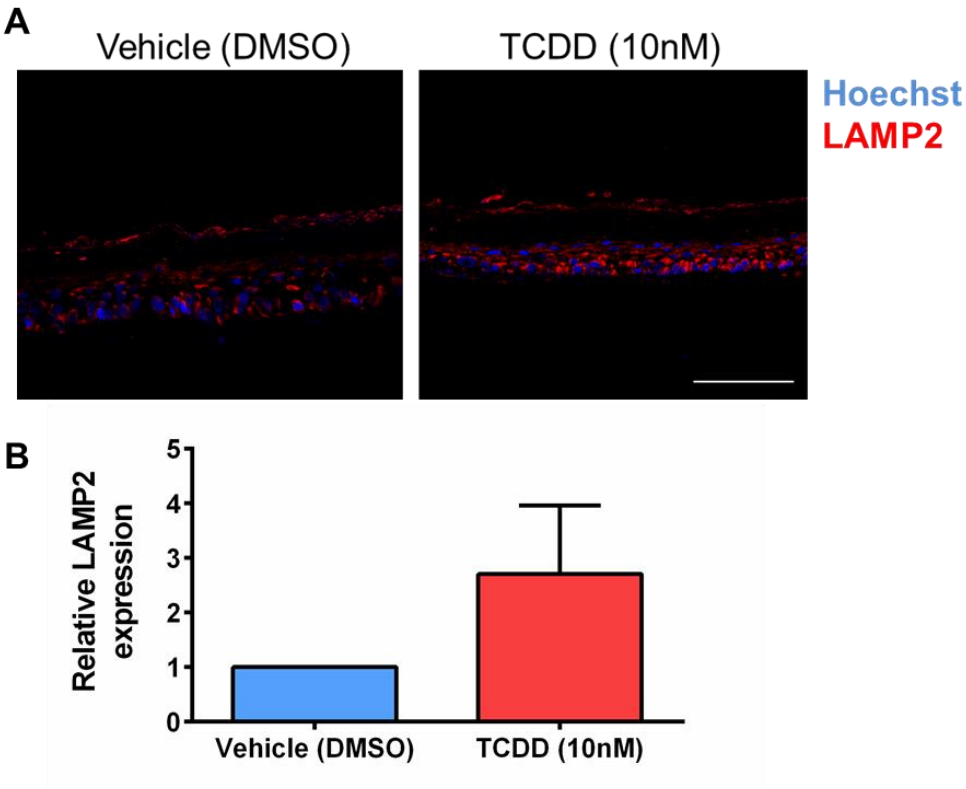

Figure 5.1 TCDD-induced LAMP2 expression in epidermal skin equivalents.

A) Representative photomicrograph of epidermal equivalents treated with vehicle (DMSO) or TCDD (10nM) every 48 hours for 7 days depicting Hoechst nuclear staining (blue fluorescence) and LAMP2 staining (red fluorescence). n=3 independent donors, scale bar 100µm. B) Mean relative LAMP2 expression in epidermal equivalents treated for 7 days with vehicle (DMSO) or TCDD (10nM). Each bar is expressed relative to vehicle (DMSO) control LAMP2 expression, n= 3 independent donors, ± SEM. Statistics were acquired by paired t test (NS).

5.2.2. Inhibition of lysosomal function alters TCDD-induced AhR degradation, LC3II accumulation and CYP1A1 expression in primary human epidermal skin equivalents.

As discussed in Chapter 4 (sections 4.2.4, 4.2.5 and 4.2.6), bafilomycin A1 can be used as an autophagy pathway inhibitor, by preventing autophagosome and lysosomal fusion. However, specifically, bafilomycin is a V-ATPase inhibitor (Yamamoto *et al*., 1998) which can prevent acidification of the lysosome and therefore successful degradation of material. As such bafilomycin can also be used to investigate lysosomal processing and function. Studies in monolayer keratinocytes indicated bafilomycin altered AhR protein expression (Chapter 4, section 4.7). To explore the potential role of the lysosomes in the TCDD-induced chloracne phenotype, human epidermal skin equivalents were treated with vehicle (DMSO), TCDD (10nM), bafilomycin (5nM) or TCDD with bafilomycin co-treatment every 48 hours for 7 days. Firstly, to confirm TCDD induced AhR degradation and LC3II induction, expression was determined by western blotting (Fig. 5.2).

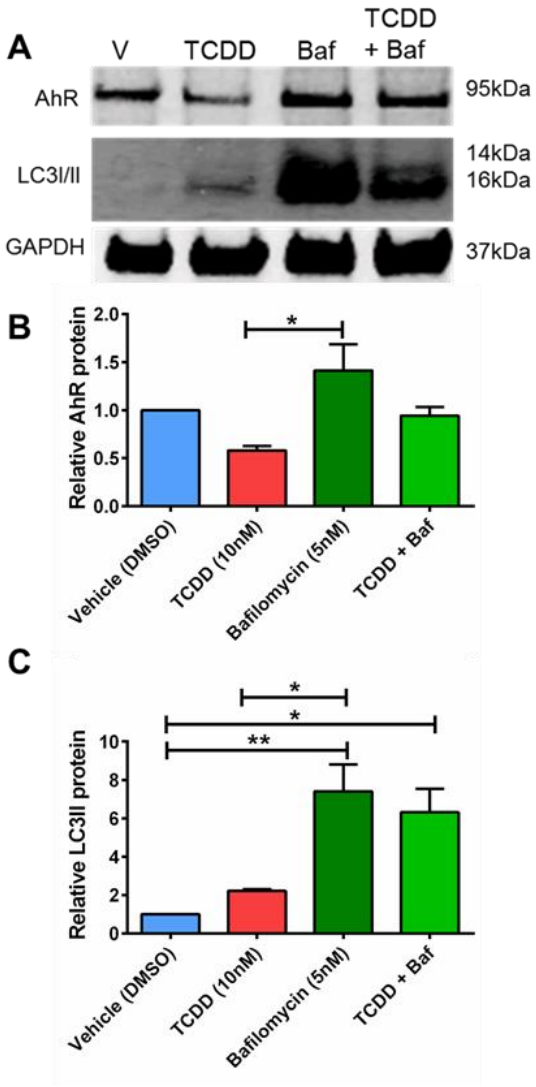

Figure 5.2 Bafilomycin co-treatment causes LC3II accumulation to be accentuated and AhR expression to increase slightly in epidermal equivalents

A) Representative western blot of AhR and LC3II protein expression following treatment of epidermal equivalents with vehicle (DMSO), TCDD (10nM), 5nM bafilomycin or TCDD with bafilomycin co-treatment every 48 hours for 7days. Densitometric analysis of AhR expression (B) or LC3II expression (C) after vehicle (blue bars), TCDD (10nM) (red bars), bafilomycin (dark green bars) or TCDD with bafilomycin co-treatment (light green bars). Each bar is normalised GAPDH loading control expressed relative to vehicle (DMSO) control. n=3 independent donors, ± SEM. Statistics were acquired by one-way ANOVA with Tukey's multiple comparison test *p= <0.05, **p=<0.01.

Results suggested AhR protein expression decreased with TCDD treatment, compared to vehicle (DMSO) control, consistent with earlier data (Chapter 3, Fig. 3.4). Interestingly, treatment with bafilomycin alone suggested an increase in AhR protein expression. Similarly, bafilomycin co-treatment caused TCDD-induced AhR degradation to be reduced. Results also showed TCDD treatment of human epidermal skin equivalents to cause LC3II accumulation, again, in keeping with earlier data in which TCDD caused a significant increase in LC3II accumulation, due to increased donor numbers (Chapter 3 Fig. 3.6, Fig. 3.7). As expected, bafilomycin

treatment caused a significant increase in LC3II expression (one-way ANOVA with Tukey's multiple comparison test, $p<0.05$, $p<0.01$ Fig. 5.2 C) thus confirming lysosomal processing and LC3I/II flux was successfully attenuated. To gain further evidence of TCDD-induced activation of AhR, mRNA levels of AhR as well as CYP1A1 (as a downstream target of AhR activation) were quantified. Epidermal skin equivalents were again treated for 7 days with vehicle (DMSO) or TCDD (10nM), bafilomycin (5nM) or TCDD with bafilomycin co-treatment (Fig. 5.3).

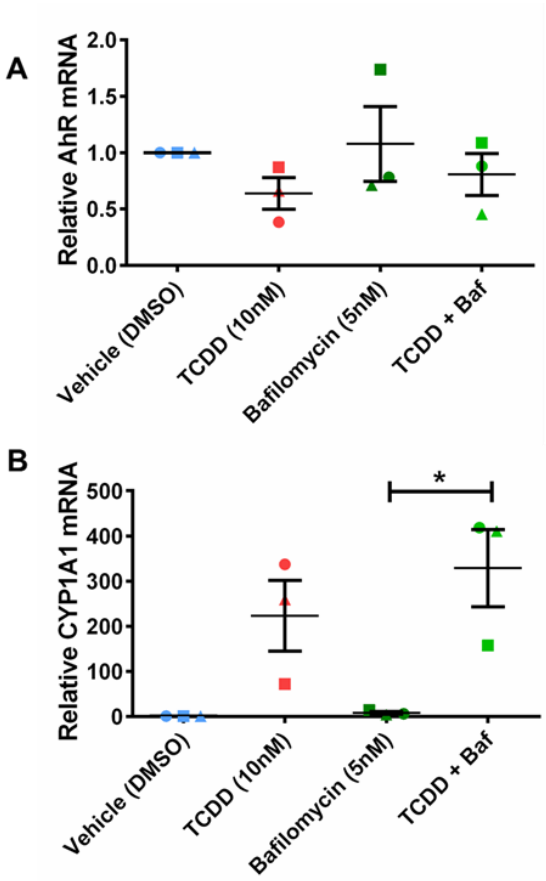

Figure 5.3 TCDD-induced AhR mRNA degradation is partially blocked and CYP1A1 mRNA induction accentuated with bafilomycin co-treatment.

A) AhR mRNA expression in epidermal equivalents (n=3 independent donors ± SEM) following treatment with vehicle (DMSO) (blue symbols), TCDD (10nM) (red symbols), bafilomycin (5nM) (dark green symbols) or TCDD with bafilomycin co-treatment (light green symbols) every 48 hours for 7 days. Each symbol represents an individual donor and is normalised to housekeeper gene H4, relative to vehicle (DMSO), line represents mean value. Statistics were acquired by one-way ANOVA with Tukey's multiple comparison test (NS) B) CYP1A1 mRNA expression in epidermal skin equivalents (n=3 independent donors ± SEM) following treatment with vehicle (DMSO) (blue symbols), TCDD (10nM) (red symbols), bafilomycin (5nM) (dark green symbols) or TCDD with bafilomycin co-treatment (light green symbols) every 48 hours for 7 days each symbol represents an individual donor and is normalised to housekeeper gene H4, relative to vehicle (DMSO) control, line represents mean value. Statistics were acquired by one-way ANOVA with Tukey's multiple comparison test *p=<0.05.

As expected, and previously shown (Fig. 3.5), TCDD treatment of epidermal skin equivalents caused AhR mRNA expression to decrease relative to vehicle control, whereas bafilomycin treatment alone caused no significant change in expression (Fig. 5.3 A). Interestingly, AhR mRNA expression in epidermal skin equivalents treated with TCDD and bafilomycin co-treatment was on average higher than in epidermal skin equivalents treated with TCDD alone, but only slightly.

TCDD treatment of epidermal skin equivalents caused an increase in CYP1A1 mRNA expression, as previously shown (Fig. 3.5), whilst bafilomycin treatment alone was found to have no significant induction of CYP1A1 mRNA (Fig. 5.3 B). In contrast, epidermal skin equivalents treated with TCDD and bafilomycin co-treatment had significantly increased CYP1A1 expression compared to bafilomycin alone (one-way ANOVA with Tukey's multiple comparison test $p<0.05$ Fig. 5.3 B) and a clear trend for increased expression in comparison to both vehicle and TCDD treated epidermal skin equivalents.

5.2.3. Inhibiting lysosomal function rescues the TCDD-induced chloracne phenotype

As previously described, treatment of human epidermal skin equivalent models with 10nM TCDD every 48 hours for 7 days induces a reproducible chloracne phenotype. TCDD treatment significantly reduces viable cell layer thickness and the stratum corneum becomes compacted, consistent with physiological features found in chloracne. To try to delineate the mechanism behind this reduction in viable cell layer, epidermal skin equivalents were treated with vehicle (DMSO), TCDD (10nM), bafilomycin (5nM) or TCDD with bafilomycin co-treatment (Fig. 5.4).

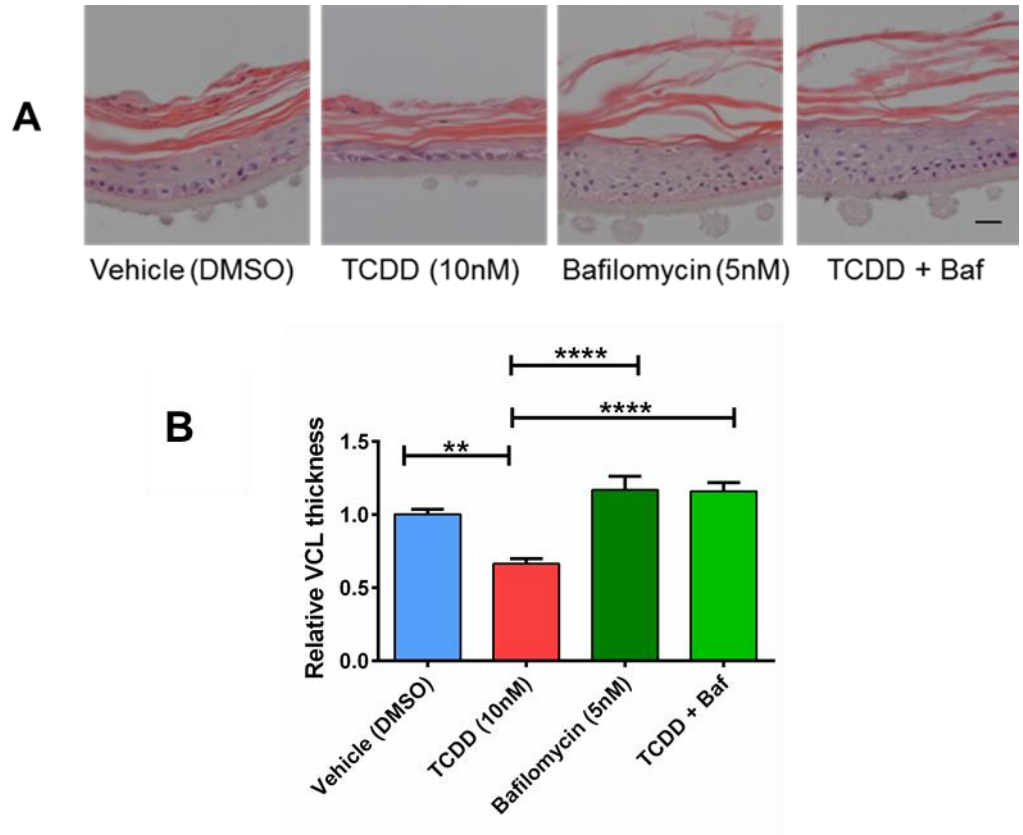

Figure 5.4 TCDD-induced reduced viable cell layer of the chloracne phenotype model is prevented by bafilomycin co-treatment.

A) Representative immunohistochemical images of epidermal equivalents stained with H&E following treatment with vehicle (DMSO), TCDD (10nM), bafilomycin (5nM) or TCDD with bafilomycin co-treatment every 48 hours for 7 days. Scale bar = 20µm B) Mean viable cell layer (VCL) thickness of epidermal equivalents treated with vehicle (DMSO) (blue bar), TCDD (red bar), bafilomycin (dark green bar) or TCDD with bafilomycin co-treatment (light green bar) Each bar is expressed relative to vehicle (DMSO) control, n=3 independent donors, ± SEM. Statistics were acquired by one-way ANOVA with Tukey's multiple comparison test **p=<0.01, ****p=<0.0001.

Histological staining of formalin fixed and paraffin embedded (FFPE) sections with haemotoxilin and eosin (H&E), again revealed a significant and consistent reduction in the viable cell layer and more compact stratum corneum with TCDD treatment as previously described (Chapter 4, Fig. 3.3) (Fig. 5.4 A). In contrast, bafilomycin co-treatment appeared to block this TCDD induced phenotype.

Quantitative analysis of the viable cell layer demonstrated a significant decrease in thickness in all epidermal skin equivalents treated for 7 days with TCDD compared to those treated with vehicle (DMSO) (one-way ANOVA with Tukey's multiple comparison test $p<0.01$ Fig. 5.4 B). Interestingly, bafilomycin co-treatment with TCDD in epidermal skin equivalents blocked this and viable cell layer thickness was increased significantly compared to TCDD treatment alone (Two-way ANOVA with Tukey's multiple comparison test $p<0.0001$ Fig. 5.4 B).

5.2.4. Bafilomycin co-treatment causes TCDD induction of late differentiation marker mRNA expression to be significantly prevented, but has no clear effect at protein level

In Chapter 3, data showed TCDD treatment of epidermal skin equivalent models to de-regulate late epidermal differentiation. In epidermal skin equivalents treated with TCDD mRNA levels of filaggrin, loricrin and cytokeratin 10 (CK10) were increased whilst expression at protein level was decreased (Fig. 3.8, Fig. 3.9). To investigate the potential influence of lysosomal processing in TCDD-induced de-regulated differentiation, mRNA expression of differentiation markers was measured in human epidermal skin equivalents treated with vehicle (DMSO), TCDD (10nM), bafilomycin (5nM) or TCDD with bafilomycin co-treatment every 48 hours for 7 days (Fig. 5.5)

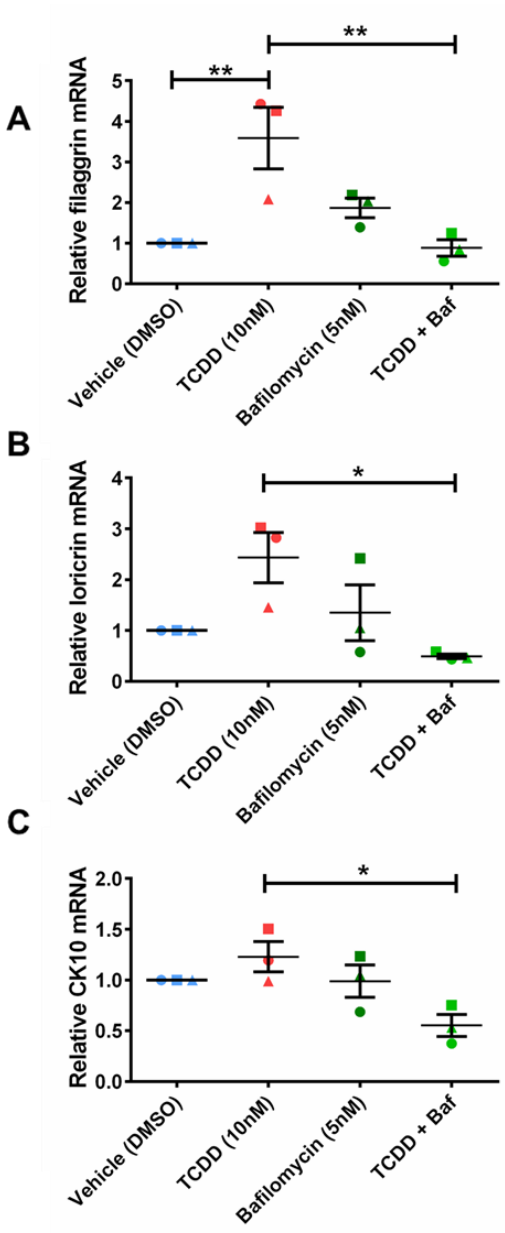

Figure 5.5 Bafilomycin co-treatment prevents TCDD induced filaggrin, loricrin and CK10 increased mRNA expression.

mRNA expression of filaggrin (A), loricrin (B) and CK10 (C) in epidermal equivalents (n=3 independent donors) ± SEM following treatment with vehicle (DMSO) (blue symbols), TCDD (10nM) (red symbols), bafilomycin (5nM) (dark green symbols) or TCDD with bafilomycin co-treatment (light green symbols) every 48 hours for 7 days. Each symbol represents an individual donor and is normalised to housekeeper gene H4, relative to vehicle (DMSO) control, line represents mean value. Statistics were acquired by one-way ANOVA with Tukey's multiple comparison test *p=<0.05, **p=<0.01.

As expected, TCDD treatment caused significantly increased mRNA expression of filaggrin and a trend in increased loricrin and CK10 expression in human epidermal skin equivalent models (Fig. 5.5). Interestingly, bafilomycin co-treatment prevented this induction and caused filaggrin, loricrin and CK10 mRNA expression to be significantly reduced compared to TCDD alone, bringing expression back to vehicle control levels, or lower (one-way ANOVA with Tukey's multiple comparison test, $p<0.05$, $p<0.01$ Fig. 5.5). Epidermal skin equivalents treated with bafilomycin alone had similar levels of filaggrin, loricrin and CK10 expression compared to vehicle (DMSO) and consistently higher expression than epidermal skin equivalents treated with TCDD and bafilomycin co-treatment.

In order to further delineate the impact of lysosomal processing on TCDD induced deregulated differentiation, the immunofluorescent expression of epidermal differentiation markers filaggrin, loricrin and CK10 was determined in epidermal equivalents treated with vehicle (DMSO), TCDD (10nM), bafilomycin (5nM) or TCDD with bafilomycin co-treatment 48 hours for 7 days (Fig. 5.6).

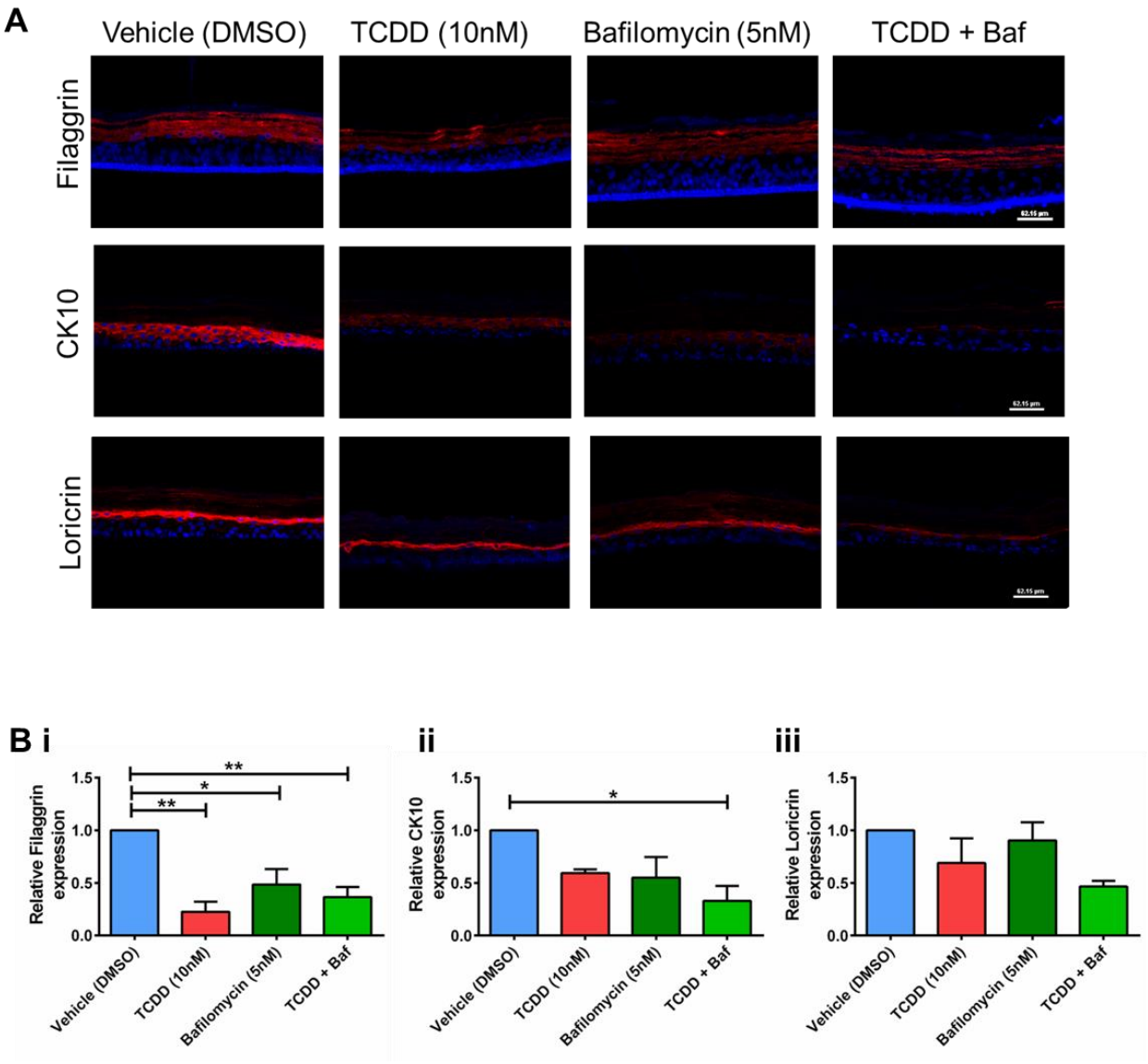

Figure 5.6 Bafilomycin co-treatment prevents TCDD induced reduction in filaggrin expression but not loricrin or CK10 reduced expression.

A) Representative photomicrographs of epidermal equivalents treated with vehicle (DMSO), TCDD (10nM), bafilomycin (5nM) or TCDD with bafilomycin every 48 hours for 7 days depicting Hoechst nuclear staining (blue fluorescence) and filaggrin, CK10 or loricrin staining (red fluorescence). N=4 independent donors, scale bar 62.15µm. B) Mean relative filaggrin (Bi) CK10 (Bii) or loricrin (Biii) expression in epidermal equivalents treated for 7 days with vehicle (DMSO) (blue bars) TCDD (10nM) (red bars) bafilomycin (5nM) (dark green bars) or TCDD with bafilomycin co-treatment (light green bars) for 7 days. Each bar is expressed relative to vehicle (DMSO) control for filaggrin (i) CK10 (ii) or loricrin (iii) expression, n= 3 independent donors, ± SEM. Statistics were acquired by one-way ANOVA with Tukey's multiple comparison test *p=<0.05, **p=<0.01

As previously found, TCDD treatment of epidermal skin equivalents caused significant decreased expression of filaggrin (Fig. 5.6 A and B i) (one-way ANOVA with Tukey's multiple comparison test, $p<0.01$) and reduced expression of CK10 and loricrin. Interestingly, bafilomycin co-treatment did not prevent TCDD induced loss of CK10 or loricrin protein expression, in fact, expression seemed further reduced (Fig. 5.6 B ii and iii). In contrast, there was a slight recovery of filaggrin expression with bafilomycin co-treatment compared to TCDD alone, although this was not significant (Fig. 5.6 B i)

5.2.5. Inhibiting lysosomal function prevents TCDD-induced caspase-3 positive staining and increases Ki67 positive staining

To explore the TCDD-induced chloracne phenotype and specifically the contribution of lysosomal activity in TCDD-induced apoptosis, the effect of bafilomycin on caspase-3 dependent cell death was investigated. Human epidermal skin equivalents were generated and then treated with vehicle (DMSO), TCDD (10nM), bafilomycin (5nM) or TCDD with bafilomycin co-treatment every 48 hours for 7 days. After harvesting, immunofluorescence staining on OCT frozen sections for caspase-3 was carried out. Images were taken along the entire length of the epidermal skin equivalents and Hoechst positive cells and caspase-3 positive cells were counted.

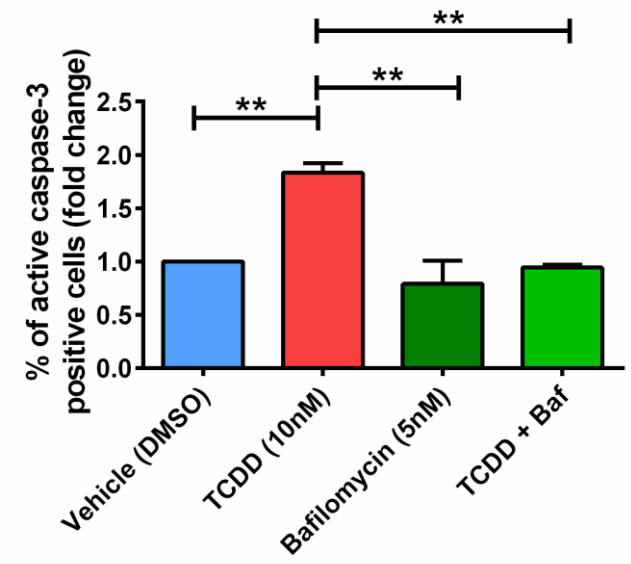

Figure 5.7 TCDD-induced increase of caspase-3 positive cells is prevented by bafilomycin co-treatment.

Mean percentage of caspase-3 positive cells to Hoechst positive cells presented as fold change in epidermal equivalents treated with vehicle (DMSO) (blue bar) TCDD (10nM) (red bar) bafilomycin (5nM) (dark green bar) or TCDD with bafilomycin co-treatment (light green bar) every 48 hours for 7 days. Each bar is expressed relative to vehicle (DMSO) control. n= 3 independent donors, ± SEM. Statistics were acquired by one-way ANOVA with Tukey's multiple comparison test. **p=<0.01.

Statistical analysis revealed TCDD treated epidermal skin equivalents had significantly increased caspase-3 positive cells compared to vehicle (DMSO) alone (one-way ANOVA with Tukey's multiple comparison test $p<0.01$ Fig. 5.7). Interestingly, co-treatment with bafilomycin reduced the TCDD induced caspase-3 positivity significantly (one-way ANOVA with Tukey's multiple comparison test

p<0.01), bringing levels back down to that of vehicle (DMSO) control treated epidermal skin equivalents (raw values are presented in Appendix J).

In epidermal skin equivalents TCDD causes differentiation to be de-regulated and significantly reduces the viable cell layer thickness compared to vehicle control. Although TCDD did not significantly alter proliferation (Chapter 3 Fig. 3.8) bafilomycin treatment did seem to cause a slight increase in viable cell layer thickness (Fig. 5.4). Therefore, the effect of blocking lysosomal function on proliferation (Ki67 positive cells) was still explored. After harvesting, immunofluorescence staining on OCT frozen sections for Ki67 was performed. Images were taken along the entire length of the epidermal skin equivalents and Hoechst positive cells and Ki67 positive cells were counted.

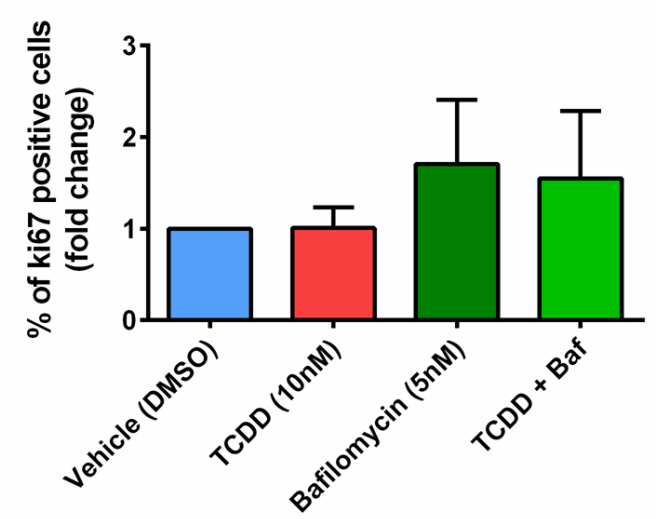

Figure 5.8 TCDD does not increase Ki67 positive cells but bafilomycin treatment does.

Mean percentage of Ki67 positive cells to Hoechst positive cells presented as fold change in epidermal equivalents treated with vehicle (DMSO) (blue bar) TCDD (10nM) (red bar) bafilomycin (5nM) (dark green bar) or TCDD with bafilomycin co-treatment (light green bar) every 48 hours for 7 days. Each bar is expressed relative to vehicle (DMSO) control. n= 3 independent donors, ± SEM. Statistics were acquired by one-way ANOVA with Tukey's multiple comparison test

Statistical analysis (one-way ANOVA with Tukey's multiple comparison test) revealed no significant change in Ki67 staining, with TCDD treatment compared to vehicle (DMSO) control treated epidermal skin equivalents (as previously presented in Chapter 3 Fig. 3.8). However, interestingly, in epidermal skin equivalents treated with bafilomycin alone or TCDD with bafilomycin co-treatment, Ki67 staining was increased above both vehicle and TCDD treatment levels, although not significant.

5.2.6. Specific chemical inhibition of cathepsin D alters TCDD-induced AhR degradation and LC3II accumulation

Although the chemical inhibitor bafilomycin, blocks lysosomal function, it also impacts the autophagy pathway as previously stated. Therefore, to further explore the influence of lysosomal processing in the chloracne phenotype model, a complementary approach was used by chemically inhibiting the lysosomal protease cathepsin D with pepstatin A.

Firstly, epidermal skin equivalents were generated and treated with vehicle (DMSO), TCDD (10nM), pepstatin A (10µg/ml) or TCDD with pepstatin A co-treatment, every 48 hours for 7 days. To confirm TCDD induced AhR degradation and LC3II induction, protein expression was determined by western blotting (Fig. 5.9).

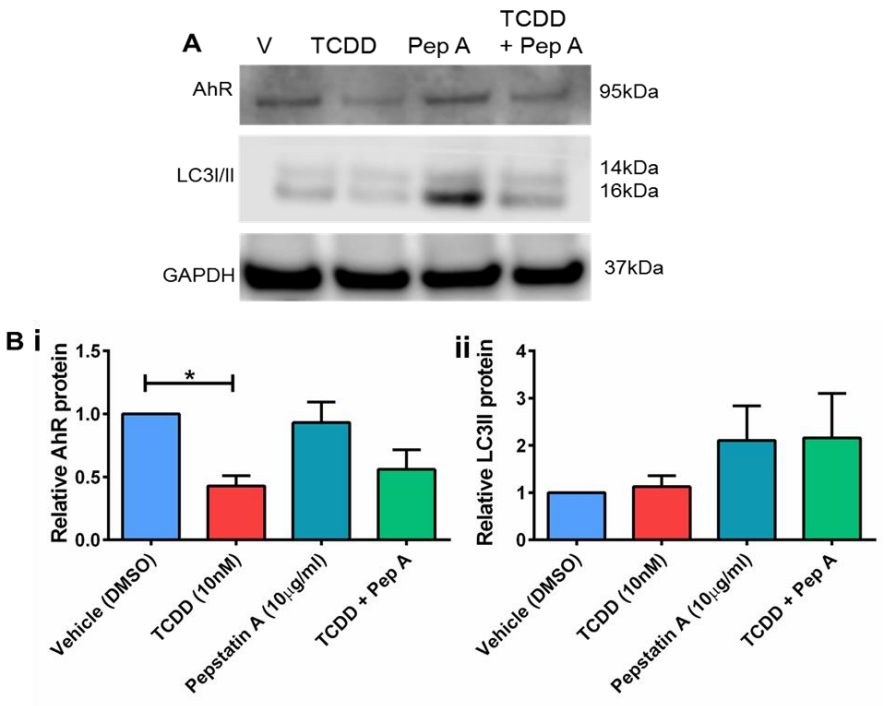

Figure 5.9 TCDD-induced AhR protein degradation is partially blocked and LC3II accumulation is accentuated by pepstatin A co-treatment.

A) Representative western blot of AhR protein expression and LC3II expression in epidermal equivalents following treatment with vehicle (DMSO), TCDD (10nM), pepstatin A (10µg/ml) or TCDD with pepstatin A co-treatment every 48 hours for 7days. B) Densitometric analysis of AhR expression (i) or LC3II expression (ii) after vehicle (blue bar), TCDD (red bar), pepstatin A (turquoise bar) or TCDD with pepstatin A co-treatment (light green bar). Each bar is normalised to GAPDH loading control expressed relative to vehicle (DMSO) control. n=3 independent donors ± SEM. Statistics were acquired by one-way ANOVA with Tukey's multiple comparison test *p= <0.05.

As expected, results showed relative to GAPDH loading control, AhR protein expression significantly decreased with TCDD compared to vehicle (DMSO) (Fig. 5.9 B i) (one-way ANOVA with Tukeys multiple comparison test $p<0.05$). In epidermal skin equivalents co-treated with pepstatin A, TCDD-induced AhR degradation was partially prevented. In epidermal skin equivalents treated with pepstatin A alone, AhR protein expression was at the same level as that found in vehicle (DMSO) treated epidermal skin equivalents.

Results also showed TCDD treatment of human epidermal skin equivalents caused a slight increase in LC3II protein expression (Fig. 5.9 B ii). Of interest, pepstatin A alone and co-treatment with pepstatin A caused an increase in LC3II expression, suggesting the inhibitor worked and lysosomal degradation or function was impaired.

5.2.7. Specific chemical inhibition of cathepsin D partially rescues the TCDD-induced chloracne phenotype

As described earlier, bafilomycin co-treatment was found to prevent the TCDD-induced reduction in viable cell layer thickness. However, it is not clear if autophagy of lysosomal processing or both processes are involved in this. To gain more information, epidermal skin equivalents were treated with vehicle (DMSO), TCDD (10nM) pepstatin A (10µg/ml) or TCDD with pepstatin A co-treatment and histological staining of formalin fixed and paraffin embedded (FFPE) sections with haemotoxilin and eoisin (H&E) was carried out (Fig. 5.10).

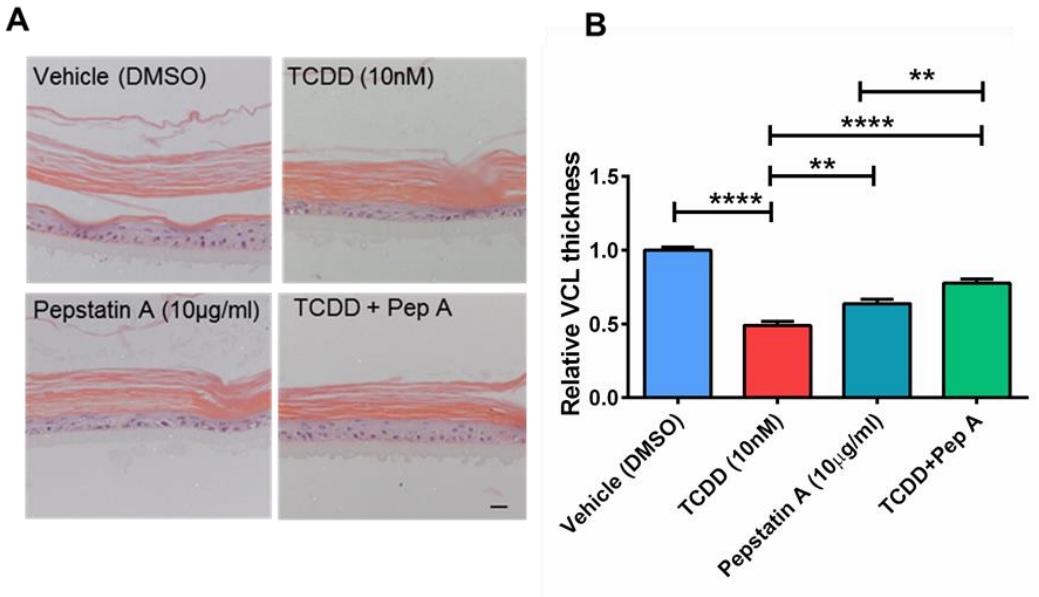

Figure 5.10 TCDD-induced reduced viable cell layer of the chloracne phenotype model is prevented by pepstatin A co-treatment.

A) Representative immunohistochemical images of epidermal equivalents stained with H&E following treatment with for 7 days with vehicle (DMSO), TCDD (10nM), pepstatin A (10µg/ml) or TCDD with pepstatin A co-treatment. Scale bar = 20µm B) Mean viable cell layer (VCL) thickness of epidermal equivalents treated every 48 hours for 7 days with vehicle (DMSO) (blue bar), TCDD (red bar), pepstatin A (turquoise bar) or TCDD with pepstatin A co-treatment (light green bar) Each bar is expressed relative to vehicle (DMSO) control, n= 3 independent donors, ± SEM. Statistics were acquired by one-way ANOVA with Tukey's multiple comparison test. **p=<0.01, ****p=<0.0001.

Imaging and subsequent quantitative analysis revealed a reduction in the viable cell layer with TCDD treatment as expected (Fig. 5.10 B) (one-way ANOVA with Tukey's multiple comparison test $p<0.0001$). Of importance, co-treatment with pepstatin A significantly increased viable cell layer thickness above that of TCDD treated epidermal skin equivalents ($p<0.0001$). Interestingly, pepstatin A treatment alone caused a reduction in viable cell layer thickness compared to vehicle treated and a significant reduction in viable cell layer thickness compared to epidermal skin equivalents with TCDD and pepstatin A co-treatment ($p<0.01$).

5.2.8. Specific chemical inhibition of cathepsin D rescues the TCDD-induced reduction in filaggrin protein expression

TCDD treatment of epidermal skin equivalents causes differentiation to be de-regulated (Fig. 3.8, Fig. 3.9). To explore more specifically the role of lysosomal processing in the chloracne phenotype and in particular its potential role in de-regulated differentiation, epidermal skin equivalents were treated in the presence and absence of pepstatin A (10µg/ml) and immunofluorescence staining for filaggrin protein expression was carried out (Fig. 5.11).

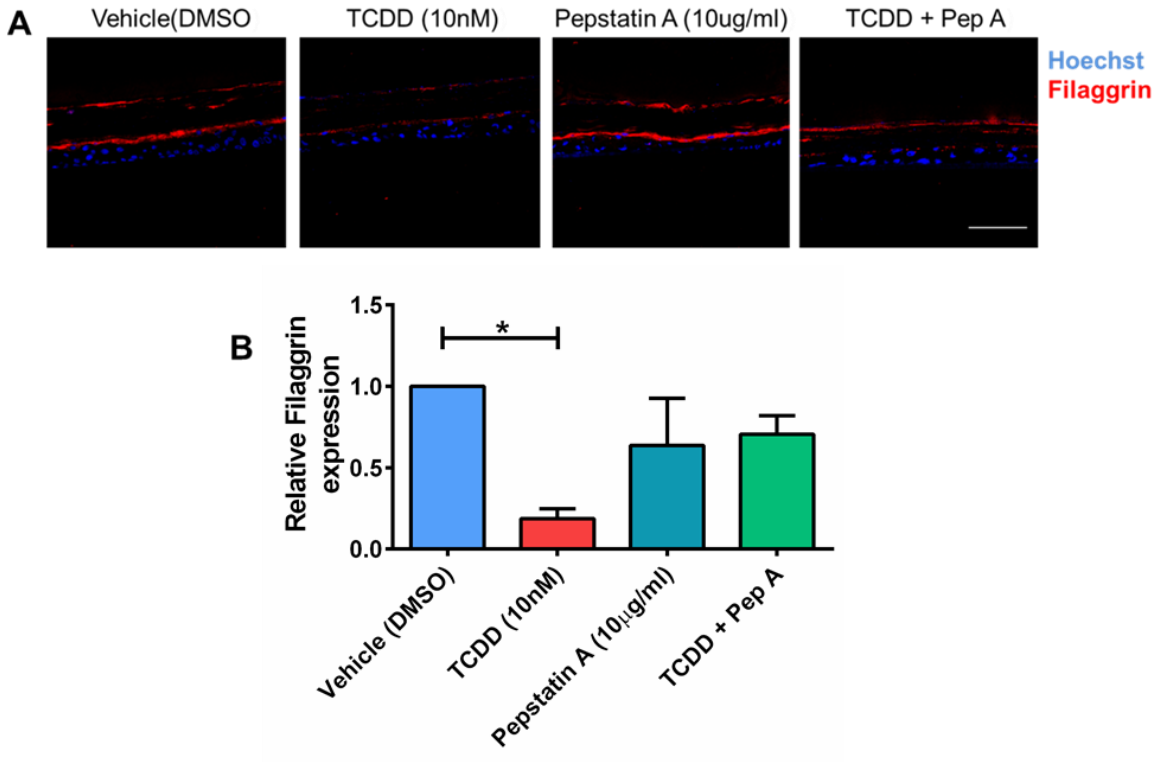

Figure 5.11 TCDD induced downregulation of filaggrin protein expression is partially blocked by pepstatin A co-treatment.

A) Representative photomicrographs of epidermal equivalents treated with vehicle (DMSO), TCDD (10nM), pepstatin A (10µg/ml) or TCDD with pepstatin A co-treatment depicting Hoechst nuclear staining (blue fluorescence) and Filaggrin expression (red fluorescence). Scale bar = 100µm B) Mean filaggrin expression of epidermal equivalents treated every 48 hours for 7 days with vehicle (DMSO) (blue bar), TCDD (red bar), pepstatin A (turquoise bar) or TCDD with pepstatin A co-treatment (light green bar). Each bar is expressed relative to vehicle (DMSO) control, n=3 independent donors, ± SEM. Statistics were acquired by one-way ANOVA with Tukey's multiple comparison test *p=<0.05

Results showed a significant reduction in filaggrin protein expression with TCDD treatment as expected (one-way ANOVA with Tukey's multiple comparison test $p<0.05$). However, data suggested pepstatin A co-treatment restored filaggrin expression and partially prevented TCDD-induced downregulation of filaggrin. Pepstatin A treatment alone caused filaggrin expression to be slightly lower than vehicle control, although again this data was not significant.

5.2.9. Specific chemical inhibition of cathepsin D prevents TCDD-induced caspase-3 positive staining

Previous data showed TCDD treatment significantly increased caspase-3 positive cells in epidermal skin equivalents and this is significantly reduced by co-treatment with bafilomycin (Fig. 5.6). To explore further the potential role of lysosomal processing, specifically the role of cathepsin D, in induction of caspase-3 positivity, epidermal equivalents were generated and treated in the presence and absence of pepstatin A and immunofluorescence staining for caspase-3 was carried out (Fig. 5.12).

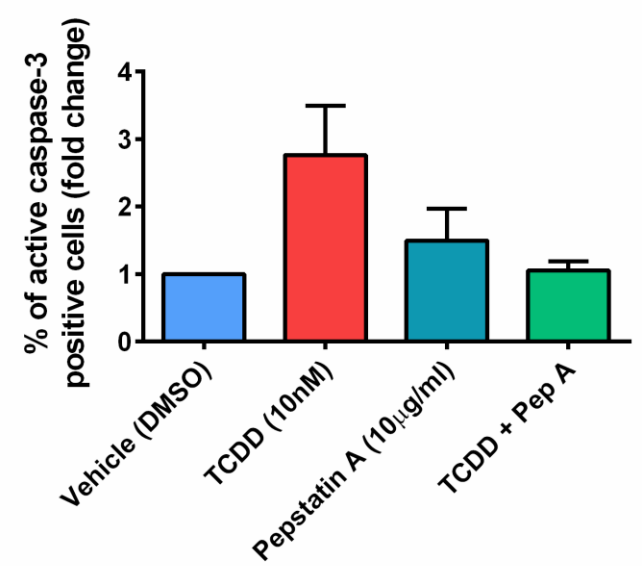

Figure 5.12 TCDD-induced increase of caspase-3 positive cells is prevented by pepstatin A co-treatment.

Mean percentage of caspase-3 positive cells to Hoechst positive cells presented as fold change in epidermal equivalents treated with vehicle (DMSO), TCDD (10nM), pepstatin A (10µg/ml) or TCDD with pepstatin A co-treatment every 48 hours for 7 days. Each bar is expressed relative to vehicle (DMSO) control. n= 3 independent donors, ± SEM. Statistics were acquired by one-way ANOVA with Tukey's multiple comparison test (NS)

Results suggested TCDD treatment caused an increase in caspase-3 positive staining compared to vehicle (DMSO) treated epidermal skin equivalents. This induction of caspase-3 positivity appeared to be reduced by pepstatin A co-treatment, whilst pepstatin A treatment alone caused a slight increase in caspase-3 positivity compared to vehicle (DMSO) control although this was not significant due to donor variability (raw values are presented in Appendix I).

5.2.10. Successful shRNA knockdown of cathepsin D was achieved in epidermal skin equivalents

Although pepstatin A is known as a specific inhibitor of cathepsin D as with any chemical inhibitor, off target affects are possible. Therefore, to verify work carried out with pepstatin A, shRNA lentiviral knockdown of cathepsin D in epidermal skin equivalents was pursued. Briefly, primary human keratinocytes were transduced with non-target control (shNT) or cathepsin D (shCTSD) shRNA lentivirus, puromycin selected and expanded. Cells were then seeded into epidermal equivalents and grown for 12 days then treated appropriately every 48 hours for a further 7 days. To establish whether successful knockdown of cathepsin D had occurred, epidermal equivalents were harvested and expression of all isoforms of cathepsin D protein (pre/pro, pro and active) was established by western blotting (Fig. 5.13)

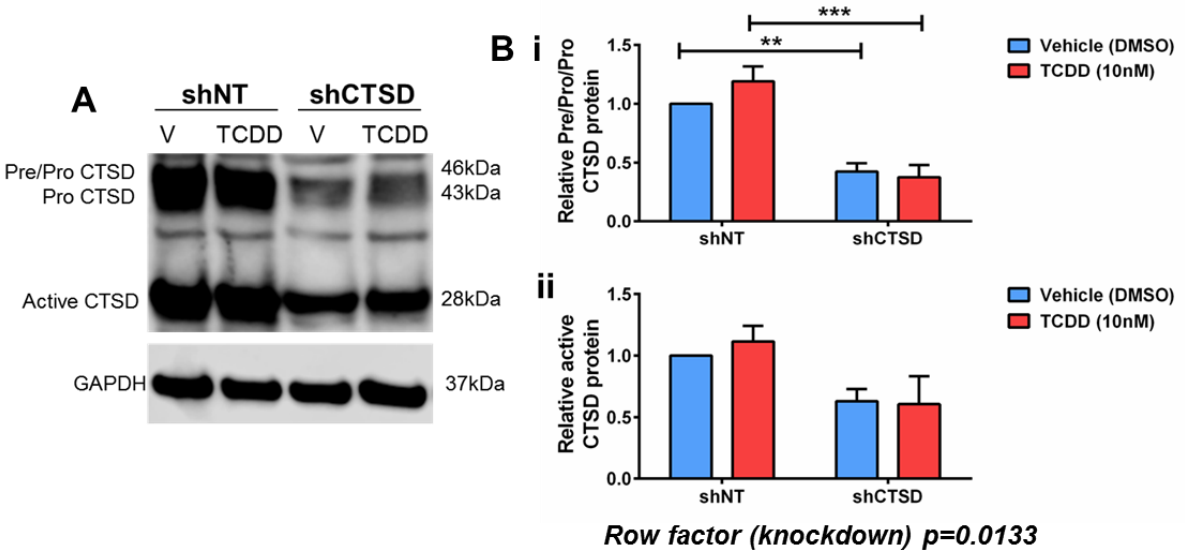

Figure 5.13 Successful knockdown of cathepsin D protein in shCTSD epidermal equivalents compared to shNT control.

A) Representative western blot of Pre/Pro, Pro and active forms of cathepsin D (CTSD) protein expression following treatment of shNT and shCTSD knockdown epidermal equivalents with vehicle (DMSO) or TCDD (10nM) every 48 hours for 7 days. B) Densitometric analysis of Pre/pro and Pro forms of cathepsin D (i) or active cathepsin D (ii) after vehicle (blue bar) or TCDD (10nM) (red bar) treatment every 48 hours for 7 days. Each bar is normalised to GAPDH loading control relative to shNT vehicle (DMSO) control. n=3 independent donors, ± SEM. Statistics were acquired by two-way ANOVA with Tukey's multiple comparison test **p= <0.01, ***p=<0.001

Results showed, relative to GAPDH loading control, pre/pro and pro isoforms of cathepsin D were significantly reduced in shCTSD epidermal equivalents compared to expression in shNT epidermal equivalents, after both vehicle (DMSO) and TCDD (10nM) treatment (one-way ANOVA with Tukey's multiple comparison test $p<0.01$ and $p<0.001$ respectively Fig. 5.13 B i, ii). Active cathepsin D protein expression was also reduced in shCTSD epidermal skin equivalents compared to shNT, with a row factor, or knockdown as a whole, significant ($p=0.0133$). Interestingly, in shNT epidermal equivalents treated with TCDD (10nM) expression of all isoforms of cathepsin D tended to increase, further supporting the involvement of cathepsin D in this phenotype.

5.2.11. shRNA knockdown of cathepsin D accentuates TCDD-induced AhR protein degradation and increases LC3II accumulation

To understand the impact of knocking down cathepsin D on AhR protein expression and LC3II accumulation, epidermal skin equivalents with shNT and shCTSD were generated and treated every 48 hours for 7 days with vehicle (DMSO) or TCDD (10nM). Western blotting was then used to determine AhR and LC3II protein expression (Fig. 5.14).

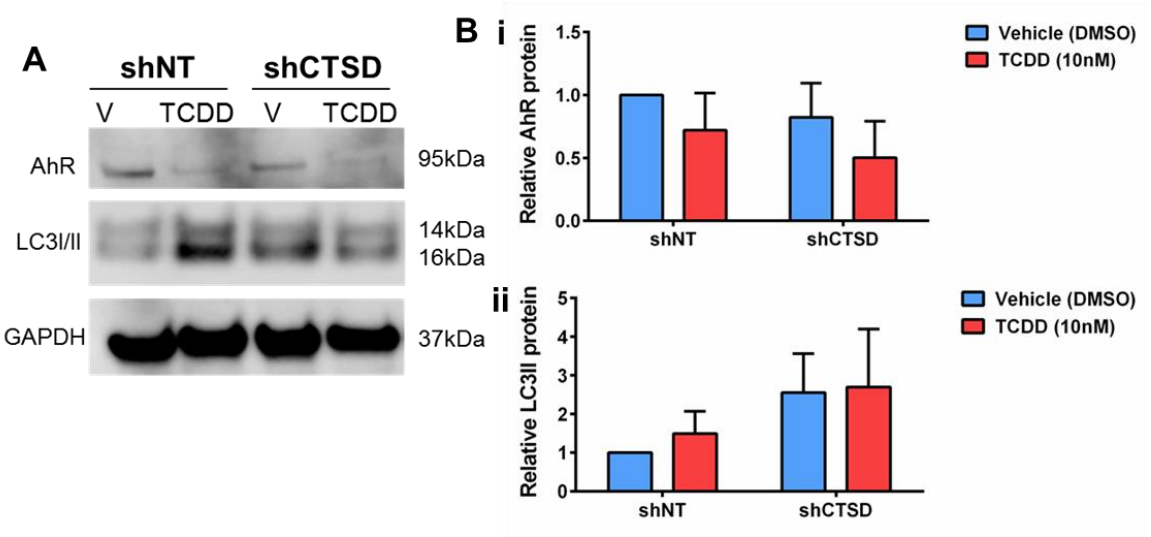

Figure 5.14 shCTSD knockdown accentuates TCDD induced AhR degradation and causes LC3II accumulation.

A) Representative western blot of AhR and LC3I/II protein expression following treatment of shNT and shCTSD knockdown epidermal equivalents with vehicle (DMSO) or TCDD (10nM) every 48 hours for 7 days. B) Densitometric analysis of AhR (i) or LC3II (ii) after vehicle (DMSO) (blue bar) or TCDD (10nM) (red bar) treatment. Each bar is normalised to GAPDH loading control expressed relative to shNT vehicle (DMSO) control. n=3 independent donors, ± SEM. Statistics were acquired by two-way ANOVA with Tukey's multiple comparison test (NS).

Data showed a trend for TCDD induced AhR degradation in both shNT and shCTSD epidermal skin equivalents as expected. Interestingly, cathepsin D knockdown in epidermal skin equivalents appeared to accentuate TCDD-induced degradation. LC3II accumulation also appeared induced by TCDD treatment in shNT epidermal equivalents as expected. Additionally, LC3II expression was increased by shCTSD knockdown regardless of treatment, confirming knockdown is actively attenuating lysosomal function. However, data was not significant due to donor variability and as such, more donors are required.

5.2.12. shRNA knockdown of cathepsin D rescues the TCDD-induced reduced viable cell layer thickness

To further explore the role of cathepsin D in the TCDD-induced chloracne phenotype, particularly the reduction in viable cell layer thickness, shNT and shCTSD epidermal equivalents were generated and treated with vehicle (DMSO) or TCDD (10nM) every 48 hours for 7 days. Histological staining of formalin fixed and paraffin embedded (FFPE) sections with haemotoxilin and eosin (H&E) was then carried out (Fig. 5.15).

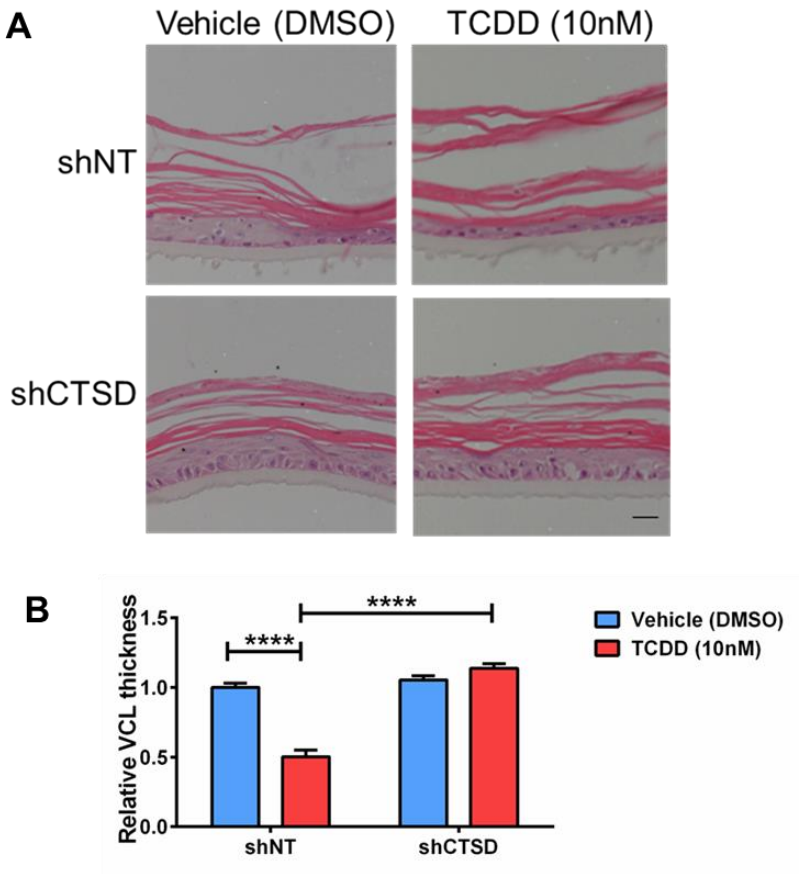

Figure 5.15 TCDD-induced reduced viable cell layer of the chloracne phenotype model is prevented by shCTSD knockdown.

A) Representative immunohistochemical images of shNT and shCTSD knockdown epidermal equivalents stained with H&E following treatment with vehicle (DMSO) or TCDD (10nM) for 7 days. Scale bar = 20µm B) Mean viable cell layer (VCL) thickness of shNT and shCTSD knockdown epidermal equivalents treated with vehicle (DMSO) (blue bar) or TCDD (red bar) every 48 hours for 7 days. Each bar is expressed relative to shNT vehicle (DMSO) control, n= 3 independent donors, ± SEM. Statistics were acquired by two-way ANOVA with Tukey's multiple comparison test ****p=<0.0001.

Quantitative analysis of viable cell layer thickness was then performed which revealed as expected, TCDD treatment of shNT epidermal skin equivalents caused a significant reduction in viable cell layer thickness (two-way ANOVA with Tukey's multiple comparison test $p<0.0001$ Fig. 5.15 B). Interestingly, shCTSD knockdown epidermal skin equivalents treated with vehicle (DMSO) control caused no significant change in viable cell layer thickness. In contrast, shCTSD knockdown significantly blocked TCDD-induced reduction in viable cell layer thickness (two-way ANOVA with Tukey's multiple comparison test, $p<0.0001$).

5.2.13. shRNA knockdown of cathepsin D partially rescues the TCDD-induced reduction in filaggrin protein expression

To explore the role of cathepsin D in the chloracne phenotype model, in particular the influence on TCDD-induced de-regulated differentiation, shNT and shCTSD knockdown epidermal skin equivalents were treated with vehicle (DMSO) or TCDD (10nM). After harvesting, immunofluorescence staining on OCT frozen sections for filaggrin was performed (Fig. 5.16).

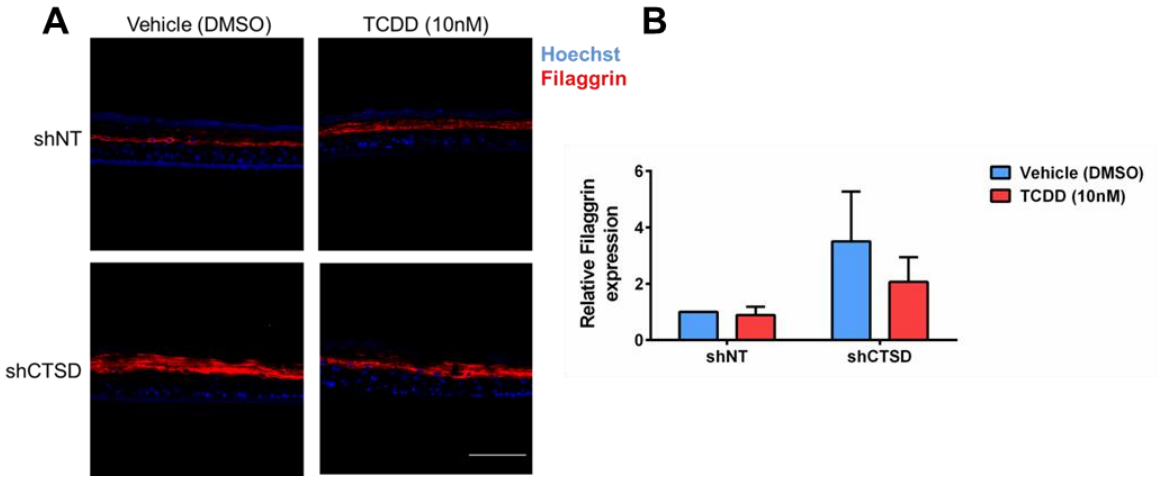

Figure 5.16 shCTSD knockdown in epidermal skin equivalents causes increased filaggrin protein expression compared to shNT control.

A) Representative photomicrographs of shNT and shCTSD knockdown epidermal equivalents (n=3 independent donors) treated with vehicle (DMSO) or TCDD (10nM) for 7 days depicting Hoechst nuclear staining (blue fluorescence) and Filaggrin expression (red fluorescence). Scale bar = 100µm. B) Mean filaggrin expression of shNT and shCTSD knockdown epidermal equivalents treated with vehicle (DMSO) (blue bar) or TCDD (10nM) (red bar) every 48 hours for 7 days. Each bar is expressed relative to shNT vehicle (DMSO) control, n=3 independent donors, ± SEM. Statistics were acquired by two-way ANOVA with Tukey's multiple comparison test (NS).

After quantification and statistical analysis (two-way ANOVA with Tukey's multiple comparison test) results surprisingly showed only a very slight decrease in filaggrin expression with TCDD (10nM) treatment in shNT epidermal equivalents. In contrast, TCDD treatment did cause reduced filaggrin expression in shCTSD epidermal skin equivalents. Surprisingly, filaggrin protein expression overall was higher in shCTSD knockdown epidermal skin equivalents compared to expression in shNT epidermal skin equivalents (Fig. 5.16). However, it is difficult to interpret this data given the donor variability and more donors would be required before firm conclusion can be drawn.

5.2.14. shRNA knockdown of cathepsin D prevents TCDD-induced caspase-3 positive staining

In order to further confirm the involvement of cathepsin D in TCDD induced caspase-3 staining, immunofluorescence was performed on frozen OCT sections of shNT and shCTSD epidermal skin equivalents treated with vehicle (DMSO) or TCDD (10nM) every 48 hours for 7 days (Fig. 5.17).

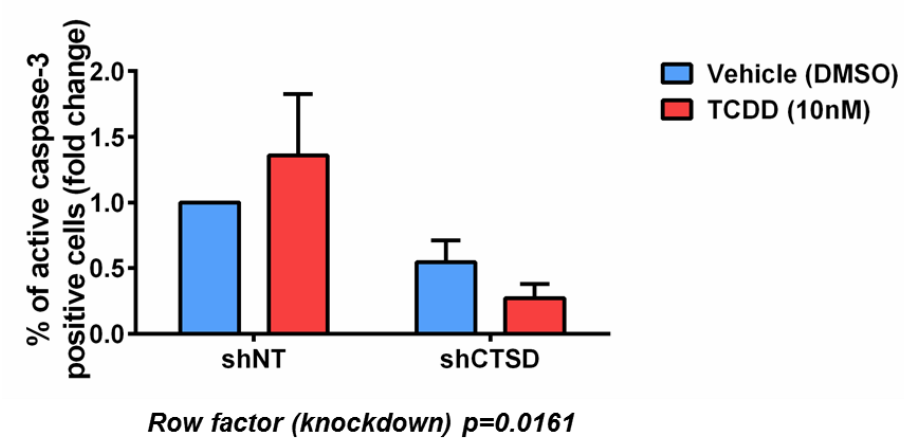

Figure 5.17 TCDD-induced increase of caspase-3 positive cells is prevented by shCTSD knockdown.

Mean percentage of caspase-3 positive cells to Hoechst positive cells presented as fold change in shNT and shCTSD knockdown epidermal equivalents treated with vehicle (DMSO) or TCDD (10nM) every 48 hours for 7 days. Each bar is expressed relative to shNT vehicle (DMSO) control. n= 3 independent donors, ± SEM. Statistics were acquired by two-way ANOVA with Tukey's multiple comparison test (NS)

After imaging the individual epidermal skin equivalent sections along their entire length, caspase-3 positive cells and Hoechst positive cells were counted, as previously described (raw values are presented in Appendix L). After quantification and statistical analysis (two-way ANOVA with Tukey's multiple comparison test) a clear trend was apparent. As previously seen, TCDD treatment of shNT epidermal skin equivalents caused increased caspase-3 positive staining relative to shNT vehicle (DMSO) treated. In general, shCTSD epidermal skin equivalents had less capase-3 positive staining overall. Of interest, TCDD treated shCTSD epidermal skin equivalents had far less caspase-3 positive cell staining compared to shNT TCDD treated epidermal skin equivalents.

5.3 Discussion

Work in this chapter focused on using the established epidermal equivalent chloracne phenotype model whilst harnessing both chemical and genetic manipulation of lysosomal function and cathepsin D activity. These novel data revealed lysosomal activity was required for the TCDD-induced reduction in viable cell layer and increased expression of active capsase-3 positive cells. Furthermore, data suggests lysosomal activity may play a role in TCDD-induced AhR degradation in this model and also implies lysosomal activity is involved in TCDD-induced de-regulated differentiation. Taken together it is likely lysosomal function plays a crucial role in the chloracne phenotype model.

5.3.1. Involvement of lysosomes in AhR degradation

As discussed in Chapter 4, section 4.3.2, results indicated autophagy, potentially chaperone mediated autophagy (CMA) may play a role in AhR degradation. Although AhR is thought to be degraded by the 26S proteasome ubiquitination pathway (Ma and Baldwin, 2000, Davarinos and Pollenz, 1999) there is known cross talk between this and chaperone mediated or selective autophagy as reviewed by Lilienbaum (2013).

LAMP2 is a lysosomal membrane protein, required for lysosomal fusion and mobility and upregulation can indicate accumulation and storage of lysosomes (Wu *et al*., 2011). Therefore, initial experiments investigated the expression LAMP2, in epidermal skin equivalents after TCDD treatment. Results demonstrated TCDD treatment induced LAMP2 expression, suggesting TCDD caused accumulation of lysosomes or increased the number of lysosomes.

Although immunofluorescence was carried out using a general LAMP2 antibody, the LAMP2 gene is known to undergo alternative splicing resulting in three isoforms: A, B and C (Cuervo and Dice, 2000, Konecki *et al*., 1995). Of interest to this study, LAMP2A is thought to be a key factor in chaperone mediated autophagy (CMA), with the chaperone-substrate complex binding to LAMP2A on the lysosomal membrane (Saftig and Eskelinen, 2008). LAMP2A has a specific 12-amino residue sequence

which forms a unique cytosolic tail and antibodies are available to target this (Patel and Cuervo, 2015). The increase in LAMP2 staining with TCDD treatment did indeed indicate lysosomal accumulation; however, staining with a LAMP2A antibody would help elucidate the role of lysosomes in chaperone mediated autophagy specifically.

Like AhR, misfolded or unfolded proteins are generally degraded by the proteasome system but when they become too large to pass through narrow proteasome channels, the autophagy pathway is often activated (Wang *et al*., 2015). To be degraded by chaperone mediated autophagy (CMA), the target protein must have a specific penta-peptide amino acid sequence, a KFERQ motif, which is recognised by hsc70 (heat shock-cognate chaperone, 70kDa) (Patel and Cuervo, 2015, Franch *et al*., 2001, Dice, 1990). Of interest, 30% of cytosolic proteins have this KFERQ motif. Interestingly, a lysosomal form of hsp90 is also involved in CMA, essential to preserve the stability of LAMP2A at the lysosomal membrane (Patel and Cuervo, 2015, Bandyopadhyay *et al*., 2008).

An association between the chaperone protein hsp90 and AhR has already been well established (as described in Chapter 1, section 1.2.2). In the cytoplasm before activation by ligands, AhR is known to bind to hsp90 as well as P23 and AIP to prepare AhR for ligand binding (Tsuji *et al*., 2014). Although hsp90 is known to chaperone over 300 proteins, this already established interaction between hsp90 and AhR may provide additional evidence of CMA being involved in AhR degradation.

Results from the present chapter support these studies and the hypothesis that CMA may be involved in AhR degradation. Data showed bafilomycin co-treatment partially blocked TCDD-induced AhR protein degradation and results indicated that the specifically the lysosomal protease cathepsin D may have a role, through experiments using the chemical inhibitor pepstatin A. In contrast, although shRNA knockdown of cathepsin D was achieved in epidermal skin equivalents, AhR protein expression data was variable, with large error bars due to donor variability, possibly because of a low donor number. However, data from experiments with bafilomycin and the pepstatin A still implies lysosomal function is somewhat required for AhR degradation in keratinocytes.

Interestingly, results also demonstrated treatment of epidermal skin equivalents with bafilomycin accentuated TCDD-induced CYP1A1 mRNA expression, indicative of AhR activity.

Accentuation of TCDD induced CYP1A1, or CYP1A1 “super induction” has been described previously in studies exploring models of AhR degradation. Mouse hepa1c1c7 cells treated with TCDD in combination with the 26S proteasome inhibitor MG-132 or another proteasome inhibitor lactacystin for 5 hours enhanced CYP1A1 gene expression 4-3.5 fold. In contrast, PMSF the serine protease inhibitor did not affect induction (Ma and Baldwin, 2000). However, although all relative, cells in the published study were only treated with 1nM TCDD compared to 10nM in the present model and as previously discussed, AhR expression and activity varies significantly between mouse and human models (as discussed in Chapter 1, section 1.3.1). Nevertheless, bafilomycin induced super induction of CYP1A1 mRNA levels in the present model suggests lysosomal degradation of AhR is also regulating ligand-bound or active AhR in the nucleus and consequently transcription of target genes.

Taken together, the data presented suggests AhR is degraded to some extent by lysosomal proteins, likely through CMA due to the unique cross talk with the 26S proteasome system.

5.3.2. Further evidence of a role for lysosomal activity and cathepsins in epidermal differentiation

Treatment of epidermal skin equivalents with TCDD over 7 days was previously found to de-regulate epidermal differentiation and potentially contributes to the chloracne phenotype (Chapter 3, section 3.2.3). As such, the role of lysosomal function in TCDD-induced de-regulated differentiation was explored. Interestingly, bafilomycin co-treatment and cathepsin D inhibition with pepstatin A or shRNA knockdown blocked the TCDD-induced reduction in filaggrin protein expression, although not significant. Similarly, at mRNA level, TCDD-induced filaggrin, loricrin and CK10 expression was blocked by bafilomycin co-treatment. Although results were somewhat variable, data suggests lysosomal activity may be required for TCDD induced de-regulated differentiation.

Although the role of lysosomes may not have been implicated in TCDD induced de-regulated epidermal differentiation before, the literature does suggest lysosomal cathepsins have a role in epidermal differentiation. For example, in rat keratinocytes,

expression of cathepsins B, H and L increased when keratinocytes were calcium differentiated (Tanabe *et al*., 1991). Similarly, cathepsin L activity has also been found to increase after 1-2 days then decrease again as differentiation progresses. Finally, in a clinical trial evaluating the efficacy and safety of the cathepsin K inhibitor balicatib for osteoporosis, one patient developed scleroderma with morphea lesions 9 months after beginning the trial (Peroni *et al*., 2008) again suggesting cathepsin activity can influence epidermal differentiation and regulation.

However, of interest to this project and data presented in this chapter, the aspartic protease cathepsin D in particular is known to have a role in epidermal differentiation. In corroboration with other cathepsin proteases, studies using primary human keratinocytes found cathepsin D expression to increase under calcium-induced differentiation (Horikoshi *et al*., 1998). Immunofluorescence staining for cathepsin D in whole skin biopsies found expression to be mainly in the stratum corneum and adjacent granular cells, with some staining present in the dermis. Data also suggested cathepsin D may be involved in the break down of pro filaggrin into filaggrin which had previously been found in rat skin (Kashima *et al*., 1988).

These studies all demonstrate cathepsin D is expressed in epidermal models and induced upon differentiation, but the function of cathepsin D was not fully explored.

Key work carried out by Egberts *et al* (2004) found that treatment with exogenous cathepsin D increased TGM-1 expression, whilst pepstatin A suppressed TGM-1 activity. In cathepsin D deficient mouse models, reduced activity of TGM-1 caused a reduction in expression and activity of a variety of cornified envelope proteins including loricrin, filaggrin and involucrin. In cathepsin D knockout mice, the epidermis was also reported to have reduced thickness and a thickened stratum corneum. In keeping with results presented in this paper, data from the present study demonstrated pepstatin A treatment alone reduced filaggrin expression, presumably through inhibition of cathepsin D causing a decrease in TGM-1 expression and activity. In contrast to Egberts *et al* (2004) cathepsin D shRNA knockdown caused a distinct increase in filaggrin expression above vehicle control, regardless of treatment.

Although surprising, differences between the present knockout model and published model are not entirely unexpected. The current study was carried out in human epidermal skin equivalents, whereas Egberts *et al* (2004) carried out

immunofluorescence on full thickness biopsies including dermis, from *in vivo* experiments in knockout mice. To confirm pepstatin A treatment is reducing filaggrin expression by TGM-1 downregulation, immunofluorescence or western blotting for TGM-1 protein expression would be valuable. It would also be interesting to investigate TGM-1 expression in shRNA knockdown epidermal equivalents, to help understand the increase in filaggrin expression above that of shNT vehicle control. It is also possible that by knocking down cathepsin D another type of cathepsin or an off target protein is upregulated or effected which could alter differentiation status, although this needs to be explored further.

Altering lysosomal function in particular cathepsin D inhibition and knockdown clearly effected epidermal differentiation but further experiments are required to truly delineate the exact role in the chloracne phenotype. Repeating experiments in more donors to gain significance would initially be beneficial as well as exploring the effect of cathepsin D blockade on more differentiation markers at both the protein and mRNA level.

In addition, to explore changes in proliferation status in the chloracne phenotype model further, and the potential role of lysosomal activity, Ki67 staining was performed. As presented previously (Chapter 3) TCDD treatment had no significant effect on Ki67 staining, but bafilomycin treatment appeared to increase Ki67 positive cells. As discussed, bafilomycin treatment reduced differentiation marker expression significantly. Epidermal differentiation is a complex balance between proliferation, differentiation and cell death. Perhaps by reducing rates of differentiation, cell proliferation was increased with bafilomycin treatment, through a feedback loop or some kind.

5.3.3 Role of lysosomes in TCDD-induced apoptosis

Lysosomes were previously thought to only have a role in necrosis or autophagic cell death, and lysosomal proteases such as cathepsin D only involved in general protein degradation (Benes *et al*., 2008). However, as previously discussed lysosome membrane permeabilisation and cathepsin activity are now thought to be involved in apoptosis. Many studies of apoptosis have demonstrated the contribution of

cathepsins and caspases. In a study by Appelqvis *et al* (2013) UVA irradiation of human keratinocytes resulted in nuclear fragmentation and a 9.5 fold increase in caspase-3 activity as well as increased caspase-8 activity. Interestingly, lysosomal exocytosis was also apparent, with lysosomes redistributing to the periphery of the cell and release of lysosomal contents including cathepsin D and the lysosomal enzyme acid sphingomyelinase. Similar to data presented in this chapter when using the inhibitor bafilomycin, prevention of lysosomal acidification with NH_4Cl reduced exocytosis and caspase-8 activation. In addition, caspase-8 activity was also reduced by pepstatin A treatment and the cysteine cathepsin inhibitor E64D. By treating keratinocytes with cathepsin D antibodies before UVA irradiation Appelqvis *et al* (2013) also determined that caspase-8 activation was downstream of cathepsin D. Of interest to this study, it was suggested that treatment with NH_4Cl, to increase the pH of the lysosome, may have attenuated caspase-8 activity by reducing the proteolytic action of cathepsins (Appelqvis *et al*., 2013).

Histological staining of epidermal skin equivalents and quantification of viable cell layer thickness revealed inhibition of lysosomal function and more specifically chemical and genetic inhibition of cathepsin D, blocked the TCDD-induced reduction of viable cell layer.

In keeping with the literature, one of the most interesting findings of this chapter was bafilomycin and pepstatin A treatment, as well as shRNA knockdown of cathepsin D all blocked TCDD-induced caspase-3 staining. Although TCDD was shown to induce caspase-3 expression in Chapter 3 (Fig. 3.8) and in siNT knockdown epidermal equivalents in Chapter 5, the present data further confirms TCDD-induced caspase-3 is robust and reproducible. The induction of apoptosis by TCDD treatment has been acknowledged in a variety of models, but the role of lysosomal function in this TCDD induced keratinocyte apoptosis may be novel.

As with most chemical inhibitors, pepstatin A is known to have off target effects including inhibition of cathepsin B and pepsin (Emert-Sedlak., *et al* 2005). Therefore, other methods, such as genetic interference of cathepsin D, are often pursued as they were in this study, to verify results and confirm involvement in apoptosis. In agreement with the present data, studies using siRNA constructs against cathepsin D in HeLa adherent cells and U937 suspension cells also found knockdown caused inhibition of cell death as well as delayed cytochrome *c* release and caspase-3

activity (Emert-Sedlak *et al*., 2005). Over expression studies in which cathepsin D was injected into the cytosol of fibroblasts (Roberg *et al*., 2002) and *in vivo* mouse models (Bewley *et al*., 2011) have also all implicated cathepsin D in apoptosis induction.

Interestingly, as cathepsin D has been linked to the activation of a variety of caspases and subsequent apoptosis induction, it has been suggested that cathepsin D may be involved in a pro-apoptotic protease cascade (Heinrich *et al*., 2004). However, the mechanism by which cathepsin D activates caspases is still not entirely understood. It has previously been suggested cathepsin D causes the apoptosis regulator Bax to be activated and relocate to the mitochondria, inducing the release of apoptosis-inducing factor (AIF) (Benes *et al*., 2008, Bidere *et al*., 2003). In another study in which cathepsin D was added to the mitochondria *in vitro* (Zhao *et al*., 2003) results suggested the release of proteases caused mitochondrial dysfunction, increasing reactive oxygen species (ROS) production which in turn caused cytochrome *c* release (Benes *et al*., 2008). However, cathepsin D is usually enzymatically active in a low pH within the lysosome; therefore, its ability to degrade material required for apoptosis induction within the cytosol, has been questioned. Whilst investigating this, Appelvist *et al* (2012) discovered three cathepsin D specific cleavage sites on pro-apoptotic Bid through which cathepsin D activated apoptosis, by inducing Bax-mediated cytochrome *c* release. Interestingly, cleavage of Bid by cathepsin D was revealed to take place at neutral pH, in contrast to previous studies in which processing of Bid did not occur above pH 6.2 (Heinrich *et al*., 2004). However, Appelvist *et al* (2012) did suggest changes in the cytosol pH may influence the contribution of different proteases to Bid activation.

Together these studies imply cathepsin D triggers apoptosis through multiple mechanisms, which are likely to be cell or model dependent, but probably involve mediators of apoptosis such as cytochrome *c*, caspases and bcl-2 family members (Benes *et al*., 2008). Therefore, the reduction in caspase-3 staining by cathepsin D knockdown and chemical inhibition through pepstatin A, or indeed treatment with bafilomycin is not surprising and is in agreement with the literature. The exact mechanism behind TCDD inducing cathepsin D mediated apoptosis will require further investigation.

As demonstrated in Chapter 4, genetic inhibition of autophagy also blocked TCDD induced caspase-3 staining. It is possible that by blocking lysosomal function or cathepsin D activity that this also attenuates the autophagy pathway/autophagic cell death, which may block the subsequent induction of apoptosis. Alternatively, TCDD induced apoptosis may be independent from autophagy. Since there is such complex cross talk between autophagy, lysosomal activity and apoptosis it is likely each process is contributing to the phenotype in some way. Due to this complexity, a proteomic study is currently being carried out in collaboration with AstraZeneca, with a particular interest in lysosomal proteins, and it is hoped this will help elucidate the contribution of these mechanisms involved in the chloracne phenotype.

5.4. Summary

- TCDD treatment caused an increase in LAMP2 expression, indicating accumulation of lysosomes

- Chemical inhibition of lysosomal function and cathepsin D through bafilomycin and pepstatin A respectively, altered TCDD-induced AhR degradation

- Lysosomal function likely contributes to TCDD-induced de-regulated epidermal differentiation

- The TCDD-induced reduced viable cell layer thickness was prevented with blockade of lysosomal function as well as chemical and genetic inhibition of cathepsin D

- TCDD-induced caspase-3 staining was reduced with blockade of lysosomal function as well as chemical and genetic inhibition of cathepsin D

Chapter 6 Concluding Remarks

6.1. Main Conclusions

The principle aim of this project was to explore the mechanisms behind a previously developed TCDD-induced chloracne phenotype model (Forrester et al., 2014). Specific aims (as described in Chapter 1, section 1.9) included investigating further potential mechanisms contributing to the morphological features observed, including the balance between cell division and cell death and the role of autophagy, arising in part from data and hypotheses generated during previous work in our lab (Forrester Thesis). Another key aim of this project was to explore the role of lysosomal function, specifically cathepsin D in the chloracne phenotype. Cross talk between autophagy and lysosomal cell death is an emerging area and as such an additional aim was to determine the impact on TCDD-induced cell death. The overall findings of this project, focussing on work in epidermal equivalents, are presented in schematic diagrams (Figure 6.1 and Figure 6.2).

The data generated provide increased insight into the physiological role of AhR in the skin and potentially highlight therapeutic targets for the treatment of chloracne. Furthermore, in the pharmaceutical industry potential drugs are often excluded if they activate AhR due to concerns of toxic side effects. Therefore, understanding the role of AhR further is potentially beneficial to the salvage of previously abandoned therapeutic compounds, as discussed by Van den Bogaard *et al* (2013) in which results demonstrated AhR activation is in fact required for epidermal barrier repair in eczema after coal tar treatment.

Initially work reported in Chapter 3 was focused on optimising a TCDD treatment regime to produce a robust and reliable chloracne phenotype model, with reduced viable cell layer thickness and compacted stratum corneum, to use for delineating targets of TCDD induced AhR activation. Whilst TCDD has previously been shown to induce a chloracne phenotype (Forrester Thesis), data demonstrating the temporal regulation and development over 7 days was novel. Combined data from 8 independent donors, found TCDD treatment significantly reduced viable cell layer thickness after 7 days, confirming the treatment regime and reproducibility of this model ($p<0.0001$, Chapter 3, Fig 3.3).

Results (Chapter 3) demonstrated significant AhR protein degradation only occurred after treatment with TCDD for 7 days, indicating delayed or prolonged AhR protein

degradation compared to monolayer keratinocyte cultures (Chapter 4, Fig 4.1, Fig 4.2, Fig 4.4A). Decreased AhR mRNA expression and induction of CYP1A1 mRNA expression were also evident after 7 days treatment, collectively indicative of TCDD interacting with AhR and subsequent degradation of the receptor. However, earlier time points were not explored in the context of mRNA expression and as such CYP1A1 mRNA induction and AhR mRNA degradation may be earlier events.

However, this late or prolonged induction of CYP1A1 is indicative of the long half-life of TCDD and the sustained induction of the AhR pathway is also seen *in vivo*. Saurat et al (2009) found CYP1A1 mRNA expression to be increased significantly above control in chloracne skin lesions 5 months after TCDD poisoning. Furthermore, a delay in AhR degradation in the epidermal skin equivalent model has been seen previously (Forrester thesis, Forrester *et al.,*2014). Results from this study revealed AhR degradation occurred after only 2 days in monolayer primary human keratinocytes, whilst AhR degradation was evident only after 7 days in epidermal skin equivalents.

Chloracne is a chronic skin disease; however, the onset of clinical symptoms is normally 2-4 weeks after exposure to chloracnegens (Ju *et al.,* 2009). Therefore, a delay in AhR degradation and delay in phenotype development is likely more patho-physiologically relevant than other cell models in which AhR degradation is detected much earlier. This might also reflect the need for chronic stimulation of the system to induce the morphological changes observed.

Another key difference noted in the present study was the differential effect of TCDD on cell viability between monolayer and epidermal equivalent models. Although TCDD was clearly activating AhR, as AhR protein expression was significantly reduced, TCDD caused no significant change to cell number in monolayer experiments. In contrast, one of the key early findings of the project was the significant induction of active caspase-3 expression after TCDD treatment, suggesting that apoptotic cell death may play a role in the development of the chloracne phenotype and specifically may account for the reduced viable cell layer. This increase in caspase-3 expression and likely apoptotic cell death is in keeping with the significant reduction in viable cell layer in the chloracne phenotype. Caspase-3 staining was detected in epidermal skin equivalents after 7 days of treatment with TCDD. This potential delayed induction of apoptosis or prolonged

apoptosis is in keeping with the delay in AhR degradation and induction of CYP1A1. Again this data supports the long half-life of TCDD and delayed clinical symptoms of chloracne *in vivo*. Furthermore, through KI67 staining, results suggested TCDD did not alter proliferative status of keratinocytes and as such it is unlikely the reduced viable cell layer is due to reduced proliferation, as no significant change in Ki67 staining was detected.

In epidermal equivalents, TCDD also clearly induced autophagic activity, with significantly increased LC3II protein expression and immunofluorescence staining revealed endogenous LC3 increased whilst P62 expression decreased, well-known markers of autophagic flux.

These results then opened up the overarching question of how cross talk between these signalling pathways might contribute to the chloracne phenotype. The approach taken was to focus on autophagy, lysosomal activation and apoptosis and investigate how these pathways interact and thereby result in AhR degradation, deregulated epidermal differentiation and the morphological changes observed.

The next chapter (Chapter 4) utilised a potential higher throughput monolayer chloracne model to study these pathways. However, results revealed differences in response to TCDD between monolayer and the epidermal equivalent model (as seen previously in these models) (Forrester thesis) and as such the monolayer model was not pursued in future chapters.

One of the key differences in comparison to work in epidermal equivalents was TCDD caused no significant change to cell number after treatment in monolayer, even across time points and at different extracellular calcium concentrations (Chapter 4, Fig 4.9 and Fig. 4.10). Another key difference was the lack of LC3II accumulation after TCDD treatment, in contrast to significant autophagy induction detected in epidermal skin equivalents. Although results generally revealed differential effects of TCDD treatment in monolayer cultures compared to epidermal equivalents, there was evidence of TCDD induced AhR degradation in monolayer and as such these differential results are likely not due to altered activation of AhR.

Nevertheless, after optimising siRNA ATG7 knockdown in monolayer this was then taken into epidermal equivalents and revealed interesting results (as demonstrated by the orange arrows in Fig. 6.1). Knockdown of ATG7 not only blocked the TCDD-

induced reduced viable cell layer but also blocked TCDD-induced caspase-3 expression, suggesting autophagy is required at least in part for apoptotic cell death in this model. Furthermore, knockdown of ATG7 blocked TCDD-induced AhR degradation suggesting autophagy may play a role in AhR degradation. As discussed in the introduction (Chapter 1), AhR is thought to be principally degraded by the 26S proteasome pathway and crosstalk between this and autophagy, specifically chaperone-mediated autophagy has been reported. Therefore, to explore the potential crosstalk between these pathways in the chloracne phenotype model, the influence of lysosomal function which is required for chaperone mediated autophagy was explored in the final chapter.

The lysosomal protease cathepsin D is of particular interest in this project after preliminary data (Forrester thesis) suggested TCDD treatment of epidermal skin equivalents and monolayer primary human keratinocytes de-regulated cathepsin D expression. In addition, studies have previously suggested a role for AhR in cathepsin D transcription (Wang *et al*., 1999) as well as a role for cathepsin D in epidermal differentiation, particularly in regulation and activation of TGM-1 (Egberts et al., 2004).

Treatment with the lysosomal chemical inhibitor bafilomycin and cathepsin D inhibitor pepstatin A as well as cathepsin D shRNA knockdown in epidermal equivalents revealed important findings. Data suggested crosstalk between lysosomal activity and TCDD induced cell death as well as AhR degradation (as demonstrated by the green arrows in Fig. 6.1). Results in Chapter 5 revealed blockade of lysosomal function prevented the TCDD-induced reduction in viable cell layer thickness as well as reduction in TCDD-induced caspase-3 expression, suggesting lysosomes, perhaps through LMP, are likely involved in the induction of apoptotic cell death. Bafilomycin treatment also increased Ki67 staining above that of vehicle, although not significantly. As demonstrated in Chapter 5 (Fig. 5.5, Fig. 5.6) bafilomycin treatment altered epidermal differentiation marker expression at both protein and mRNA level. Epidermal differentiation is a complex balance between proliferation, differentiation and cell death and as such, it is not surprising bafilomycin also effects proliferation status of cells.

TCDD-induced AhR degradation was also prevented with bafilomycin and pepstatin A co-treatment, although results with cathepsin D shRNA knockdown were variable.

Another novel result was the accentuated TCDD-induced CYP1A1 expression observed after co-treatment with bafilomycin.

Although ATG7 knockdown in epidermal equivalents resulted in variable epidermal differentiation marker expression, bafilomycin, pepstatin A and cathepsin D knockdown all blocked TCDD-induced reduction in filaggrin protein expression. These results suggest a role for lysosomal function in TCDD de-regulated differentiation.

Together, these novel data suggest apoptosis, autophagy and de-regulated differentiation all contribute to the development of a TCDD-induced chloracne phenotype. Results specifically demonstrated autophagy and lysosomal function are likely involved in this apoptotic activity. Furthermore, lysosomal activity and autophagy are required at least in part for the degradation of AhR after TCDD treatment, and we hypothesise this is through chaperone mediated autophagy. However, the intricate cross-talk between apoptosis, lysosomal activity and autophagy adds to the complexity of these findings.

Although TCDD has previously been reported to induce apoptosis in other systems, and lysosomes are known to play a role in apoptosis through LMP (as discussed in Chapter 5, section 5.3.3), the involvement of lysosomes in TCDD-induced apoptosis in keratinocytes is a novel finding. Furthermore, only two studies reporting TCDD-induced autophagy have been published, one of which in a bovine kidney cell line (Fiorito et al., 2011) and the other in the human neuroblastoma cell line SH-SY5Y (Zhao et al., 2015). In contrast to the present data, Zhao et al, (2015) suggest autophagy protects against TCDD induced apoptosis in cells and found blockade of autophagy through treatment with 3-MA led to increased apoptosis. However, crosstalk between apoptosis and autophagy is complex and studies have reported conflicting results as reviewed by Mukhopadhyay et al (2014). Indeed, as demonstrated above, autophagy can promote cell survival and block apoptosis in the same system but under alternative conditions. Thus, autophagy can result in cell death through apoptosis or independently through non-apoptotic pathways (Mukhopadhyay *et al*., 2014). Therefore, the precise pathway and interaction between TCDD-induced apoptosis and induction of autophagy remains unclear and requires further delineation.

Conflicting data on TCDD induced de-regulated differentiation are also reported in the literature. Generally, results suggest TCDD treatment accelerates differentiation in corroboration with this, studies have shown TCDD treatment to increase differentiation marker expression in keratinocyte models (Loertscher *et al*., 2001b, Gaido and Maness, 1994, Sutter *et al*., 2009). However, in the present model, TCDD treatment induced downregulation of differentiation marker protein expression, whilst mRNA expression was increased. Interestingly, in agreement with results from the present study, Hu *et al* (2014) also demonstrated through proteomic analysis, treatment of keratinocytes with TCDD for two weeks induced downregulation of filaggrin, keratin 1 and keratin 10 protein expression. In addition, Geusau *et al* (2005) found TCDD treatment of organotypic models, revealed an increase in involucrin expression but decrease in keratin 1 and 10. The author suggests although hyperkeratosis is a known feature of chloracne, parakeratosis and loss of granular layer is also displayed and as such differentiation may be de-regulated rather than simply induced, in agreement with the present study. It has also been reported that induction of ROS, specifically TCDD-mediated production of hydrogen peroxide (H_2O_2) is essential for the TCDD-induced acceleration of differentiation (Kennedy *et al*., 2013). Therefore, differences in ROS generation likely contribute to differences in TCDD-induced de-regulated differentiation between studies. In addition, the technical and cellular differences between models, treatment regimens and culture conditions may all influence the effect of TCDD treatment.

Collectively this study has demonstrated epidermal skin equivalents provide a physiologically relevant, reproducible tool to explore pathways and molecular targets of interest in disease models and environmental exposure. The data presented further delineates the pathophysiology of chloracne and has highlighted novel outcomes of TCDD-induced AhR pathway activation. As reviewed by Mulero-Navarro and Fernandez-Salguero (2016) the AhR is already implicated in significantly more cellular processes than initially thought and as evidenced by this project, likely to be involved in many more.

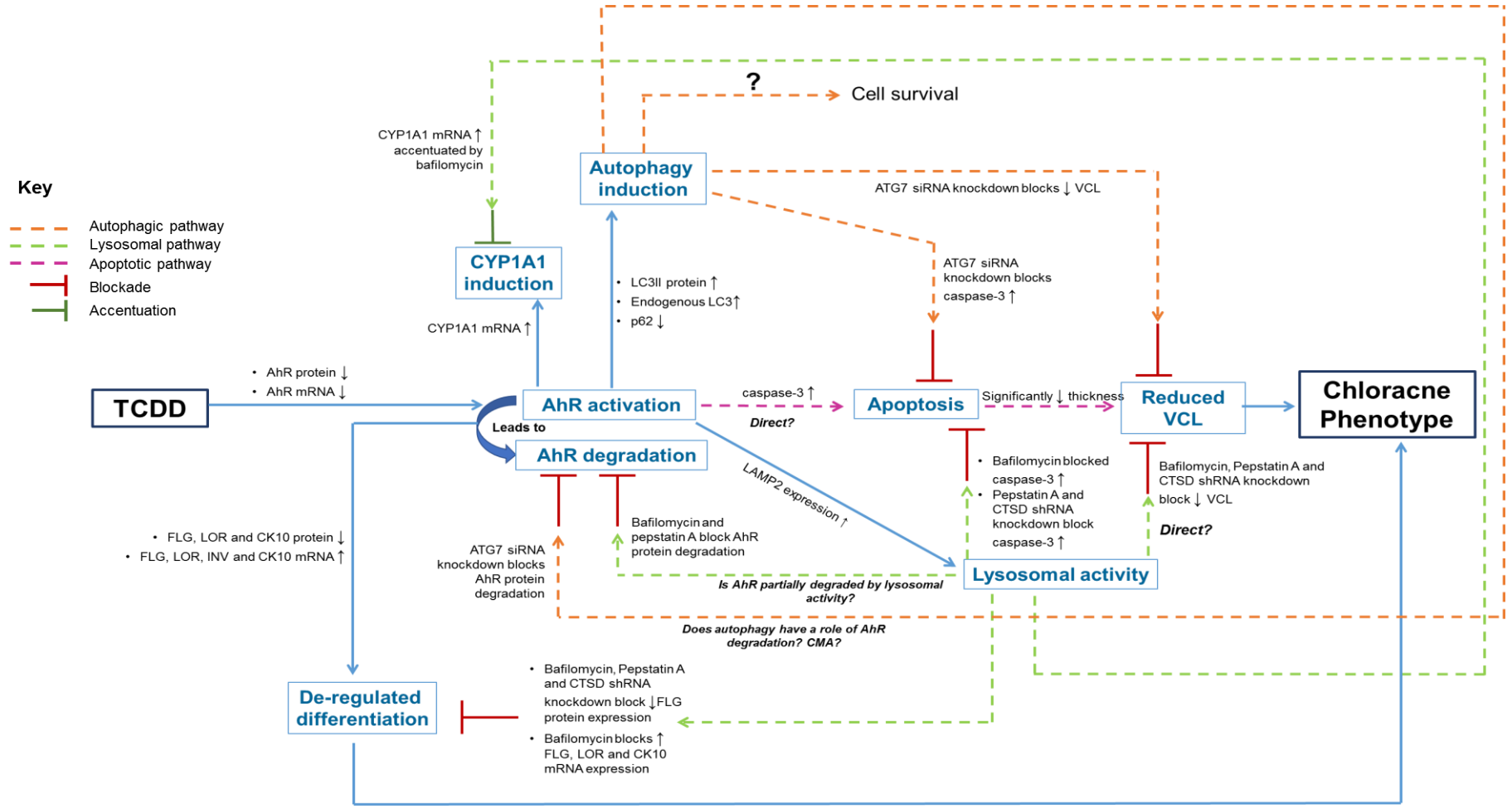

Figure 6.1. Detailed overview of findings in epidermal skin equivalents

Schematic demonstrating the pathways involved in development of the chloracne phenotype model and potential crosstalk.

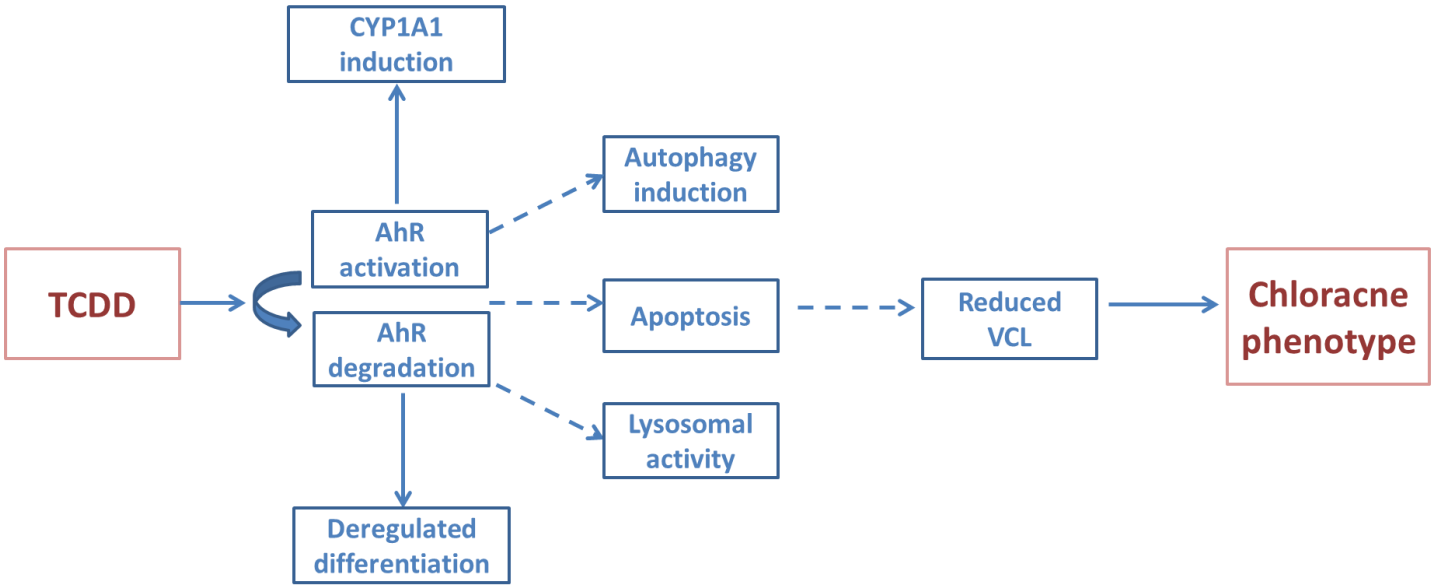

Figure 6.2 Summary of findings in epidermal skin equivalents

Schematic demonstrating the pathways involved in development of the chloracne phenotype model

6.2. Future Work

One of the key areas for future work would be to explore the role of chaperone mediated autophagy in AhR degradation. Although results strongly suggested lysosomal function and autophagy were required for AhR degradation in this model, delineating whether this is specifically chaperone mediated autophagy would require further experiments.

There are a number of approaches to take when exploring chaperone mediated autophagy (Patel and Cuervo. 2015). To assess activity, post translational changes in key components of the pathway can be determined by immunoblotting or immunofluorescence. For example, staining for LAMP2A or lysosomal hsc-70, both of which known to be required for chaperone mediated autophagy activity (Agarraberes *et al*., 1997, Cuervo and Dice, 1996). Co-localisation of markers LAMP2A, hsc-70 or P62 in combination with AhR could also be valuable to determine whether this was specifically involved in AhR degradation. To determine whether a protein of interest, in this case AhR, is a chaperone mediated autophagy substrate there are also a number of readouts. Principally these are focused on determining the cellular localisation/levels of the protein or the effect of modulation of chaperone mediated autophagy on protein degradation. However, it should be noted that blocking chaperone mediated autophagy can alter other autophagy pathways and can increase protein degradation by alternative pathways (Kaushik and Cuervo 2009, Patel and Cuervo, 2015).

Another area for future work would be determining if apoptosis was the primary mechanism responsible for the TCDD reduced viable cell layer. It would also be interesting to establish the relationship between autophagy and apoptosis in this model, as results suggested blocking autophagy blocked caspase-3 expression, but the precise order of events needs further investigation. Alternatively, epidermal equivalents could be treated with a pan-caspase inhibitor. However, it has been reported that at high concentrations, caspase inhibitors can also block cathepsins which can cause misinterpretations of data (Foghsgaard *et al*., 2001, Gomez-Sintes *et al*., 2016). To specifically determine if LMP is occurring can be quite difficult as lysosomes are heterogeneous and have differential sensitivity to agents.

In addition, blocking lysosomal function prevented TCDD induced caspase-3 expression; suggesting LMP is occurring and inducing apoptosis. However, blocking lysosomal function may simply be attenuating autophagy and as such confirmation of LMP and its time course (relative to caspase-3 activation) would be required to firmly establish the role of lysosomes in regulating apoptosis in this model. To explore the role of apoptosis further, knockdown of key regulatory genes involved in the intrinsic apoptosis pathway could be pursued, such as BAX or BAK.

However, as well as cathepsin inhibitors used in this study, serpins (serine protease inhibitors) have also been found to inhibit caspases and cathepsins and block lysosomal cell death (Law *et al*., 2006). In addition, antioxidants can also be used to prevent ROS induced LMP inhibiting LMP and subsequent cell death (Zang *et al*., 2001). It can be technically difficult to explore cellular activity in epidermal equivalents, however, if LysoTracker®, or indeed staining of cathepsin B or D to explore their release from lysosomes, could be optimised these would also be useful tools. The use of super-resolution microscopy or two photon microscopy would also enable us to explore localisation within the model further.

Finally, proteomics analysis of TCDD-treated epidermal equivalents is on-going, with the specific aim of exploring lysosome-related proteins. Results from this will also help determine specific proteins of interest and confirm the involvement of lysosomes.

Of note, although results demonstrated consistent trends in data there was often a lack of statistical significance. This is due to donor variability and relatively low sample number (in part because of the logistical/time considerations); although trends in donors were often exactly the same, values between donors varied, as such these trends were often deemed not significant. Therefore, repeating these experiments in more donors may be required to make firm conclusions.

6.3. Potential molecular targets of interest

A commentary paper of interest to this study has recently been published, focussing on the elucidation of dioxin-mediated chloracne and AhR (Bock, 2016). Although the paper focuses on sebaceous glands and TCDD activation of the AhR pathway in sebocytes it brings to light molecular targets which may be relevant to the present model.

The proposed relationship between AhR and Blimp1 (B lymphocyte-induced maturation protein 1) is of particular importance. In murine sebaceous glands, AhR co-localised with Blimp1, known to regulate cell number, cell size and activity of sebaceous glands (Ikuta *et al*., 2010). Expression of Blimp1 mRNA was also induced in SZ95 sebocytes and HaCaT keratinocytes after treatment with AhR ligands and this was found to be dependent on AhR and ARNT (Ikuta *et al*., 2010). In a later study, TCDD treatment of *ex vivo* human skin samples and cultured SZ95 sebocytes was noted to induce irregular differentiation in the sebaceous gland cells (Ju *et al*., 2011). Taken together, Ju *et al* (2011) hypothesise that TCDD causes hypoplasia of the sebaceous gland by induction of Blimp1 which represses c-Myc. Blimp1 is known to regulate the transcription factor c-Myc, which plays a role in the balance between pro-genitor cell self-renewal and differentiation (Bock, 2016, Wilson *et al*., 2004).

Interestingly, Blimp1 has also been implicated in epidermal differentiation; with conditional knockout mice displaying enlarged granular layer cells and corneocytes, and a morphologically abnormal cornified layer (Magnúsdóttir *et al*., 2007). However, key to the present study, c-Myc plays a pivotal role in in the apoptosis pathway as reviewed by Hoffman and Liberman (2008). A recent paper has also suggested AMBRA-1 facilitates the de-phosphorylation and degradation of c-Myc, demonstrating potential crosstalk between c-Myc and the autophagy signalling network (Cianfanelli *et al*., 2015). In addition, Mandavia (2015) hypothesises TCDD may directly, or indirectly (via AhR cross-talk) up regulate c-Myc via EGFR-ERK axis stimulation, increasing epidermal stem cell turnover in chloracne. Together this data suggests Blimp1 may be implicated in the TCDD induced de-regulated differentiation in the present model. In addition, the potential interaction with c-Myc and subsequent effect on the autophagic and/or apoptotic pathway, in the present model would be interesting to explore.

Bock (2016) also comments on the involvement of AhR in modulation of cell cycle through p21/Cip1. Interestingly, a recent study has suggested p21 is key in the response of HaCat keratinocytes to UVB exposure (although HaCaTs are effectively p53 null) (Chen *et al*., 2015). UVB exposure downregulated p21 and was associated with significantly increased apoptosis, decreased proliferation, and increased G2 phase arrest. Given the similarity between phenotypes, interaction between AhR and p21/Cip1 could possibly be involved in the current model. In corroboration with this, a microarray analysis of TCDD-treated multipotential C3H10T1/2 fibroblasts found altered expression of over 1000 genes, including a 1.8 fold reduction in the p21 gene (Hanlon *et al*., 2005).

As discussed, there are a variety of potential molecular targets to further explore and as demonstrated by the present study, the robust and reproducible chloracne phenotype model represents an ideal environment to take these studies forward and understand their functional and pathophysiological relevance.

Appendices

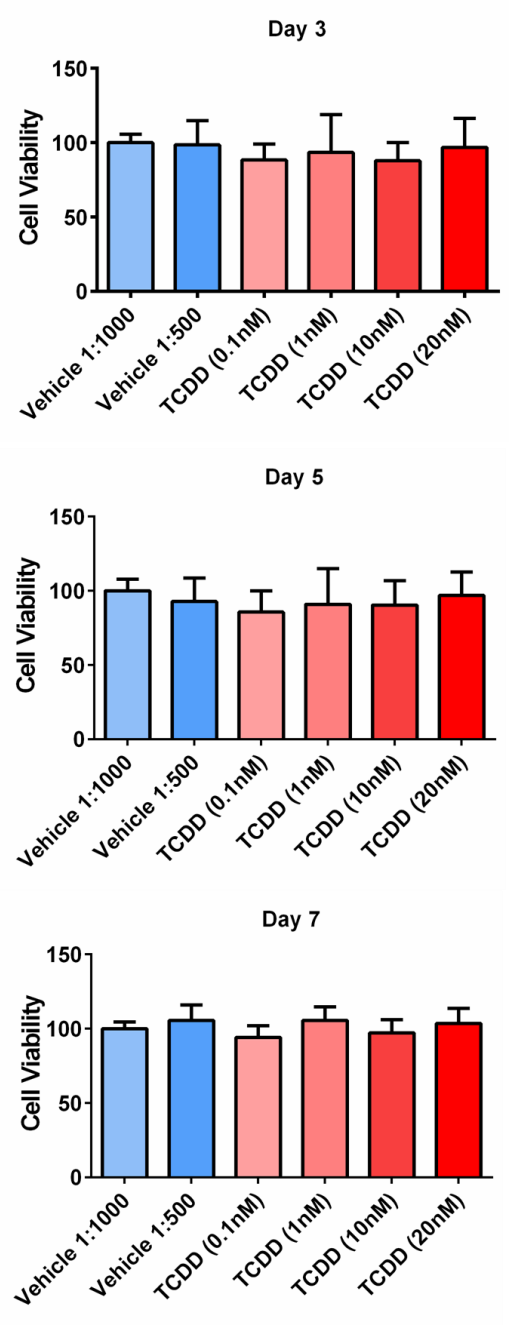

Appendix A. TCDD causes no significant induction of reduced keratinocyte viability at day 3, 5 or 7 days in monolayer culture.

Analysis of cell viability (SRB assay) in monolayer primary human keratinocytes following treatment with vehicle (DMSO) control (blue bars), TCDD (0.1, 1, 10 or 20nM) (red bars) every 48 hours for 3, 5 and 7 days. Each bar is expressed relative to vehicle (DMSO) 1:100 control. n=3 independent donors, in triplicate (N=9) ± SEM. Statistics were acquired by one-way ANOVA with Dunnett's multiple comparison test (NS)

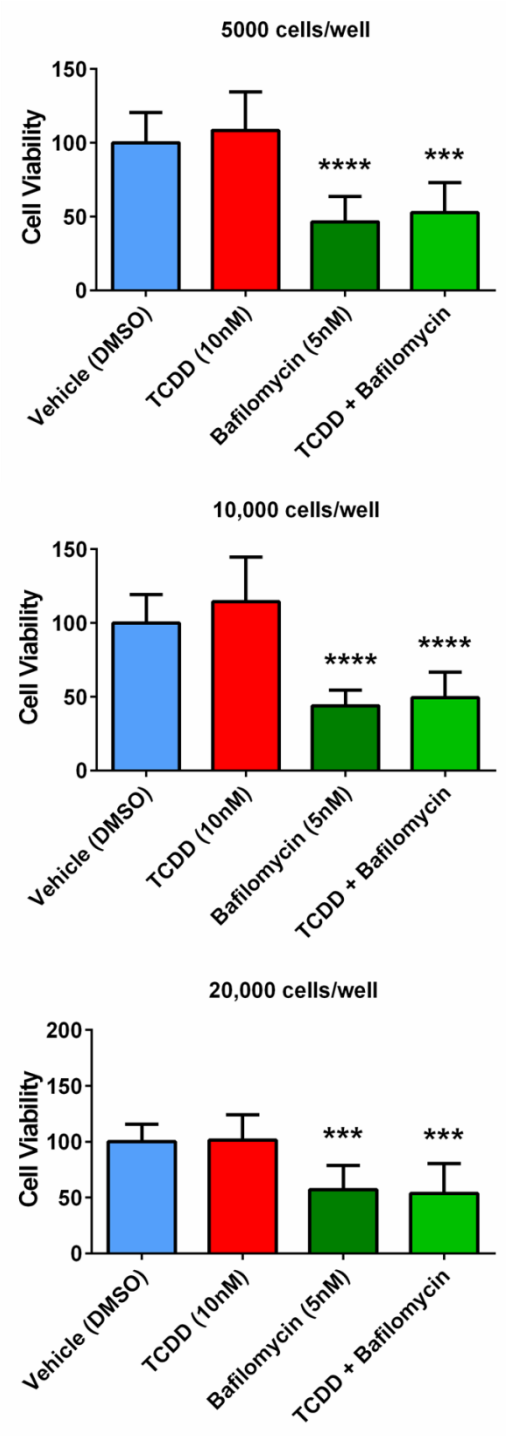

Appendix B. TCDD causes no significant induction of reduced keratinocyte viability in monolayer culture even at different seeding densities.

Analysis of cell viability (SRB assay) in monolayer primary human keratinocytes, seeded at 5,000, 10,000 or 20,000 cells per well of a 48 well plate, following treatment with vehicle (DMSO) control (blue bars), TCDD (10nM) (red bars) bafilomycin (5nM) (dark green bars) or TCDD with bafilomycin (light green bars) every 48 hours for 5 days. Each bar is expressed relative to vehicle (DMSO) control. n=3 independent donors, in triplicate (N=9) ± SEM. Statistics were acquired by one-way ANOVA with Dunnett's multiple comparison test ***p<0.001 ****p<0.0001

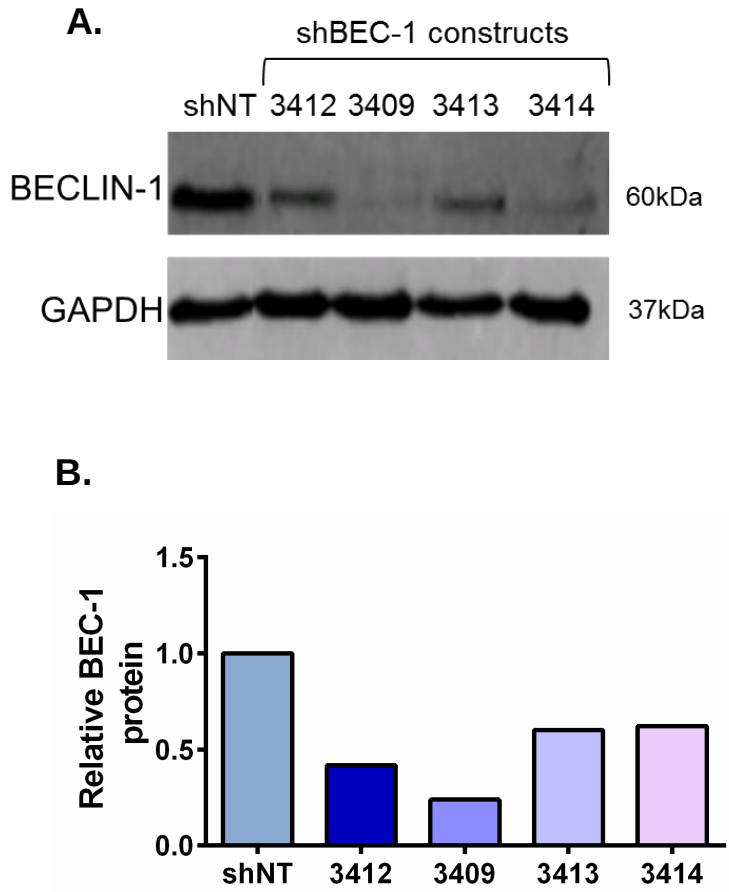

Appendix C. Optimisation of BECLIN-1 shRNA knockdown in monolayer primary human keratinocytes

A) Representative western blot of BECLIN-1 (BEC-1) protein expression in monolayer primary human keratinocytes with either shNT or 3412, 3409, 3413, or 3414 BECLIN-1 shRNA constructs. B) Densitometric analysis of BECLIN-1 expression in shNT and shBEC-1 knockdown monolayer primary human keratinocytes. Expression is normalised to GAPDH loading control expressed relative to shNT, n=1 independent donor and therefore no statistical analysis could be performed.

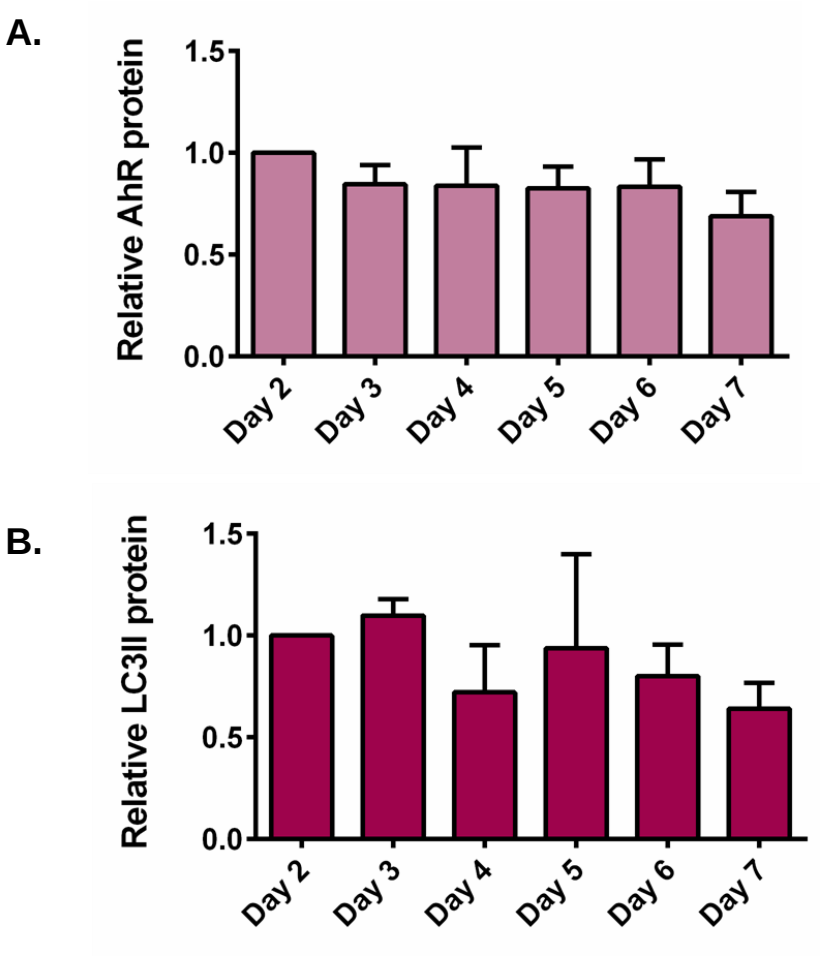

Appendix D. Treatment with vehicle (DMSO) causes no significant change in AhR or LC3II protein expression in monolayer primary keratinocyte cultures, over time.

Densitometric analysis of A) AhR or B) LC3II protein expression in monolayer primary human keratinocytes vehicle (DMSO) treatment every 48 hours over 7 days. Each bar is normalised to GAPDH loading control expressed relative to vehicle (DMSO) control at day 2 n=3 independent donors, ± SEM. Statistics were acquired by one-way ANOVA with Dunnett's multiple comparison test. A) (NS) B) (NS)

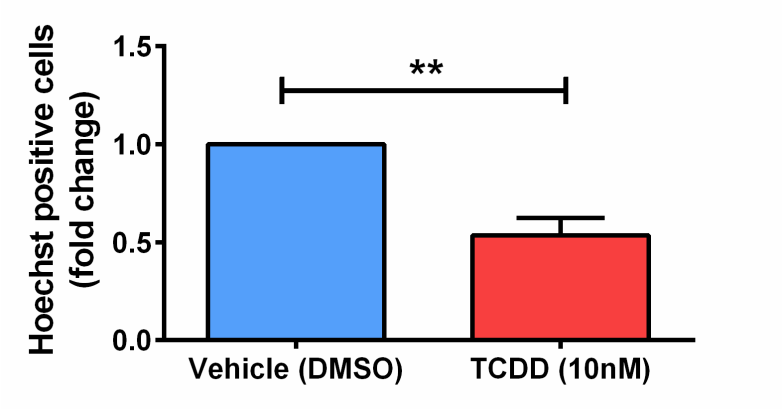

Appendix E. TCDD significantly reduced Hoechst positive cells in human epidermal equivalents.

Mean fold change of Hoechst positive cells in epidermal equivalents treated with vehicle (DMSO) (blue bar) or TCDD (10nM) (red bar) every 48 hours for 7 days normalised relative to vehicle (DMSO) control. n=7 independent donors, ± SEM. Statistics were acquired by paired t-test **p=<0.01

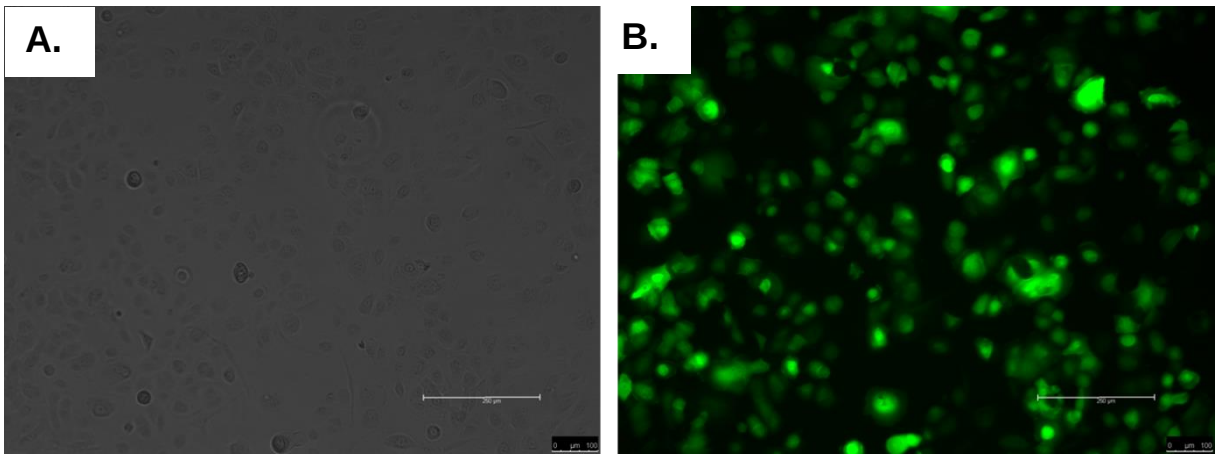

Appendix F. Transduction efficiency of shRNA BECLIN-1 3409 construct.

Representative photomicrographs of monolayer primary human keratinocytes 48 hours post transduction with shBECLIN-1 3409 depicting A) bright field or B) GFP fluorescence of the same field of view of cells. Scale bar= 250µm

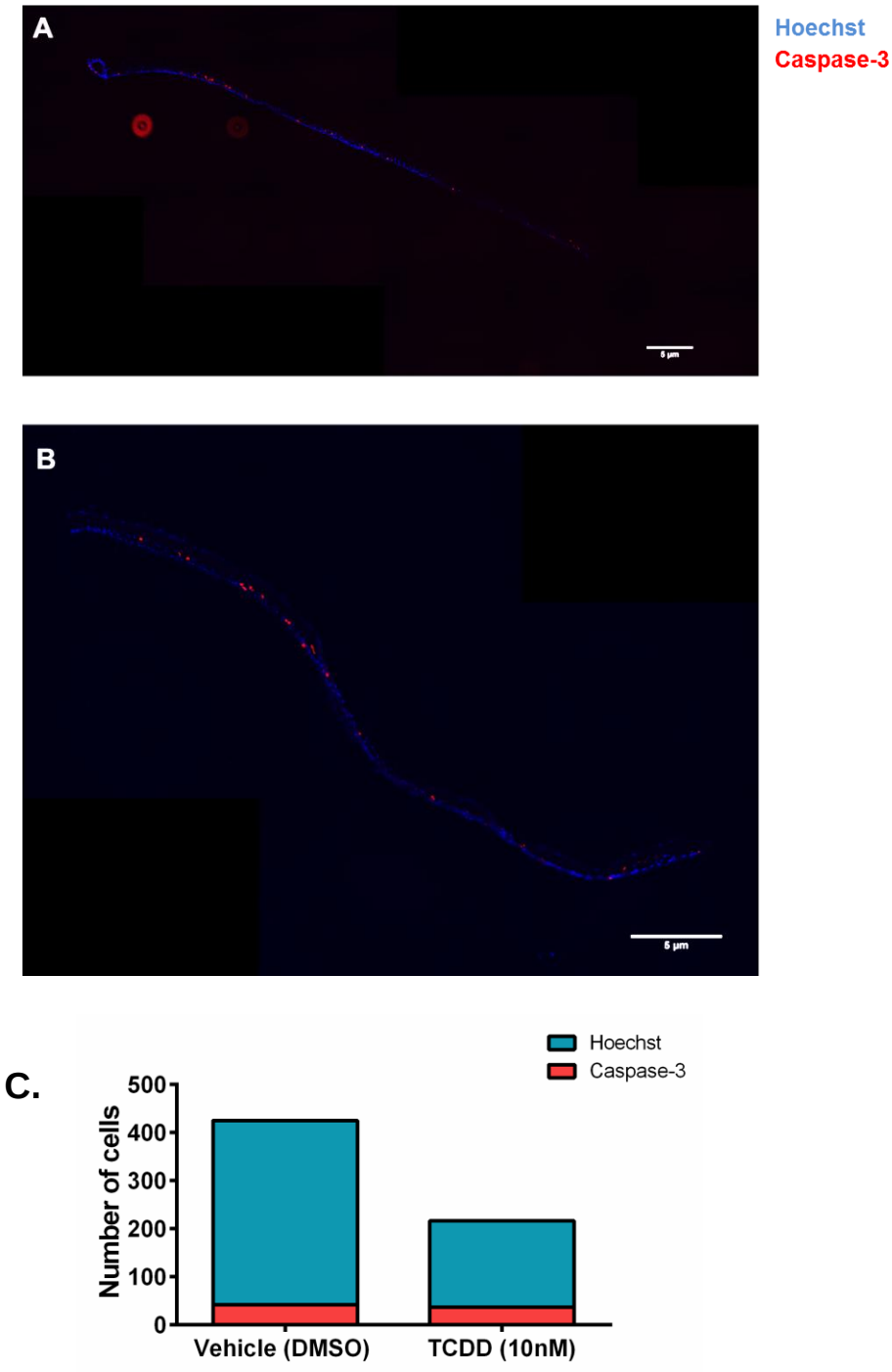

Appendix G. Raw number of Caspase-3 and Hoechst positive cells after vehicle and TCDD treatment.

Representative tiled photomicrographs taken at 10x magnification from one donor of epidermal skin equivalents treated with vehicle (DMSO) (A) or TCDD (10nM) (B) every 48 hours for 7 days depicting Hoechst nuclear staining (blue fluorescence) or caspase-3 expression (red fluorescence). Scale bar=5µm. C) Raw number of cells with Hoechst or caspase-3 expression in the epidermal skin equivalent photomicrographs presented, treated with vehicle (DMSO) or TCDD (10nM) every 48 hours for 7 days. Data is from one representative donor so no statistical test was used.

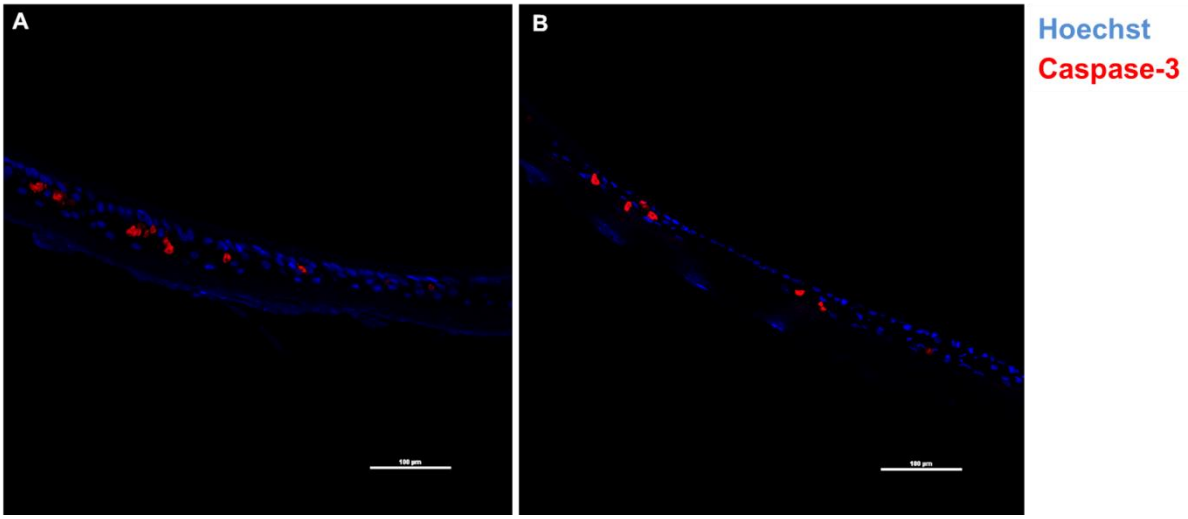

Appendix H. Higher magnification images of Caspase-3 and Hoechst staining in epidermal skin equivalents after vehicle and TCDD treatment.

Representative photomicrographs taken at 20x magnification from one donor of epidermal skin equivalents treated with vehicle (DMSO) (A) or TCDD (10nM) (B) every 48 hours for 7 days depicting Hoechst nuclear staining (blue fluorescence) or caspase-3 expression (red fluorescence). Scale bar=100µm.

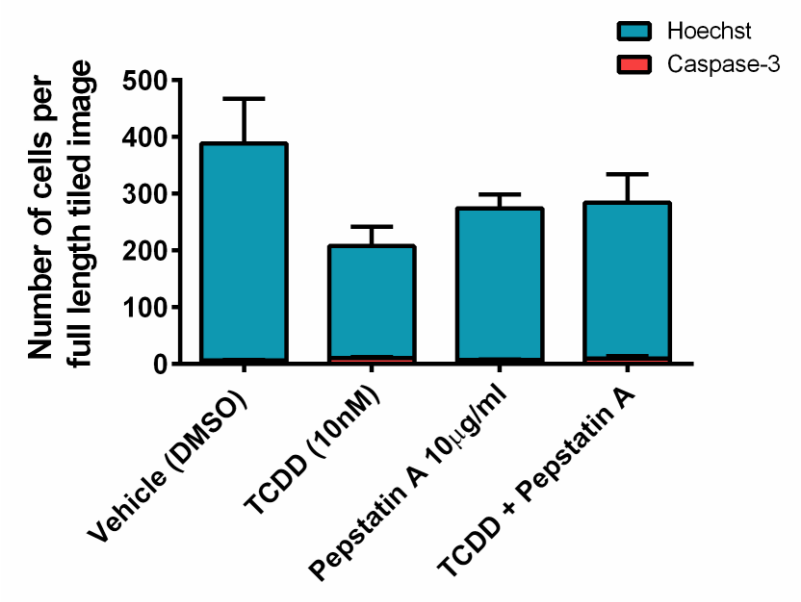

Appendix I. Raw number of Caspase-3 and Hoechst positive cells in epidermal skin equivalents after chemical inhibition of cathepsin D

Raw number of cells with Hoechst or caspase-3 expression in epidermal skin equivalents, treated with vehicle (DMSO), TCDD (10nM) Pepstatin A (10µg/ml) or TCDD with pepstatin A co-treatment every 48 hours for 7 days, n=4 independent donors, ± SEM. Statistics were acquired by two-way ANOVA with Bonferroni's multiple comparison test (NS)

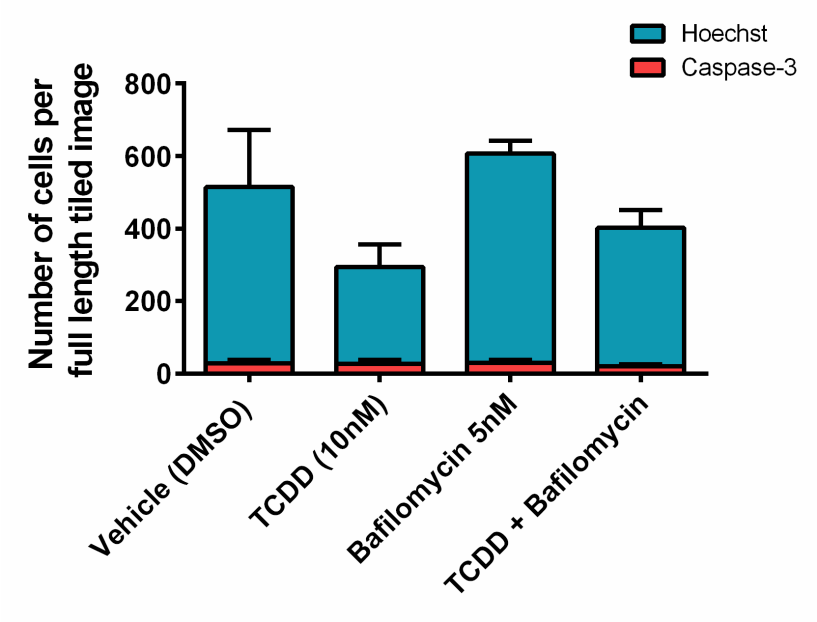

Appendix J. Raw number of Caspase-3 and Hoechst positive cells in epidermal skin equivalents after blockade of lysosomal function

Raw number of cells with Hoechst or caspase-3 expression in epidermal skin equivalents, treated with vehicle (DMSO), TCDD (10nM) bafilomycin (5nM) or TCDD with bafilomycin co-treatment every 48 hours for 7 days, n=4 independent donors, ± SEM. Statistics were acquired by two-way ANOVA with Bonferroni's multiple comparison test (NS)

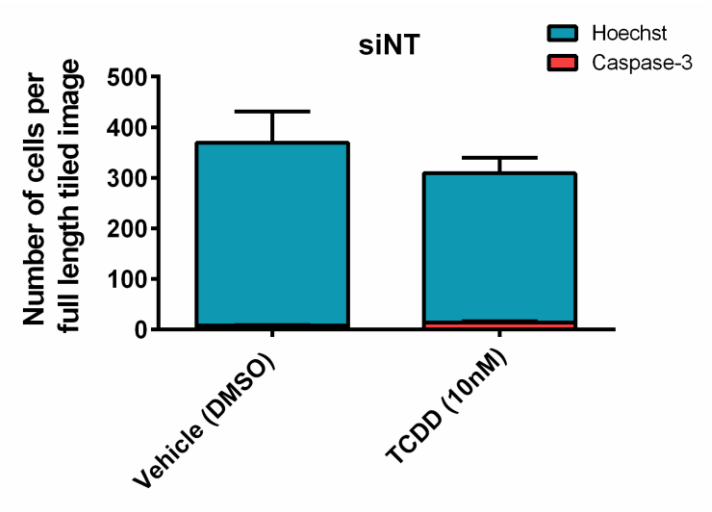

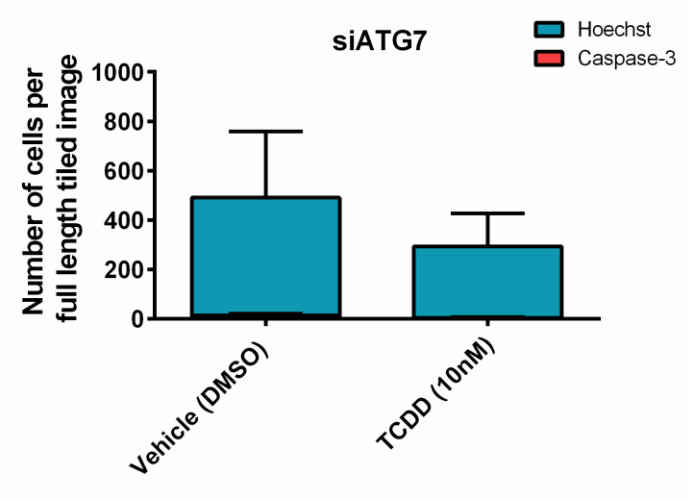

Appendix K. Raw number of Caspase-3 and Hoechst positive cells in epidermal skin equivalents after siRNA ATG7 knockdown

Raw number of cells with Hoechst or caspase-3 expression in siNT and siATG7 epidermal skin equivalents, treated with vehicle (DMSO) or TCDD (10nM) every 48 hours for 7 days, n=3 independent donors, ± SEM. Statistics were acquired by two-way ANOVA with Bonferroni's multiple comparison test (NS)

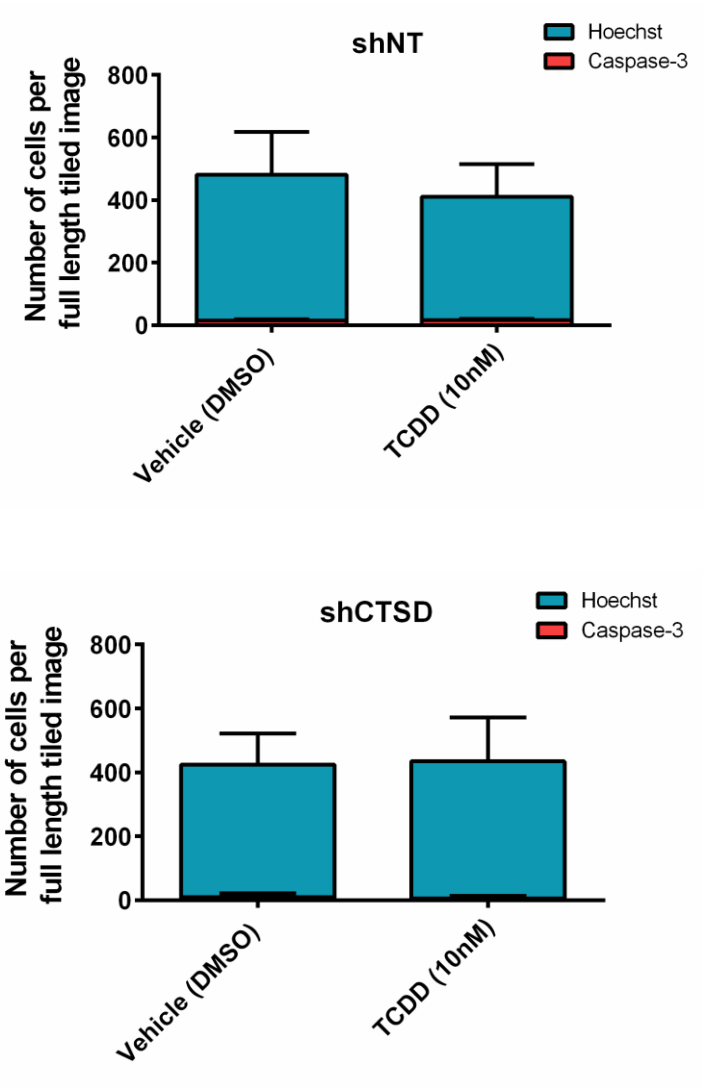

Appendix L. Raw number of Caspase-3 and Hoechst positive cells in epidermal skin equivalents after shRNA cathepsin D knockdown

Raw number of cells with Hoechst or caspase-3 expression in shNT and shCTSD epidermal skin equivalents, treated with vehicle (DMSO) or TCDD (10nM) every 48 hours for 7 days, n=3 independent donors, ± SEM. Statistics were acquired by two-way ANOVA with Bonferroni's multiple comparison test (NS)

References

Abel, J. and Haarmann-Stemmann, T. (2010) 'An introduction to the molecular basics of aryl hydrocarbon receptor biology', *Biological chemistry*, 391(11), pp. 1235-48.

Agarraberes, F.A., Terlecky, S.R. and Dice, J.F. (1997) 'An intralysosomal hsp70 is required for a selective pathway of lysosomal protein degradation', *The Journal of cell biology*, 137(4), pp. 825-34.

Aits, S. and Jaattela, M. (2013) 'Lysosomal cell death at a glance', *Journal of cell science*, 126(Pt 9), pp. 1905-12.

Akinduro, O., Sully, K., Patel, A., Robinson, D.J., Chikh, A., McPhail, G., Braun, K.M., Philpott, M.P., Harwood, C.A., Byrne, C., O'Shaughnessy, R.F. and Bergamaschi, D. (2016) 'Constitutive autophagy and nucleophagy during epidermal differentiation', *The Journal of investigative dermatology*.

Allombert-Blaise, C., Tamiji, S., Mortier, L., Fauvel, H., Tual, M., Delaporte, E., Piette, F., DeLassale, E.M., Formstecher, P., Marchetti, P. and Polakowska, R. (2003) 'Terminal differentiation of human epidermal keratinocytes involves mitochondria- and caspase-dependent cell death pathway',*Cell death and differentiation*, 10(7), pp. 850-2.

Ananthaswamy, H.N. and Pierceall, W.E. (1990) 'Molecular mechanisms of ultraviolet radiation carcinogenesis', *Photochemistry and photobiology*, 52(6), pp. 1119-36.

Anglade, P., Vyas, S., Javoy-Agid, F., Herrero, M.T., Michel, P.P., Marquez, J., Mouatt-Prigent, A., Ruberg, M., Hirsch, E.C. and Agid, Y. (1997) 'Apoptosis and autophagy in nigral neurons of patients with Parkinson's disease', *Histology and histopathology*, 12(1), pp. 25-31.

Appelqvist, H., Waster, P., Eriksson, I., Rosdahl, I. and Ollinger, K. (2013) 'Lysosomal exocytosis and caspase-8-mediated apoptosis in UVA-irradiated keratinocytes', *Journal of cell science*, 126(Pt 24), pp. 5578-84.

Ashkenazi, A. and Dixit, V.M. (1998) 'Death receptors: signaling and modulation', *Science*, 281(5381), pp. 1305-8.

Axe, E.L., Walker, S.A., Manifava, M., Chandra, P., Roderick, H.L., Habermann, A., Griffiths, G. and Ktistakis, N.T. (2008) 'Autophagosome formation from membrane compartments enriched in phosphatidylinositol 3-phosphate and dynamically connected to the endoplasmic reticulum', *The Journal of cell biology*, 182(4), pp. 685-701.

Aymard, E., Barruche, V., Naves, T., Bordes, S., Closs, B., Verdier, M. and Ratinaud, M.H. (2011) 'Autophagy in human keratinocytes: an early step of the differentiation?', *Experimental dermatology*, 20(3), pp. 263-8.

Baccarelli, A., Pfeiffer, R., Consonni, D., Pesatori, A.C., Bonzini, M., Patterson, D.G., Jr., Bertazzi, P.A. and Landi, M.T. (2005) 'Handling of dioxin measurement data in the presence of non-detectable values: overview of available methods and their application in the Seveso chloracne study',*Chemosphere*, 60(7), pp. 898-906.

Bandyopadhyay, U., Kaushik, S., Varticovski, L. and Cuervo, A.M. (2008) 'The chaperone-mediated autophagy receptor organizes in dynamic protein complexes at the lysosomal membrane', *Molecular and cellular biology*, 28(18), pp. 5747-63.

Baron, J.M. and Merk, H.F. (2001) 'Drug metabolism in the skin', *Current opinion in allergy and clinical immunology*, 1(4), pp. 287-91.

Baroni, A., Buommino, E., De Gregorio, V., Ruocco, E., Ruocco, V. and Wolf, R. (2012) 'Structure and function of the epidermis related to barrier properties', *Clinics in dermatology*, 30(3), pp. 257-62.

Benes, P., Vetvicka, V. and Fusek, M. (2008) 'Cathepsin D--many functions of one aspartic protease', *Critical reviews in oncology/hematology*, 68(1), pp. 12-28.

Berkers, J.A., Hassing, I., Spenkelink, B., Brouwer, A. and Blaauboer, B.J. (1995) 'Interactive effects of 2,3,7,8-tetrachlorodibenzo-p-dioxin and retinoids on proliferation and differentiation in cultured human keratinocytes: quantification of cross-linked envelope formation', *Archives of toxicology*, 69(6), pp. 368-78.

Bewley, M.A., Marriott, H.M., Tulone, C., Francis, S.E., Mitchell, T.J., Read, R.C., Chain, B., Kroemer, G., Whyte, M.K. and Dockrell, D.H. (2011) 'A cardinal role for cathepsin d in co-ordinating the host-mediated apoptosis of macrophages and killing of pneumococci', *PLoS pathogens*, 7(1), p. e1001262.

Bidere, N., Lorenzo, H.K., Carmona, S., Laforge, M., Harper, F., Dumont, C. and Senik, A. (2003) 'Cathepsin D triggers Bax activation, resulting in selective apoptosis-inducing factor (AIF) relocation in T lymphocytes entering the early commitment phase to apoptosis', *The Journal of biological chemistry*, 278(33), pp. 31401-11.

Bikle, D.D., Xie, Z. and Tu, C.L. (2012) 'Calcium regulation of keratinocyte differentiation', *Expert review of endocrinology & metabolism*, 7(4), pp. 461-472.

Bock, K.W. (2016) 'Toward elucidation of dioxin-mediated chloracne and Ah receptor functions', *Biochemical pharmacology*, 112, pp. 1-5.

Bove, J., Martinez-Vicente, M., Dehay, B., Perier, C., Recasens, A., Bombrun, A., Antonsson, B. and Vila, M. (2014) 'BAX channel activity mediates lysosomal disruption linked to Parkinson disease', *Autophagy*, 10(5), pp. 889-900.

Boya, P., Gonzalez-Polo, R.A., Poncet, D., Andreau, K., Vieira, H.L., Roumier, T., Perfettini, J.L. and Kroemer, G. (2003) 'Mitochondrial membrane permeabilization is a critical step of lysosome-initiated apoptosis induced by hydroxychloroquine', *Oncogene*, 22(25), pp. 3927-36.

Boya, P. and Kroemer, G. (2008) 'Lysosomal membrane permeabilization in cell death', *Oncogene*, 27(50), pp. 6434-51.

Candi, E., Schmidt, R. and Melino, G. (2005) 'The cornified envelope: a model of cell death in the skin', *Nature reviews. Molecular cell biology*, 6(4), pp. 328-40.

Cantrell, S.M., Joy-Schlezinger, J., Stegeman, J.J., Tillitt, D.E. and Hannink, M. (1998) 'Correlation of 2,3,7,8-tetrachlorodibenzo-p-dioxin-induced apoptotic cell death in the embryonic vasculature with embryotoxicity', *Toxicology and applied pharmacology*, 148(1), pp. 24-34.

Caruso, J.A., Mathieu, P.A., Joiakim, A., Leeson, B., Kessel, D., Sloane, B.F. and Reiners, J.J., Jr. (2004) 'Differential susceptibilities of murine hepatoma 1c1c7 and Tao cells to the lysosomal photosensitizer NPe6: influence of aryl hydrocarbon receptor on lysosomal fragility and protease contents', *Molecular pharmacology*, 65(4), pp. 1016-28.

Caruso, J.A., Mathieu, P.A., Joiakim, A., Zhang, H. and Reiners, J.J., Jr. (2006) 'Aryl hydrocarbon receptor modulation of tumor necrosis factor-alpha-induced apoptosis and lysosomal disruption in a hepatoma model that is caspase-8-independent', *The Journal of biological chemistry*, 281(16), pp. 10954-67.

Carvajal-Gonzalez, J.M., Roman, A.C., Cerezo-Guisado, M.I., Rico-Leo, E.M., Martin-Partido, G. and Fernandez-Salguero, P.M. (2009) 'Loss of dioxin-receptor expression accelerates wound healing in vivo by a mechanism involving TGFbeta', *Journal of cell science*, 122(Pt 11), pp. 1823-33.

Castino, R., Bellio, N., Nicotra, G., Follo, C., Trincheri, N.F. and Isidoro, C. (2007) 'Cathepsin D-Bax death pathway in oxidative stressed neuroblastoma cells', *Free radical biology & medicine*, 42(9), pp. 1305-16.

Chen, A., Huang, X., Xue, Z., Cao, D., Huang, K., Chen, J., Pan, Y. and Gao, Y. (2015) 'The Role of p21 in Apoptosis, Proliferation, Cell Cycle Arrest, and Antioxidant Activity in UVB-Irradiated Human HaCaT Keratinocytes', *Medical science monitor basic research*, 21, pp. 86-95.

Chen, S.C., Liao, T.L., Wei, Y.H., Tzeng, C.R. and Kao, S.H. (2010) 'Endocrine disruptor, dioxin (TCDD)-induced mitochondrial dysfunction and apoptosis in human trophoblast-like JAR cells', *Molecular human reproduction*, 16(5), pp. 361-72.

Chinnaiyan, A.M. (1999) 'The apoptosome: heart and soul of the cell death machine', *Neoplasia*, 1(1), pp. 5-15.

Chipuk, J.E. and Green, D.R. (2008) 'How do BCL-2 proteins induce mitochondrial outer membrane permeabilization?', *Trends in cell biology*, 18(4), pp. 157-64.

Chwieralski, C.E., Welte, T. and Buhling, F. (2006) 'Cathepsin-regulated apoptosis', *Apoptosis : an international journal on programmed cell death*, 11(2), pp. 143-9.

Cianfanelli, V., Fuoco, C., Lorente, M., Salazar, M., Quondamatteo, F., Gherardini, P.F., De Zio, D., Nazio, F., Antonioli, M., D'Orazio, M., Skobo, T., Bordi, M., Rohde, M., Dalla Valle, L., Helmer-Citterich, M., Gretzmeier, C., Dengjel, J., Fimia, G.M., Piacentini, M., Di Bartolomeo, S., Velasco, G. and Cecconi, F. (2015) 'AMBRA1 links autophagy to cell proliferation and tumorigenesis by promoting c-Myc dephosphorylation and degradation', *Nature cell biology*, 17(5), p. 706.

Cocchiaro, P., Fox, C., Tregidgo, N.W., Howarth, R., Wood, K.M., Situmorang, G.R., Pavone, L.M., Sheerin, N.S. and Moles, A. (2016) 'Lysosomal protease cathepsin D; a new driver of apoptosis during acute kidney injury', *Scientific reports*, 6, p. 27112.

Colonna, M. (2014) 'AHR: making the keratinocytes thick skinned', *Immunity*, 40(6), pp. 863-4.

Cory, S. and Adams, J.M. (2002) 'The Bcl2 family: regulators of the cellular life-or-death switch', *Nature reviews. Cancer*, 2(9), pp. 647-56.

Cuervo, A.M. and Dice, J.F. (1996) 'A receptor for the selective uptake and degradation of proteins by lysosomes', *Science*, 273(5274), pp. 501-3.

Cuervo, A.M. and Dice, J.F. (2000) 'Unique properties of lamp2a compared to other lamp2 isoforms', *Journal of cell science*, 113 Pt 24, pp. 4441-50.

Cumberbatch, M., Dearman, R.J., Griffiths, C.E. and Kimber, I. (2003) 'Epidermal Langerhans cell migration and sensitisation to chemical allergens', *APMIS : acta pathologica, microbiologica, et immunologica Scandinavica*, 111(7-8), pp. 797-804.

Davarinos, N.A. and Pollenz, R.S. (1999) 'Aryl hydrocarbon receptor imported into the nucleus following ligand binding is rapidly degraded via the cytosplasmic proteasome following nuclear export', *The Journal of biological chemistry*, 274(40), pp. 28708-15.

De Abrew, K.N., Thomas-Virnig, C.L., Rasmussen, C.A., Bolterstein, E.A., Schlosser, S.J. and Allen-Hoffmann, B.L. (2014) 'TCDD induces dermal accumulation of keratinocyte-derived matrix metalloproteinase-10 in an organotypic model of human skin', *Toxicology and applied pharmacology*, 276(3), pp. 171-8.

de Breij, A., Haisma, E.M., Rietveld, M., El Ghalbzouri, A., van den Broek, P.J., Dijkshoorn, L. and Nibbering, P.H. (2012) 'Three-dimensional human skin equivalent as a tool to study Acinetobacter baumannii colonization', *Antimicrobial agents and chemotherapy*, 56(5), pp. 2459-64.

Denison, M.S., Fisher, J.M. and Whitlock, J.P., Jr. (1988) 'The DNA recognition site for the dioxin-Ah receptor complex. Nucleotide sequence and functional analysis', *The Journal of biological chemistry*, 263(33), pp. 17221-4.

Denison, M.S. and Nagy, S.R. (2003) 'Activation of the aryl hydrocarbon receptor by structurally diverse exogenous and endogenous chemicals', *Annual review of pharmacology and toxicology*, 43, pp. 309-34.

Deruy, E., Nassour, J., Martin, N., Vercamer, C., Malaquin, N., Bertout, J., Chelli, F., Pourtier, A., Pluquet, O. and Abbadie, C. (2014) 'Level of macroautophagy drives senescent keratinocytes into cell death or neoplastic evasion', *Cell death & disease*, 5, p. e1577.

Di Meglio, P., Duarte, J.H., Ahlfors, H., Owens, N.D., Li, Y., Villanova, F., Tosi, I., Hirota, K., Nestle, F.O., Mrowietz, U., Gilchrist, M.J. and Stockinger, B. (2014) 'Activation of the aryl hydrocarbon receptor dampens the severity of inflammatory skin conditions', *Immunity*, 40(6), pp. 989-1001.

Dice, J.F. (1990) 'Peptide sequences that target cytosolic proteins for lysosomal proteolysis', *Trends in biochemical sciences*, 15(8), pp. 305-9.

Ding, W.X., Ni, H.M., Gao, W., Yoshimori, T., Stolz, D.B., Ron, D. and Yin, X.M. (2007) 'Linking of autophagy to ubiquitin-proteasome system is important for the regulation of endoplasmic reticulum stress and cell viability', *The American journal of pathology*, 171(2), pp. 513-24.

Dong, Q., Oh, J.E., Yi, J.K., Kim, R.H., Shin, K.H., Mitsuyasu, R., Park, N.H. and Kang, M.K. (2013) 'Efavirenz induces autophagy and aberrant differentiation in normal human keratinocytes', *International journal of molecular medicine*, 31(6), pp. 1305-12.

Dong, W., Teraoka, H., Yamazaki, K., Tsukiyama, S., Imani, S., Imagawa, T., Stegeman, J.J., Peterson, R.E. and Hiraga, T. (2002) '2,3,7,8-tetrachlorodibenzo-p-dioxin toxicity in the zebrafish embryo: local circulation failure in the dorsal midbrain is associated with increased apoptosis',*Toxicological sciences : an official journal of the Society of Toxicology*, 69(1), pp. 191-201.

Droga-Mazovec, G., Bojic, L., Petelin, A., Ivanova, S., Romih, R., Repnik, U., Salvesen, G.S., Stoka, V., Turk, V. and Turk, B. (2008) 'Cysteine cathepsins trigger caspase-dependent cell death through cleavage of bid and antiapoptotic Bcl-2 homologues', *The Journal of biological chemistry*, 283(27), pp. 19140-50.

Eckert, R.L., Sturniolo, M.T., Broome, A.M., Ruse, M. and Rorke, E.A. (2005) 'Transglutaminase function in epidermis', *The Journal of investigative dermatology*, 124(3), pp. 481-92.

Eckhart, L., Lippens, S., Tschachler, E. and Declercq, W. (2013) 'Cell death by cornification', *Biochimica et biophysica acta*, 1833(12), pp. 3471-80.

Egberts, F., Heinrich, M., Jensen, J.M., Winoto-Morbach, S., Pfeiffer, S., Wickel, M., Schunck, M., Steude, J., Saftig, P., Proksch, E. and Schutze, S. (2004) 'Cathepsin D is involved in the regulation of transglutaminase 1 and epidermal differentiation', *Journal of cell science*, 117(Pt 11), pp. 2295-307.

El Ghalbzouri, A., Siamari, R., Willemze, R. and Ponec, M. (2008) 'Leiden reconstructed human epidermal model as a tool for the evaluation of the skin corrosion and irritation potential according to the ECVAM guidelines', *Toxicology in vitro : an international journal published in association with BIBRA*, 22(5), pp. 1311-20.

Elmore, S. (2007) 'Apoptosis: a review of programmed cell death', *Toxicologic pathology*, 35(4), pp. 495-516.

Ema, M., Ohe, N., Suzuki, M., Mimura, J., Sogawa, K., Ikawa, S. and Fujii-Kuriyama, Y. (1994) 'Dioxin binding activities of polymorphic forms of mouse and human arylhydrocarbon receptors', *The Journal of biological chemistry*, 269(44), pp. 27337-43.

Emert-Sedlak, L., Shangary, S., Rabinovitz, A., Miranda, M.B., Delach, S.M. and Johnson, D.E. (2005) 'Involvement of cathepsin D in chemotherapy-induced cytochrome c release, caspase activation, and cell death', *Molecular cancer therapeutics*, 4(5), pp. 733-42.

Eskelinen, E.L. (2005) 'Maturation of autophagic vacuoles in Mammalian cells', *Autophagy*, 1(1), pp. 1-10.

Eskelinen, E.L. (2006) 'Roles of LAMP-1 and LAMP-2 in lysosome biogenesis and autophagy', *Molecular aspects of medicine*, 27(5-6), pp. 495-502.

Espert, L., Denizot, M., Grimaldi, M., Robert-Hebmann, V., Gay, B., Varbanov, M., Codogno, P. and Biard-Piechaczyk, M. (2006) 'Autophagy is involved in T cell death after binding of HIV-1 envelope proteins to CXCR4', *The Journal of clinical investigation*, 116(8), pp. 2161-72.

Feng, S., Cao, Z. and Wang, X. (2013) 'Role of aryl hydrocarbon receptor in cancer', *Biochimica et biophysica acta*, 1836(2), pp. 197-210.

Fiorito, F., Ciarcia, R., Granato, G.E., Marfe, G., Iovane, V., Florio, S., De Martino, L. and Pagnini, U. (2011) '2,3,7,8-tetrachlorodibenzo-p-dioxin induced autophagy in a bovine kidney cell line', *Toxicology*, 290(2-3), pp. 258-70.

Foghsgaard, L., Wissing, D., Mauch, D., Lademann, U., Bastholm, L., Boes, M., Elling, F., Leist, M. and Jaattela, M. (2001) 'Cathepsin B acts as a dominant execution protease in tumor cell apoptosis induced by tumor necrosis factor', *The Journal of cell biology*, 153(5), pp. 999-1010.

Follo, C., Barbone, D., Richards, W.G., Bueno, R. and Broaddus, V.C. (2016) 'Autophagy initiation correlates with the autophagic flux in 3D models of mesothelioma and with patient outcome', *Autophagy*, 12(7), pp. 1180-94.

Forrester, A.R., Elias, M.S., Woodward, E.L., Graham, M., Williams, F.M. and Reynolds, N.J. (2014) 'Induction of a chloracne phenotype in an epidermal equivalent model by 2,3,7,8-tetrachlorodibenzo-p-dioxin (TCDD) is dependent on aryl hydrocarbon receptor activation and is not reproduced by aryl hydrocarbon receptor knock down', *Journal of dermatological science*, 73(1), pp. 10-22.

Franch, H.A., Sooparb, S., Du, J. and Brown, N.S. (2001) 'A mechanism regulating proteolysis of specific proteins during renal tubular cell growth', *The Journal of biological chemistry*, 276(22), pp. 19126-31.

Franke, W.W., Cowin, P., Schmelz, M. and Kapprell, H.P. (1987) 'The desmosomal plaque and the cytoskeleton', *Ciba Foundation symposium*, 125, pp. 26-48.

Fuchs, E. (1990) 'Epidermal differentiation: the bare essentials', *The Journal of cell biology*, 111(6 Pt 2), pp. 2807-14.

Fuchs, Y. and Steller, H. (2015) 'Live to die another way: modes of programmed cell death and the signals emanating from dying cells', *Nature reviews. Molecular cell biology*, 16(6), pp. 329-44.

Furue, M., Takahara, M., Nakahara, T. and Uchi, H. (2014) 'Role of AhR/ARNT system in skin homeostasis', *Archives of dermatological research*, 306(9), pp. 769-79.

Gaido, K.W. and Maness, S.C. (1994) 'Regulation of gene expression and acceleration of differentiation in human keratinocytes by 2,3,7,8-tetrachlorodibenzo-p-dioxin', *Toxicology and applied pharmacology*, 127(2), pp. 199-208.

Galluzzi, L., Vitale, I., Abrams, J.M., Alnemri, E.S., Baehrecke, E.H., Blagosklonny, M.V., Dawson, *et al*., (2012) 'Molecular definitions of cell death subroutines: recommendations of the Nomenclature Committee on Cell Death 2012', *Cell death and differentiation*, 19(1), pp. 107-20.

Gawkrodger, D.J., Harris, G. and Bojar, R.A. (2009) 'Chloracne in seven organic chemists exposed to novel polycyclic halogenated chemical compounds (triazoloquinoxalines)', *The British journal of dermatology*, 161(4), pp. 939-43.

Geng, S., Mezentsev, A., Kalachikov, S., Raith, K., Roop, D.R. and Panteleyev, A.A. (2006) 'Targeted ablation of Arnt in mouse epidermis results in profound defects in desquamation and epidermal barrier function', *Journal of cell science*, 119(Pt 23), pp. 4901-12.

Geusau, A., Khorchide, M., Mildner, M., Pammer, J., Eckhart, L. and Tschachler, E. (2005) '2,3,7,8-tetrachlorodibenzo-p-dioxin impairs differentiation of normal human epidermal keratinocytes in a skin equivalent model', *The Journal of investigative dermatology*, 124(1), pp. 275-7.

Gomez-Sintes, R., Ledesma, M.D. and Boya, P. (2016) 'Lysosomal cell death mechanisms in aging', *Ageing research reviews*.

Gonzalez-Polo, R.A., Boya, P., Pauleau, A.L., Jalil, A., Larochette, N., Souquere, S., Eskelinen, E.L., Pierron, G., Saftig, P. and Kroemer, G. (2005) 'The apoptosis/autophagy paradox: autophagic vacuolization before apoptotic death', *Journal of cell science*, 118(Pt 14), pp. 3091-102.

Gosselin, K., Deruy, E., Martien, S., Vercamer, C., Bouali, F., Dujardin, T., Slomianny, C., Houel-Renault, L., Chelli, F., De Launoit, Y. and Abbadie, C. (2009) 'Senescent keratinocytes die by autophagic programmed cell death', *The American journal of pathology*, 174(2), pp. 423-35.

Gozuacik, D. and Kimchi, A. (2007) 'Autophagy and cell death', *Current topics in developmental biology*, 78, pp. 217-45.

Graham, F.L., Smiley, J., Russell, W.C. and Nairn, R. (1977) 'Characteristics of a human cell line transformed by DNA from human adenovirus type 5', *The Journal of general virology*, 36(1), pp. 59-74.

Guicciardi, M.E., Deussing, J., Miyoshi, H., Bronk, S.F., Svingen, P.A., Peters, C., Kaufmann, S.H. and Gores, G.J. (2000) 'Cathepsin B contributes to TNF-alpha-mediated hepatocyte apoptosis by promoting mitochondrial release of cytochrome c', *The Journal of clinical investigation*, 106(9), pp. 1127-37.

Hacker, G. (2000) 'The morphology of apoptosis', *Cell and tissue research*, 301(1), pp. 5-17.

Hailey, D.W., Rambold, A.S., Satpute-Krishnan, P., Mitra, K., Sougrat, R., Kim, P.K. and Lippincott-Schwartz, J. (2010) 'Mitochondria supply membranes for autophagosome biogenesis during starvation', *Cell*, 141(4), pp. 656-67.

Hankinson, O. (2009) 'Repression of aryl hydrocarbon receptor transcriptional activity by epidermal growth factor', *Molecular interventions*, 9(3), pp. 116-8.

Hanlon, P.R., Zheng, W., Ko, A.Y. and Jefcoate, C.R. (2005) 'Identification of novel TCDD-regulated genes by microarray analysis', *Toxicology and applied pharmacology*, 202(3), pp. 215-28.

Hao, N. and Whitelaw, M.L. (2013) 'The emerging roles of AhR in physiology and immunity', *Biochemical pharmacology*, 86(5), pp. 561-70.

Hara, T., Nakamura, K., Matsui, M., Yamamoto, A., Nakahara, Y., Suzuki-Migishima, R., Yokoyama, M., Mishima, K., Saito, I., Okano, H. and Mizushima, N. (2006) 'Suppression of basal autophagy in neural cells causes neurodegenerative disease in mice', *Nature*, 441(7095), pp. 885-9.

Haselsberger, K., Peterson, D.C., Thomas, D.G. and Darling, J.L. (1996) 'Assay of anticancer drugs in tissue culture: comparison of a tetrazolium-based assay and a protein binding dye assay in short-term cultures derived from human malignant glioma', *Anti-cancer drugs*, 7(3), pp. 331-8.

He, C. and Klionsky, D.J. (2009) 'Regulation mechanisms and signaling pathways of autophagy', *Annual review of genetics*, 43, pp. 67-93.

Heinrich, M., Neumeyer, J., Jakob, M., Hallas, C., Tchikov, V., Winoto-Morbach, S., Wickel, M., Schneider-Brachert, W., Trauzold, A., Hethke, A. and Schutze, S. (2004) 'Cathepsin D links TNF-induced acid sphingomyelinase to Bid-mediated caspase-9 and -3 activation', *Cell death and differentiation*, 11(5), pp. 550-63.

Hennings, H., Holbrook, K., Steinert, P. and Yuspa, S. (1980) 'Growth and differentiation of mouse epidermal cells in culture: effects of extracellular calcium', *Current problems in dermatology*, 10, pp. 3-25.

Hoffman, B. and Liebermann, D.A. (2008) 'Apoptotic signaling by c-MYC', *Oncogene*, 27(50), pp. 6462-72.

Horikoshi, T., Arany, I., Rajaraman, S., Chen, S.H., Brysk, H., Lei, G., Tyring, S.K. and Brysk, M.M. (1998) 'Isoforms of cathepsin D and human epidermal differentiation', *Biochimie*, 80(7), pp. 605-12.

Hu, Q., Rice, R.H., Qin, Q., Phinney, B.S., Eigenheer, R.A., Bao, W. and Zhao, B. (2013) 'Proteomic analysis of human keratinocyte response to 2,3,7,8-tetrachlorodibenzo-p-dioxin (TCDD) exposure', *Journal of proteome research*, 12(11), pp. 5340-7.

Hua, C.T., Hopwood, J.J., Carlsson, S.R., Harris, R.J. and Meikle, P.J. (1998) 'Evaluation of the lysosome-associated membrane protein LAMP-2 as a marker for lysosomal storage disorders', *Clinical chemistry*, 44(10), pp. 2094-102.

Huang, P., Tofighi, R., Emgard, M. and Ceccatelli, S. (2005) 'Cell death induced by 2,3,7,8-tetrachlorodibenzo-p-dioxin (2,3,7,8-TCDD) in AtT-20 pituitary cells', *Toxicology*, 207(3), pp. 391-9.

Ikuta, T., Eguchi, H., Tachibana, T., Yoneda, Y. and Kawajiri, K. (1998) 'Nuclear localization and export signals of the human aryl hydrocarbon receptor', *The Journal of biological chemistry*, 273(5), pp. 2895-904.

Ikuta, T., Kobayashi, Y. and Kawajiri, K. (2004) 'Cell density regulates intracellular localization of aryl hydrocarbon receptor', *The Journal of biological chemistry*, 279(18), pp. 19209-16.

Ikuta, T., Namiki, T., Fujii-Kuriyama, Y. and Kawajiri, K. (2009) 'AhR protein trafficking and function in the skin', *Biochemical pharmacology*, 77(4), pp. 588-96.

Ikuta, T., Ohba, M., Zouboulis, C.C., Fujii-Kuriyama, Y. and Kawajiri, K. (2010) 'B lymphocyte-induced maturation protein 1 is a novel target gene of aryl hydrocarbon receptor', *Journal of dermatological science*, 58(3), pp. 211-6.

Itakura, E. and Mizushima, N. (2013) 'Syntaxin 17: the autophagosomal SNARE', *Autophagy*, 9(6), pp. 917-9.

Jahn, R. and Scheller, R.H. (2006) 'SNAREs--engines for membrane fusion', *Nature reviews. Molecular cell biology*, 7(9), pp. 631-43.

Jin, U.H., Lee, S.O., Pfent, C. and Safe, S. (2014) 'The aryl hydrocarbon receptor ligand omeprazole inhibits breast cancer cell invasion and metastasis', *BMC cancer*, 14, p. 498.

Johansson, A.C., Appelqvist, H., Nilsson, C., Kagedal, K., Roberg, K. and Ollinger, K. (2010) 'Regulation of apoptosis-associated lysosomal membrane permeabilization', *Apoptosis : an international journal on programmed cell death*, 15(5), pp. 527-40.

Johansson, A.C., Steen, H., Ollinger, K. and Roberg, K. (2003) 'Cathepsin D mediates cytochrome c release and caspase activation in human fibroblast apoptosis induced by staurosporine', *Cell death and differentiation*, 10(11), pp. 1253-9.

Jones, C.L. and Reiners, J.J., Jr. (1997) 'Differentiation status of cultured murine keratinocytes modulates induction of genes responsive to 2,3,7,8-tetrachlorodibenzo-p-dioxin', *Archives of biochemistry and biophysics*, 347(2), pp. 163-73.

Ju, Q., Fimmel, S., Hinz, N., Stahlmann, R., Xia, L. and Zouboulis, C.C. (2011) '2,3,7,8-Tetrachlorodibenzo-p-dioxin alters sebaceous gland cell differentiation in vitro', *Experimental dermatology*, 20(4), pp. 320-5.

Ju, Q., Kuochia, Y., Zouboulis, C., Ring, J. and Chen, W. (2012) ‘Chloracne: From clinic to research’, *Dermatologica Sinica,* 30(1), pp.2-6

Ju, Q., Zouboulis, C.C. and Xia, L. (2009) 'Environmental pollution and acne: Chloracne', *Dermato-endocrinology*, 1(3), pp. 125-8.

Kaewpiboon, C., Surapinit, S., Malilas, W., Moon, J., Phuwapraisirisan, P., Tip-Pyang, S., Johnston, R.N., Koh, S.S., Assavalapsakul, W. and Chung, Y.H. (2014) 'Feroniellin A-induced autophagy causes apoptosis in multidrug-resistant human A549 lung cancer cells', *International journal of oncology*, 44(4), pp. 1233-42.

Kagedal, K., Zhao, M., Svensson, I. and Brunk, U.T. (2001) 'Sphingosine-induced apoptosis is dependent on lysosomal proteases', *The Biochemical journal*, 359(Pt 2), pp. 335-43.

Karlsson, T., Vahlquist, A. and Torma, H. (2010) 'Keratinocyte differentiation induced by calcium, phorbol ester or interferon-gamma elicits distinct changes in the retinoid signalling pathways', *Journal of dermatological science*, 57(3), pp. 207-13.

Kashima, M., Fukuyama, K., Kikuchi, M. and Epstein, W.L. (1988) 'Limited proteolysis of high molecular weight histidine-rich protein of rat epidermis by epidermal proteinases', *The Journal of investigative dermatology*, 90(6), pp. 829-33.

Kaur, J. and Debnath, J. (2015) 'Autophagy at the crossroads of catabolism and anabolism', *Nature reviews. Molecular cell biology*, 16(8), pp. 461-72.

Kaushik, S. and Cuervo, A.M. (2009) 'Methods to monitor chaperone-mediated autophagy', *Methods in enzymology*, 452, pp. 297-324.

Kawai, A., Uchiyama, H., Takano, S., Nakamura, N. and Ohkuma, S. (2007) 'Autophagosome-lysosome fusion depends on the pH in acidic compartments in CHO cells', *Autophagy*, 3(2), pp. 154-7.

Kennedy, L.H., Sutter, C.H., Leon Carrion, S., Tran, Q.T., Bodreddigari, S., Kensicki, E., Mohney, R.P. and Sutter, T.R. (2013) '2,3,7,8-Tetrachlorodibenzo-p-dioxin-mediated production of reactive oxygen species is an essential step in the mechanism of action to accelerate human keratinocyte differentiation', *Toxicological sciences : an official journal of the Society of Toxicology*, 132(1), pp. 235-49.

Kerr, J.F., Wyllie, A.H. and Currie, A.R. (1972) 'Apoptosis: a basic biological phenomenon with wide-ranging implications in tissue kinetics', *British journal of cancer*, 26(4), pp. 239-57.

Kim, H.O., Kim, J.H., Chung, B.Y., Choi, M.G. and Park, C.W. (2014) 'Increased expression of the aryl hydrocarbon receptor in patients with chronic inflammatory skin diseases', *Experimental dermatology*, 23(4), pp. 278-81.

Kirkegaard, T. and Jaattela, M. (2009) 'Lysosomal involvement in cell death and cancer', *Biochimica et biophysica acta*, 1793(4), pp. 746-54.

Kischkel, F.C., Hellbardt, S., Behrmann, I., Germer, M., Pawlita, M., Krammer, P.H. and Peter, M.E. (1995) 'Cytotoxicity-dependent APO-1 (Fas/CD95)-associated proteins form a death-inducing signaling complex (DISC) with the receptor', *The EMBO journal*, 14(22), pp. 5579-88.

Klages, N., Zufferey, R. and Trono, D. (2000) 'A stable system for the high-titer production of multiply attenuated lentiviral vectors', *Molecular therapy : the journal of the American Society of Gene Therapy*, 2(2), pp. 170-6.

Klionsky, D.J., Abdelmohsen, K., Abe, A., Abedin, M.J., Abeliovich, H., Acevedo Arozena, A., *et al*. (2016) 'Guidelines for the use and interpretation of assays for monitoring autophagy (3rd edition)', *Autophagy*, 12(1), pp. 1-222.

Klionsky, D.J., Abeliovich, H., Agostinis, P., Agrawal, D.K., Aliev, G., Askew, D.S., Baba, M., *et al*. (2008) 'Guidelines for the use and interpretation of assays for monitoring autophagy in higher eukaryotes', *Autophagy*, 4(2), pp. 151-75.

Knerr, S. and Schrenk, D. (2006) 'Carcinogenicity of 2,3,7,8-tetrachlorodibenzo-p-dioxin in experimental models', *Molecular nutrition & food research*, 50(10), pp. 897-907.

Knutson, J.C. and Poland, A. (1982) 'Response of murine epidermis to 2,3,7,8-tetrachlorodibenzo-p-dioxin: interaction of the ah and hr loci', *Cell*, 30(1), pp. 225-34.

Komatsu, M., Waguri, S., Chiba, T., Murata, S., Iwata, J., Tanida, I., Ueno, T., Koike, M., Uchiyama, Y., Kominami, E. and Tanaka, K. (2006) 'Loss of autophagy in the central nervous system causes neurodegeneration in mice', *Nature*, 441(7095), pp. 880-4.

Konecki, D.S., Foetisch, K., Zimmer, K.P., Schlotter, M. and Lichter-Konecki, U. (1995) 'An alternatively spliced form of the human lysosome-associated membrane protein-2 gene is expressed in a tissue-specific manner', *Biochemical and biophysical research communications*, 215(2), pp. 757-67.

Korolchuk, V.I., Menzies, F.M. and Rubinsztein, D.C. (2009) 'A novel link between autophagy and the ubiquitin-proteasome system', *Autophagy*, 5(6), pp. 862-3.

Kraft, C., Peter, M. and Hofmann, K. (2010) 'Selective autophagy: ubiquitin-mediated recognition and beyond', *Nature cell biology*, 12(9), pp. 836-41.

Kroemer, G. and Levine, B. (2008) 'Autophagic cell death: the story of a misnomer', *Nature reviews. Molecular cell biology*, 9(12), pp. 1004-10.

Kwon, J.Y., Park, B.S., Kim, Y.H., Kim, Y.D., Kim, C.H., Yoon, J.Y. and Yoon, J.U. (2015) 'Remifentanil protects human keratinocytes against hypoxia-reoxygenation injury through activation of autophagy', *PloS one*, 10(1), p. e0116982.

Kypriotou, M., Huber, M. and Hohl, D. (2012) 'The human epidermal differentiation complex: cornified envelope precursors, S100 proteins and the 'fused genes' family', *Experimental dermatology*, 21(9), pp. 643-9.

Lahvis, G.P., Lindell, S.L., Thomas, R.S., McCuskey, R.S., Murphy, C., Glover, E., Bentz, M., Southard, J. and Bradfield, C.A. (2000) 'Portosystemic shunting and persistent fetal vascular structures in aryl hydrocarbon receptor-deficient mice', *Proceedings of the National Academy of Sciences of the United States of America*, 97(19), pp. 10442-7.

Lanzafame, M., Botta, E., Teson, M., Fortugno, P., Zambruno, G., Stefanini, M. and Orioli, D. (2015) 'Reference genes for gene expression analysis in proliferating and differentiating human keratinocytes', *Experimental dermatology*, 24(4), pp. 314-6.

Li, Y., Wang, K., Jiang, Y.Z., Chang, X.W., Dai, C.F. and Zheng, J. (2014) '2,3,7,8-Tetrachlorodibenzo-p-dioxin (TCDD) inhibits human ovarian cancer cell proliferation', *Cellular oncology*, 37(6), pp. 429-37.

Lichter-Konecki, U., Moter, S.E., Krawisz, B.R., Schlotter, M., Hipke, C. and Konecki, D.S. (1999) 'Expression patterns of murine lysosome-associated membrane protein 2 (Lamp-2) transcripts during morphogenesis', *Differentiation; research in biological diversity*, 65(1), pp. 43-58.

Lilienbaum, A. (2013) 'Relationship between the proteasomal system and autophagy', *International journal of biochemistry and molecular biology*, 4(1), pp. 1-26.

Lin, P.H., Lin, C.H., Huang, C.C., Chuang, M.C. and Lin, P. (2007) '2,3,7,8-Tetrachlorodibenzo-p-dioxin (TCDD) induces oxidative stress, DNA strand breaks, and poly(ADP-ribose) polymerase-1 activation in human breast carcinoma cell lines', *Toxicology letters*, 172(3), pp. 146-58.

Lin, Y.C., Boone, M., Meuris, L., Lemmens, I., Van Roy, N., Soete, A., Reumers, J., Moisse, M., Plaisance, S., Drmanac, R., Chen, J., Speleman, F., Lambrechts, D., Van de Peer, Y., Tavernier, J. and Callewaert, N. (2014) 'Genome dynamics of the human embryonic kidney 293 lineage in response to cell biology manipulations', *Nature communications*, 5, p. 4767.

Lippens, S., Denecker, G., Ovaere, P., Vandenabeele, P. and Declercq, W. (2005) 'Death penalty for keratinocytes: apoptosis versus cornification', *Cell death and differentiation*, 12 Suppl 2, pp. 1497-508.

Lippens, S., Kockx, M., Knaapen, M., Mortier, L., Polakowska, R., Verheyen, A., Garmyn, M., Zwijsen, A., Formstecher, P., Huylebroeck, D., Vandenabeele, P. and Declercq, W. (2000) 'Epidermal differentiation does not involve the pro-apoptotic executioner caspases, but is associated with caspase-14 induction and processing', *Cell death and differentiation*, 7(12), pp. 1218-24.

Livak, K.J. and Schmittgen, T.D. (2001) 'Analysis of relative gene expression data using real-time quantitative PCR and the 2(-Delta Delta C(T)) Method', *Methods*, 25(4), pp. 402-8.

Locksley, R.M., Killeen, N. and Lenardo, M.J. (2001) 'The TNF and TNF receptor superfamilies: integrating mammalian biology', *Cell*, 104(4), pp. 487-501.

Loertscher, J.A., Lin, T.M., Peterson, R.E. and Allen-Hoffmann, B.L. (2002) 'In utero exposure to 2,3,7,8-tetrachlorodibenzo-p-dioxin causes accelerated terminal differentiation in fetal mouse skin', *Toxicological sciences : an official journal of the Society of Toxicology*, 68(2), pp. 465-72.

Loertscher, J.A., Sadek, C.S. and Allen-Hoffmann, B.L. (2001) 'Treatment of normal human keratinocytes with 2,3,7,8-tetrachlorodibenzo-p-dioxin causes a reduction in cell number, but no increase in apoptosis', *Toxicology and applied pharmacology*, 175(2), pp. 114-20. (A)

Loertscher, J.A., Sattler, C.A. and Allen-Hoffmann, B.L. (2001) '2,3,7,8-Tetrachlorodibenzo-p-dioxin alters the differentiation pattern of human keratinocytes in organotypic culture', *Toxicology and applied pharmacology*, 175(2), pp. 121-9. (B)

Ma, Q. (2001) 'Induction of CYP1A1. The AhR/DRE paradigm: transcription, receptor regulation, and expanding biological roles', *Current drug metabolism*, 2(2), pp. 149-64.

Ma, Q. (2011) 'Influence of light on aryl hydrocarbon receptor signaling and consequences in drug metabolism, physiology and disease', *Expert opinion on drug metabolism & toxicology*, 7(10), pp. 1267-93.

Ma, Q. and Baldwin, K.T. (2000) '2,3,7,8-tetrachlorodibenzo-p-dioxin-induced degradation of aryl hydrocarbon receptor (AhR) by the ubiquitin-proteasome pathway. Role of the transcription activaton and DNA binding of AhR', *The Journal of biological chemistry*, 275(12), pp. 8432-8.

Magnusdottir, E., Kalachikov, S., Mizukoshi, K., Savitsky, D., Ishida-Yamamoto, A., Panteleyev, A.A. and Calame, K. (2007) 'Epidermal terminal differentiation depends on B lymphocyte-induced maturation protein-1', *Proceedings of the National Academy of Sciences of the United States of America*, 104(38), pp. 14988-93.

Maiuri, M.C., Zalckvar, E., Kimchi, A. and Kroemer, G. (2007) 'Self-eating and self-killing: crosstalk between autophagy and apoptosis', *Nature reviews. Molecular cell biology*, 8(9), pp. 741-52.

Mandavia, C. (2015) 'TCDD-induced activation of aryl hydrocarbon receptor regulates the skin stem cell population', *Medical hypotheses*, 84(3), pp. 204-8.

Marques-Gallego, P., den Dulk, H., Backendorf, C., Brouwer, J., Reedijk, J. and Burke, J.F. (2010) 'Accurate non-invasive image-based cytotoxicity assays for cultured cells', *BMC biotechnology*, 10, p. 43.

Mauvezin, C., Nagy, P., Juhasz, G. and Neufeld, T.P. (2015) 'Autophagosome-lysosome fusion is independent of V-ATPase-mediated acidification', *Nature communications*, 6, p. 7007.

McIlwain, D.R., Berger, T. and Mak, T.W. (2015) 'Caspase functions in cell death and disease', *Cold Spring Harbor perspectives in biology*, 7(4).

Menzies, F.M., Moreau, K., Puri, C., Renna, M. and Rubinsztein, D.C. (2012) 'Measurement of autophagic activity in mammalian cells', *Current protocols in cell biology / editorial board, Juan S. Bonifacino ... [et al.]*, Chapter 15, p. Unit 15 16.

Mimura, J., Ema, M., Sogawa, K. and Fujii-Kuriyama, Y. (1999) 'Identification of a novel mechanism of regulation of Ah (dioxin) receptor function', *Genes & development*, 13(1), pp. 20-5.

Mindell, J.A. (2012) 'Lysosomal acidification mechanisms', *Annual review of physiology*, 74, pp. 69-86.

Misovic, M., Milenkovic, D., Martinovic, T., Ciric, D., Bumbasirevic, V. and Kravic-Stevovic, T. (2013) 'Short-term exposure to UV-A, UV-B, and UV-C irradiation induces alteration in cytoskeleton and autophagy in human keratinocytes', *Ultrastructural pathology*, 37(4), pp. 241-8.

Mizushima, N. (2010) 'The role of the Atg1/ULK1 complex in autophagy regulation', *Current opinion in cell biology*, 22(2), pp. 132-9.

Mizushima, N. (2014) 'Sugar modification inhibits autophagosome-lysosome fusion', *Nature cell biology*, 16(12), pp. 1132-3.

Mizushima, N., Yoshimori, T. and Levine, B. (2010) 'Methods in mammalian autophagy research', *Cell*, 140(3), pp. 313-26.

Mizushima, N., Yoshimori, T. and Ohsumi, Y. (2011) 'The role of Atg proteins in autophagosome formation', *Annual review of cell and developmental biology*, 27, pp. 107-32.

Moirangthem, V., Katz, W.S., Su, W., Choi, E.Y., Dingle, R.W., Zeigler, G.M., Everson, W.V., Jennings, C.D., Gong, M. and Swanson, H.I. (2013) 'Impact of 2,3,7,8-tetrachlorodibenzo-p-dioxin on cutaneous wound healing', *Experimental and toxicologic pathology : official journal of the Gesellschaft fur Toxikologische Pathologie*, 65(1-2), pp. 61-7.

Morales-Hernandez, A., Sanchez-Martin, F.J., Hortigon-Vinagre, M.P., Henao, F. and Merino, J.M. (2012) '2,3,7,8-Tetrachlorodibenzo-p-dioxin induces apoptosis by disruption of intracellular calcium homeostasis in human neuronal cell line SHSY5Y', *Apoptosis : an international journal on programmed cell death*, 17(11), pp. 1170-81.

Mukhopadhyay, S., Panda, P.K., Sinha, N., Das, D.N. and Bhutia, S.K. (2014) 'Autophagy and apoptosis: where do they meet?', *Apoptosis : an international journal on programmed cell death*, 19(4), pp. 555-66.

Mulero-Navarro, S. and Fernandez-Salguero, P.M. (2016) 'New Trends in Aryl Hydrocarbon Receptor Biology', *Frontiers in cell and developmental biology*, 4, p. 45.

Murase, D., Hachiya, A., Takano, K., Hicks, R., Visscher, M.O., Kitahara, T., Hase, T., Takema, Y. and Yoshimori, T. (2013) 'Autophagy has a significant role in determining skin color by regulating melanosome degradation in keratinocytes', *The Journal of investigative dermatology*, 133(10), pp. 2416-24.

Murray, I.A., Patterson, A.D. and Perdew, G.H. (2014) 'Aryl hydrocarbon receptor ligands in cancer: friend and foe', *Nature reviews. Cancer*, 14(12), pp. 801-14.

Naldini, L., Blomer, U., Gage, F.H., Trono, D. and Verma, I.M. (1996) 'Efficient transfer, integration, and sustained long-term expression of the transgene in adult rat brains injected with a lentiviral vector', *Proceedings of the National Academy of Sciences of the United States of America*, 93(21), pp. 11382-8.

Nelson, W.G. and Sun, T.T. (1983) 'The 50- and 58-kdalton keratin classes as molecular markers for stratified squamous epithelia: cell culture studies', *The Journal of cell biology*, 97(1), pp. 244-51.

Neuberger, M., Landvoigt, W. and Derntl, F. (1991) 'Blood levels of 2,3,7,8-tetrachlorodibenzo-p-dioxin in chemical workers after chloracne and in comparison groups', *International archives of occupational and environmental health*, 63(5), pp. 325-7.

Nguyen, L.P. and Bradfield, C.A. (2008) 'The search for endogenous activators of the aryl hydrocarbon receptor', *Chemical research in toxicology*, 21(1), pp. 102-16.

Oesch, F., Fabian, E., Guth, K. and Landsiedel, R. (2014) 'Xenobiotic-metabolizing enzymes in the skin of rat, mouse, pig, guinea pig, man, and in human skin models', *Archives of toxicology*, 88(12), pp. 2135-90.

Oesch, F., Fabian, E., Oesch-Bartlomowicz, B., Werner, C. and Landsiedel, R. (2007) 'Drug-metabolizing enzymes in the skin of man, rat, and pig', *Drug metabolism reviews*, 39(4), pp. 659-98.

Ouyang, L., Shi, Z., Zhao, S., Wang, F.T., Zhou, T.T., Liu, B. and Bao, J.K. (2012) 'Programmed cell death pathways in cancer: a review of apoptosis, autophagy and programmed necrosis', *Cell proliferation*, 45(6), pp. 487-98.

Pagliacci, M.C., Spinozzi, F., Migliorati, G., Fumi, G., Smacchia, M., Grignani, F., Riccardi, C. and Nicoletti, I. (1993) 'Genistein inhibits tumour cell growth in vitro but enhances mitochondrial reduction of tetrazolium salts: a further pitfall in the use of the MTT assay for evaluating cell growth and survival', *European journal of cancer*, 29A(11), pp. 1573-7.

Pankiv, S., Lamark, T., Bruun, J.A., Overvatn, A., Bjorkoy, G. and Johansen, T. (2010) 'Nucleocytoplasmic shuttling of P62/SQSTM1 and its role in recruitment of nuclear polyubiquitinated proteins to promyelocytic leukemia bodies', *The Journal of biological chemistry*, 285(8), pp. 5941-53.

Pannatier, A., Jenner, P., Testa, B. and Etter, J.C. (1978) 'The skin as a drug-metabolizing organ', *Drug metabolism reviews*, 8(2), pp. 319-43.

Pastor, M.A., Carrasco, L., Izquierdo, M.J., Farina, M.C., Martin, L., Renedo, G. and Requena, L. (2002) 'Chloracne: histopathologic findings in one case', *Journal of cutaneous pathology*, 29(4), pp. 193-9.

Patel, B. and Cuervo, A.M. (2015) 'Methods to study chaperone-mediated autophagy', *Methods*, 75, pp. 133-40.

Pelclova, D., Urban, P., Preiss, J., Lukas, E., Fenclova, Z., Navratil, T., Dubska, Z. and Senholdova, Z. (2006) 'Adverse health effects in humans exposed to 2,3,7,8-tetrachlorodibenzo-p-dioxin (TCDD)', *Reviews on environmental health*, 21(2), pp. 119-38.

Peroni, A., Zini, A., Braga, V., Colato, C., Adami, S. and Girolomoni, G. (2008) 'Drug-induced morphea: report of a case induced by balicatib and review of the literature', *Journal of the American Academy of Dermatology*, 59(1), pp. 125-9.

Pillai, S., Bikle, D.D., Mancianti, M.L., Cline, P. and Hincenbergs, M. (1990) 'Calcium regulation of growth and differentiation of normal human keratinocytes: modulation of differentiation competence by stages of growth and extracellular calcium', *Journal of cellular physiology*, 143(2), pp. 294-302.

Pollenz, R.S. and Buggy, C. (2006) 'Ligand-dependent and -independent degradation of the human aryl hydrocarbon receptor (hAHR) in cell culture models', *Chemico-biological interactions*, 164(1-2), pp. 49-59.

Proksch, E., Brandner, J.M. and Jensen, J.M. (2008) 'The skin: an indispensable barrier', *Experimental dermatology*, 17(12), pp. 1063-72.

Puhvel, S.M., Sakamoto, M., Ertl, D.C. and Reisner, R.M. (1982) 'Hairless mice as models for chloracne: a study of cutaneous changes induced by topical application of established chloracnegens', *Toxicology and applied pharmacology*, 64(3), pp. 492-503.

Quintana, F.J. (2013) 'The aryl hydrocarbon receptor: a molecular pathway for the environmental control of the immune response', *Immunology*, 138(3), pp. 183-9.

Quintanilla-Dieck, M.J., Codriansky, K., Keady, M., Bhawan, J. and Runger, T.M. (2009) 'Expression and regulation of cathepsin K in skin fibroblasts', *Experimental dermatology*, 18(7), pp. 596-602.

Raj, D., Brash, D.E. and Grossman, D. (2006) 'Keratinocyte apoptosis in epidermal development and disease', *The Journal of investigative dermatology*, 126(2), pp. 243-57.

Ramadoss, P. and Perdew, G.H. (2004) 'Use of 2-azido-3-[125I]iodo-7,8-dibromodibenzo-p-dioxin as a probe to determine the relative ligand affinity of human versus mouse aryl hydrocarbon receptor in cultured cells', *Molecular pharmacology*, 66(1), pp. 129-36.

Ravikumar, B., Moreau, K., Jahreiss, L., Puri, C. and Rubinsztein, D.C. (2010) 'Plasma membrane contributes to the formation of pre-autophagosomal structures', *Nature cell biology*, 12(8), pp. 747-57.

Ray, S. and Swanson, H.I. (2009) 'Activation of the aryl hydrocarbon receptor by TCDD inhibits senescence: a tumor promoting event?', *Biochemical pharmacology*, 77(4), pp. 681-8.

Ray, S.S. and Swanson, H.I. (2003) 'Alteration of keratinocyte differentiation and senescence by the tumor promoter dioxin', *Toxicology and applied pharmacology*, 192(2), pp. 131-45.

Repnik, U., Stoka, V., Turk, V. and Turk, B. (2012) 'Lysosomes and lysosomal cathepsins in cell death', *Biochimica et biophysica acta*, 1824(1), pp. 22-33.

Repnik, U. and Turk, B. (2010) 'Lysosomal-mitochondrial cross-talk during cell death', *Mitochondrion*, 10(6), pp. 662-9.

Rice, R.H. and Green, H. (1979) 'Presence in human epidermal cells of a soluble protein precursor of the cross-linked envelope: activation of the cross-linking by calcium ions', *Cell*, 18(3), pp. 681-94.

Roberg, K., Kagedal, K. and Ollinger, K. (2002) 'Microinjection of cathepsin d induces caspase-dependent apoptosis in fibroblasts', *The American journal of pathology*, 161(1), pp. 89-96.

Rossiter, H., Konig, U., Barresi, C., Buchberger, M., Ghannadan, M., Zhang, C.F., Mlitz, V., Gmeiner, R., Sukseree, S., Fodinger, D., Eckhart, L. and Tschachler, E. (2013) 'Epidermal keratinocytes form a functional skin barrier in the absence of Atg7 dependent autophagy', *Journal of dermatological science*, 71(1), pp. 67-75.

Runger, T.M., Quintanilla-Dieck, M.J. and Bhawan, J. (2007) 'Role of cathepsin K in the turnover of the dermal extracellular matrix during scar formation', *The Journal of investigative dermatology*, 127(2), pp. 293-7.

Saeki, M., Saito, Y., Nagano, M., Teshima, R., Ozawa, S. and Sawada, J. (2002) 'mRNA expression of multiple cytochrome p450 isozymes in four types of cultured skin cells', *International archives of allergy and immunology*, 127(4), pp. 333-6.

Saelens, X., Festjens, N., Vande Walle, L., van Gurp, M., van Loo, G. and Vandenabeele, P. (2004) 'Toxic proteins released from mitochondria in cell death', *Oncogene*, 23(16), pp. 2861-74.

Saftig, P. and Eskelinen, E.L. (2008) 'Live longer with LAMP-2', *Nature medicine*, 14(9), pp. 909-10.

Saftig, P., Schroder, B. and Blanz, J. (2010) 'Lysosomal membrane proteins: life between acid and neutral conditions', *Biochemical Society transactions*, 38(6), pp. 1420-3.

Sandilands, A., Sutherland, C., Irvine, A.D. and McLean, W.H. (2009) 'Filaggrin in the frontline: role in skin barrier function and disease', *Journal of cell science*, 122(Pt 9), pp. 1285-94.

Saraste, A. and Pulkki, K. (2000) 'Morphologic and biochemical hallmarks of apoptosis', *Cardiovascular research*, 45(3), pp. 528-37.

Saurat, J.H., Kaya, G., Saxer-Sekulic, N., Pardo, B., Becker, M., Fontao, L., Mottu, F., Carraux, P., Pham, X.C., Barde, C., Fontao, F., Zennegg, M., Schmid, P., Schaad, O., Descombes, P. and Sorg, O. (2012) 'The cutaneous lesions of dioxin exposure: lessons from the poisoning of Victor Yushchenko', *Toxicological sciences : an official journal of the Society of Toxicology*, 125(1), pp. 310-7.

Savill, J. and Fadok, V. (2000) 'Corpse clearance defines the meaning of cell death', *Nature*, 407(6805), pp. 784-8.

Shen, H.M. and Mizushima, N. (2014) 'At the end of the autophagic road: an emerging understanding of lysosomal functions in autophagy', *Trends in biochemical sciences*, 39(2), pp. 61-71.

Shimohama, S. (2000) 'Apoptosis in Alzheimer's disease--an update', *Apoptosis : an international journal on programmed cell death*, 5(1), pp. 9-16.

Shpilka, T., Mizushima, N. and Elazar, Z. (2012) 'Ubiquitin-like proteins and autophagy at a glance', *Journal of cell science*, 125(Pt 10), pp. 2343-8.

Shrestha, C., Tang, Y., Fan, H., Li, L., Zeng, Q., Pennypacker, S.D., Bikle, D.D. and Xie, Z. (2016) 'Phosphoprotein Phosphatase 1 Is Required for Extracellular Calcium-Induced Keratinocyte Differentiation', *BioMed research international*, 2016, p. 3062765.

Slee, E.A., Adrain, C. and Martin, S.J. (2001) 'Executioner caspase-3, -6, and -7 perform distinct, non-redundant roles during the demolition phase of apoptosis', *The Journal of biological chemistry*, 276(10), pp. 7320-6.

Song, J., Clagett-Dame, M., Peterson, R.E., Hahn, M.E., Westler, W.M., Sicinski, R.R. and DeLuca, H.F. (2002) 'A ligand for the aryl hydrocarbon receptor isolated from lung', *Proceedings of the National Academy of Sciences of the United States of America*, 99(23), pp. 14694-9.

Sorg, O. (2014) 'AhR signalling and dioxin toxicity', *Toxicology letters*, 230(2), pp. 225-33.

Sorg, O., Zennegg, M., Schmid, P., Fedosyuk, R., Valikhnovskyi, R., Gaide, O., Kniazevych, V. and Saurat, J.H. (2009) '2,3,7,8-tetrachlorodibenzo-p-dioxin (TCDD) poisoning in Victor Yushchenko: identification and measurement of TCDD metabolites', *Lancet*, 374(9696), pp. 1179-85.

Stockert, J.C., Blazquez-Castro, A., Canete, M., Horobin, R.W. and Villanueva, A. (2012) 'MTT assay for cell viability: Intracellular localization of the formazan product is in lipid droplets', *Acta histochemica*, 114(8), pp. 785-96.

Sutter, C.H., Bodreddigari, S., Campion, C., Wible, R.S. and Sutter, T.R. (2011) '2,3,7,8-Tetrachlorodibenzo-p-dioxin increases the expression of genes in the human epidermal differentiation complex and accelerates epidermal barrier formation', *Toxicological sciences : an official journal of the Society of Toxicology*, 124(1), pp. 128-37.

Sutter, C.H., Yin, H., Li, Y., Mammen, J.S., Bodreddigari, S., Stevens, G., Cole, J.A. and Sutter, T.R. (2009) 'EGF receptor signaling blocks aryl hydrocarbon receptor-mediated transcription and cell differentiation in human epidermal keratinocytes', *Proceedings of the National Academy of Sciences of the United States of America*, 106(11), pp. 4266-71.

Svensson, C.K. (2009) 'Biotransformation of drugs in human skin', *Drug metabolism and disposition: the biological fate of chemicals*, 37(2), pp. 247-53.

Swanson, H.I. and Bradfield, C.A. (1993) 'The AH-receptor: genetics, structure and function', *Pharmacogenetics*, 3(5), pp. 213-30.

Takasawa, R., Nakamura, H., Mori, T. and Tanuma, S. (2005) 'Differential apoptotic pathways in human keratinocyte HaCaT cells exposed to UVB and UVC', *Apoptosis : an international journal on programmed cell death*, 10(5), pp. 1121-30.

Tanabe, H., Kumagai, N., Tsukahara, T., Ishiura, S., Kominami, E., Nishina, H. and Sugita, H. (1991) 'Changes of lysosomal proteinase activities and their expression in rat cultured keratinocytes during differentiation', *Biochimica et biophysica acta*, 1094(3), pp. 281-7.

Tang, N.J., Liu, J., Coenraads, P.J., Dong, L., Zhao, L.J., Ma, S.W., Chen, X., Zhang, C.M., Ma, X.M., Wei, W.G., Zhang, P. and Bai, Z.P. (2008) 'Expression of AhR, CYP1A1, GSTA1, c-fos and TGF-alpha in skin lesions from dioxin-exposed humans with chloracne', *Toxicology letters*, 177(3), pp. 182-7.

Tanida, I., Yamasaki, M., Komatsu, M. and Ueno, T. (2012) 'The FAP motif within human ATG7, an autophagy-related E1-like enzyme, is essential for the E2-substrate reaction of LC3 lipidation', *Autophagy*, 8(1), pp. 88-97.

Thakoersing, V.S., Gooris, G.S., Mulder, A., Rietveld, M., El Ghalbzouri, A. and Bouwstra, J.A. (2012) 'Unraveling barrier properties of three different in-house human skin equivalents', *Tissue engineering. Part C, Methods*, 18(1), pp. 1-11.

Thomas, P.E., Kouri, R.E. and Hutton, J.J. (1972) 'The genetics of aryl hydrocarbon hydroxylase induction in mice: a single gene difference between C57BL-6J and DBA-2J', *Biochemical genetics*, 6(2), pp. 157-68.

Thomason, H.A., Scothern, A., McHarg, S. and Garrod, D.R. (2010) 'Desmosomes: adhesive strength and signalling in health and disease', *The Biochemical journal*, 429(3), pp. 419-33.

Thorburn, A. (2008) 'Studying autophagy's relationship to cell death', *Autophagy*, 4(3), pp. 391-4.

Tian, J., Feng, Y., Fu, H., Xie, H.Q., Jiang, J.X. and Zhao, B. (2015) 'The Aryl Hydrocarbon Receptor: A Key Bridging Molecule of External and Internal Chemical Signals', *Environmental science & technology*, 49(16), pp. 9518-31.

Tigges, J., Weighardt, H., Wolff, S., Gotz, C., Forster, I., Kohne, Z., Huebenthal, U., Merk, H.F., Abel, J., Haarmann-Stemmann, T., Krutmann, J. and Fritsche, E. (2013) 'Aryl hydrocarbon receptor repressor (AhRR) function revisited: repression of CYP1 activity in human skin fibroblasts is not related to AhRR expression', *The Journal of investigative dermatology*, 133(1), pp. 87-96.

Tobin, D.J., Foitzik, K., Reinheckel, T., Mecklenburg, L., Botchkarev, V.A., Peters, C. and Paus, R. (2002) 'The lysosomal protease cathepsin L is an important regulator of keratinocyte and melanocyte differentiation during hair follicle morphogenesis and cycling', *The American journal of pathology*, 160(5), pp. 1807-21.

Todd, C. and Reynolds, N.J. (1998) 'Up-regulation of p21WAF1 by phorbol ester and calcium in human keratinocytes through a protein kinase C-dependent pathway', *The American journal of pathology*, 153(1), pp. 39-45.

Tsuji, N., Fukuda, K., Nagata, Y., Okada, H., Haga, A., Hatakeyama, S., Yoshida, S., Okamoto, T., Hosaka, M., Sekine, K., Ohtaka, K., Yamamoto, S., Otaka, M., Grave, E. and Itoh, H. (2014) 'The activation mechanism of the aryl hydrocarbon receptor (AhR) by molecular chaperone HSP90',*FEBS open bio*, 4, pp. 796-803.

Tsujimoto, Y. and Shimizu, S. (2005) 'Another way to die: autophagic programmed cell death', *Cell death and differentiation*, 12 Suppl 2, pp. 1528-34.

van den Bogaard, E.H., Bergboer, J.G., Vonk-Bergers, M., van Vlijmen-Willems, I.M., Hato, S.V., van der Valk, P.G., Schroder, J.M., Joosten, I., Zeeuwen, P.L. and Schalkwijk, J. (2013) 'Coal tar induces AHR-dependent skin barrier repair in atopic dermatitis', *The Journal of clinical investigation*, 123(2), pp. 917-27.

van den Bogaard, E.H., Podolsky, M.A., Smits, J.P., Cui, X., John, C., Gowda, K., Desai, D., Amin, S.G., Schalkwijk, J., Perdew, G.H. and Glick, A.B. (2015) 'Genetic and pharmacological analysis identifies a physiological role for the AHR in epidermal differentiation', *The Journal of investigative dermatology*, 135(5), pp. 1320-8.

van Tonder, A., Joubert, A.M. and Cromarty, A.D. (2015) 'Limitations of the 3-(4,5-dimethylthiazol-2-yl)-2,5-diphenyl-2H-tetrazolium bromide (MTT) assay when compared to three commonly used cell enumeration assays', *BMC research notes*, 8, p. 47.

Veldhoen, M., Hirota, K., Christensen, J., O'Garra, A. and Stockinger, B. (2009) 'Natural agonists for aryl hydrocarbon receptor in culture medium are essential for optimal differentiation of Th17 T cells', *The Journal of experimental medicine*, 206(1), pp. 43-9.

Venderova, K. and Park, D.S. (2012) 'Programmed cell death in Parkinson's disease', *Cold Spring Harbor perspectives in medicine*, 2(8).

Vitale, N., Kisslinger, A., Paladino, S., Procaccini, C., Matarese, G., Pierantoni, G.M., Mancini, F.P. and Tramontano, D. (2013) 'Resveratrol couples apoptosis with autophagy in UVB-irradiated HaCaT cells', *PloS one*, 8(11), p. e80728.

Voigt, W. (2005) 'Sulforhodamine B assay and chemosensitivity', *Methods in molecular medicine*, 110, pp. 39-48.

Vyas, P.M., Roychowdhury, S., Khan, F.D., Prisinzano, T.E., Lamba, J., Schuetz, E.G., Blaisdell, J., Goldstein, J.A., Munson, K.L., Hines, R.N. and Svensson, C.K. (2006) 'Enzyme-mediated protein haptenation of dapsone and sulfamethoxazole in human keratinocytes: I. Expression and role of cytochromes P450', *The Journal of pharmacology and experimental therapeutics*, 319(1), pp. 488-96.

Wang, D.W., Peng, Z.J., Ren, G.F. and Wang, G.X. (2015) 'The different roles of selective autophagic protein degradation in mammalian cells', *Oncotarget*, 6(35), pp. 37098-116.

Wang, F., Wang, W. and Safe, S. (1999) 'Regulation of constitutive gene expression through interactions of Sp1 protein with the nuclear aryl hydrocarbon receptor complex', *Biochemistry*, 38(35), pp. 11490-500.

Wei, M.C., Zong, W.X., Cheng, E.H., Lindsten, T., Panoutsakopoulou, V., Ross, A.J., Roth, K.A., MacGregor, G.R., Thompson, C.B. and Korsmeyer, S.J. (2001) 'Proapoptotic BAX and BAK: a requisite gateway to mitochondrial dysfunction and death', *Science*, 292(5517), pp. 727-30.

Wei, Y.D., Helleberg, H., Rannug, U. and Rannug, A. (1998) 'Rapid and transient induction of CYP1A1 gene expression in human cells by the tryptophan photoproduct 6-formylindolo[3,2-b]carbazole', *Chemico-biological interactions*, 110(1-2), pp. 39-55.

Wickett, R.R. and Visscher, M.O. (2006) ‘Structure and function of the epidermal barrier’, *American journal of infection control,* 34(10), pp.S98-S110.

Wilson, A., Murphy, M.J., Oskarsson, T., Kaloulis, K., Bettess, M.D., Oser, G.M., Pasche, A.C., Knabenhans, C., Macdonald, H.R. and Trumpp, A. (2004) 'c-Myc controls the balance between hematopoietic stem cell self-renewal and differentiation', *Genes & development*, 18(22), pp. 2747-63.

Wincent, E., Amini, N., Luecke, S., Glatt, H., Bergman, J., Crescenzi, C., Rannug, A. and Rannug, U. (2009) 'The suggested physiologic aryl hydrocarbon receptor activator and cytochrome P4501 substrate 6-formylindolo[3,2-b]carbazole is present in humans', *The Journal of biological chemistry*, 284(5), pp. 2690-6.

Wong, R.S. (2011) 'Apoptosis in cancer: from pathogenesis to treatment', *Journal of experimental & clinical cancer research : CR*, 30, p. 87.

Wormke, M., Stoner, M., Saville, B. and Safe, S. (2000) 'Crosstalk between estrogen receptor alpha and the aryl hydrocarbon receptor in breast cancer cells involves unidirectional activation of proteasomes', *FEBS letters*, 478(1-2), pp. 109-12.

Wu, G., Huang, J., Wei, G., Liu, L., Pang, S. and Yan, B. (2011) 'LAMP-2 gene expression in peripheral leukocytes is increased in patients with coronary artery disease', *Clinical cardiology*, 34(4), pp. 239-43.

Wu, Y.T., Tan, H.L., Shui, G., Bauvy, C., Huang, Q., Wenk, M.R., Ong, C.N., Codogno, P. and Shen, H.M. (2010) 'Dual role of 3-methyladenine in modulation of autophagy via different temporal patterns of inhibition on class I and III phosphoinositide 3-kinase', *The Journal of biological chemistry*, 285(14), pp. 10850-61.

Xue, L., Fletcher, G.C. and Tolkovsky, A.M. (1999) 'Autophagy is activated by apoptotic signalling in sympathetic neurons: an alternative mechanism of death execution', *Molecular and cellular neurosciences*, 14(3), pp. 180-98.

Yamamoto, A., Tagawa, Y., Yoshimori, T., Moriyama, Y., Masaki, R. and Tashiro, Y. (1998) 'Bafilomycin A1 prevents maturation of autophagic vacuoles by inhibiting fusion between autophagosomes and lysosomes in rat hepatoma cell line, H-4-II-E cells', *Cell structure and function*, 23(1), pp. 33-42.

Yazdankhah, M., Farioli-Vecchioli, S., Tonchev, A.B., Stoykova, A. and Cecconi, F. (2014) 'The autophagy regulators Ambra1 and Beclin 1 are required for adult neurogenesis in the brain subventricular zone', *Cell death & disease*, 5, p. e1403.

Yoshihara, N., Ueno, T., Takagi, A., Oliva Trejo, J.A., Haruna, K., Suga, Y., Komatsu, M., Tanaka, K. and Ikeda, S. (2015) 'The significant role of autophagy in the granular layer in normal skin differentiation and hair growth', *Archives of dermatological research*, 307(2), pp. 159-69.

Yoshimori, T., Yamamoto, A., Moriyama, Y., Futai, M. and Tashiro, Y. (1991) 'Bafilomycin A1, a specific inhibitor of vacuolar-type H(+)-ATPase, inhibits acidification and protein degradation in lysosomes of cultured cells', *The Journal of biological chemistry*, 266(26), pp. 17707-12.

Youle, R.J. and Strasser, A. (2008) 'The BCL-2 protein family: opposing activities that mediate cell death', *Nature reviews. Molecular cell biology*, 9(1), pp. 47-59.

Yu, H., Du, Y., Zhang, X., Sun, Y., Li, S., Dou, Y., Li, Z., Yuan, H. and Zhao, W. (2014) 'The aryl hydrocarbon receptor suppresses osteoblast proliferation and differentiation through the activation of the ERK signaling pathway', *Toxicology and applied pharmacology*, 280(3), pp. 502-10.

Yuspa, S.H., Kilkenny, A.E., Steinert, P.M. and Roop, D.R. (1989) 'Expression of murine epidermal differentiation markers is tightly regulated by restricted extracellular calcium concentrations in vitro', *The Journal of cell biology*, 109(3), pp. 1207-17.

Zang, Y., Beard, R.L., Chandraratna, R.A. and Kang, J.X. (2001) 'Evidence of a lysosomal pathway for apoptosis induced by the synthetic retinoid CD437 in human leukemia HL-60 cells', *Cell death and differentiation*, 8(5), pp. 477-85.

Zhang, F., White, R.L. and Neufeld, K.L. (2001) 'Cell density and phosphorylation control the subcellular localization of adenomatous polyposis coli protein', *Molecular and cellular biology*, 21(23), pp. 8143-56.

Zhang, S., Qin, C. and Safe, S.H. (2003) 'Flavonoids as aryl hydrocarbon receptor agonists/antagonists: effects of structure and cell context', *Environmental health perspectives*, 111(16), pp. 1877-82.

Zhang, W., Li, Q., Song, C. and Lao, L. (2015) 'Knockdown of autophagy-related protein 6, Beclin-1, decreases cell growth, invasion, and metastasis and has a positive effect on chemotherapy-induced cytotoxicity in osteosarcoma cells', *Tumour biology: the journal of the International Society for Oncodevelopmental Biology and Medicine*, 36(4), pp. 2531-9.

Zhao, J., Tang, C., Nie, X., Xi, H., Jiang, S., Jiang, J., Liu, S., Liu, X., Liang, L., Wan, C. and Yang, J. (2016) 'Autophagy potentially protects against 2,3,7,8-tetrachlorodibenzo-p-Dioxin induced apoptosis in SH-SY5Y cells', *Environmental toxicology*, 31(9), pp. 1068-79.

Zhao, M., Antunes, F., Eaton, J.W. and Brunk, U.T. (2003) 'Lysosomal enzymes promote mitochondrial oxidant production, cytochrome c release and apoptosis', *European journal of biochemistry / FEBS*, 270(18), pp. 3778-86.